Design and performance of energy pile foundations

Precast quadratic pile heat exchangers for shallow geothermal energy systems

Alberdi-Pagola, Maria

[Link to publication from Aalborg University](#)

DESIGN AND PERFORMANCE OF ENERGY PILE FOUNDATIONS

PRECAST QUADRATIC PILE HEAT EXCHANGERS FOR SHALLOW GEOTHERMAL ENERGY SYSTEMS

BY
MARIA ALBERDI-PAGOLA

DISSERTATION SUBMITTED 2018

AALBORG UNIVERSITY
DENMARK

DESIGN AND PERFORMANCE OF ENERGY PILE FOUNDATIONS

PRECAST QUADRATIC PILE HEAT EXCHANGERS FOR SHALLOW GEOTHERMAL ENERGY SYSTEMS

by

Maria Alberdi-Pagola

AALBORG UNIVERSITY
DENMARK

Dissertation submitted

CURRICULUM VITAE

Name	Maria Alberdi-Pagola
Date of birth	24/08/1988
Nationality	Spanish
Email	maria-alberdi4@hotmail.com
Phone	+45 52 52 02 37
LinkedIn	https://www.linkedin.com/in/maria-alberdi-pagola-3a063066/
Research Gate	https://www.researchgate.net/profile/Maria_Alberdi-Pagola

Professional Experience

Feb 2015 – Jun 2018	Industrial PhD student at Centrum Pæle A/S and the Department of Civil Engineering at Aalborg University, Denmark.
Sep 2013 – Feb 2015	Assistant professor at VIA University College, Horsens, Denmark.

Education

Sep 2012 – Sep 2013	MSc in Civil Engineering, University of Cantabria, Spain.
Sep 2006 – Sep 2012	Graduated in Civil Engineering, specialised in roads, canals and ports, University of Burgos, Spain.

Research Areas

Ground source heat pump systems, thermal response testing, laboratory measurements of thermal properties.

ENGLISH SUMMARY

Ground source heat pump (GSHP) systems are sustainable and cost-effective space conditioning systems based on shallow geothermal energy. In combination with other renewable energies, GSHP systems have great potential for realising the transition from fossil fuels to renewable energy resources in Denmark.

Pile heat exchangers, also known as energy piles, are concrete piles with built in geothermal pipes. Thus, the foundation of a building performs as a structural and a heating/cooling supply element.

The thermal dimensioning of energy pile foundations is typically addressed by methods originally developed for borehole heat exchangers. However, those methods are not always well suited for analysing the thermal dynamics of energy piles. Piles are shorter and wider than boreholes and while boreholes typically are arranged in regular grids, energy piles are placed irregularly and in clusters, constrained by the structural requirements of the building. Moreover, the influence of temperature changes induced in the foundation on the bearing properties of the energy piles must be considered in the geotechnical and structural dimensioning. Hence, reliable temperature calculations are required.

There is a lack of documentation on the long-term thermal and structural sustainability of energy foundations and a lack of unified guidelines for practitioners. This PhD project focuses on developing a tool to calculate the temperature changes occurring in the energy piles given a thermal load of a building. It will serve to assist feasibilities studies and dimensioning.

First, a full 3D finite element model (FEM) is set to include the geometry of the pile and the embedded geothermal pipe arrangement, for calculating the heat transport inside the pipes, in the concrete, as well as in the ground. The model is validated with measured temperatures from thermal response tests (TRT) of existing energy piles, where the energy pile is continuously heated for over 60 hours. It is demonstrated that the model reproduces the measured TRT temperatures within measurement uncertainty, thus, the model is considered validated. The 3D FEM model is then used to calculate dimensionless temperature responses over dimensionless time (Fourier's number), which are adjusted with simple polynomials. Fluid temperatures are calculated for a group of energy piles that thermally affect each other with time and space superposition of the temperature responses for a given energy requirement of the building. Hence, the calculation of the temperature response is reduced to simple addition of polynomials instead of time consuming transient 3D FEM modelling, enabling practical application of the developed calculation method for dimensioning energy pile foundations.

In the las publication, the dimensioning tool is used in a case study high school in Denmark, where 219 energy piles supply the building with heating and cooling. Initially, measured and calculated temperatures were compared and showed a fair predictive capability of the model. Subsequently, the number of piles and their arrangement is optimised based on the heating and cooling needs of the building and the fluid temperatures leaving the heat pump. The optimisation minimises the number of energy piles, maximises the distance between them and ensures safe temperatures in the ground loop. It is shown that the number of energy piles required to cover the energy needs of the building could be reduced by 32 %.

Regarding thermo-mechanical aspects, an extensive literature review and a numerical study are carried out. The results show that a typical geothermal utilisation of the energy foundation does not generate significant structural implications on the geotechnical capacity of a single energy pile. However, ground thermal loads need to be considered in the design phase to account for potential extreme temperature changes. These findings are in line with the literature.

DANSK RESUME

Jordvarmepumper (GSHP) udgør en bæredygtig og omkostningseffektiv energiforsyning, der udnytter jorden som køle- og varmekilde. GSHP-systemer har, i kombination med andre vedvarende energikilder, et betydeligt potentiale i omstillingen til vedvarende energikilder i Danmark.

Energipælen er en traditionel funderingspæl med indstøbte jordvarmeslanger, hvori cirkulation af væske optager eller afgiver varme fra/til pælen og jorden. Bygningens fundament sørger således både for den mekaniske stabilisering af bygningen men også som varme- og køleforsyning.

Den termiske dimensionering af energipælefundamenter baserer sig typisk på matematiske metoder, der oprindeligt er udviklet til jordvarmeboringer. Disse metoder er imidlertid ikke altid velegnede til analyse af energipæle pga. af betydelige forskelle i geometri, materialer og opbygning. Energipæle er kortere og bredere end borehuller og sidstnævnte placeres typisk i en velordnet geometri, hvorimod førstnævnte ofte placeres uregelmæssigt og i klynger af hensyn til funderingen af bygningen. Endvidere skal indflydelsen, af temperaturændringer i fundamentet på de bærende egenskaber af pælene vurderes i den geotekniske dimensionering, hvorfor pålidelige temperaturberegninger er nødvendige.

På verdensplan mangler der dokumentation af den langsigtede udvikling i de termiske og geotekniske egenskaber af energipælefundamenter, hvorfor der også mangler retningslinjer for praktikere. Arbejdet i dette Ph.D.-projekt har til formål at udvikle beregningsmetoder til termisk dimensionering af energipælefundamenter. Indledningsvis opstilles en fuld 3D finite element model (FEM), der inkluderer geometrien af pælen og jordvarmeslangerne til beregning af varmetransport i jordvarmeslangen (og strømning), betondelen af pælen samt i jorden. Modellen valideres med målte temperaturer fra termisk respons test (TRT) af eksisterende energipæle, hvor jordvarmekredsen opvarmes kontinuerligt over mindst 60 timer. Det demonstreres at modellen reproducerer de målte TRT-temperaturer indenfor måleusikkerheden, hvorfor modellen betragtes som værende valideret. FEM-modellen anvendes derefter til beregning af det dimensionsløse temperaturrespons i dimensionsløs tid (Fourier-tallet), der efterfølgende tilpasses med et simpelt polynomium. Væsketemperaturerne beregnes for en gruppe af pæle, der termisk påvirker hinanden ved superposition i tid og rum af temperaturresponser (de tilpassede polynomier) for et givet energibehov for bygningen samt de termiske egenskaber af pælene og jorden. Dermed reduceres beregningerne af temperaturresponset til simpel addition af polynomier i stedet for tidskrævende, transient 3D FEM modellering, hvilket muliggør praktisk anvendelse af den udviklede beregningsmetode til dimensionering af energipælefundamenter.

I det afsluttende arbejde anvendes dimensioneringsværktøjet i et case studie af Rosborg Gymnasium, hvor 219 energipæle forsyner bygningen med varme og køl. Indledningsvis påvises der god overensstemmelse imellem målte og de med dimensioneringsværktøjet beregnede temperaturer. Efterfølgende optimeres antallet af pæle og arrangementet heraf ud fra bygningens varme- og kølebehov samt væsketemperaturerne til varmepumpen. Optimeringen minimerer antallet af pæle samt variansen i den indbyrdes afstand herimellem og sikrer minimumstemperaturer til varmepumpen. Det påvises at antallet af pæle, der er nødvendige for at dække bygningens energibehov, er ca. 150, hvilket er 32% færre end de aktuelle 219 pæle.

Med hensyn til termisk-mekaniske egenskaber, udføres et omfattende litteraturstudie og numeriske undersøgelser. Resultaterne viser at en typisk geotermisk udnyttelse af energipæle ikke genererer signifikante strukturelle implikationer på den geotekniske kapacitet i forhold til den enkelte energipæl. Imidlertid bør jordvarmebelastninger overvejes i designfasen med henblik på at tage højde for ekstreme temperaturudsving. Disse resultater er i overensstemmelse med den eksisterende litteratur.

PREFACE

LIST OF PUBLICATIONS

The core of this thesis is comprised by the following collection of publications:

Paper A   Alberdi-Pagola, M., Poulsen, S.E., Loveridge, F., Madsen, S. & Jensen, L.J., 2018. "Comparing heat flow models for interpretation of precast quadratic pile heat exchanger thermal response tests", *Energy*, 145, pp. 721-733. https://doi.org/10.1016/j.energy.2017.12.104.

Paper B   Alberdi-Pagola, M., Poulsen, S.E. Jensen, L.J. & Madsen, S. (under review). "Design methodology for precast quadratic pile heat exchanger-based shallow geothermal ground-loops: multiple pile g-functions", *Geothermics*.

Paper C   Alberdi-Pagola, M., Poulsen, S.E., Jensen, L.J. & Madsen, S. (under consideration). "A case study of the sizing and optimisation of an energy pile foundation (Rosborg, Denmark)", *Renewable Energy.*

Paper D   Alberdi-Pagola, M., 2018. "Thermal Response Test data of five quadratic cross section precast pile heat exchangers", *Data in Brief*, 18, pp. 13-15. https://doi.org/10.1016/j.dib.2018.02.080.

Conference Paper I   Alberdi-Pagola, M., Poulsen, S.E. & Jensen, L.J., 2016. "A performance case study of energy pile foundation at Rosborg Gymnasium (Denmark)", in *Proceedings of the 12th REHVA World Congress Clima2016*, May 2016, Aalborg, Denmark. Vol. 3, pp. 10. Aalborg University, Department of Civil Engineering, http://vbn.aau.dk/files/233716932/paper_472.pdf.

Conference Paper II   Alberdi-Pagola, M., Madsen, S., Jensen, L.J. & Poulsen, S.E., 2017. "Numerical investigation on the thermo-mechanical

behavior of a quadratic cross section pile heat exchanger", in *Proceedings of the IGSHPA Technical/Research Conference and Expo Denver*, USA, March 14-16, 2017. http://dx.doi.org/10.22488/okstate.17.000520.
Available online:
https://shareok.org/bitstream/handle/11244/49304/oksd_igshpa_2017_Alberdi-Pagola.pdf?sequence=1&isAllowed=y

Technical Report I   Alberdi-Pagola, M., Poulsen, S.E., Jensen, L.J. & Madsen, S., 2017. "Thermal response testing of precast pile heat exchangers: fieldwork report". Aalborg: Department of Civil Engineering, Aalborg University. DCE Technical Reports, nr. 234, pp. 43.
Available online:
http://vbn.aau.dk/files/266379225/Thermal_response_testing_of_precast_pile_heat_exchangers_fieldwork_report.pdf.

Technical Report II   Alberdi-Pagola, M., Jensen, L.J., Madsen, S. & Poulsen, S.E., 2017. "Measurement of thermal properties of soil and concrete samples". Aalborg: Department of Civil Engineering, Aalborg University. DCE Technical Reports, nr. 235, pp. 30. Available online:
http://vbn.aau.dk/files/266378485/Measurement_of_thermal_properties_of_soil_and_concrete_samples.pdf.

Technical Report III Alberdi-Pagola, M., Jensen, L.J., Madsen, S. & Poulsen, S.E., 2018. "Method to obtain g-functions for multiple precast quadratic pile heat exchangers". Aalborg: Department of Civil Engineering, Aalborg University. DCE Technical Reports; nr. 243, pp. 34. Available online:
http://vbn.aau.dk/files/274763046/Method_to_obtain_g_functions_for_multiple_precast_quadratic_pile_heat_exchangers.pdf

Technical Report IV   Alberdi-Pagola, M., Madsen, S., Jensen, L.J. & Poulsen, S.E., 2018. "Thermo-mechanical aspects of pile heat exchangers: background and literature review". Aalborg: Department of Civil Engineering, Aalborg University. DCE Technical Reports, nr. 250, pp. 37. Available online:
http://vbn.aau.dk/files/281634409/Thermo_mechanical_aspects_of_pile_heat_exchangers_background_and_literature_review.pdf

This thesis has been submitted for assessment in partial fulfilment of the PhD degree. The thesis is based on the submitted or published scientific papers which are listed

above. As part of the assessment, co-author statements have been made available to the assessment committee and are also available at the Faculty.

ACKNOWLEDGEMENTS

TABLE OF CONTENTS

NOMENCLATURE-ABBREVIATIONS

AR	Aspect ratio
BHE	Borehole heat exchanger
COP	Coefficient of performance
d_{ij}	Pile distance [m]
d_i	Individual desirability [-]
D	Overall desirability [-]
FEM	Finite element method - model
f	Heat carrier fluid flow [m^3/s]
Fo	Normalised time, Fourier's number [-]
g	Multiple energy pile g-function [-]
G_c	Transient Concrete response g-function [-]
G_g	Ground temperature response g-function [-]
GSHP	Ground source heat pump
h_i	Heat transfer coefficient [W/m^2/K]
k	number of responses [-]
L	Energy pile length [m]
L_i, U_i, T_i	Lower, upper and target values for definition of desirability function, respectively
n	Number of pipes in the pile cross section [-]
n_p	Number of pile heat exchangers [-]
q	Heat transfer rate per metre length of energy pile [W/m]

Q	Thermal power [W]
r_b	Pile or borehole radius [m]
r_i	Inner radius of pipe [m]
r_o	Outer radius of pipe [m]
R_c	Steady state concrete thermal resistance [K·m/W]
R_p	Steady state pile thermal resistance [K·m/W]
R_{pipe}	Steady state pipe thermal resistance [K·m/W]
s and t	desirability parameters
S	Pile spacing [m]
SLS	Service limit state
SPF	Seasonal performance factor
T_0	Undisturbed soil temperature [°C]
T_b	average pile wall temperature [°C]
T_{in}, T_{out}	Inlet and outlet temperatures [°C]
T_f	Average fluid temperature in the ground loop [°C]
T_p	Average temperature on the outer wall of the pipe [°C]
t	Time [s]
TRT	Thermal response test
ULS	Ultimate limit state
UTES	Underground thermal energy storage
x	Specific parameter for response calculation Y_i
Y_i	Calculated response for a specific parameter

<u>Greek symbols</u>

α   Thermal diffusivity [m^2/s]

ΔT   Change in temperature [K]

λ   Thermal conductivity [W/m/K]

ρc_p Volumetric heat capacity [J/m^3/K]

Φ   Normalised temperature change [-]

<u>Material subscripts</u>

c   Concrete

s   Soil

CHAPTER 1. INTRODUCTION

1.1. BACKGROUND OF THE PHD PROJECT

The harmful consequences derived from global warming and climate change have forced countries worldwide to reach agreements to alleviate the effects, to the benefit of general wellbeing. The Paris Agreement within the United Nations Framework Convention on Climate Change aims to reduce greenhouse gas emissions to keep the global warming below 2 °C [1]. To meet this target, the European Commission aims to reduce by 2020 greenhouse gas emissions by 20% compared to 1990 levels. The Danish government has increased this share to 30% and has set two additional targets: by 2030, 50% of the gross energy use will be covered with renewable energies and by 2050 the energy system in Denmark will be independent of fossil fuels [2].

In combination with other renewable energies, shallow geothermal energy and ground source heat pump (GSHP) systems have great potential for realising the transition from fossil fuels to renewable energy resources [3]. Subsurface energy systems are important for alleviating energy storage problems related to the intermittent generation of heat and electricity by renewable resources, such as wind and sun [3–5]. The Danish Energy Agency predicts an increase in heat pump technology utilisation between 2017-2030. The net heating demand will drop over the years, yet, as shown in Figure 1-1a, heat pumps are expected to replace biomass and become the most used heating technology for households by 2030 [6]. District heating also plays a role in the transition towards renewable energies. Figure 1-1b shows that the share of renewable energies in the generation of district heating will increase, until it reaches 74% by 2030. Its use is not expected to increase throughout the period 2017-2030 but the contributions from each energy source will suffer changes [6].

Biomass consumption rises by almost 5% annually by 2020, to the detriment of coal and natural gas consumption. In 2020 the coal consumption remains stable, while natural gas consumption falls by almost 8% annually. Consumption of solar heat and biogas rises 2-3% yearly, while the consumption of waste and surplus heat remains constant during the period. District heating production from heat pumps and electric boilers rises from 0.8 PJ in 2017 to 5.3 PJ in 2030, corresponding to a 16% annual increase, associated to tax reduction on electricity generated by renewable resources. Heat pumps and electric boilers are expected to account for 4% of total district heating production by 2030 [6].

Despite the positive forecasts, the application of shallow geothermal and GSHP systems is limited in Denmark mainly due to groundwater flow legislation [7,8] and low cost of district heating [9,10]. Currently there are approximately 40,000 ground source heat pump installations in Denmark. This corresponds to an installed capacity of 320 MWt and annual energy use of 3,400 TJ/year [9,11].

a)

b)
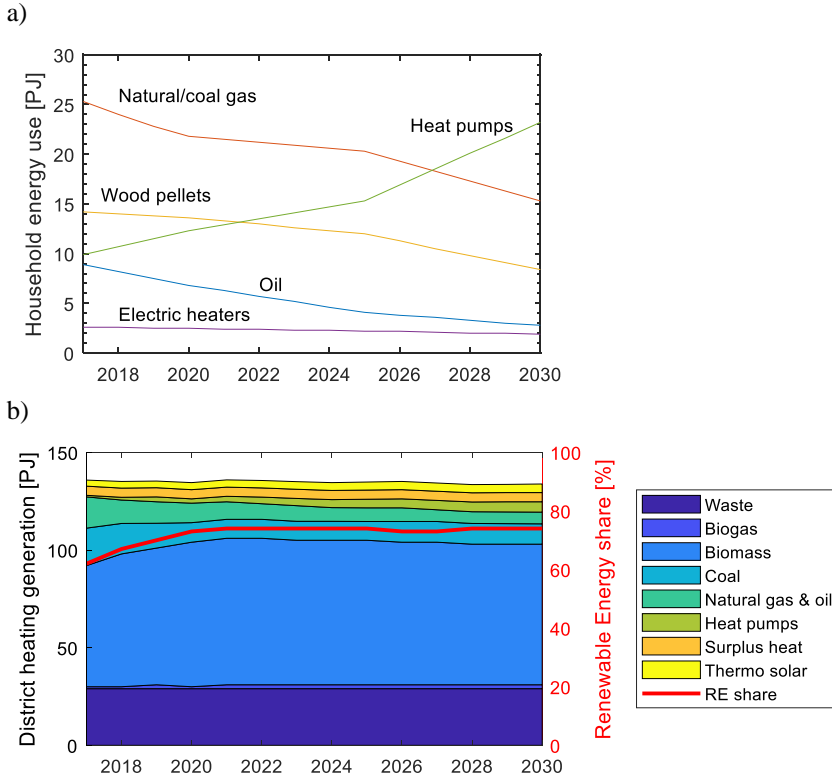
Figure 1-1: a) Danish household energy consumption by selected heating technologies. Heat pump energy consumption includes electricity consumption, based on data from [6]; b) District heating production by energy technologies and renewable energy production share in Denmark, based on data from [6].

Centrum Pæle A/S is a manufacturer of precast foundation piles. In Denmark, 90% of the piles installed are precast [12] and the main share is addressed to the building industry. The Danish based company, founded on 1965, employs more than 60 people in its headquarters in Vejle. Centrum Pæle A/S has sister companies in Germany, Sweden, Poland and United Kingdom and currently produces a total of 2,500,000 m of piles per year all together. In Centrum Pæle A/S, the ambition to be market leader incites innovation as a key factor for reaching cost-effective development and competitiveness, and product development is a pillar in the strategy of the organization.

The environmental objectives set by policy makers have facilitated new markets for sustainable energy technologies. Hence, and being aware of the future energy challenges, Centrum Pæle A/S launched the precast pile heat exchangers (Figure 1-2), also known as energy piles, by fitting geothermal pipes to the steel reinforcement

of the piles. The company has produced the energy pile foundations at Rosborg Gymnasium in Vejle (2011 and 2017) and Horsens Vand's waste-water plant in Horsens (2012) among other smaller installations.

a)
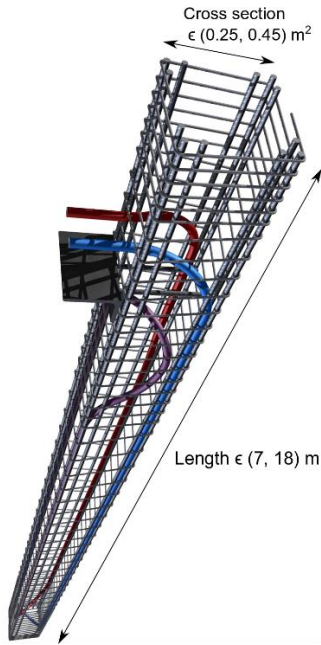
b)

Figure 1-2: a) Demonstration model of the precast energy pile. The concrete has been omitted for illustration. Courtesy of Centrum Pæle A/S. b) 18 m long energy pile driving.

Centrum Pæle A/S has raised concerns about the possibilities of increasing sales of energy piles, taking advantage of their dual role as structural and heating/cooling supply element. The company states that potential customers are reluctant to purchase the technology due to a lack of documentation of the long-term thermal and structural sustainability of energy pile foundations. To address these concerns, it is necessary to understand their behaviour. The existing design standards do not consider the nature of thermo-active foundations and, in general, conservative considerations are employed in the sizing. Structural reliability of the product is the most vital feature of energy pile foundations and, therefore, scientific evidence is vital.

The primary initiator of this project is the pile producer company, which had previously collaborated with VIA University College during initial investigations that leaded to the PhD study, together with Aalborg University. This thesis, thus, is part of

an industrial PhD project carried out in collaboration between Centrum Pæle A/S, Aalborg University and VIA University College.

1.2. OBJECTIVES OF THE THESIS

This research project aims to create a framework for the analysis and design of GSHP systems based on precast quadratic pile heat exchangers to cover the heating and/or cooling needs of a building, without compromising the structural role of the piles.

Pile heat exchangers are structural elements, and, therefore, first, the structural integrity of the pile must be guaranteed. To treat the thermo-mechanical aspects, an updated literature study will be developed. Analyses of the implications of the geothermal use will be carried out to quantify the thermally induced changes in displacements and stresses.

Because the thermally induced stresses and strains will depend on the resulted temperature change, it is important to develop models that accurately determine these temperature changes in the soil and the piles, in the short and long-terms. For this, a method that considers the thermal processes occurring within the geothermal pile foundation is required. To reach it, specific objectives will be breakdown, building up from a single energy pile and to a group of energy piles:

- Characterise the thermal response of single pile heat exchangers and the ground response.
- Assess the applicability of thermal response testing TRT of pile heat exchangers.
- Characterise the thermal response of groups of pile heat exchangers.
- Optimise the energy pile foundation arrangement to simultaneously fulfil certain conditions, e.g., minimise the number of required energy piles and avoid a significant fluid temperature depletion in the ground loop over time.
- Assess the operational demonstration of a case study building.

1.3. THESIS STRUCTURE AND READING GUIDE

The thesis is paper-based but it is presented as monograph to avoid endless self-citations and unnecessary duplication of work. Therefore, Papers A to C and Conference Paper I have been integrated directly into the main body of the text. Paper D, Conference Paper II and the technical reports are appended with references in the main text.

The main body is divided in 8 chapters, with assigned corresponding documents, as shown in Figure 1-3.
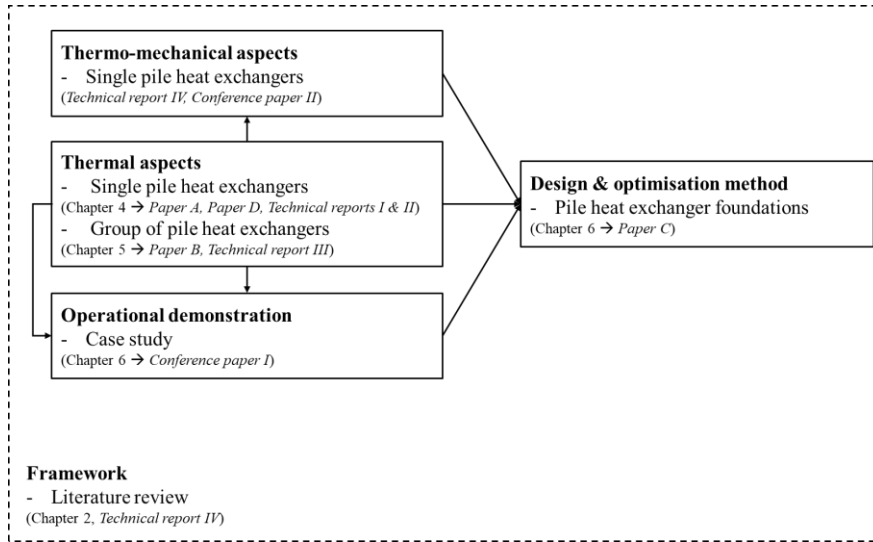
Figure 1-3: Breakdown of the contents of the thesis and related publications.

Chapter 1 has presented the background and the objectives of this PhD project.

Chapter 2 provides a literature review to frame the field of research. It deals with the principles of shallow geothermal and GSHP systems and it presents the main challenges related to energy piles, both mechanically and thermally. The literature review assists in setting the course of the main research focus of the thesis.

Chapter 3 presents the studied quadratic cross section pile heat exchangers and summarises the methodologies that have been used along the PhD thesis, providing the reader with an overview of the experimental and numerical methods that have been applied in the different papers.

Chapter 4 presents the challenges to model single quadratic cross section pile heat exchangers. Different heat flux models are compared to obtain the most suitable one for the studied energy piles. Paper A is introduced.

Chapter 5 investigates the thermal interactions of groups of energy piles. It aims to propose a design method for pile heat exchangers which is easy to implement and still provides acceptable accuracy. Paper B is introduced.

Chapter 6 applies the design method to a case study and extends it to ease the optimisation of the energy pile foundation, in terms of minimising the number of pile heat exchangers required to supply a thermal need of a building. Conference Paper I describes the case study and after, Paper C is introduced.

Chapter 7 discusses the suitability of the methods applied along the thesis and provides general conclusions drawn from the results.

Chapter 8 gives recommendations for further research work on the topics treated in this PhD project.

Appendixes I to VI contain the papers, conference papers and technical reports that complete the thesis and have not been included in the main body.

Two reference lists are provided. The first list, denoted as "References in summary", involves the references used in the main body, excluding the references covered in Papers A, B, and C. The second list (attached as Appendix VII) covers all the references used in the thesis, including journal papers, conference papers and technical reports.

CHAPTER 2. LITERATURE REVIEW

2.1. SCOPE AND MOTIVATION

This chapter provides the current state of knowledge and research areas related to pile heat exchangers. It starts with describing the main principles of shallow geothermal and GSHP systems and it presents the main challenges associated to the mechanical and thermal aspects of pile heat exchangers. The literature review assists in identifying the set the course of the main research focus of the thesis.

2.2. SHALLOW GEOTHERMAL SYSTEMS

Ground source heat pump (GSHP) systems produce renewable thermal energy that offer high levels of efficiency for space heating and cooling [13] and have the potential to be used anywhere in the world [11]. GSHP systems have a significant impact on the direct use of geothermal energy, accounting for 70% of the worldwide installed capacity. The installed capacity for heating reaches 50,258 MWt with an annual energy use of 326,848 TJ/year, while space cooling covers 53 MWt with an annual energy use of 273 TJ/year [11].

2.2.1. BACKGROUND

The ground acts as a huge energy store. In summer, the surface of the earth heats up due to increased solar radiation and elevated air temperatures. This heating effect propagates a few meters down into the subsurface. Below a few meters depth, the temperature remains stable. Figure 2-1 shows measurements taken in Denmark. Throughout the year, the temperature varies 15 °C at 1 m depth and below 7-8 m the temperature variation is no more than 1 °C [14]. The daily thermal disturbance is on the order of 0.3-0.8 m [15].

The depth of heat penetration and the response time depend on the thermal properties of the ground. The thermal properties of soils are affected by several parameters, among others: mineralogy, particle shape, contact between soil particles, volumetric ratio of the constituents, porosity, grainsize distribution and degree of saturation [15]. It is assumed that for GSHP applications thermal properties of soils and rocks remain constant [14]. Table 2-1 provides an overview for some types.

a)

b)
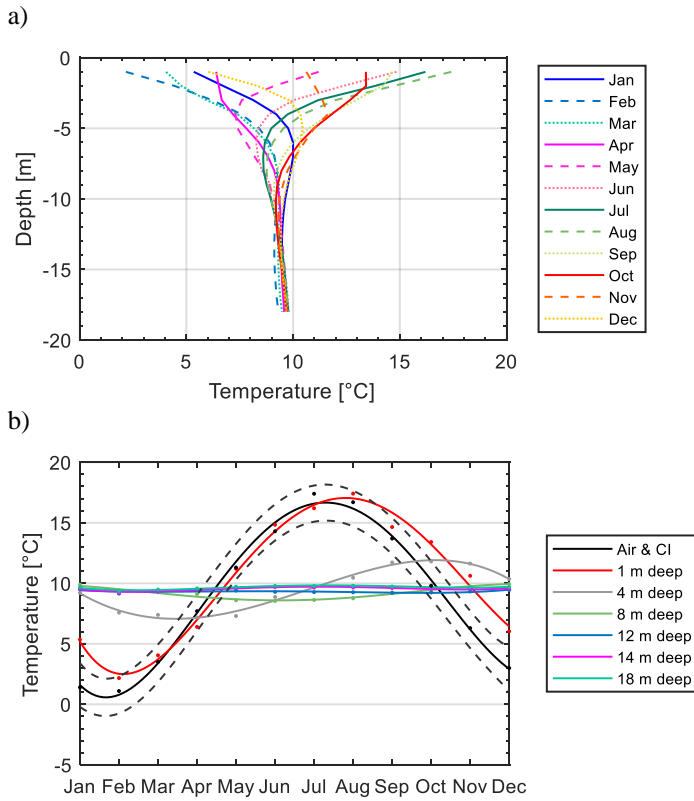
Figure 2-1: Undisturbed soil temperatures. Measurements observed at Langmarksvej test site, in Horsens, Denmark: a) monthly profiles; b) temperature variation with time for selected depths. CI states for confidence intervals. Measurements courtesy of VIA University College. Air temperatures from [16].

Table 2-1: Ranges of thermal properties, after [17].

	Thermal conductivity [W/m/K]	Volumetric heat capacity [MJ/m^3/K]	Density [kg/m^3]
Dry clay	0.4 - 1.0	1.5 - 1.6	1.8 - 2.0
Water saturated clay	1.1 - 3.1	2.0 - 2.8	2.0 - 2.2
Dry sand	0.3 - 0.9	1.3 - 1.6	1.8 - 2.2
Water saturated sand	2.0 - 3.0	2.2 - 2.8	1.9 - 2.3
Dry gravel	0.4 - 0.9	1.3 - 1.6	1.8 - 2.2
Water saturated gravel	1.6 - 2.5	2.2 - 2.6	1.9 - 2.3
Quartzite rock	5.0 - 6.0	2.1	2.5 - 2.7

The thermal energy stored in the ground can be used as a heat source in winter and a heat sink in summer [14] in two ways: i) increasing or decreasing the ground temperature to usable levels using heat pumps (GSHP) or ii) increasing or decreasing the temperature in the ground by storing heat when there is a surplus and extracting heat when is necessary (UTES) [18]. Ground temperatures vary less over the year than air temperatures and they are closer to room temperatures. This benefits the performance of the coupled water to water heat pump [13].

Ground heat exchangers are critical components in any GSHP system since they comprise the elements that extract or inject heat from or to the ground. They can be connected to the heat pump by open or closed loops. This thesis focuses on the latter. Closed loops consist of anti-freeze water mixtures circulating through pipe loops buried in the ground (either vertically or horizontally). In heating mode, the ground loop exchanges heat with the cold side of the heat pump (evaporator), which covers the heating needs of a building.

The main heat transfer mechanisms occurring in shallow geothermal energy systems are [14]: transient conduction through soils, conduction through the ground heat exchanger and heat transfer pipes, convection at the pipe-fluid boundary and convection due to groundwater motion. Radiation is usually neglected [19].

2.2.2. PILE HEAT EXCHANGERS

Horizontal heat exchangers, vertical borehole heat exchangers (BHE) and energy piles comprise the main different types of closed loop ground heat exchangers (Figure 2-2). Energy piles are concrete piles with built in geothermal pipes, i.e., they are thermo-active ground structures that utilise reinforced concrete foundation piles as vertical closed-loop heat exchangers [20]. The number of energy pile installations registered in the world are estimated to be around 115 in 2017, where almost 60% of them are built in the UK [21]. Relative to BHEs, energy piles have lower initial costs [21,22] and their potential to minimise the overall environmental impact of a structure has been demonstrated [23].

Pile heat exchangers vary in length from 7 to 50 m with a cross section of 0.3 to 1.5 m. The methods of construction include: cast-in-place concrete piles, 0.3-1.5 m in diameter [24–27]; precast concrete piles with side lengths spanning 0.27-0.6 m [28–31]; hollow concrete precast piles [32] and driven steel piles [33,34]. Collections of energy pile case studies are available in [20,22].

The foundation of the building both serves as a structural and a heating and/or cooling component. Thermal aspects affect the mechanical behaviour of piles and soil and affect the hydraulic conditions of the latter (changes in pore pressure and heat transfer through pores), whereas the influence of the mechanical loads on the temperature field

is usually insignificant. Hence, the analysis of pile heat exchangers is mainly governed by thermo-mechanical influences, treated in the following.
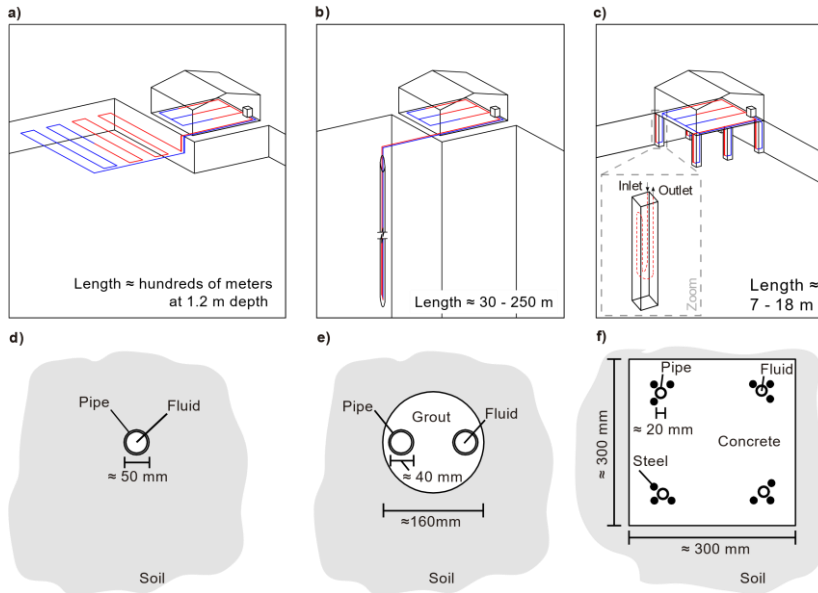
Figure 2-2: Description of main closed loop GSHP systems: a) horizontal heat exchangers; b) vertical borehole heat exchangers; c) pile heat exchangers. d), e) and f) illustrate the cross sections for horizontal, borehole and pile heat exchangers, respectively. Reproduced after [35].

2.3. MECHANICAL ASPECTS OF PILE HEAT EXCHANGERS

Some of the material presented in this section has been published in [36] (Appendix VI in this thesis), where the thermo-mechanical aspects of energy piles have been treated. This section summarises the main aspects: load transfer mechanisms, influence of temperature on mechanical properties of soils, full scale studies of energy piles, numerical methods applied for thermo-mechanical analysis of energy piles, operational demonstration and existing thermo-mechanical design approaches for energy pile foundations.

Pile heat exchangers are ground structures subject to time varying thermal loads, additional to those resulted from axial loading. Hence, an assessment of the structural and geotechnical implications needs to be carried out in any project. Pile design procedures in Europe are based on the verification of the ultimate and serviceability limit states, ULS and SLS respectively, within the Eurocode 7 frame [37]. Yet regulations do not consider the geothermal use in the foundation design.

Energy piles will be subject to a change in temperature relative to the initial condition over time, generating thermal stresses and head displacements. The pile will not expand or contract freely since it is confined, at different levels of restrain, by the structure on top and the surrounding soil (Figure 2-3). Thus, the measured strain changes due to temperature change will be less than the free axial thermal strain and the restrained strain induces a thermal stress [38].
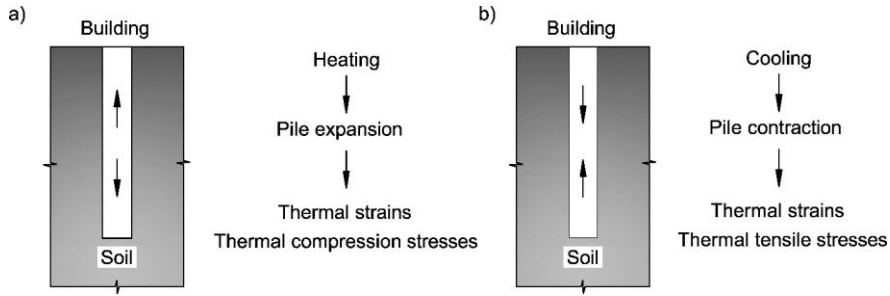
Figure 2-3: Response mechanism of a pile heat exchanger to thermal loading; a) for heating and b) for cooling. Reproduced after [39]

The null point represents the plane where zero thermally displacements occur in the pile [40]. The section of the pile above the null point experiences upward displacements when heated and downward displacements during cooling. Pile cooling results in a reverse behaviour. As a result, the mobilised bearing capacities of energy piles (end-bearing and shaft resistances) will rearrange with temperature according to the position of the null point [41].

The pile-soil interaction under working mechanical and thermal loads confers complex systems depending on: ground conditions, different levels of pile confinement and magnitude of the thermal loads. Descriptive frameworks have been established from observed behaviours [42–44].

The temperature range imposed by the geothermal exploitation of the foundations are relatively modest, falling between 2 °C to 30 °C [44]. E.g., [45] shows operational energy pile ground loop temperatures in cooling mode: the temperature of the fluid in the geothermal pipes shows quick variation in response to the building thermal needs while the temperature changes near the edge of the pile are smoother. The changes in pile temperature in the centre vary from 12.5 °C to 27 °C, while the corresponding temperatures near the edge vary from 14 °C to 19 °C, showing temperature changes of seasonal period and rather small amplitude.

The principal thermo-hydro-mechanical processes that affect the mechanical behaviour of soils are the thermal hardening, the thermally induced water flow, the excess pore pressure development and the volume changes due to thermal consolidation, possibly the most critical factor [45,46]. When a thermal load is

transmitted from the pile to the soil, the soil reacts by changing its volume (expansion or contraction of the porewater and soil structure) and by modifying the strength of contact between soil particles [38,47–54]. The thermally induced volumetric strains expected for energy pile applications are very low. According to [45], soft normally consolidated clays require main attention because large plastic volume changes may occur upon heating.

The energy pile investigation has been leaded by two main full-scale studies: the Lambeth College setup in London [42,55], which behaves as a floating pile, and the EPFL setup in Lausanne [56–58], showing a semi-floating behaviour. Both studies conclude: i) short-term plastic response of soils has not been observed due to the geothermal use since effective stresses of the soil typically are within yield surfaces, i.e., within the thermo-elastic domain; ii) the additional stresses produced in the energy pile due to temperature change depend on the level of restraint of the pile.

Full scale demonstrations of precast energy piles have also been reported in [59]. The energy pile is subjected to cycles of heat injection, resembling cooling operation mode. The measurements show a thermo-elastic behaviour, with an increase of the axial load in the pile (relative to the existing mechanical) in the order of 12%. The maximum increase of temperature in the pile during the test does not reach 5 °C at any depth and the maximum displacement observed during 0.4 mm.

A similar behaviour has been reported in [60], where the thermal strains and stresses for intermittent tests of heat extraction are cyclic and return to initial values. The maximum thermal strain measured 0.09 mm downwards and the thermally induced average stress are around 0.9 MPa for 8 hours working cycles. The absolute decrease of temperature in the pile at the end of the test is 9 °C for 8-hour operation cycles. It was concluded that intermittent operation is advantageous in terms of generating lower pile thermal loading for long term operations.

Ref. [58,61–64] treat the analysis of energy pile group effects. Combined experimental and numerical studies of energy piles operating in groups [65] suggest that the assessment of thermally induced vertical strains needs to be assessed by considering group effects.

Different numerical methods have been used to explore the thermo-mechanical phenomena of energy piles. Ref. [56,66–69] encompass good examples of finite element models validated with experimental data. The load transfer method [44,70], modified to account for thermal loads has been used by [41,44,71–73]. This method allows reliable analysis of mechanical and monotonic thermal changes in a practical way and it is implemented in computational tools such as ThermoPile [74] (verified with energy pile data) and Oasys Pile [75]. Ref. [73,76–78] have adapted the load transfer model to account for degradation of the pile-soil interface under cyclic thermal loads.

Regarding case study operational demonstration, [79] analyses two energy piles that have been coupled to a conventional GSHP system. Measurements over a period of 658 days show fluid temperatures ranging from 7 to 35 °C. It concludes that the values of thermal axial displacement and the thermo-mechanical axial stresses are within reasonable limits and are not expected to cause any structural damage to the building. Ref. [20] states that appropriate operating conditions of energy pile installations, where the temperatures range from 5 to 20 °C over 3 years, hardly affect the shaft resistance of the pile.

2.3.1. THERMO-MECHANICAL DESIGN OF ENERGY PILE FOUNDATIONS

To ensure that the geotechnical performance of the pile is not negatively affected, conservative safety procedures are applied, which potentially reduce their cost-effectiveness. The fluid temperature in the ground loop is not allowed to go below 0 - 2 °C, to avoid freezing of the pile interface and the pore water in the concrete [17,38,57,80–82].

To ease the implementation of this technology, the need of a design method incorporated within the Eurocode agenda has been suggested [72,83]. It should consider the effects of the temperature changes resulted from the geothermal use in the foundation design with regards to geotechnical and structural requirements. In this sense, it needs to be decided the way these thermal actions are considered in the load combination processes and whether their consideration is relevant just for SLS or it also needs to be addressed in ULS [83].

The analysed research suggests that the thermal loads and displacements resulted from the geothermal use of the energy piles are not likely to lead to geotechnical failure. Ref. [41] demonstrated that under monotonic thermal loading the null point will always move towards the pile end in order to maintain the equilibrium, even if the ultimate bearing force (friction and base) is mobilised, as it happened at the Lambeth College pile [42]. This happens because the null point will prevent excessive settlement/heave since at least this point remains stable under temperature variations, ensuring equilibrium concerning a collapse mechanism. In terms of induced thermal strains, the same authors [41] demonstrated that over-sizing energy piles, by projecting a longer length, can have a negative impact. If a pile is over dimensioned structurally, the head heave or settlement will increase with temperature because there is a considerable amount of bearing force that the pile could still mobilise after mechanical loading. This has been observed in the EPFL test pile [41]. Therefore, enlengthening for geothermal reasons could go against safety.

Based on these findings, the EPFL research team has continued developing a method to consider the thermal loads within the Eurocode framework. The latest work is still under review [84], but the author of this thesis has recently attended an intensive

course in EPFL [85], where the method was presented. Here, the thermally induced loads are treated as deformation related problems. For these verifications, numerical models based on the load transfer method [41,44,71–73] (e.g., Thermo-Pile software [44]), can be used. Stresses caused by thermal loads may be generated in the reinforced concrete section. Hence, sufficient compressive and tensile strengths need to be ensured to verify structural ULS as well. Extensive reviews about these topics are available in [77,83,86,87].

Energy piles are structural elements and they need to be treated as such. Therefore, the energy pile design needs to integrate geotechnical, structural and heat transfer considerations [69].

2.4. THERMAL ASPECTS OF PILE HEAT EXCHANGERS

The temperature disturbance in the pile-soil system depends as well on the thermal properties of the concrete and the surrounding soil, the geometry of the pile and the foundation pile arrangement. Hence, an assessment of the induced temperature changes with respect to the initial undisturbed temperature needs to be carried out to estimate the induced thermal stresses and strains expected in an energy pile foundation. This section overviews the existing options for thermal analysis of energy pile foundations.

The thermal dimensioning of energy pile foundations (i.e., the amount of energy piles required to cover a given building thermal need) is typically addressed by methods developed for borehole heat exchangers which are implemented in commercial software, e.g.: GLHEPro [88], EED [89], LoopLink PRO [90], GLD [91] or the ASHRAE method [92]. However, standard methods for BHEs are not always well suited for analysing the thermal dynamics of energy piles and foundation arrangements.

Firstly, piles are shorter and wider than boreholes. Energy pile aspect ratios (length to diameter ratio), typically fall below 50, while corresponding ratios for BHEs range 200-1500. For instance, the volume per length ratio of a standard borehole is 0.02 m^3/m while a 30x30 cm^2 energy pile has 4.5 times higher ratio, 0.09m^3/m. Secondly, while BHEs typically are arranged in regular grids, piles are placed irregularly in clusters (from singles to fours) which is determined by the structural requirements of the building. The small pile spacing causes significant thermal interaction between neighbouring piles. Thirdly, fluid temperatures in energy piles must be kept above 2 °C to ensure structural integrity, avoiding freezing of concrete and surrounding soil [17,38]. And finally, energy piles (despite the steel piles) are made of concrete instead of grouting, which confers them a different thermal performance.

Due to the variety in types of energy piles, several experimental and numerical studies attempt to develop novel approaches that characterize the heat transfer in and around

such structures. Some of the methodologies used to characterize the temperature field involve: i) finite element modelling (FEM) [32,93,94]; ii) line and cylindrical source finite solutions suggested in [95] and iii) empirical equations for pile and concrete thermal responses which account for the axial effects ignored by the infinite source approaches [94,96,97].

Infinite line and cylinder solutions are not appropriate for pile heat exchangers and they should be avoided for the long-term analysis of energy piles [53,98]. The importance of considering the thermal inertia of the pile concrete, primarily in the short term, has also been demonstrated in [94]. Ignoring this fact would lead to a reduction in the assessed energy capacity of the system. This is relevant for energy piles because their operational temperature range is tighter than that of BHEs. Further discussions regarding heat flow models are provided in [53,99].

The long-term performance of energy pile foundations must consider the thermal interaction between piles. A common approach used for BHE analysis is the application of the so-called g-functions for multiple ground heat exchangers, first introduced by [100]. The g-function is a type curve of dimensionless time and ground heat exchanger wall temperatures assuming a constant, applied power. Thermal interaction is calculated by spatial superposition of single BHE temperatures, based on a finite difference model.

Multiple ground heat exchanger g-functions can also be calculated by spatial superposition of analytical solutions for single ground heat exchangers that permit calculation of the radial temperature distribution [101–106]. A different approach is the ASHRAE method, where the temperature penalty concept is defined to account for thermal interactions between individual heat exchangers [107–110]. Multiple heat exchanger g-functions have been calculated by means of numerical methods as well [111,112].

The duct storage model [113], implemented in the PILESIM software [114] for analysing pile heat exchangers, has been validated with field data in [115], however, this method does not allow the analysis of irregular pile configurations. To overcome this drawback, [96] proposed the use of semi-empirical models based on numerical analyses, following a similar method to that proposed by [116,117] for BHE fields. For further details on these topics, see [96,100,106,110].

Optimisation strategies for sizing ground heat exchanger fields have also been reported in literature. Ref. [118] minimises the soil temperature change over time by adjusting the individual heat extraction rate in each borehole; Ref. [119] adjusts the position of each borehole individually. Ref. [120] adjusts irregular configurations to regular grids, so does the latest version of EED [89]. Ref. [121] uses multi objective optimisation to find a balance between the borehole field configuration and economic

parameters. In principle, the thermal design of energy pile foundations should follow a similar approach.

The dimensioning of GSHP installations typically relies on thermal response testing of one or more ground heat exchangers. Thermal response testing (TRT) is a widely used field method of BHEs for estimation of soil thermal conductivity, borehole thermal resistance and undisturbed ground temperature [122]. Occasionally, the TRT method has been adopted for analysing the thermal behaviour of energy piles [123]. It has been demonstrated that using interpretations models that neglect three-dimensional effects and the thermal dynamics of the pile, yield biased values of soil thermal conductivity [32,34,97,124–127]. As such, there is a need for developing the theoretical framework for analysing such data for precast pile heat exchangers.

Typically, the dominant heat transfer mechanism occurring in shallow geothermal energy applications is conduction, yet flowing groundwater can provide significant additional heat transfer by advection [128]. The impact of the groundwater flow in the system performance differs depending on the thermal load needs of the building. For instance, a heating-dominated system exposed to high groundwater flow velocities would experience a more effective heat transfer of energy to the ground because the ground will be recharged quicker. According to [129], heat extraction/injection capacity can increase up to four times and a sufficient groundwater flow of approximately 35 m/year conducts to a natural thermal regeneration of the ground [76]. Correspondingly, in a cooling-dominated system the injected heat would be taken away, keeping a high performance of the system. Conversely, the groundwater flow would adversely affect a balanced system that relies on seasonal storage, since it would remove the stored heat [45]. According to [80], the seasonal heat storage becomes unfeasible when the Darcy's velocity exceeds 0.5 – 1 m/day.

Lack of actual published operational data limits the optimisation of the systems under working conditions. Several studies have been published in the field of BHEs [130–132]. Energy management applied to thermo-active geostructures potentially improves cost-effectiveness of the system [133]. More case studies will contribute to this knowledge.

2.5. PRELIMINARY WORK, DISCUSSION & MAIN RESEARCH FOCUS

Once the status of the energy pile technology is analysed, an assessment of the research gaps and the needs of the company is carried out.

Precast energy piles did not have a considerable attention on the published research. The main full-scale setup has been reported in [28,59], where thermo-mechanical aspects are treated. Operational installations utilising similar precast energy piles are

found in Germany [134,135] and in the Netherlands [136] but very limited information has transcended.

A pilot project of precast energy pile foundation (2011) is used to point out challenges and limitations when facing the planning and design of such projects. Due to the lack of flexible tools to dimension energy pile ground loops, the project partners had to rely on conservative rules of thumb.

A preliminary study based on this pilot case study and written by the author of this thesis before the PhD project started [29], highlighted the need to develop appropriate thermal models for quadratic cross section energy pile foundations, suggesting that the installation could be over dimensioned.

As a first step of this PhD project, and to understand the thermal performance of this type of energy piles, an assessment of the operational parameters of the case study was carried out. This work is presented in Conference Paper I (introduced in Chapter 6) and it determines, among other things, the ground thermal load.

As a second step, this thermal load is used to assess the thermo-mechanical behaviour of the case study energy piles. A preliminary numerical study, appended in this thesis as Conference Paper, is carried out. Transient simulations over a year show that a typical operation of the energy pile foundation does not generate significant structural and geotechnical implications on a single thermal pile in terms of induced thermal stresses and strains. However, it shows the importance of calculating and controlling the thermal loads to assess the temperature changes generated in the pile. Extreme thermal loads could lead to compressive combined thermal and mechanical loads undesirable in design.

The literature review has revealed a large amount of information and research groups working on the thermo-mechanical aspects of energy piles. The induced thermal stresses and strains depend on the nature of the of the thermal loads, i.e., depend on the ground thermal load resulted from the building heating and/or cooling needs, and the development of the temperature field depends on the thermal properties and the foundation arrangement. Hence, a prior assessment of the induced temperature changes with respect to the initial undisturbed temperature needs to be carried out in design.

Consequently, there is a fundamental need, at scientific and commercial levels, to understand the thermal behaviour of the energy pile foundations. The partners of this PhD project have identified the need to develop a tool that yields the temperature changes that the energy pile foundation would be subject to in the long-term given a building thermal profile and, therefore, our most valuable contribution to the field will focus on these aspects.

CHAPTER 3. METHODOLOGY

3.1. SCOPE AND MOTIVATION

This chapter provides an overview of the main methods used along this PhD thesis to help the reader in the better understanding of the coming chapters. It is structured to address the analysis of thermal aspects from the single energy pile to groups of piles. In each sub-section, the applied experimental and analysis methods are shortly described. Table 3-1 provides an overview of the experimental data, from laboratory work to case study level, and the addressed objective:

Table 3-1: Overview of experimental methods and addressed aims.

Experimental methods	Objective
Laboratory measurements of thermal properties	Analysis of single energy pile
Field thermal response test	
Field thermal response test complemented with soil temperatures	Analysis of multiple energy piles
Case study operational data	

An in deep development of each method is available in the papers and appendices accompanying this thesis. Henceforth, "energy pile" and "pile heat exchanger" terms involve a quadratic cross section pile heat exchanger whose length is limited between 7 to 18 m, such as the described in Figure 3-1.
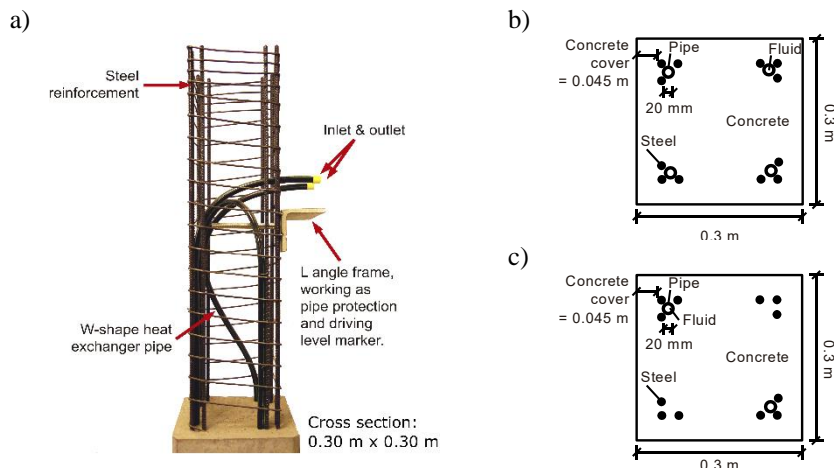
Figure 3-1: a) Demonstration model of the precast energy pile with W-shaped heat exchanger pipes fitted to the reinforcement bars; b and c) horizontal cross sections of the W-shape and single-U energy piles, respectively. After [35].

3.2. THERMAL ASPECTS OF SINGLE PILES

The experimental and analysis methods are described, after definitions of the main terms, are introduced.

3.2.1. DEFINITIONS

The average fluid temperature T_f [°C] circulating through the ground-loop is one of the main parameters required to choose the most adequate heat pump for a GSHP installation. The average fluid temperature T_f is defined as:

$$T_f = T_0 + \frac{q}{2\pi\lambda_s} G_g + qR_c G_c + qR_{pipe} \tag{1}$$

where T_0 [°C] is the undisturbed soil temperature, q [W/m] is the heat transfer rate per metre length of pile heat exchanger, λ_s [W/m/K] is the thermal conductivity of the soil, G_g is the g-function describing the ground temperature response, R_c [K·m/W] is the steady state concrete thermal resistance, G_c is the concrete g-function describing the transient concrete response and R_{pipe} [K·m/W] is the thermal resistance of the pipes. The temperatures and thermal resistance arrangement are shown in Figure 3-2.

a)
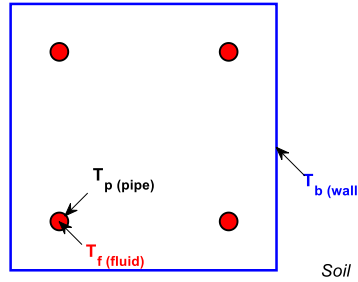
b)
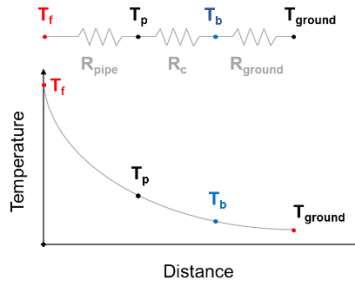
Figure 3-2: a) Temperature definitions in the energy pile cross section;
b) fundamentals of thermal resistances in the energy pile cross section.

G-functions are dimensionless response factors that describe the change in temperature in the ground around a heat exchanger with time as a result of an applied thermal load q [100]. Usually, both temperature change and time are normalised. In this study, the normalised temperature changes Φ and time Fo are defined as:

$$\Phi = \frac{2\pi\lambda_s\Delta T}{q} \tag{2}$$

$$Fo = \frac{\alpha_s t}{r_b^2} \tag{3}$$

where ΔT [K] is the temperature change between the undisturbed soil temperature T_0 [°C] and the average pile wall temperature T_b [°C], α_s [m²/s] is the thermal diffusivity, i.e., the ratio between the thermal conductivity λ_s [W/m/K] and the volumetric heat capacity of the soil ρc_{ps} [J/m³/K], t [s] is the time and r_b [m] is the pile equivalent radius. The pile radius is the radius that provides an equivalent circumference to the square perimeter.

For a single pile, the pile wall temperature depends on time and its aspect ratio AR $(L/2r_b)$, and it can be determined as:

$$T_b = T_0 + \frac{q}{2\pi\lambda_s} \cdot G(Fo, \frac{L}{2r_b}) \tag{4}$$

G-functions can be obtained by analytical, numerical and empirical methods. Figure 3-3 shows different types:
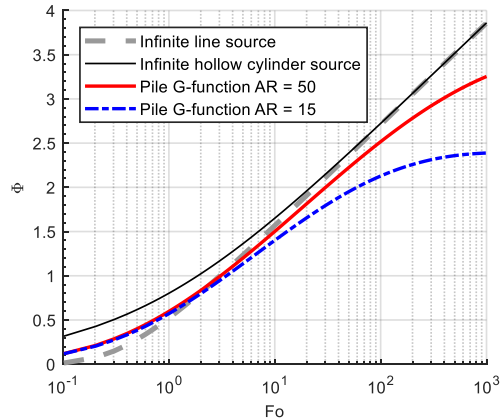
Figure 3-3: The infinite line [137] *and infinite hollow cylinder* [138] *source solutions together with semi-empirical pile G-functions reported in* [94].

The concrete G-function G_c, as defined by [94,139], describes the transient thermal resistance of the pile heat exchangers. It depends on the shape of the pile cross section, the position of the pipes and the thermal conductivity of the concrete λ_c. That is, it defines the thermal resistance of the concrete part. To incorporate the transient response of the pile concrete into the overall temperature response function (Equation 1), the proportion of the steady state thermal resistance that has been achieved at a given value of time Fo needs to be determined as:

$$R_c = \frac{T_p - T_b}{q} \tag{5}$$

where T_p [°C] is the average temperature on the outer wall of the pipe

Finally, the pipe thermal resistance R_{pipe} [K·m/W] is defined in Equation 6 as the sum of the pipe convective (first term on right hand side) and conductive (second term on right hand side) resistances:

$$R_{pipe} = \frac{1}{2n\pi r_i h_i} + \frac{\ln(r_o/r_i)}{2n\pi\lambda_{pipe}} \tag{6}$$

where n is the number of pipes in the pile heat exchanger cross section, r_i [m] is the inner radius of the pipe, r_o [m] is the outer radius of the pipe, h_i [W/m^2/K] is the heat transfer coefficient and λ_{pipe} [W/m/K] is the thermal conductivity of the pipe material. h_i can be calculated using the Gnielinski correlation as described in [140,141].

3.2.2. EXPERIMENTAL DATA

The experimental work related to the thermal aspects of the energy piles has been carried out in two test sites in Denmark (Figure 3-4). The work mainly consists of thermal response testing (TRT) of energy piles and laboratory measurements of the thermal properties of the soil at both test sites and of the concrete used in the piles.

The TRT is a field method of ground heat exchangers for estimation of soil thermal conductivity λ_s, ground heat exchanger thermal resistance (hereon concrete thermal resistance R_c) and undisturbed ground temperature T_0 [122].

During the TRT, the heat carrier fluid (water) is circulated in the ground heat exchanger while being continuously heated at a specified rate. Heat dissipates to the ground heat exchanger and subsequently to the ground. The test records fluid inlet- and outlet temperatures and the fluid flowrate and logs them in 10-min intervals for at least 48h. Figure 3-5 shows the test setup and an example for the measurements.
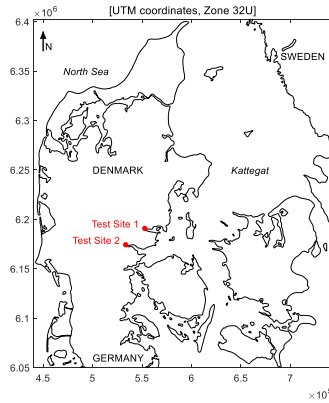
Figure 3-4: Location of test sites, in Denmark.

Several tests are carried out in energy piles with different depths and pipe configurations (single-U and W-shape). During one of the tests, soil temperatures at a distance from the energy pile were also recorded at given depths (Figure 3-5). Detailed information regarding the fieldwork is provided in [142], Appendix III.

a)   b)
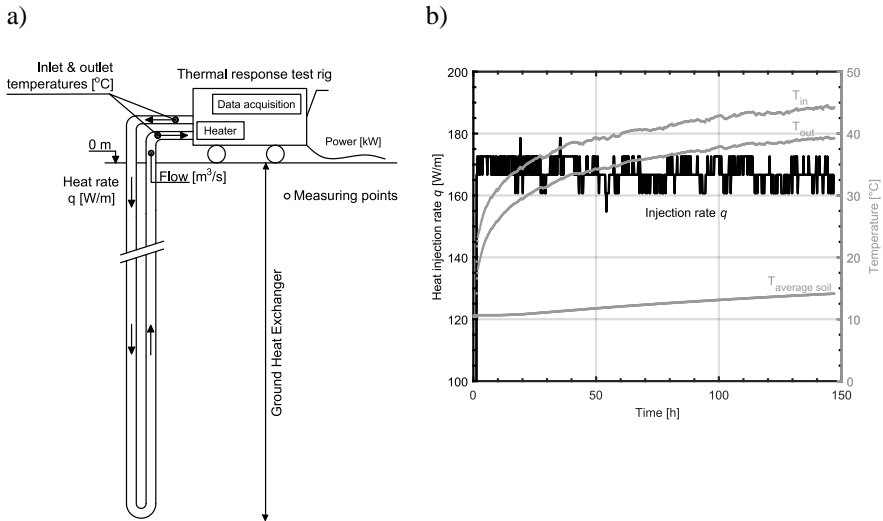
Figure 3-5: a) Thermal response test setup, after [143]*; b) TRT field data of pile heat exchanger and weighted soil temperatures at 0.9 m from pile, after* [144]*.*

Independent measurements of the thermal properties of the soil and the concrete have been carried out by means of the Hot Disk apparatus [145]. The Hot Disk equipment (Figure 3-6) relies on the transient plane source method [146], which yields estimations on the thermal conductivity and volumetric heat capacity. An 18-m bore is drilled in each test site, where soil samples are collected every 0.5 m. Water content

and bulk and dry density measurements are also given for each sample. Details on the equipment, sample treatment and measurement procedures are provided in [147], Appendix IV.
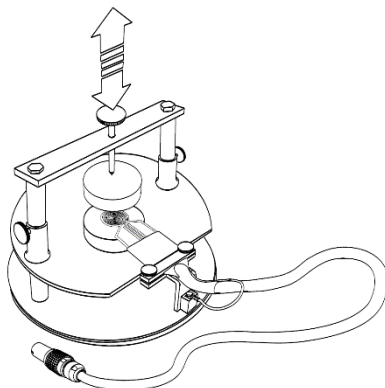
Figure 3-6: Hot Disk sensor in between halved sample and room temperature sample holder. Courtesy of Hot Disk ® [145].

3.2.3. ANALYSIS METHODS

In practice, the TRT data is analysed with analytical models in order to estimate the soil thermal conductivity and the concrete thermal resistance. In this study, the TRTs of energy piles are interpreted with analytical, semi-empirical and numerical models by means of non-linear regression. First, the soil thermal conductivity is estimated by inverse 3D finite element modelling (Figure 3-7) of the TRT data and then compared to corresponding, independent laboratory measurements.

A fully 3D based TRT interpretation is not feasible for routine practical applications due to the computational cost of solving the inverse problem. Consequently, the study also explores the applicability of simpler analytical and semi-empirical models for interpretation of the TRT data. The tested models are summarised in Table 3-2.

The parameter estimation is performed with PEST Model-Independent Parameter Estimation software [148]. PEST employs the Gauss-Marquardt-Levenberg algorithm for minimising the weighted, squared difference between computed and observed fluid temperatures. PEST calculates linear confidence intervals for estimated parameter following the non-linear regression procedure. This algorithm is applied to all the models.
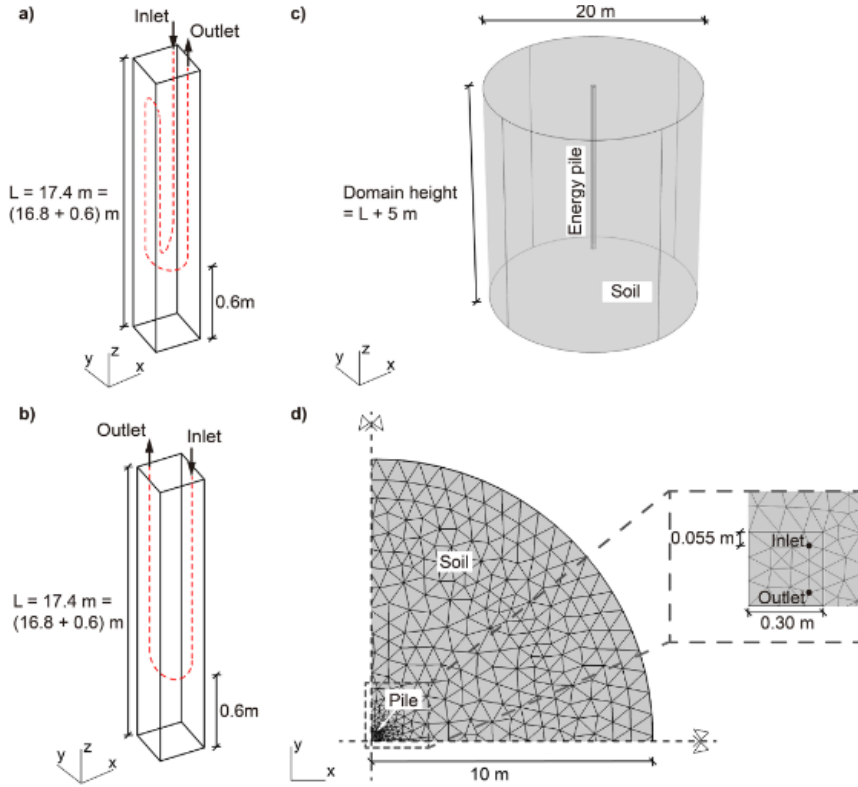
Figure 3-7: Description of the 3D finite element model: a) Schematic of the W-shape pile heat exchanger; b) Schematic of the Single-U pile heat exchanger; c) Simulated meshed domains; d) Top view of a quarter of domain, after [35].

Table 3-2: Summary of models selected to evaluate the pile heat exchanger TRT data, after [35].

	Model description
Analytical approaches	Infinite line source [137].
	Infinite cylinder source [138].
	Infinite solid cylinder source [95]
	Finite solid cylinder source [95].
Semi-empirical approach	G-function for pile heat exchangers [94]. The finite length of the pile is considered.
Numerical approach	Equivalent pipe model [149]. It neglects the finite length of the pile.
	2D horizontal cross section finite element model.

3.3. THERMAL ASPECTS OF MULTIPLE PILES

In the long-term performance, energy pile foundations must consider the thermal interaction between piles. Building on the work published in [96], where the potential of semi-empirical models to account for irregular pile positions was highlighted, this study aims to investigate their applicability and accuracy in the analysis of precast energy piles. Hence, semi-empirical g-functions for calculating average fluid temperatures in energy pile foundation based GSHP systems are developed. The simulated average temperatures are compared to corresponding full 3D finite element models of groups of quadratic precast energy piles.

To analyse interacting energy piles is important to understand how the temperature field evolves in the ground. Firstly, single pile 3D finite element modelled fluid and soil temperatures are compared to corresponding field observations which include thermal response test data and simultaneous temperature measurements at a distance (shown in Figure 3-5). The thermal interaction between the energy pile and the surrounding soil is modelled by conduction and advection in the heat exchanger pipes, in a similar way to the models developed for the single pile analysis described before (Figure 3-7). The validated 3D model is then extended to include multiple piles prearranged in different patterns: regular groups with constant pile spacing and irregular arrangements.

However, the analysis of hundreds of energy piles becomes impracticable during feasibility and sizing processes. Therefore, we extract temperature fields from single pile 3D models and we apply temporal and spatial superposition to obtain the temperature field for an ensemble of piles assuming a dynamic thermal load. The generation process is described in the following.

The multiple pile g-functions provide the change in the average pile wall temperature over time of all the piles comprising the foundation. I.e., the g-function provides the pile wall temperature for a specific foundation configuration due to a constant heat input rate [150]:

$$T_b = T_0 - \frac{q}{2\pi\lambda_s} \cdot g(Fo, \frac{L}{2r_b}, \frac{S}{2r_b}) \tag{7}$$

where T_b [°C] is the pile wall temperature common to all piles, T_0 [°C] is the undisturbed ground temperature, q [W/m] is the average heat extraction rate per pile length, λ_s [W/m/K] is the ground thermal conductivity and g [-] is the multiple pile g-function. For the case of pile heat exchanger foundations or groups, the multiple g-functions depend on three non-dimensional parameters: the dimensionless time Fo, the AR ($L/2r_b$), being L [m] the active length of the pile heat exchanger, and the foundation aspect ratio $S/2r_b$, being S the centre to centre pile spacing, as defined in [96].

As mentioned, the multiple pile heat exchanger g-functions herein analysed are based on the temperature fields extracted from single 3D FEM. The simulations are used to obtain, in addition to the pile wall temperature, soil temperatures at required radial distances that would resemble pile spacing. For easier implementation of the temperature response functions curve fitting has been carried out, in a similar way to the process followed by [94,151].

For various piles, the multiple pile g-function can be calculated by applying temporal and spatial superposition of the single pile G-function and radial temperatures. This principle relies on the heat conduction equation and boundary conditions on being linear [150].

In the spatial superposition the temperature distributions around every ground heat exchanger are added in order to calculate the overall temperature variation at the pile walls [105]:

$$\Delta T_b(t) = \frac{1}{n_p} \sum_{i=1}^{n_p} \sum_{j=1}^{n_p} \Delta \overline{T_b}(d_{ij}, t) \tag{8}$$

$$d_{ij} = \begin{cases} r_b, & i = j \\ \sqrt{(x_i - x_j)^2 + (y_i - y_j)^2}, & i \neq j \end{cases} \tag{9}$$

where ΔT_b [K] is the average temperature variation at the pile heat exchanger wall, (x_i, y_i) [m] are the coordinates of the ith pile heat exchanger, n_p is the number of pile heat exchangers in the foundation and d_{ij} [m] is the pile distance.

Time variations can be applied by deconvolution of the time varying heat transfer rate [150]. The temperature at discrete time step in the pile heat exchanger foundation is computed as:

$$\Delta T_n = \sum_{i=1}^{i=n} \frac{q_i}{2\pi\lambda_s} \left(G\left(Fo_n - Fo_{(i-1)}\right) - G\left(Fo_n - Fo_i\right) \right) \tag{10}$$

where n is the point in normalised time in which the superposition is evaluated.

In an energy foundation, the pile heat exchangers can be connected in series and/or in parallel. This study analyses pile heat exchangers connected in parallel, assuming uniform and equal heat extraction rates for all the energy piles. Because of this boundary condition, the average temperatures along the length of all the piles are unequal. Hence, the average of the mean pile wall temperatures is used in the

evaluation of the g-function. The type curves and further details are provided in [152], Appendix V.

3.4. OPTIMISATION OF THE NUMBER OF ENERGY PILES

Piles are usually placed irregularly in clusters, from singles to fours, occasionally spaced less than 1 m apart. The small pile spacing causes significant thermal interaction between neighbouring piles. This increases the required number of piles and entails higher costs during construction and operation. Hence, it appears reasonable to equip only a subset of the foundation piles as ground source heat exchangers as far as the foundation is able to cover the thermal requirements of the building [96]. This compromise leads to an optimisation problem in which the number of energy piles and which piles to pick as ground source heat exchangers are constrained by a need to maintain long term sustainable ground temperatures and to meet the thermal requirements of the building.

This study is developed in the Rosborg Gymnasium case school, in Denmark, founded on 269 piles, 219 of which are energy piles (Figure 3-8). The driven, quadratic cross section (30 cm by 30 cm), precast 15 m energy piles are equipped with W-shaped heat exchanger piping. The control and monitoring system of the building logs ground loop fluid temperatures and flow, heat pump and circulation pump electricity consumptions and energy generation by the heat pump, among other parameters. A comprehensive description of the operational conditions and performance coefficients of the case study is also carried out.
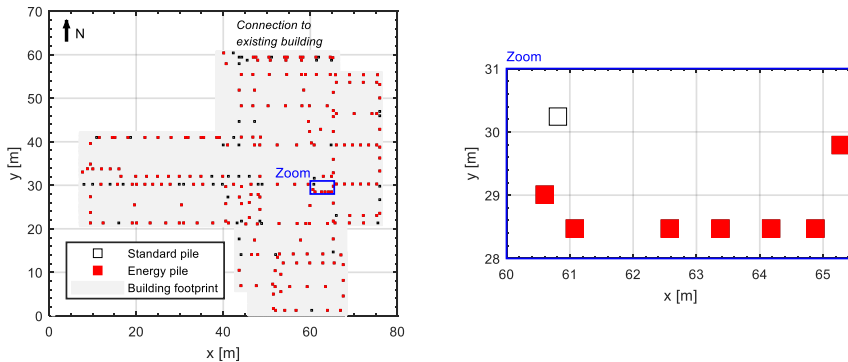
Figure 3-8: Top view of foundation pattern of the case study. a) Overview; b) Zoom to a high pile density area. The legend is common for both subplots. Reproduced after [153].

The data from the case study is used to validate the multiple energy pile semi-empirical model described in the previous section, i.e., the ground thermal load measured from the case study is applied to the model and the simulated average fluid temperatures in the ground loop are compared to corresponding observations.

The temperature model is then utilised in an optimisation algorithm that yields the minimum number of energy piles required by simultaneously maximising the energy pile spacing, to generate a homogeneous distribution of the energy piles below the building and reduce their interaction and taking into consideration the thermal load of the building.

The geometrical arrangement of foundation piles is determined solely by the structural requirements of the building. However, it is important that the spatial arrangement of the energy piles is as uniform as possible to avoid significant local changes in the soil temperature. Once an energy pile pattern is chosen from the predefined grid of foundation piles, corresponding fluid temperatures are estimated with the multiple pile g-functions. The energy pile pattern is then adjusted until the desired temperatures are achieved while fulfilling the thermal requirements of the building.

The ideal way to place ground heat exchangers in a field is by minimising the influence between them which corresponds to maximising the pile spacing. To provide the energy pile arrangement that maximises the pile spacing, given the structural constraints, a constrained optimisation scheme is proposed. The scheme accepts as input the coordinates of the foundation piles, the number of required energy piles and a minimum initial pile spacing. The MATLAB "*patternsearch*" subroutine [154] is utilised for determining the arrangement of the required energy piles, while maximising pile spacing.

The multiple pile g-function model is applied to the pile arrangement determined by the optimisation scheme to yield average fluid temperatures in the ground loop. Now, the optimum number of pile heat exchangers required to supply a given building need is determined by maximising a so-called desirability function. The desirability function approach [155], also described in [156,157], is used for optimisation of multiple response processes by assigning a desirability function $d_i(Y_i)$ value between 0 and 1 to each response $Y_i(x)$, where $d_i(Y_i) = 0$ and $d_i(Y_i) = 1$ represent unacceptable and ideal responses, respectively. The individual desirabilities are combined using the geometric mean, to give the overall desirability D (hereby the notation used in [157] is adopted):

$$D = (d_1(Y_1)d_2(Y_2)\dots d_k(Y_k))^{1/k} \tag{11}$$

where k is the number of responses. Clearly, if any response Y_i is completely undesirable, i.e., $d_i(Y_i) = 0$, then the overall desirability is zero.

Different desirability functions $d_i(Y_i)$ are defined, depending on whether a response Y_i is to be maximised, minimised or assigned a target value. Let define L_i, U_i and T_i as lower, upper and target values, respectively. According to this, the desired response Y_i needs to fall within $L_i \leq T_i \leq U_i$.

When a specific value needs to be assigned to a response (a.k.a. target is best), its desirability functions is defined as:

$$
d_i(Y_i) = \begin{cases} 0 & \text{if} \quad Y_i(x) < L_i \\ \left(\dfrac{Y_i(x) - L_i}{T_i - L_i}\right)^s & \text{if} \quad L_i \leq Y_i(x) \leq T_i \\ \left(\dfrac{Y_i(x) - U_i}{T_i - U_i}\right)^t & \text{if} \quad T_i \leq Y_i(x) \leq U_i \\ 0 & \text{if} \quad Y_i(x) > U_i \end{cases}
\tag{12}
$$

where s and t determine the importance to hit the target value. When $s = t = 1$, the desirability function increases linearly towards the target value T_i.

When a response needs to be maximised, its desirability function is defined as:

$$
d_i(Y_i) = \begin{cases} 0 & \text{if} \quad Y_i(x) < L_i \\ \left(\dfrac{Y_i(x) - L_i}{T_i - L_i}\right)^s & \text{if} \quad L_i \leq Y_i(x) \leq T_i \\ 1 & \text{if} \quad Y_i(x) > T_i \end{cases}
\tag{13}
$$

where T_i is understood as a large enough value for the response.

Lastly, when a response needs to be minimised, its desirability function is defined as:

$$
d_i(Y_i) = \begin{cases} 1 & \text{if} \quad Y_i(x) < T_i \\ \left(\dfrac{Y_i(x) - U_i}{T_i - U_i}\right)^s & \text{if} \quad T_i \leq Y_i(x) \leq U_i \\ 0 & \text{if} \quad Y_i(x) > U_i \end{cases}
\tag{14}
$$

where T_i is understood as a small enough value for the response.

The desirability approach penalises the values that differ from the target values or admissible limits and allows the assignment of weights to each response into the weighted geometric mean (Equation 11).

In this study, the desirability function is defined by adjusting three responses simultaneously: i) the number of energy piles, which needs to be minimised (Equation 14); ii) the return temperature to the ground loop, which should always be around 2 °C ("target is best", Equation 12); iii) the long-term average fluid temperature, which must be as close as possible to the initial soil temperature ("target is best").

The desirability function approach and its flexibility allow more conditions and features to be considered in future improvements, such as costs and the use of complementary energy sources.

3.5. CONCLUSION

The main methods applied in this PhD thesis have been shown and now Table 3-3 sums up the main content of the journal papers comprising the body of this thesis.

Paper A aims to find appropriate models to interpret TRT data of energy piles. From here, the potential of semi-empirical models to account for thermal interactions between piles is noticed, due to its simple implementation. Hence, Paper B develops semi-empirical thermal models for multiple piles by utilising 3D finite element model heat transport simulations with temporal and spatial superposition techniques. These models are compared to full 3D finite element models of different pile arrangements to check their accuracy and limitations.

Finally, Paper C applies the multiple pile method for estimating operational average fluid temperatures in an actual energy pile foundation in Denmark. The thermal model is then utilised in an optimisation algorithm that yields the minimum number of energy piles required by simultaneously maximising the energy pile spacing and taking into consideration the thermal load of the building. In addition, to provide a wider knowledge about the case study, a conference paper where the operational data from 2015 is treated is introduced before Paper C.

Table 3-3: Link between the papers comprising the main body of the thesis.

Sequence	TESTING ⟶	METHOD DEVELOPMENT ⟶	PROVE OF CONCEPT
Main goal	Benchmark different options to model thermal behaviour of single energy piles.	Analyse thermal influences between piles and develop a design method.	Apply the method (Paper B) to a case study and develop an optimisation tool.
Time scale	[0 – 150 hours]	[1 – 25 years]	[1 – 25 years]
Modelled domain	Single pile and surrounded soil.	Regular and irregular groups, up to 16 piles.	Actual foundations (hundreds of piles).
Methodology	- Experimental: field TRT and lab measurements. - Numerical: analytical, semi-empirical and 2D - 3D finite element models.	- Experimental: TRT and soil temperatures. - Numerical: 3D finite element and semi-empirical models.	- Experimental: operational temperatures from case study. - Numerical: semi-empirical models and optimisation algorithm.
Paper name	Paper A	Paper B	Paper C

In the following, the papers are directly introduced in the thesis, either in the published or in the submitted versions. The latter follow the citation and referencing requirements of the specific journals.

For further information, please refer to Appendixes III, IV and VI.

CHAPTER 4. THERMAL ANALYSIS OF SINGLE PILE HEAT EXCHANGERS

4.1. SCOPE AND MOTIVATION

In the previous literature review we highlighted the importance of considering the geometrical characteristics of the energy pile to simulate the temperature field in and around such structures. In this sense, it is equally relevant to use adequate thermal properties of the materials.

Dimensioning of vertical GSHP systems, such as boreholes and energy piles, requires the determination of the soil thermal conductivity and heat exchanger thermal resistance. These parameters are usually determined by in situ TRT.

In Paper A we use the TRT to investigate the internal response of the energy piles and the thermal response of the ground surrounding it. We interpret TRT data with different heat flow models by inverse modelling. The estimates of soil thermal conductivity and pile thermal resistance are compared to independent measurements. Hence, we assess the suitability of different models to thermally simulate energy piles.

4.1.1. PAPER A

The following article, denoted Paper A, has been published in Energy.

Alberdi-Pagola, M., Poulsen, S.E., Loveridge, F., Madsen, S. & Jensen, L.J., 2018. "Comparing heat flow models for interpretation of precast quadratic pile heat exchanger thermal response tests", *Energy*, 145, pp. 721-733.

https://doi.org/10.1016/j.energy.2017.12.104.

Reprinted by permission from Elsevier.

Comparing heat flow models for interpretation of precast quadratic pile heat exchanger thermal response tests

Maria Alberdi-Pagola [a], [*], Søren Erbs Poulsen [b], Fleur Loveridge [c], Søren Madsen [a], Rasmus Lund Jensen [a]

[a] Department of Civil Engineering, Aalborg University, Denmark
[b] VIA Building, Energy & Environment, VIA University College, Denmark
[c] School of Civil Engineering, University of Leeds, United Kingdom

ARTICLE INFO

ABSTRACT

This paper investigates the applicability of currently available analytical, empirical and numerical heat flow models for interpreting thermal response tests (TRT) of quadratic cross section precast pile heat exchangers. A 3D finite element model (FEM) is utilised for interpreting five TRTs by inverse modelling. The calibrated estimates of soil and concrete thermal conductivity are consistent with independent laboratory measurements. Due to the computational cost of inverting the 3D model, simpler models are utilised in additional calibrations. Interpretations based on semi-empirical pile G-functions yield soil thermal conductivity estimates statistically similar to those obtained from the 3D FEM inverse modelling, given minimum testing times of 60 h. Reliable estimates of pile thermal resistance can only be obtained from type curves computed with 3D FEM models. This study highlights the potential of applying TRTs for sizing quadratic, precast pile heat exchanger foundations.

© 2017 Elsevier Ltd. All rights reserved.

1. Introduction

Ground source heat pump (GSHP) systems are sustainable and cost effective space conditioning systems based on shallow geothermal energy [1]. Utilisation of geothermal energy supports the reduction of the greenhouse gas emissions proposed by the Paris Agreement within the United Nations Framework Convention on Climate Change [2].

Sizing guidelines for closed loop horizontal and vertical ground heat exchangers have been developed over the last decades (Fig. 1, a and b) [3,4]. Several factors must be taken into consideration when dimensioning GSHP installations including the dynamics of the cooling and heating demands of the building, the thermal properties of the soil and the backfilling material, the geometry and spacing of the ground heat exchangers, the thermal influence of the ground surface and the presence of groundwater flow, if any (Fig. 1).

Foundation pile heat exchangers were developed during the 1980's as an alternative to traditional borehole heat exchangers [5]

(Fig. 1, c). Pile heat exchangers, typically referred to as energy piles, consist of traditional foundation piles with embedded heat exchanger pipes. Energy piles differ from conventional borehole heat exchangers by their length and cross section, being both shorter and wider, and materials. Energy pile aspect ratios (length/ diameter) are typically less than 50, while for traditional borehole heat exchangers aspect ratios range 200–1500.

Pile heat exchangers vary in length from 7 to 50 m with a cross section of 0.3–1.5 m. The methods of construction include: cast-in-place concrete piles, 0.3–1.5 m in diameter [6–9]; precast concrete piles with side lengths spanning 0.27–0.6 m [10–13]; hollow concrete precast piles [14] and driven steel piles [15,16].

1.1. Thermal response testing

Dimensioning of vertical ground heat exchangers such as boreholes and energy piles requires the determination of the soil thermal conductivity, λ_s [W/m/K], and heat exchanger thermal resistance, R_b [K m/W]. The thermal conductivity λ_s is a measure of the ease with which soil conducts heat, while the heat exchanger thermal resistance R_b is the integrated thermal resistance between the GSHP carrier fluid and the ground; it serves as an efficiency measure for the heat exchanger. For borehole heat exchangers

* Corresponding author. Department of Civil Engineering, Thomas Manns Vej 23, 9220 Aalborg Ø, Denmark.
E-mail address: mapa@civil.aau.dk (M. Alberdi-Pagola).
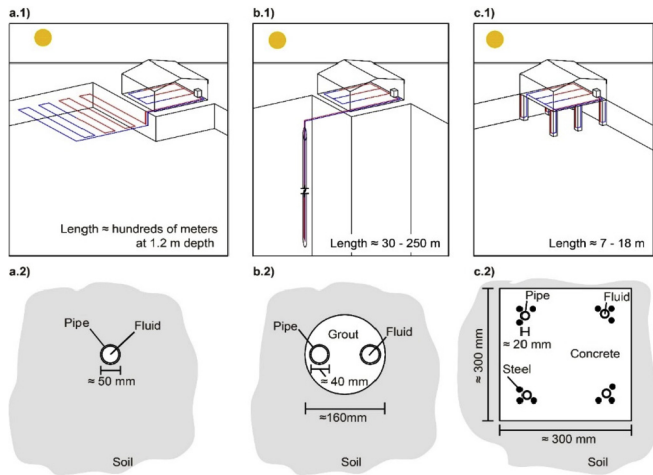
Fig. 1. Closed loop ground source heat pump GSHP systems: a.1) GSHP system based on horizontal heat exchangers; a.2) horizontal heat exchanger cross section; b.1) GSHP system based on vertical borehole heat exchangers; b.2) borehole heat exchanger cross section; c.1) GSHP systems based on pile heat exchangers and c.2) precast pile heat exchanger cross section.

these parameters are usually determined in situ using thermal response testing (TRT) of one or more ground heat exchangers [17–19]. During the TRT, the heat carrier fluid (water) is circulated in the ground heat exchanger while being continuously heated at a specified rate. Heat dissipates to the ground heat exchanger and subsequently to the ground. The test records fluid inlet- and outlet temperatures, the fluid flow rate and energy consumption and logs them in 10-min intervals for at least 48 h (Fig. 2).

The TRT data is evaluated by regression methods applied to analytical, semi-empirical or numerical models designed to link the heat applied to the ground heat exchanger and the resulting temperature change. Due to its simplicity, the most widely used method of interpretation is based on the infinite line source (ILS) model [20]. However, there is a wide range of heat flow models that describe heat transport in the heat exchanger and the soil, including the infinite cylinder source model [21] and the finite line source model [22,23]. These models assume thermal steady-state conditions in the borehole heat exchanger. More complex models,

such as the composite medium line source [24] and the infinite and finite solid cylinder source models [25] account for the heat capacity of the heat exchanger. For further details see Refs. [26,19,27].

The uncertainty on line-source based TRT estimates of soil thermal conductivity is in the order of ±10% [18]. Ref. [28] demonstrated that propagation of measurement errors for TRTs is expected to be approximately 5% for the soil thermal conductivity λ_s and 10–15% for the borehole resistance R_b. Ref. [29] showed that the line-source analysis provides reliable results under ideal simulated situations however the added effects of model simplification errors are up to 10%.

1.2. Pile thermal response testing

Occasionally, the TRT method has been adopted for analysing the thermal behaviour of energy piles [30]. Table 1 provides a summary of previous research in which the TRT has been deployed for estimating the soil thermal conductivity λ_s and the pile thermal resistance (called R_p herein). Refs. [30–33] suggest that the TRT is applicable to piles with a diameter less than 0.3 m. Testing times increase for larger piles due to the greater thermal mass of the heat exchanger.

The ILS model has been used in previous studies to evaluate TRT data from energy piles [16,14,33–37]. Depending on the geometry of the pile, line source model simplifications potentially bias estimates of soil thermal conductivity and pile thermal resistance by neglecting three-dimensional effects and the thermal dynamics of the pile. The ILS based interpretation overestimates soil thermal conductivity as measured temperatures tend to fall below the line source modelled temperatures due to vertical heat transport. In previous research ILS estimates of soil thermal conductivity exceed corresponding values obtained with the composite cylinder model [34], capacitance models [37] and numerical models [35] by 22%, 80% and 230%, respectively.

Ref. [35] analyse TRT data with 2D FEM temperature models of horizontal cross sections of a cylindrical energy pile seated in geological layers with contrasting thermal properties. The authors find soil thermal conductivities in agreement with the laboratory derived values (Table 1). However [35], ignores vertical heat transport and heat loss at the foot of the pile in their modelling. Refs. [16,7,36], listed in Table 1, report higher values of soil thermal conductivity than the lab- or in-situ derived values, up to 22% [16],
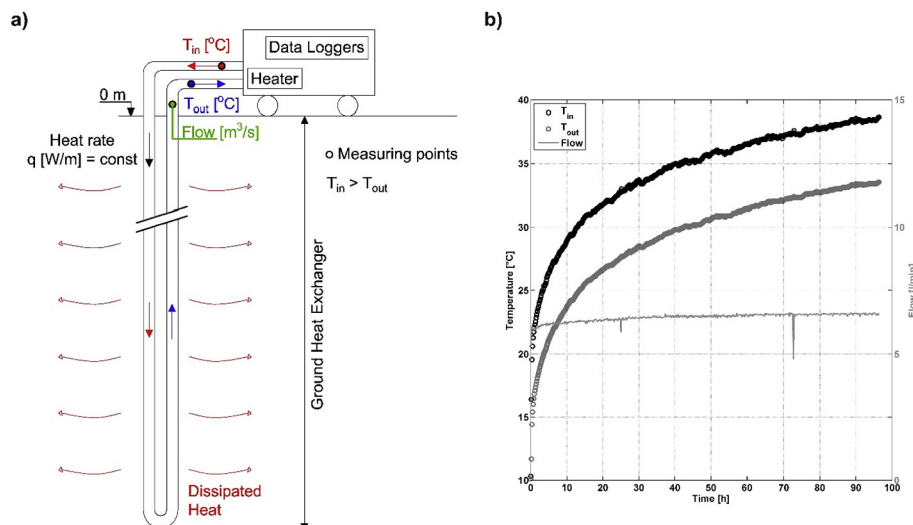
Fig. 2. Thermal response test TRT process: a) TRT setup and principle of the in-situ test, after [18]; b) Typical TRT measurements.

Table 1
Summary of pile heat exchanger TRT studies. The concrete cover is defined as the distance from the pipe edge to the pile wall.

Pile type, pipe configuration[a]	Dimensions [m]: length, diameter or size, concrete cover	TRT duration	Interpretation methodology[b]	Soil thermal conductivity λ_s [W/m/K]	Pile thermal resistance R_p [K m/W]	Deviation from reference values λ_s[c]	Ref.
Precast square, 1U	12.0, 0.27 x 0.27, 0.10	30 h	ILS	2.56	0.170	22% higher than BHE TRT	[16]
Cast-in-place, W	45.0, 0.60, 0.13	48 h	ILS	2.96	–	–	[34]
		48 h	CCM	2.42	–		
Cast-in-place, 2U	18.3, 0.305, 0.09	96 h	G-function ts	2.90	0.061	From −3% lower to 20% higher than lab	[7], data from Ref. [8]
Cast-in-place, 1U	18.3, 0.305, 0.09	67 h	G-function ts	3.45	0.104		
Cast-in-place, 2U	18.3, 0.457, 0.16	100 h	G-function ts	3.20	0.104		
Cast-in-place, 1U	18.3, 0.457, 0.16	110 h	G-function ts	3.55	0.135		
Cast-in-place, 1U	26.8, 0.30, 0.08	72 h	G-function	2.40	0.125	–	[33]
		72 h	ILS	2.60	0.125		
Cast-in-place, 1U	16.1, 0.60, 0.05	72 h	ILS	4.19	–	Considered inaccurate	[35]
		72 h	2D FEM λ_s parameter change	1.20–2.00	–	Within range of lab (1.50 −2.40)	
Precast square, 2U	17.0, 0.35 x 0.35, -	120 h	ILS	2.70	0.160	15% higher than lab	[36]
Cast-in-place, 2U	20.0, 0.62, 0.11	110 h	CaRM inverse analysis	1.50	0.120	–	[37]
		110 h	ILS	2.80	–	–	

[a] 1U: Single-U; 2U: Double-U; 3U: Three-U; W: W-shape (continuous pipe).
[b] ILS: Infinite Line Source; CCM: Composite Cylindrical Model; FEM: Finite Element Model, CaRM: Capacity Resistance Model; ts: time superposition.
[c] BHE: borehole heat exchanger.

20% [7] and 15% [36]. Determining the pile thermal resistance requires further analysis.

1.3. Scope of this study

In this study, five TRTs of quadratic cross section energy piles carried out in Denmark are interpreted with analytical, semi-empirical and numerical models by means of non-linear regression. Initially, soil thermal conductivity is estimated by inverse 3D FEM modelling of the TRT data and then compared to corresponding, independent laboratory measurements. A fully 3D based TRT interpretation is not feasible for routine practical applications, due to the immense computational burden of solving the inverse problem, which could last days. Consequently, the study also explores the applicability of simpler analytical and semi-empirical models for interpretation of the TRT data. The tested models include the infinite and finite line and cylinder (hollow and solid) source models and the empirically-based G-functions (see e.g. Ref. [38]).

2. Experimental data

The precast quadratic cross section energy piles studied in this paper have so far been used in Denmark [39], Germany [40] and Austria [41]. Fig. 3 shows the studied energy pile with W-shaped and single-U pipe heat exchangers, respectively. The length of these precast piles is usually limited to 18 m due to transportation logistics.
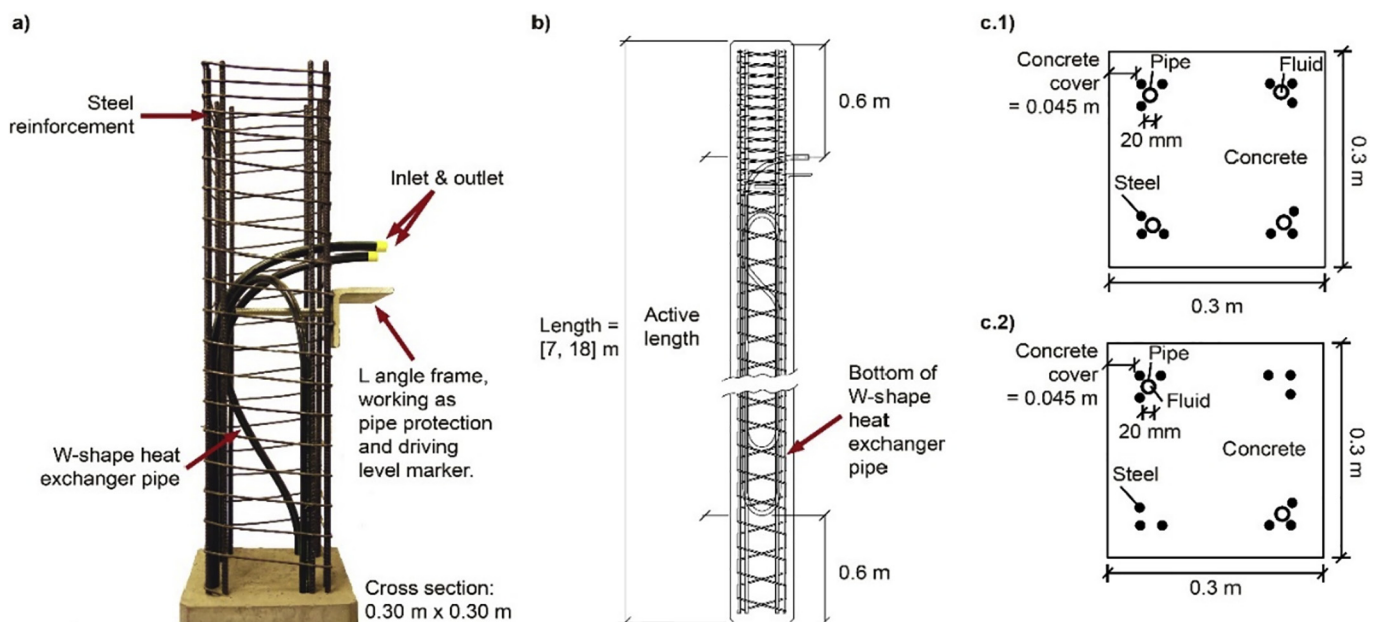
Fig. 3. a) Demonstration model of the precast energy pile with W-shaped heat exchanger pipes fitted to the reinforcement bars; b) vertical profile; c.1) horizontal cross section of the W-shape energy pile and; c.2) horizontal cross section of the single-U energy pile.

Table 2
Test parameters for the five TRTs. The quadratic cross section piles have a side length of 30 cm. The measurement interval was 10 min. The outer and inner diameters of the PEX pipes are 2 cm and 1.6 cm, respectively and water serves as the heat carrier fluid. The piping between the TRT instrument and the tested piles (1.2 m approx.) is carefully insulated to reduce ambient temperature effects.

Test site	Langmarksvej (LM)	Langmarksvej (LM)	Langmarksvej (LM)	Rosborg South (RS)	Rosborg North (RN)
Pile heat exchanger ID	LM1	LM2	LM3	RS1	RN1
Heat exchanger pipe configuration	1U	W	W	W	W
Active length [m]	10.8	10.8	16.8	15.0	14.8
Aspect ratio (AR = active length/diameter)	28	28	44	39	39
Undisturbed soil temperature T_0 [°C]	12.1	11.4	10.4	10.2	9.9
Volumetric flow rate [m³/h]	0.50	0.56	0.51	0.39	0.54
Average heat injection rate q [W/m]	101.4	159.4	167.6	152.5	157.8
Heat injection rate, standard deviation as % of average	4.3	4.7	3.7	4.3	3.1
TRT duration [h]	120	114	147	96	49

The data analysed have been collected from two different locations in Denmark: the Langmarksvej test site in Horsens (55° 51′ 43″ N, 9° 51′ 7″ E) where three energy piles have been tested and the Rosborg test site in Vejle (55° 42′ 30″ N, 9° 32′ 0″ E), with two tested energy piles. The experimental data consist of TRT temperatures and laboratory measurements of the thermal properties of soil and concrete samples. The test sites and the field work are further described in Ref. [42].

2.1. Thermal response test data

Five TRTs were performed on energy piles differing in length and the configuration of the geothermal piping (W-shaped and single-U, refer to Table 2). The dimensionless TRT temperatures Φ (Equation (1)) are plotted in Fig. 4 with corresponding Fourier numbers Fo (Equation (2)).

$$\Phi = \frac{2\pi\lambda_s \Delta T}{q} \qquad (1)$$

$$Fo = \frac{\alpha_s t}{r_b^2} \qquad (2)$$

where q [W/m] is the heat injection rate normalized by the active length of the heat exchanger, ΔT [K] is the temperature change between the undisturbed soil temperature T_0 [°C] and the measured average fluid temperature T_f [°C], α_s is the thermal diffusivity [m²/s], i.e., the ratio between the thermal conductivity λ_s
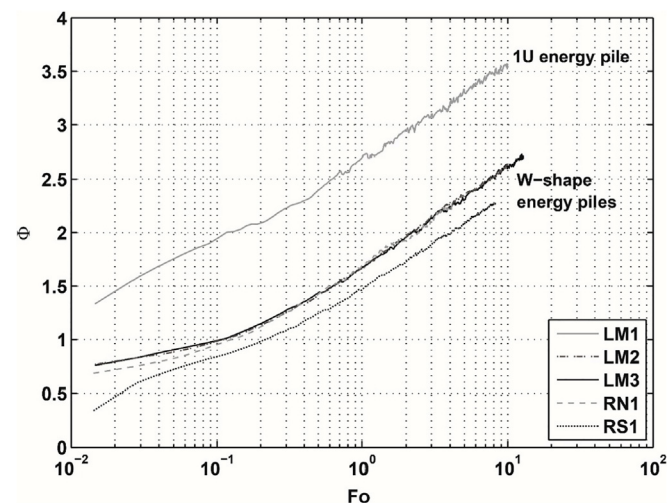
and the volumetric heat capacity ρc_p [J/m³/K], t [s] is the time and r_b [m] is the pile radius. The corresponding laboratory estimates of soil thermal conductivity λ_s are used in Equation (1). In Equation (2), the pile radius r_b is the radius that provides an equivalent circumference to the square perimeter. This radius closely maintains the position of the pipes and the concrete cover within the pile cross section, as compared to the quadratic cross section shown in Fig. 3, c.1. The five TRT data sets are available in [dataset] [43].

Test parameters are summarised in Table 2.

2.2. Laboratory measurements

The thermal properties of the soil and the concrete have been measured with a Hot Disk apparatus which measures the sample thermal conductivity and diffusivity with an accuracy of ±5% and ±10%, respectively [44]. Five repeated measurements were performed on each sample at a room temperature (20–23 °C).

Soil samples were collected every 50 cm from borings at both test sites. The samples were immediately placed in sealed bags and tested within 48 h. The cohesive samples were kept intact while for the non-cohesive samples, the natural water content was preserved, as best possible.

The borehole at Langmarksvej is located approximately 90 cm from the energy pile LM3 and 5–6 m from piles LM1 and LM2. At Rosborg the drilling is placed 50 m and 100 m from RN1 and RS1, respectively. The test site at Langmarksvej show 4–5 m of man-made fill topping glacial clay till. Glacial sand and gravel situated at 5–6 m below terrain are topped by postglacial organic clay at the Rosborg test site. Table 3 provides the layer-thickness-weighted arithmetic mean of the measured characteristics, with full results for the soil borings shown in Fig. 5.

The concrete samples were measured in both dry and saturated conditions to infer the range of feasible thermal conductivities and diffusivities. The laboratory measurements are summarised in Table 3.

3. Methods

The 3D FEM model is described first and the selected analytical, empirical and numerical models are presented afterwards. Lastly, the parameter estimation procedure, applied to all the models, is described.

3.1. Finite element model

The software COMSOL Multiphysics has been used to calculate the subsurface temperature response in and near the energy pile [45]. COMSOL solves the governing Equation (3) for transient thermal conduction in solids by means of the finite element method:

Fig. 4. Dimensionless, average fluid TRT temperatures. The pile IDs and corresponding details are provided in Table 2.

Table 3
Summary of the laboratory measurements. The thermal conductivity and volumetric heat capacity are estimated by the layer-weighted arithmetic mean of the measurements over the active length of the heat exchanger.

Material	Bulk density [kg/m³]	Thermal conductivity λ [W/m/K]	Volumetric heat capacity ρcₚ [MJ/m³/K]
Soil, Langmarksvej (18 m deep drilling)	2030	2.30 ± 0.13	2.61 ± 0.27
Soil, Rosborg North (16 m deep drilling)	1850	2.14 ± 0.11	2.47 ± 0.29
Concrete, oven dry (0% water content in mass)	2320	2.30 ± 0.28	1.69 ± 0.29
Concrete, saturated (4% water content in mass)	2410	2.75 ± 0.15	2.37 ± 0.28

$$\rho c_p \frac{\partial T}{\partial t} = \nabla(\lambda \nabla T) + Q \qquad (3)$$

where ρc_p [J/m³/K] is the volumetric heat capacity, T [K] the temperature, t [s] the time, λ [W/m/K] is the bulk thermal conductivity tensor and Q [W/m³] is the heat generation rate. The presence of groundwater flow is ignored in the simulations and the ground is assumed to be thermally isotropic and homogeneous. The thermal interaction of the pile heat exchanger with the surrounding soil is modelled by conduction (heat transfer within concrete and soil) and advection in the heat exchanger pipes. The 3D model contains three domains (Fig. 6): the soil, the concrete pile and the heat exchanger pipe, embedded in the concrete, which contains the fluid. The upper 60 cm of the pile do not contain heat exchanger pipes and are not included in the model (see Fig. 3).

The 3D model utilises two modules in COMSOL: transient heat transfer in solids (applied to all the domains) and non-isothermal pipe flow (applied to the pipe). The non-isothermal pipe flow model approximates advective, 1D transport of heat by the circulating heat carrier fluid in hollow tubes along lines represented in 2D or 3D [46]. The 1D simplification is justified due to the high slenderness ratio of the heat pipe. It is assumed that the velocity profile is fully developed, it does not change within a section, and a negligible temperature change within the pipe in the radial direction occurs. This avoids the more challenging mesh compatibility of the full pipe cross section and the 3D solid materials since edge elements are used to solve for the tangential cross-section averaged velocity. Turbulent pipe flow is specified in accordance with the actual TRT conditions. The diameter of the PEX pipe is 20 mm with a wall thickness of 2 mm and the thermal conductivity of the pipe material is 0.42 W/m/K. Flow in the pipe is simulated with Churchill's friction model [47] which accounts for the internal advective thermal resistance. Both the W-shaped and the single-U pipe configurations are modelled (Fig. 6a and b). The thermal effects of the steel reinforcement bars are negligible as shown by Refs. [48,49], and as such they are not included in the modelling.

Model tests were made to ensure that modelled temperatures are independent of chosen level of temporal and spatial discretisation and to ensure that the simulated temperature changes at the boundaries are negligible. The model extends 20 m horizontally and from the surface to 5 m below the energy pile (Fig. 6). The mesh is refined in the immediate vicinity of the pile. A fine mesh with tetrahedral, prismatic, triangular, quadrilateral, linear and vertex elements has been created. The minimum element size is 3.4 cm and the maximum element size is 78.4 cm.

The initial temperature in the model domain is set equal to the undisturbed ground temperature measured prior to the TRT. Specified temperature conditions equal to the measured initial temperature are imposed at the soil domain boundaries. The measured inlet temperature during the TRTs is specified for the
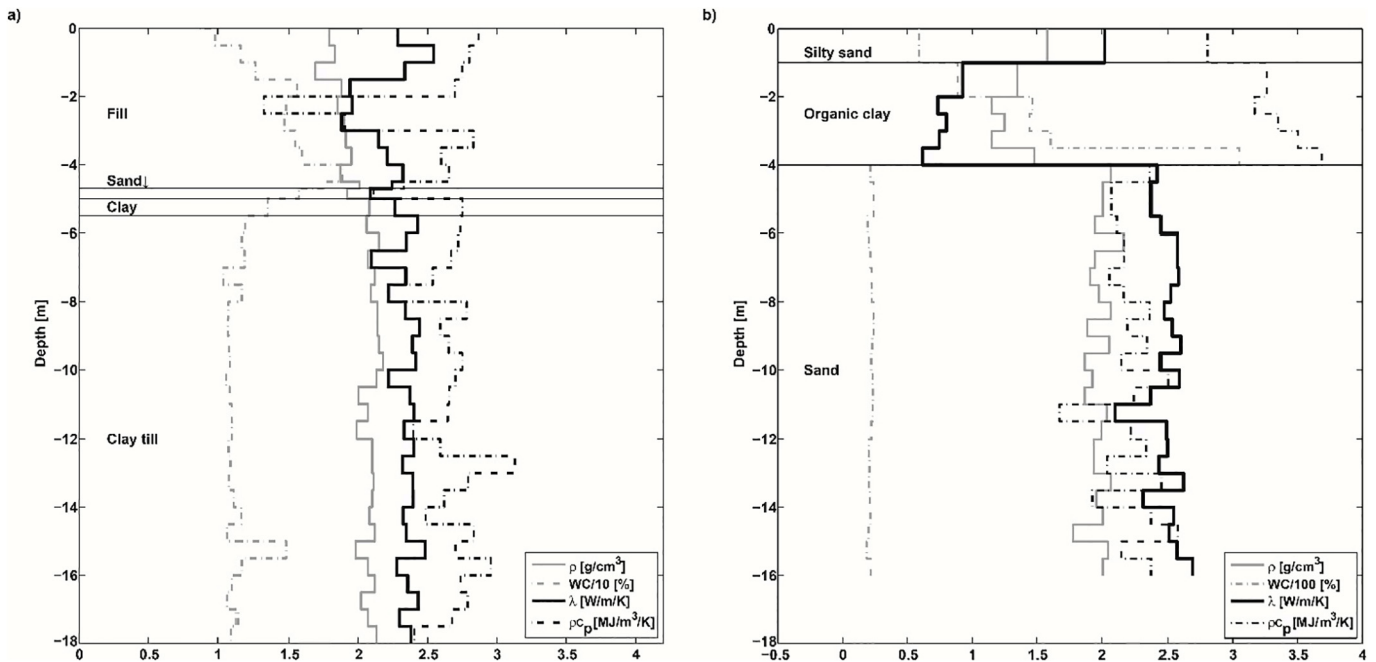
Fig. 5. Density, water content, thermal conductivity and volumetric heat capacity profiles at the a) Langmarksvej and b) Rosborg test sites. Depth is relative to the ground surface. Notice that the plotted water content is scaled differently for the two test sites.
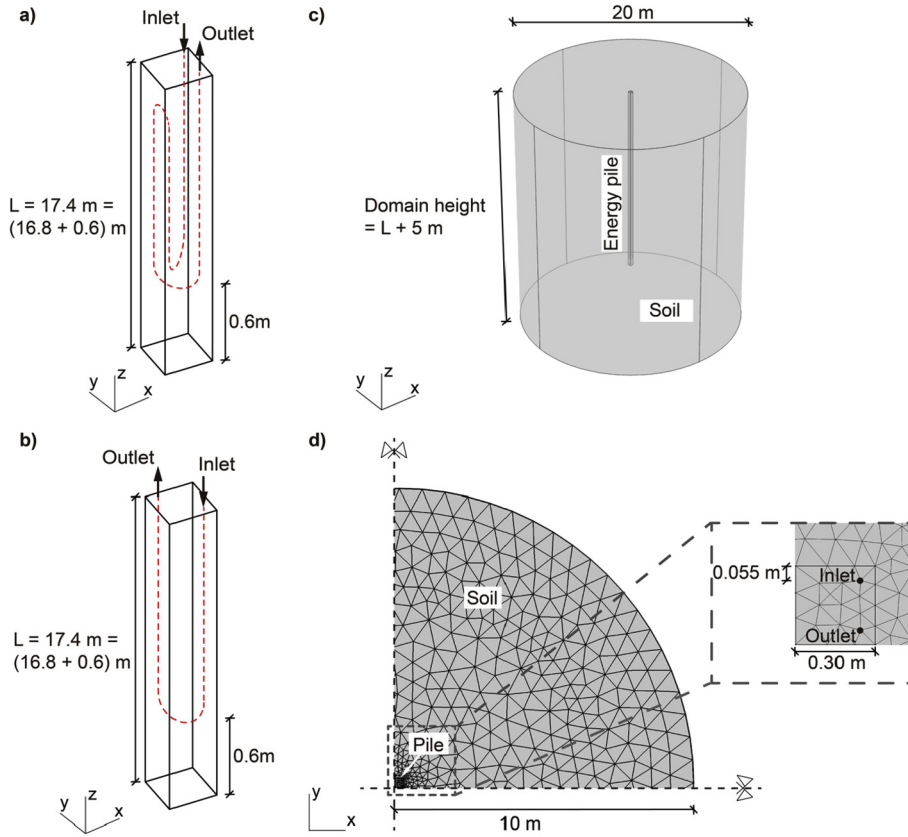
Fig. 6. Description of the 3D finite element model simulated in COMSOL: a) Schematic of the W-shape pile heat exchanger; b) Schematic of the Single-U pile heat exchanger; c) Simulated meshed domains; d) Top view of a quarter of domain.

inlet node of the pipe (Fig. 6d).

3.1.1. Model verification

The 3D FEM modelled temperatures are compared to short- and long-time pile-wall temperature responses calculated with existing analytical models including finite and infinite line and solid cylinder sources (see Section 3.2 for model details) in Fig. 7.

The curves are computed assuming a constant heat injection rate considering identical soil and concrete thermal conductivities. The temperature change θ is defined as the difference between the initial soil temperature T_0 and the computed average pile wall temperature T_b.

The largest difference in calculated, normalised temperatures between the 3D finite element model and the finite source is 0.17 for Fo = 900. This corresponds to a temperature difference of 0.90 °C at approximately 415 days. This discrepancy is considered acceptable since analytical solutions do not capture the influence of the square cross section and 3D effects such as the thermal short circuiting between pipes, causing overestimated long-term temperatures. As shall be seen in Section 4.1, the 3D FEM model also allows excellent representation of the field results, providing full confidence in its suitability for the inverse analysis.

3.1.2. Pile thermal resistance

The thermal conductivity of the concrete largely impacts the pile thermal resistance R_p [K m/W], which also depends on the position, size and number of pipes, the circulating fluid and flow regime and the dimensions of the pile. Pile thermal resistance is defined as:

$$R_p = \frac{T_f - T_b}{q} \tag{4}$$

where T_f [°C] is the average fluid temperature and T_b [°C] is the pile heat exchanger average wall temperature computed from the 3D finite element model and q [W/m] is the heat injection rate normalized by the active length of the heat exchanger. To uncouple the influence of the convective heat transfer within the pipes, the term pile concrete thermal resistance R_c [K m/W] is defined. It is determined from subtracting the convective and conductive resistances of the pipe R_{pipe} from the pile thermal resistance [38,50]:

$$R_c = R_p - R_{pipe} \tag{5}$$

$$R_{pipe} = \frac{1}{2n\pi r_i h_i} + \frac{\ln(r_o/r_i)}{2n\pi \lambda_{pipe}} \tag{6}$$

where n is the number of pipes in the pile heat exchanger cross section, r_i [m] is the inner radius of the pipe, r_o [m] is the outer radius of the pipe, h_i [W/m²/K] is the heat transfer coefficient and λ_{pipe} [W/m/K] is the thermal conductivity of the PEX pipe. R_c can also be determined as:

$$R_c = \frac{T_p - T_b}{q} \tag{7}$$

where T_p [°C] is the average temperature on the outer wall of the pipe.
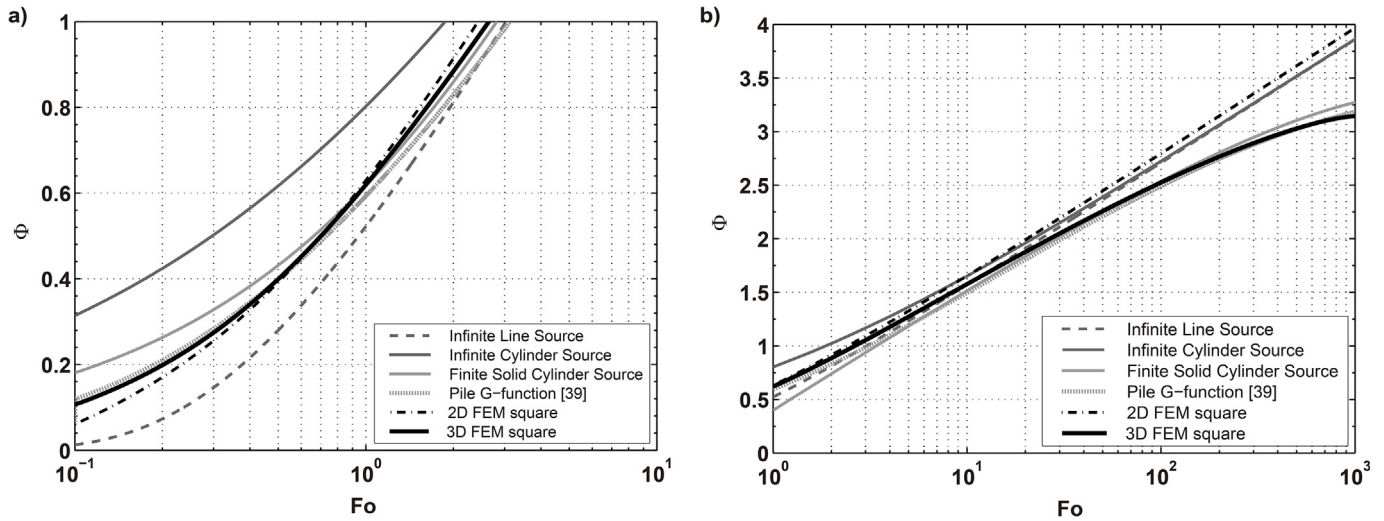
Fig. 7. Pile wall temperature responses for the 3D finite element model and selected corresponding analytical models assuming an aspect ratio of 44. a) Short-term and b) long-term responses.

3.2. Selected analytical, empirical and numerical heat flow models

The investigated models comprise analytical models, where the heat transfer in the ground heat exchanger is assumed to be in steady-state and semi-empirical and numerical models, where transient heat transfer in the ground heat exchanger is considered. The models are listed in Table 4 and are further described in Table A.1 in Appendix A. The finite line source model is not considered as it does not differ significantly from the ILS solution for the considered testing times [51] and aspect ratios between 25 and 50.

G-functions are dimensionless, time dependent temperature response functions for computing the temperature T_b on the energy pile wall (shown here in their general form):

$$T_b = \frac{q}{4\pi\lambda_s} G(r = r_b, \text{ Fo}) \qquad (8)$$

where G is the G-function. All the analytical expressions in Table 4 and Appendix A can be expressed in this form. Additionally, in this study the semi-empirical pile G-functions [38] were also used. These were estimated by 3D modelling of cylindrical energy piles. In all cases the average fluid temperature in the heat exchanger pipes is calculated as:

$$T_f = T_0 + qR_p + T_b \qquad (9)$$

For the analytical models qR_p is constant since the pile is assumed steady. For the pile G-functions qR_p is also a function of Fo, as set out in Appendix A. When time variations of the heat rate need to be considered, the temperature change is computed as:

$$\Delta T_n = \sum_{i=1}^{i=n} \frac{q_i}{2\pi\lambda_s} \left(G\left(\text{Fo}_n - \text{Fo}_{(i-1)}\right) - G\left(\text{Fo}_n - \text{Fo}_{(i)}\right) \right) \qquad (10)$$

where n is the point in normalised time in which the superposition is evaluated.

3.3. Parameter estimation

The parameter estimation is performed with PEST Model-Independent Parameter Estimation software [56]. PEST employs the Gauss-Marquardt-Levenberg algorithm for minimizing the weighted, squared difference between computed and observed fluid temperatures. PEST calculates linear confidence intervals for estimated parameter following the non-linear regression procedure.

For the 3D FEM inverse modelling, the measured outlet temperatures serve as calibration data assigned with equal observation weights. The average of the late-time in- and outlet temperatures ($t_c > 5r_b^2/\alpha$) serve as calibration data for the analytical models. In the interpretation of the TRT of RN1, the aforementioned time criterion was lowered by a factor of 1.5 due to the short duration of the test.

Table 4
Summary of models selected to evaluate the pile heat exchanger TRT data.

	Model description and reference	Analysed time range
Analytical approaches	Infinite line source ILS by Ref. [52].	Fo > 5, steady state in the pile.
	Infinite cylinder source ICS by Ref. [21]. The simplification by Ref. [53] is used in this study.	Fo > 5, steady state in the pile.
	Infinite solid cylinder source ISCS by Ref. [25].	Fo > 4, steady state in the pile.
	Finite solid cylinder source FSCS by Ref. [25].	Fo > 4, steady state in the pile.
Semi-empirical approach	G-function for pile heat exchangers (G-flov) by Ref. [38]. The finite length of the pile is considered. Variable heating rates can be considered by time superposition (G-flovts).	Fo > 0.1, transient in the pile.
Numerical approaches	Equivalent pipe model EQpipe by Ref. [54]. The model presented in Ref. [55] is used in this study. The model neglects the finite length of the pile.	Fo > 0, transient in the pile.
	2D horizontal cross section FEM 2D FEM developed for this study. It neglects the finite length of the pile.	Fo > 0, transient in the pile.
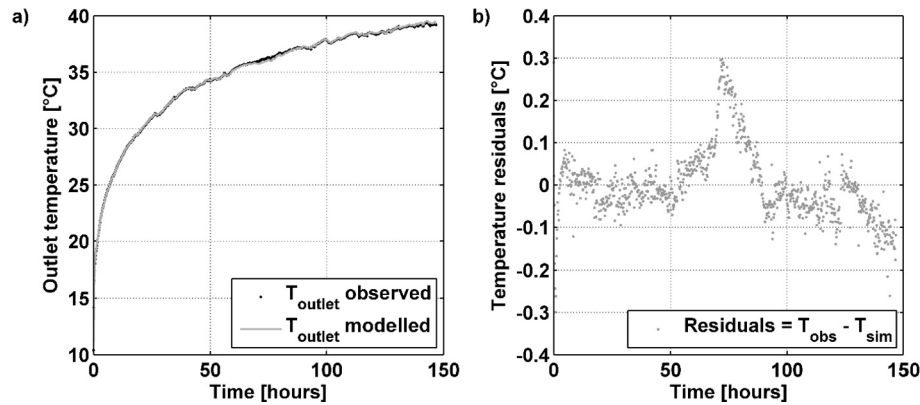
Fig. 8. Model calibration of LM3. a) Observed and modelled outlet temperatures; b) residuals, defined as the difference between the observed and the simulated temperatures.

Table 5
Calibration estimates and linear 95% confidence levels for the soil and concrete thermal conductivities determined from 3D FEM.

Energy pile ID	Thermal conductivity soil λ_s [W/m/K]	Thermal conductivity concrete λ_c [W/m/K]	Root Mean Squared Error RMSE
LM1	2.50 ± 0.16	2.33 ± 0.19	0.036
LM2	2.21 ± 0.05	2.85 ± 0.14	0.029
LM3	2.22 ± 0.07	2.46 ± 0.15	0.083
RN1	2.20 ± 0.22	2.35 ± 0.19	0.065
RS1	2.21 ± 0.06	3.05 ± 0.13	0.047

All measured temperatures are considered in the calibration of the semi-empirical and numerical models. The initial parameter values in the parameter estimation are set equal to the corresponding laboratory measurements (Table 3). The thermal conductivities are allowed to vary from 1.0 to 3.5 W/m/K while the volumetric heat capacities in the 3D FEM model are constrained to ±10% of the corresponding laboratory measurements. For the analytical approaches, the pile thermal resistance R_p is restricted to 0.01–0.30 K m/W. For the semi-empirical approach the pile concrete thermal resistance R_c is allowed to vary between 0.01 and 0.30 K m/W.

4. Results and discussion

Firstly, the 3D FEM calibrated parameter estimates are compared to corresponding laboratory measurements. Secondly, the estimated parameters from calibration of the heat flow models listed in Section 3.2 are compared to corresponding estimates obtained from the inverse 3D FEM modelling and discrepancies are discussed. Next, the pile thermal resistance in the context of square cross section energy piles is further explored. Finally, recommendations on applying TRT in the dimensioning of quadratic cross section precast pile heat exchanger foundations are provided.

4.1. 3D FEM parameter estimation and concrete thermal resistance

The 3D FEM modelling closely matches the observed outlet fluid temperatures as shown in Fig. 8 for the case of pile LM3.

The resulting thermal conductivity values from the inverse calculations are given for all piles in Table 5.

Fig. 9 compares the inverse 3D FEM modelling estimates with the laboratory measurements. Overlapping confidence bounds, demonstrate good agreement between computed estimates and the laboratory conductivity measurements. The estimates of soil thermal conductivity are consistent with geological profiles that show similar geology nearby the tested piles [57]. The estimated concrete thermal conductivity for RS1 slightly exceeds the laboratory measurements. While the concrete production process is strictly controlled, it is not unlikely that some compositional variation exists between different batches of concrete.

Previous research indicate that TRT based soil conductivity estimates exceed corresponding laboratory measurements [58–60]. The inconsistency is attributed to drilling and sampling methods, variations in the natural moisture content, thermal anisotropy and variations in confining pressure. Advanced interpretation methods,
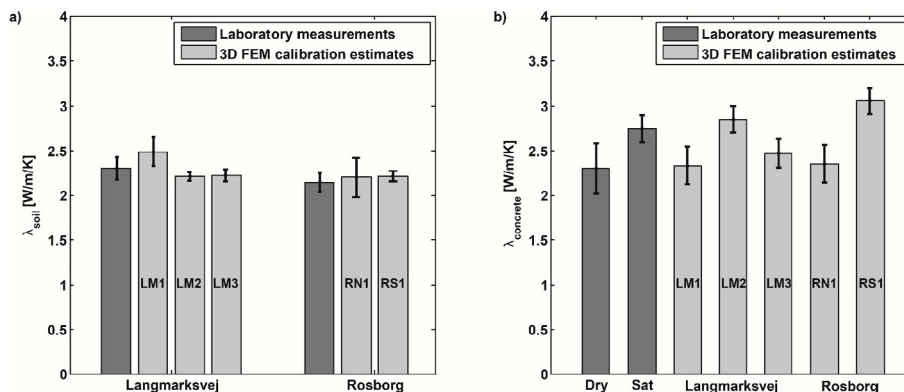
Fig. 9. Laboratory measurements of thermal conductivity compared to 3D model calibration estimates. a) Soil thermal conductivity with weighted, averaged laboratory measurements; b) concrete thermal conductivity, "Sat" indicates saturated conditions. The error bars correspond to the 95% linear confidence intervals.

Table 6
3D FEM model based estimates of concrete thermal resistance R_c.

Pile ID	LM1	LM2	LM3	RN	RS
R_c [K m/W]	0.095	0.045	0.045	0.049	0.039

such as inverse 3D finite element modelling, yield better agreement between laboratory and calibrated conductivity estimates (Table 1). Therefore, if sufficient caution is taken in the sampling and measuring processes and adequate interpretation methods are used, the influence of the aforementioned factors are minimised. It is concluded that the inverse 3D FEM modelling provides accurate estimates of the thermal conductivity of the soil and the concrete.

The 3D FEM computed average pile wall temperature forms the basis for estimating the pile concrete thermal resistance following Equation (7) (Table 6).

The W-shaped and single-U pile heat exchangers yield an average concrete thermal resistance R_c of 0.044 and 0.095 K m/W, respectively.

4.2. Comparison with simpler heat flow models

The inversion of the 3D FEM model is associated with excessive computational time (days), rendering it impractical for routine interpretation. It is therefore investigated to what extent simplifications of the forward model influence parameter estimates. The models described in Section 3.2 form the basis for reinterpretations of the five TRTs to compare calibration estimates to those of the inverse 3D FEM modelling.

Fig. 10 shows parameter estimates from calibration of simpler, numerical, analytical and semi-empirical heat flow models, normalised by the 3D FEM results (Table 5).

Models that do not account for the initial transient behaviour (both finite and infinite approaches) tend to overestimate the thermal conductivity of the soil λ_s by up to 38% for the single-U pile LM1 and up to 25% for W-shape pile heat exchangers, relative to the reference values (Fig. 10a). This discrepancy is greater for the single-U pile due to its larger pile resistance. The time superposition G-function (G-flovts) model was also calibrated to take into account heating fluctuations during the TRTs. Both G-flov and G-flovts estimates consistently fall within the uncertainty of the 3D FEM estimates although slightly underestimating the reference value. The maximum difference of 8% for the model G-flovts is obtained for the RN1 test (pile RN1), which relative to the four other test, has the shortest duration and the largest parameter estimate uncertainties.
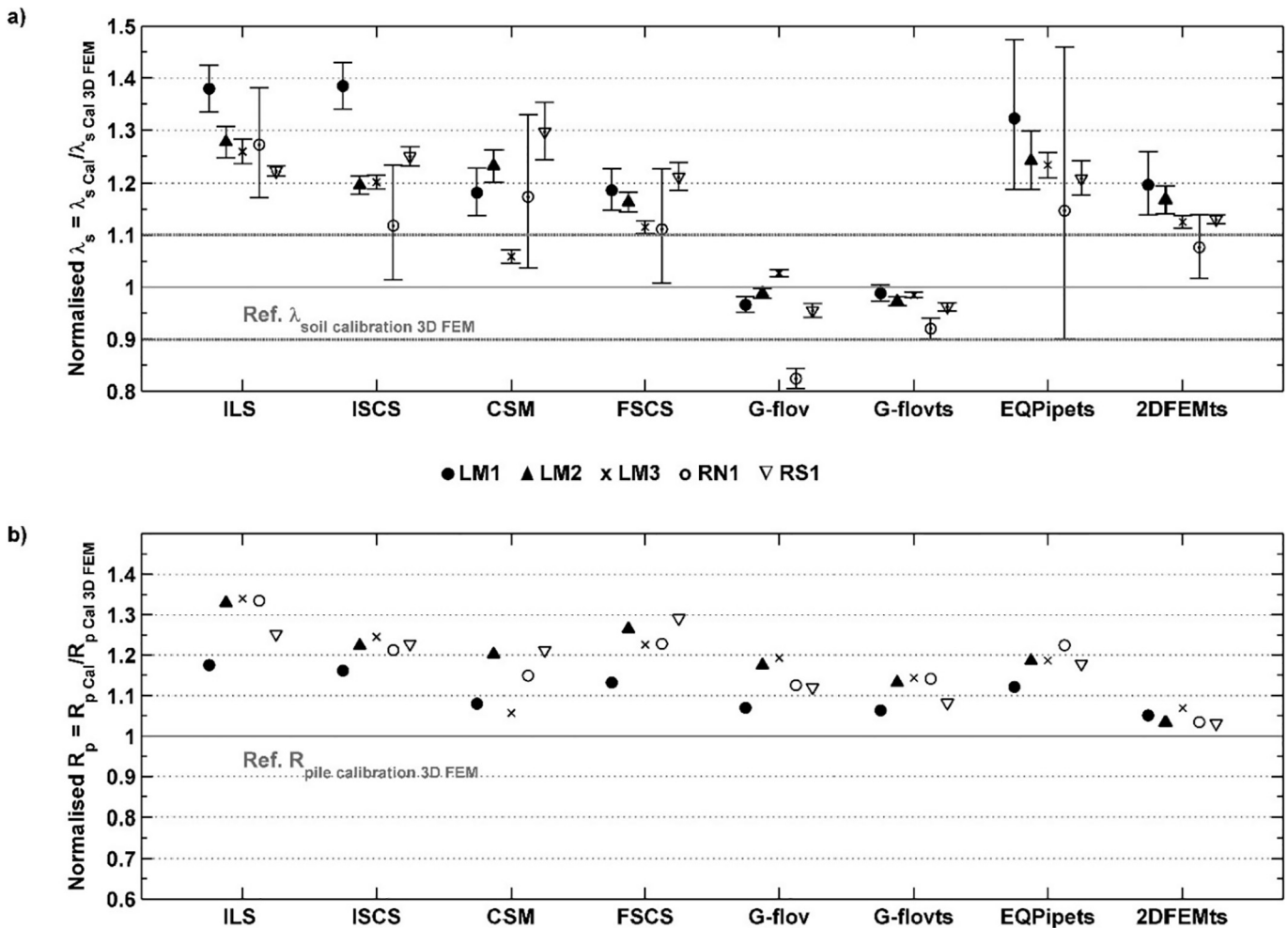
Fig. 10. Parameter estimates from calibration of the heat flow models normalised by the 3D FEM based estimates. G-flovts accounts for variable heating rates. a) The uncertainty bounds depicted (grey) in a) correspond to the largest uncertainty obtained in the calibration of the 3D FEM models (test RN1). b) Uncertainties are not shown for the pile thermal resistance R_p as they are insignificant (order of 10^{-2} K m/W).
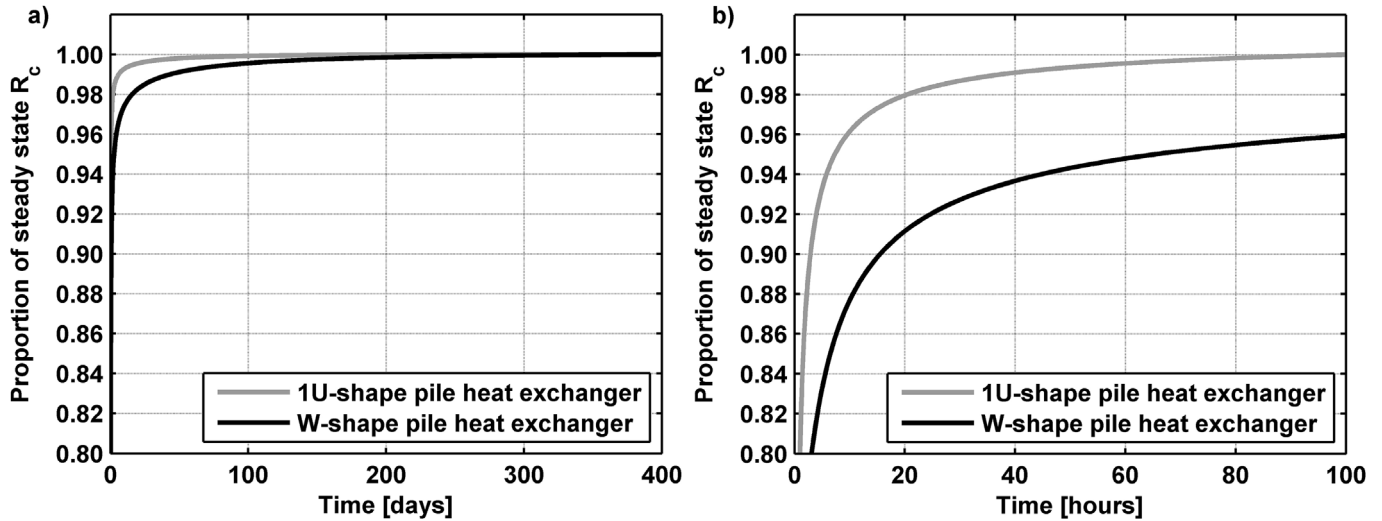
Fig. 11. Evolution of pile concrete thermal resistance Rc over time, computed with the 3D finite element model as synthetic TRT data: a) Long-term behaviour and b) Short-term zoom.

As temperature responses of the infinite source models eventually become linear in logarithmic time, the lower, actual temperatures due to downward heat loss, are compensated for by increasing the soil thermal conductivity in the parameter estimation (refer to Fig. 7). The difference in 2D and 3D FEM modelled temperatures for Fo = 10 exceed 5% for the LM3 pile with an aspect ratio of 44 and the deviation is expected to increase for lower aspect ratios. This is in accordance with the findings in Ref. [38]. For the G-functions by Ref. [38] temperatures fall slightly below those of the 3D FEM model causing a slight underestimation of the soil thermal conductivity.

Fig. 10b shows the estimated pile thermal resistance R_p. Generally, the models consistently overestimate the concrete thermal resistance, up to 35% for the ILS model. The 2D FEM model provides the closest match however it systematically overestimates the reference value by 5–9%. This model considers the square cross section of the pile but it does not take into account the convective resistance associated with pipe fluid flow (first term on right-hand side of Equation (6)). The higher measured temperatures during the initial hours (refer to 2D FEM curve in Fig. 7), result in a lower estimated thermal conductivity of concrete λ_c, compared to the 3D

FEM estimate. This yields a higher pile thermal resistance R_p.

For the analysed models, the thermal conductivity of the soil λ_s and the pile thermal resistance R_p are positively correlated implying that the parameters can be increased simultaneously without seriously compromising the model fit to measured temperatures. Consequently, the systematic overestimation of the soil thermal conductivity illustrated in Fig. 10a is compensated for by increasing the thermal resistance of the pile in the model calibration.

4.3. Concrete thermal resistance

The pile concrete thermal resistance R_c measures the efficiency of the ground heat exchanger in steady state conditions (Equation (5)). The time required for establishing steady-state conditions in the pile was computed with the 3D FEM model (Fig. 11).

Steady-state conditions exist in the single-U pile after 100 h of testing while 96% of the steady-state concrete thermal resistance is reached for the W-shaped heat exchanger pile. As such, the TRT of
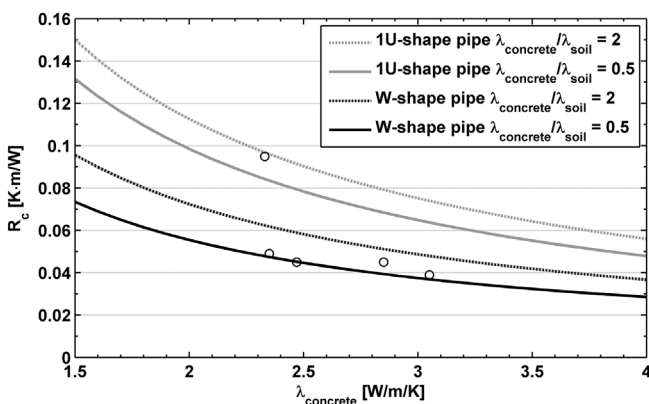
Fig. 12. Upper and lower bounds for the concrete thermal resistance R_c for square precast pile heat exchangers with single-U- and W-shape pipes obtained from 3D FEM modelling for a range of concrete thermal conductivities. Calibrated 3D FEM model based estimates of R_c are indicated with circles.
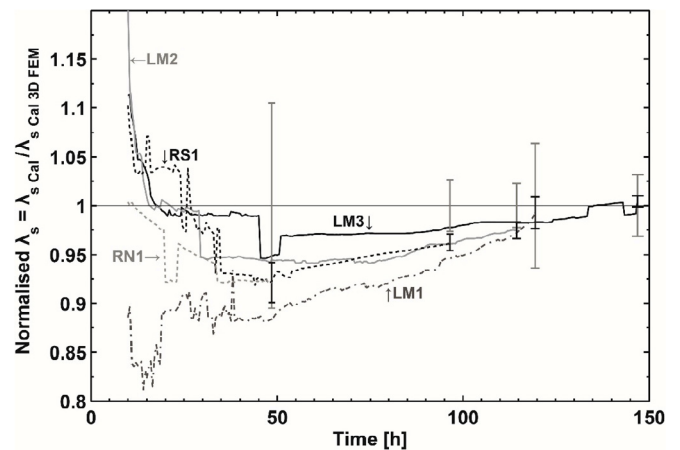
Fig. 13. Stepwise interpretation of the five TRTs with the G-functions proposed by Ref. [39] and with corresponding soil thermal conductivity estimates. The time increment is 30 min. Error bars are indicated for the duration of the test: black) uncertainty bands for the G-flovts calibrated estimates; grey) uncertainty bands for the 3D FEM calibrated estimates.

Appendix A

Table A.1
Description of models selected to evaluate the pile heat exchanger TRT data.

	Model description	Equations	Analysed time range
Analytical approaches	**Infinite line source (ILS):** Approximates the ground heat exchanger by an infinite line source with a vanishing cross section in an infinite, isotropic and homogeneous medium [52]. A constant far-field temperature is assumed.	Late-time approximation valid for $5 < \alpha \cdot t/r^2$. $$T_b(r,t) = \frac{q}{4\pi\lambda_s}\left(\ln\left(\frac{4\alpha t}{r_b}\right) - \gamma\right) \quad (11)$$ where t is time and γ is Euler's constant.	Fo > 5, steady state in the pile.
	Infinite cylinder source (ICS): Approximates the ground heat exchanger by an infinite hollow cylinder in an infinite, isotropic and homogeneous medium. A specified heating rate is imposed at a radius equal to the cylinder surface wall [21] assuming a constant far-field temperature. The simplification by Ref. [53] is used.	$$T_b(r,t) = \frac{q}{2\pi^2\lambda_s r_b}\sum_{j=1}^{10}\left[\frac{V_j}{j}\frac{K_0(\omega_j r)}{\omega_j K_1(\omega_j r_b)}\right]; \quad (12)$$ $$\omega_j(t) = \sqrt{\frac{j\ln(2)}{\alpha t}} \quad (13)$$ $$V_j = \sum_{k=\text{Int}\left(\frac{j+1}{2}\right)}^{\min(j,5)}\frac{(-1)^{j-5}k^5(2k)!}{(5-k)!k!(j-k)!(2k-j)!} \quad (14)$$	Fo > 5, steady state in the pile.
	Infinite solid cylinder source (ISCS): Approximates the ground heat exchanger by a solid cylinder with an infinite length in an infinite, isotropic and homogeneous medium. A specified heating rate is applied at the outer surface of the cylinder and heat can dissipate radially towards the centre of the cylinder and to the soil. The analytical formulation and corresponding simplifications are given by Ref. [25]. Here, the simplified equations are used.	where K_0 and K_1 are modified Bessel functions of the second kind of order 0 and 1, respectively. The approximation is valid for $(p+1)^2 \leq$ Fo $\ll\infty$. $$G(r,t) = \frac{1}{2}\left[-\gamma - \ln\frac{r^2 + r_b + |r^2 - r_b|}{8 r_b Fo} + \frac{1+p^2}{4Fo}\right] \quad (15)$$ where $p = r/r_b$	Fo > 4, transient in the pile.
	Finite solid cylinder source (FSCS): Identical to the model proposed by Ref. [25] except that the cylinder source has a finite length. The simplified approximation presented by Ref. [25] is used in the present study.	The approximation is valid for $(p+1)^2 \leq$ Fo H^2/r_b^2. $$G = \frac{1}{2}\left[-\gamma - \ln\frac{r^2 + r_b^2 + |r^2 - r_b^2|}{8 r_b^2 Fo} + 3\frac{r+r_b}{H}\frac{2}{\pi}\frac{E_0}{(r+r_b)^2} + 3\sqrt{\frac{4t}{t_z}} - \frac{3}{\sqrt{\pi}}\frac{r^2 + r_b^2}{\sqrt{4Fo_b}H} + \frac{p^2 + 1}{4Fo}\right] \quad (16)$$ Where $p = r/r_b$, $E_0(m)$ is the complete elliptic integral of the second kind of order 0 and t_z is H^2/α.	Fo > 4, transient in the pile.
Semi-empirical approach	**G-functions for pile heat exchangers (G-flov):** Ref. [38] proposed semi-empirical functions for the transient behaviour of energy piles. The solutions are based on 3D finite element model curve fitting. The G-functions combine G-functions for the concrete Gc, and pile G-functions Gg, which describe the temperature response of the ground surrounding the pile. They account for different properties of the pile and the soil and have been computed for upper and lower bound temperature responses for different aspect ratios. The upper bound is defined by a large diameter pile with pipes near the edge of the pile and where the ratio between concrete and soil thermal conductivity is equal to 2. The lower bound is defined by a large diameter pile with centred pipes and where the ratio between concrete and soil thermal conductivity is equal to 0.5. G-functions take into account heating rate variations by temporal superposition and considers the finite length of the pile.	Ground temperature response Gg for upper bound solution and for lower bound solutions, for Fo > 0.1 and Fo > 0.25, respectively: $$G_g = a[\ln(Fo)]^7 + b[\ln(Fo)]^6 + c[\ln(Fo)]^5 + d[\ln(Fo)]^4 + e[\ln(Fo)]^3 + f[\ln(Fo)]^2 + g[\ln(Fo)] + h \quad (17)$$ Concrete G-function Gc for Fo < 10: $$G_c = a[\ln(Fo)]^6 + b[\ln(Fo)]^5 + c[\ln(Fo)]^4 + d[\ln(Fo)]^3 + e[\ln(Fo)]^2 + f[\ln(Fo)] + g \quad (18)$$ The curve fitting parameters are given in Appendix A and B in Ref. [38]. To get the average fluid temperatures, the previous equations are combined as: $$T_f = T_0 + qR_{pipe} + qR_cG_c + \frac{q}{2\pi\lambda_s}G_g \quad (19)$$	Fo > 0.1 and Fo > 0.1, transient in the pile.
Numerical app.	**Equivalent pipe model (EQpipe):** Simplifies the cross section of the heat exchanger to a centred pipe with an area equivalent to that of the ground heat exchanger pipes. It was first proposed by Ref. [54]. It does not consider the finite length of the ground heat exchanger but it does consider its thermal mass. The model used in this paper is the one presented in Ref. [55]. The model takes into account heating rate variations by temporal superposition.		Fo > 0, transient in the pile.
	2D horizontal cross section finite element model (2D FEM): 2D cross section model of the square energy pile. Two models are considered: single-U and double U heat exchangers. The soil domain extends to a radius of 5 m. The initial temperature is set equal to the undisturbed ground temperature measured prior to the TRT. Dirichlet boundary conditions, equal to the undisturbed temperature, are imposed on vertical boundaries. Heating is simulated by a time varying source condition imposed on the elements comprising the heat exchanger fluid. The source is equally distributed in the heat exchanger pipes. The model does not consider the finite length of the pile.		Fo > 0, transient in the pile.

RN1 (49 h) most likely was too short yielding the greatest deviation and uncertainty on estimated parameters (Fig. 10).

The investigations presented in the previous sections have not provided reliable models for estimating the pile concrete thermal resistance R_c. Therefore, the pile concrete thermal resistance must be estimated with the 3D FEM model. Imposing a constant heat injection rate in steady state conditions, upper and lower bounds of the concrete thermal resistance R_c for different λ_c/λ_s ratios are computed, for single U- and W-configuration energy piles. The upper bound corresponds to a λ_c/λ_s ratio of 2, while the lower bound corresponds to a λ_c/λ_s ratio of 0.5. 7 m and 18 m are considered as upper and lower bounds on the pile length, respectively. The calculated concrete thermal resistances R_c are shown in Fig. 12.

The computed curves for 7 m and 18 m piles differ only slightly and, therefore, the most conservative estimates are shown for the single U and W-shape pipes in Fig. 12. The thermal resistance is higher for single-U energy piles and decreases as the thermal conductivity of the concrete increases. The TRT estimates obtained from the 3D FEM calibration (Table 6), indicated with circles in Fig. 12, fall within the computed resistance bounds, as expected. Concrete thermal resistance varies moderately for the expected range of concrete thermal conductivity (approx. 2.3–3.1 W/m/K). Within this range, the thermal conductivity of the soil barely affects the concrete thermal resistance (less than 13%).

4.4. Testing times

The G-functions proposed by Ref. [38] provide consistent soil thermal conductivity λ_s values for the five TRTs analysed. It is of interest to examine plots of the stepwise estimates of soil thermal conductivity for the five TRTs. Sequential plots give indications as to whether calibrated conductivities converge to a particular value as further data are included in the interpretation. Fig. 13 shows the calibrated soil thermal conductivity at different testing times: the initial time is 10 h with a time increment of 30 min in the stepwise interpretation of the five TRTs.

The duration of the analysed TRTs in this study range from 49 to 150 h (i. e., Fourier's number 4.5 to 10). As shown in Fig. 13, the G-functions by Ref. [38] yield estimates of soil thermal conductivity λ_s that fall well within the 3D FEM uncertainty bounds. Beyond 100 h, the G-function calibrated conductivities converge to the corresponding 3D FEM estimate, suggesting that testing times should be longer than 120 h. However, G-function and 3D FEM modelled temperatures tend to diverge at later times (see Fig. 7) which potentially leads to overestimation of the soil thermal conductivity λ_s. Hence, dimensionless testing times for the studied precast pile heat exchangers should not exceed Fo = 10 (150 h) nor be less than Fo = 5 (60 h, approximately). The 49-h TRT of pile RN1 is likely to be too short (Fo < 4.5).

5. Conclusions

We apply 3D finite element models to interpret five thermal response tests of square cross section foundation pile heat exchangers (energy piles) with contrasting lengths and pipe configurations. The FEM model accepts measured fluid inlet temperatures as input and computes outlet temperatures. The interpretation procedure is based on inverse modelling of observed outlet temperatures to estimate the bulk thermal conductivity of the soil and the concrete. The 3D finite element model accurately reproduces the observed outlet temperatures of the TRTs and estimates are in close agreement with corresponding laboratory measurements. The pile concrete thermal resistances are computed from the simulated pipe and pile wall temperatures, respectively.

Due to immense computational burden of calibrating the 3D model, the TRTs are reinterpreted with simpler analytical, empirical and numerical models. Parameter estimates from the reinterpretation of soil thermal conductivity and pile thermal resistance are compared to corresponding 3D FEM model estimates.

Interpretations based on infinite source 2D finite element models do not yield reliable conductivity and resistance estimates, in the present case up to 22% discrepancy for soil thermal conductivity and 9% for pile thermal resistance. The models that do not account for the transient thermal behaviour of the pile and, in particular, the models that do not consider the pile length, consistently overestimate soil thermal conductivity and pile thermal resistance. The overestimation of pile thermal resistance is due to negative, statistical correlation between the soil and concrete thermal conductivity. The pile heat exchanger G-functions reported by Ref. [38] accurately match the thermal conductivity of the soil for the five TRTs between 60 and 150 h. Except for the 3D FEM model, it is not possible to obtain reliable estimates of the thermal resistance of the pile with the simpler heat flow models. This is likely caused by 3D effects influencing the pile thermal resistance. Moreover, the simpler heat flow models assume a circular rather than square cross section the energy pile. To overcome this issue, potential upper and lower bounds for the pile concrete thermal resistance, for a range of thermal conductivities of concrete, are computed with the 3D model.

To summarize, TRTs are useful for inferring the thermal conductivity of the soil in the dimensioning of square cross section energy pile foundations. Tests should be carried out during the geotechnical investigations where piles are driven to assess the depth of the foundation. Interpretation of TRTs must be done with pile G-functions, either for steady (G-flov) or variable (G-flovts) heating rates depending on test conditions. It is recommended that pile thermal resistance is estimated by type curves computed with 3D FEM models.

References

[1] EPA. Space conditioning: the next frontier. The potential of advanced residential space conditioning technologies for reducing pollution and saving money. Environmental Protection Agency; 1993.

[2] Rogelj J, Den Elzen M, Höhne N, Fransen T, Fekete H, Winkler H, Schaeffer R, Sha F, Riahi K, Meinshausen M. Paris Agreement climate proposals need a boost to keep warming well below 2 C. Nature 2016;534:631–9. https://doi.org/10.1038/nature18307.

[3] ASHRAE. 2009 ASHRAE handbook. Fundamentals. 1791 Tullie circle, N.E. Atlanta: American Society of Heating, Refrigerating and Air-Conditioning Engineers, Inc; 2009. GA 30329.

[4] Oklahoma State University. In: Closed-loop/ground source heat pump systems. Installation guide. UNIVERSITY, O. S. International Ground Source Heat Pump Association; 1988, ISBN 0-929974-01-8.

[5] Brandl H. Energy foundations and other thermo-active ground structures. Geotechnique 2006;56:81–122. https://doi.org/10.1680/geot.2006.56.2.81.

[6] Park S, Lee D, Choi HJ, Jung K, Choi H. Relative constructability and thermal performance of cast-in-place concrete energy pile: coil-type GHEX (ground heat exchanger). Energy 2015;81:56–66. https://doi.org/10.1016/j.energy.2014.08.012.

[7] Loveridge F, Olgun CG, Brettmann T, Powrie W. The thermal behaviour of three different auger pressure grouted piles used as heat exchangers. Geotech Geol Eng 2014;33(2):273–89. https://doi.org/10.1007/s10706-014-9757-4.

[8] Brettman TPE, Amis T, Kapps M. Thermal conductivity analysis of geothermal energy piles. In: Proceedings of the geotechnical challenges in Urban

regeneration conference, London, UK; 2010.

[9] Laloui L, Nuth M. Investigations on the mechanical behaviour of a heat exchanger Pile. In: Van Impe, Van Impe, editors. Proceedings of the Fifth International conference on deep foundations on Bored and Auger Piles,, Frankfurt, Germany, 15 may 2009. London: Taylor & Francis Group; 2009, ISBN 978-0-415-47556-3.

[10] De Groot M, De Santiago C, Pardo De Santayana F. Heating and cooling an energy pile under working load in Valencia. In: Proceedings of the 23rd European Young geotechnical Engineers conference. Barcelona; 2013.

[11] Alberdi-Pagola M, Poulsen SE. Thermal response testing and performance of quadratic cross section energy piles (Vejle, Denmark). In: Proceedings of the XVI European conference on soil mechanics and geotechnical Engineering 2015. Edinburgh, United Kingdom. ICE Institution of Civil Engineers; September 2015. https://doi.org/10.1680/ecsmge.60678.vol5.379.

[12] Pahud D. Geothermal energy and heat storage. Cannobio: SUPSI – DCT – LEEE. Scuola Universitaria Professionale della Svizzera Italiana; 2002.

[13] Balfour Beatty Ground Engineering. Geothermal driven piles. 2016. Available online, URL, https://www.balfourbeatty.com/media/29535/geothermal-driven-piles.pdf.

[14] Park H, Lee S-R, Yoon S, Choi JC. Evaluation of thermal response and performance of PHC energy pile: field experiments and numerical simulation. Appl Energy 2013;103:12–24. https://doi.org/10.1016/j.apenergy.2012.10.012.

[15] Jalaluddin AM, Tsubaki K, Inoue S, Yoshida K. Experimental study of several types of ground heat exchanger using a steel pile foundation. Renew Energy 2011;36:764–71. https://doi.org/10.1016/j.renene.2010.08.011.

[16] Lennon DJ, Watt E, Suckling TP. Energy piles in Scotland. In: Van Impe, Van Impe, editors. Proceedings of the Fifth International conference on deep foundations on Bored and Auger Piles, Frankfurt, Germany, 15 may 2009. Taylor & Francis Group, London; 2009.

[17] Mogensen P. Fluid to Duct wall heat transfer in Duct system heat storage. In: Proceedings of the International conference on subsurface heat storage in theory and practice, Stockholm, Sweden. Swedish Council for Building Research; June 6-8, 1983. p. 652–7.

[18] Gehlin S. Thermal response test. Method development and evaluation. PhD Thesis. Luleå, Sweden: Luleå University of Technology; 2002.

[19] Spitler JD, Gehlin SEA. Thermal response testing for ground source heat pump systems - an historical review. Renew Sustain Energy Rev 2015;50:1125–37. https://doi.org/10.1016/j.rser.2015.05.061.

[20] Carslaw HS, Jaeger JC. Conduction of heat in solids. UK: Clarendon Press, Oxford Science Publications; 1959, ISBN 0-19-853368-3.

[21] Ingersoll LR, Zobel OJ, Ingersoll AC. Heat conduction with engineering, geological, and other applications. Madison, Wisconsin: Ed. The University of Wisconsin Press; 1954.

[22] Eskilson P. Thermal analysis of heat extraction. PhD Thesis. Lund, Sweden: University of Lund; 1987.

[23] Philippe M, Bernier M, Marchio D. Validity ranges of three analytical solutions to heat transfer in the vicinity of single boreholes. Geothermics 2009;38: 407–13. https://doi.org/10.1016/j.geothermics.2009.07.002.

[24] Li M, Lai ACK. New temperature response functions (G functions) for pile and borehole ground heat exchangers based on composite-medium line-source theory. Energy 2012;38:255–63. https://doi.org/10.1016/j.energy.2011.12.004.

[25] Bandos TV, Campos-Celador Á, López-González LM, Sala-Lizarraga JM. Finite cylinder-source model for energy pile heat exchangers: effects of thermal storage and vertical temperature variations. Energy 2014;78:639–48. https://doi.org/10.1016/j.energy.2014.10.053.

[26] Li M, Lai AC. Review of analytical models for heat transfer by vertical ground heat exchangers (GHEs): a perspective of time and space scales. Appl Energy 2015;151:178–91. https://doi.org/10.1016/j.apenergy.2015.04.070.

[27] Javed S, Fahlén P, Claesson J. Vertical ground heat exchangers: a review of heat flow models. In: Proceedings of Effstock 2009; 14–17 June 2009. Stockholm, Sweden.

[28] Witte HJL. Error analysis of thermal response tests. Appl Energy 2013;109: 302–11. https://doi.org/10.1016/j.apenergy.2012.11.060.

[29] Signorelli S, Bassetti S, Pahud D, Kohl T. Numerical evaluation of thermal response tests. Geothermics 2007;36:141–66. https://doi.org/10.1016/j.geothermics.2006.10.006.

[30] Loveridge FA, Brettmann T, Olgun CG, Powrie W. Assessing the applicability of thermal response testing to energy piles. In: At global perspectives on the sustainable Execution of foundations works, Sweden; May 2014. p. 21–3.

[31] Loveridge F. The thermal performance of foundation piles used as heat exchangers in ground energy systems. PhD Thesis. Southampton, UK: University of Southampton; 2012.

[32] GSHP Association. Thermal pile: design, installation & materials standards. National energy centre, Davy Avenue. Knowlhill, Milton Keynes: Ground Source Heat Pump Association; 2012.

[33] Loveridge F, Powrie W, Nicholson D. Comparison of two different models for

pile thermal response test interpretation. Acta Geotech 2014;9:367–84. https://doi.org/10.1007/s11440-014-0306-3.

[34] Hu P, Zha J, Lei F, Zhu N, Wu T. A composite cylindrical model and its application in analysis of thermal response and performance for energy pile. Energy Build 2014;84:324–32. https://doi.org/10.1016/j.enbuild.2014.07.046.

[35] Yu K, Singh R, Bouazza A, Bui H. Determining soil thermal conductivity through numerical simulation of a heating test on a heat exchanger pile. Geotech Geol. Eng. 2015;33:239–52. https://doi.org/10.1007/s10706-015-9870-z.

[36] Badenes B, De Santiago C, Nope F, Magraner T, Urchueguía J, De Groot M, Pardo De Santayana F, Arcos JL, Martín F. Thermal characterization of a geothermal precast pile in Valencia (Spain). In: Proceedings of the European geothermal congress 2016, Strasbourg, France; September 2016. p. 19–24.

[37] Zarrella A, Emmi G, Zecchin R, De Carli M. An appropriate use of the thermal response test for the design of energy foundation piles with U-tube circuits. Energy Build 2017;134:259–70. https://doi.org/10.1016/j.enbuild.2016.10.053.

[38] Loveridge F, Powrie W. Temperature response functions (G-functions) for single pile heat exchangers. Energy 2013;57:554–64. https://doi.org/10.1016/j.energy.2013.04.060.

[39] Alberdi-Pagola M, Jensen RL, Poulsen SE. A performance case study of energy pile foundation at Rosborg Gymnasium (Denmark). In: Proceedings of the 12th REHVA world congress clima 2016. Aalborg, Denmark: Department of Civil Engineering, Aalborg University; 22-25 May 2016. p. 10.

[40] Centrum Paele A/S. Energipæle. 2002 [Online]. Available, http://www.centrumpaele.dk/paele/energipaele.html. [Accessed 3 August 2017].

[41] Bourne-Webb P, Bernard J-B, Friedemann W, Von Der Hude N, Pralle N, Uotinen VM, Widerin B. Delivery of energy geostructures. In: Laloui L, Di Donna A, editors. Energy geostructures. John Wiley & Sons, Inc; 2013.

[42] Alberdi-Pagola M, Poulsen SE, Jensen RL, Madsen S. Thermal response testing of precast pile heat exchangers: fieldwork report. In: Aalborg University, department of civil Engineering; 2016. Aalborg, Denmark.

[43] Alberdi-Pagola M. Thermal Response Test data of five quadratic cross section precast pile heat exchangers. Data in Brief 2017.

[44] Hot Disk AB. Hot Disk thermal constants analyser TPS 1500 unit. In: Instruction manual; 2014.

[45] COMSOL Multiphysics. In: COMSOL Multiphysics version 5.1: user's guide. Burlington: COMSOL; 2015.

[46] COMSOL Multiphysics. In: Pipe flow module - user's guide. COMSOL; 2012.

[47] Churchill SW. Friction factor equations spans all fluid-flow regimes. Chem Eng J 1977;84:94–5.

[48] Abdelaziz SLAM. Deep energy foundations: geotechnical challenges and design considerations. PhD Thesis. Virginia Polytechnic Institute and State University; 2013.

[49] Loveridge F, Cecinato F. Thermal performance of thermoactive continuous flight auger piles. Environ Geotech 2016;3(4):265–79.

[50] Al-Khoury R. Computational modeling of shallow geothermal systems. Leiden, The Netherlands: CRC Press; 2011.

[51] Spitler JD, Bernier M. Vertical borehole ground heat exchanger design methods. In: Rees SJ, editor. Advances in ground-source heat pump systems. Woodhead Publishing; 2016.

[52] Kelvin TW. Mathematical and physical papers. London: Cambridge University Press; 1882.

[53] Baudoin A. Stockage intersaisonnier de chaleur dans le sol par batterie d'échangeurs baïonnette verticaux modèle de prédimensionnement. PhD Thesis. France: Université de Reims; 1988.

[54] Shonder JA, Beck JV. Field test of a new method for determining soil formation thermal conductivity and borehole resistance. ASHRAE Transactions 2000;106:843–50.

[55] Poulsen SE, Alberdi-Pagola M. Interpretation of ongoing thermal response tests of vertical (BHE) borehole heat exchangers with predictive uncertainty based stopping criterion. Energy 2015;88:157–67. https://doi.org/10.1016/j.energy.2015.03.133.

[56] Doherty J. PEST model-independent parameter estimation. User manual. Watermark Numerical Computing; 2010. http://www.pesthomepage.org/Downloads.php.

[57] Dansk Geoteknik A/S. Geoteknisk rapport. Grundundersøgelser for Amtsgymnasium i Vejle, Vestre Engvej, Vejle. 1973.

[58] Austin WA. Development of an in-situ system and analysis procedure for measuring ground thermal properties. ASHRAE Trans 2000;106(1):365–79.

[59] Witte HJL, Gelder GJV, Spitler JD. In situ measurement of ground thermal conductivity: a Dutch Perspective. ASHRAE Trans 2002;108:263–72.

[60] Low JE, Loveridge FA, Powrie W, Nicholson D. A comparison of laboratory and in situ methods to determine soil thermal conductivity for energy foundations and other ground heat exchanger applications. Acta Geotech 2014;10: 209–18. https://doi.org/10.1007/s11440-014-0333-0.

4.2. LESSONS LEARNT

Figure 10 in Paper A shows that the 2D FEM provide a good estimation of the pile concrete thermal resistance. This indicates that not just the length of the pile but also the cross-section shape need to be considered to get reliable estimates from TRT data.

When selecting an equivalent radius r_b to approximate the square shape to a circle, three options are considered (Figure 4-1): the hydraulic radius, i.e., half of the side length for square ducts; a radius that provides an equivalent circumference to the square perimeter, called equivalent perimeter; and a radius that provides the same area as the area of the square, named equivalent area. This affects the location of the pipes, varying the space between them, also known as shank spacing. As shown in Figure 4-1, the pipes would rearrange so that the distance from the centre of the pipe to the pile wall is kept to 5 cm to respect the concrete cover.

Shape	Radius [m]	Shank spacing [m]	Volume per meter length [m³/m]
Square 0.3x0.3 m²	-	0.269	0.090
Equivalent perimeter	0.191	0.272	0.115
Equivalent area	0.169	0.229	0.090
Hydraulic diameter	0.150	0.190	0.071

— Original square shape
- - - Equivalent perimeter
- - - - Equivalent area
- - - - Hydraulic diameter
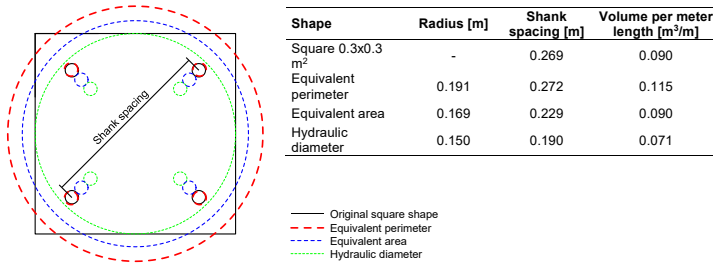
Figure 4-1: Options to establish an equivalent radius to approximate a square to a circle.

The equivalent perimeter option has been chosen as it closely maintains the original position of the pipes in the cross-section geometry. According to [158], for short time simulations a model that accounts for the geometry of the ground heat exchanger is required.

To understand the disagreement between the concrete thermal resistances R_c determined by the methods that do not account for the square shape, 3D FEM simulations of cylindrical piles have been carried out. A hundred hours TRTs are simulated for cylindrical piles with equivalent perimeter and equivalent area cross sections. The active length of the pile heat exchangers is 16.8 m and single-U and W-shape pipe arrangements are used. The concrete thermal resistances R_c and the thermal field of horizontal cross sections are compared to square prism FEM, used as references.

Figure 4-2 shows the thermal resistances obtained with the cylindrical piles, normalised with the thermal resistance of the square pile. It shows that the use of a radius providing an equivalent perimeter, or an equivalent area hardly affects the estimated concrete thermal resistance. It could be expected that a bigger ground heat

exchanger would have a higher thermal resistance, however, the bigger influence between the pipes going up and down (short circuiting) in the smaller geometries counteracts the effect of the size.
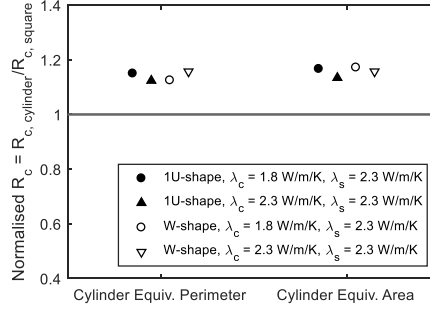
Figure 4-2: Normalised pile concrete thermal resistances R_c calculated with 3D FEM of cylindrical piles heat exchanger with an equivalent perimeter and with an equivalent area, for different soil concrete thermal conductivity ratios.

Figure 4-3 shows temperature contour maps in and around a pile heat exchanger after 100 hours of constant heat injection. The cross sections belong to a slide that halves the pile length.
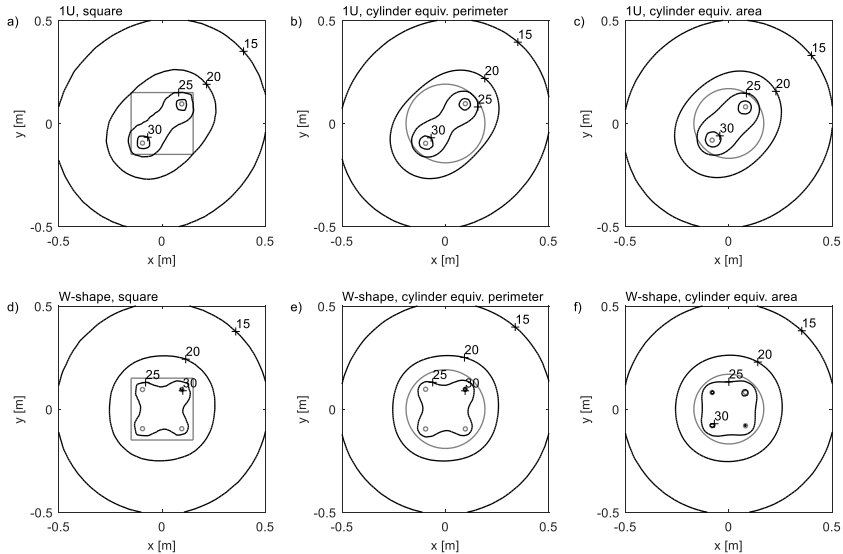
Figure 4-3: Temperature contour maps in and around a pile heat exchanger after 100 hours of constant heat injection. The cross sections belong to a slide that halves the pile length. The pile cross section shape is drawn in grey.

When using a cylindrical ground heat exchanger instead of a square prism, the temperature field is not distributed the same way nor over the horizontal cross section of the pile, nor along the pile wall. Due to the square shape, there is a higher average temperature distribution on the pile wall compared to the circular shaped, what provides a thermal resistance 15% lower than for the latter. The different thermal field distribution also provokes that the concrete thermal resistance is higher for the single-U pipes compared to the W-shape pipes, as obtained in Table 6 in Paper A. However, the temperature contours radially develop very similar in all cases meaning that to tens of centimetres from the pile wall, the temperature field distribution is independent of the shape of the pile.

For further information, please refer to Appendixes I, III and IV.

CHAPTER 5. THERMAL DESIGN METHOD FOR MULTIPLE PILE HEAT EXCHANGERS

5.1. SCOPE AND MOTIVATION

Based on the findings from Paper A, the semi-empirical models for single piles provided acceptable estimates at a low computational cost, we decide to generate our own semi-empirical dimensionless temperature g-functions for multiple energy piles, utilising 3D FEM simulations of single energy piles with temporal and spatial superposition techniques. To check the reliability and accuracy of this method for simulating thermally interacting energy piles, full 3D FEM of groups of energy piles are used as reference. We compare average fluid temperatures of small energy pile arrangements, up to 16 energy piles.

5.1.1. PAPER B

The following manuscript, denoted Paper B, is under review by Geothermics.

Alberdi-Pagola, M., Poulsen, S.E., Jensen, L.J. and Madsen, S., (under review). "Design methodology for precast quadratic pile heat exchanger-based shallow geothermal ground-loops: multiple pile g-functions", *Geothermics*.

Reprinted by permission from Elsevier.

Design methodology for precast quadratic pile heat exchanger-based shallow geothermal ground-loops: multiple pile g-functions

Maria Alberdi-Pagola [a, *], Søren Erbs Poulsen [b],

Rasmus Lund Jensen [a], Søren Madsen [a]

[a] *Department of Civil Engineering, Aalborg University, Denmark.*

[b] *VIA Building, Energy & Environment, VIA University College, Denmark.*

* Corresponding author. Department of Civil Engineering, Thomas Manns Vej 23, 9220 Aalborg Øst, Denmark. E-mail address: mapa@civil.aau.dk (M. Alberdi-Pagola).

_____

Abstract

This paper investigates the applicability of numerical and semi-empirical heat flow models for calculating average fluid temperatures in groups of quadratic, precast pile heat exchangers. A 3D finite element model (FEM), verified with experimental data, is extended to account for multiple pile heat exchangers. We develop semi-empirical dimensionless temperature g-functions for multiple piles by utilising 3D FEM heat transport simulations with temporal and spatial superposition techniques to account for the thermal interaction between piles. We find that the multiple pile g-functions yield fluid temperatures similar to those obtained with full 3D modelling, at minimal computational cost.

Keywords: Pile heat exchanger, energy pile, g-functions, multiple piles, interaction, 3D finite element model, semi-empirical model.

1. Introduction

Ground source heat pump (GSHP) systems yield renewable thermal energy that offer high levels of efficiency for space heating and cooling (Ahmad, 2017; Rees, 2016). The use of GSHP systems has risen 50% between 2010 and 2015, primarily, due to their ability to use relatively steady ground temperatures anywhere in the world (Ahmad, 2017; Olgun and McCartney, 2014).

Energy piles are traditional foundation piles with embedded fluid pipes that serve as ground heat exchangers (Alberdi-Pagola et al., 2018a; Bourne-Webb et al., 2013; Brettman et al., 2010; Jalaluddin et al., 2011; Laloui and Nuth, 2009; Li and Lai, 2012; Loveridge et al., 2014a; Pahud, 2002; Park et al., 2013, 2015; Vieira et al., 2017). The thermal analysis of energy pile foundations is typically addressed by methods developed for borehole heat exchanger (BHE) fields (ASHRAE, 2009; Buildingphysics, 2008; Oklahoma State University, 1988; Spitler, 2000; Spitler and Bernier, 2016). However, standard methods for BHEs are not well suited for analysing the thermal dynamics of energy piles (Figure 1).
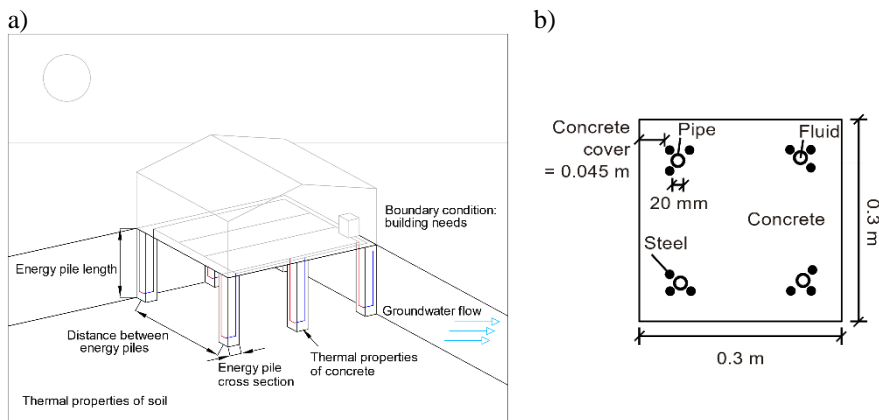
Figure 1: a) Main parameters affecting the thermal behaviour of energy pile foundations. b) Horizontal cross section of the W-shape energy pile studied in this paper.

Firstly, piles are shorter and wider than boreholes. Energy pile aspect ratios (length to diameter ratio), typically fall below 50, while corresponding ratios for BHEs range 200-1500. Secondly, while BHEs typically are arranged in regular grids, piles are placed irregularly in clusters (from singles to fours) which is determined by the structural requirements of the building. Thirdly, fluid temperatures in energy piles must be kept above 0 to 2 °C to ensure structural integrity and to avoid soil freezing and deterioration of the bearing capacity (GSHP Association, 2012; VDI, 2001).

Heat transfer in energy pile foundations is governed by the dynamics of the thermal requirements of the building, the thermal properties of the soil, concrete and heat carrier fluid, the aspect ratio and spacing between the energy piles, the thermal

influence of the ground surface and the presence of groundwater flow, if any (Figure 1a).

The thermal dynamics of a single energy pile can be analysed by: i) analytical solutions such as the infinite line (Kelvin, 1882), the infinite cylinder (Baudoin, 1988) and the infinite solid sources (Bandos et al., 2014), their finite equivalents (Bandos et al., 2014; Lamarche and Beauchamp, 2007; Philippe et al., 2009; Zeng et al., 2002) and the composite medium model (Li and Lai, 2012); ii) numerical models (Alberdi-Pagola et al., 2018a; Signorelli et al., 2007) and iii) semi-empirical models (Loveridge and Powrie, 2013; Zanchini and Lazzari, 2013). Yet, the long-term performance of energy pile foundations must take into account the thermal interaction between piles.

A common approach to address the thermal influence between piles is the application of the so-called g-functions for multiple ground heat exchangers, first introduced by Eskilson (1987). The g-function is a type curve of dimensionless time and ground heat exchanger wall temperatures assuming a constant, applied power. Eskilson (1987) calculated the thermal interaction by spatial superposition of single BHE temperatures, based on the finite difference method. A similar approach was adopted by Maragna (2016) and Maragna and Rachez (2015).

In general, multiple heat exchanger g-functions can be calculated by spatial superposition of single ground heat exchanger analytical solutions that permit calculation of the radial temperature distribution (Cimmino et al., 2013; Cimmino and Bernier, 2014; Fossa, 2011; Fossa et al., 2009; Fossa and Rolando, 2014; Katsura et al., 2008). A different approach is the ASHRAE method, where the temperature penalty concept is defined to account for thermal interactions between individual heat exchangers (Bernier et al., 2008, 2004; Fossa and Rolando, 2015; Philippe et al., 2010). Multiple heat exchanger g-functions have been calculated by means of numerical methods as well (Acuña et al., 2012).

The PILESIM software (Pahud et al., 1999), that utilises the duct storage model (Hellström, 1991) for analysing pile heat exchangers, has been validated with field data in Pahud and Hubbuch (2007), however, it does not allow the analysis of irregular pile configurations. To overcome this drawback, Loveridge and Powrie (2013 and 2014a) proposed the use of semi-empirical models based on numerical analyses, following a similar method to that proposed by Zanchini and Lazzari (2013 and 2014) for borehole heat exchanger fields. For further details on these topics, see (Cimmino and Bernier, 2014; Eskilson, 1987; Fossa and Rolando, 2015; Loveridge and Powrie, 2014a).

Alberdi-Pagola et al. (2018a) and Vieira et al. (2017) suggest that semi-empirical g-functions are potentially suitable for the thermal analysis of pile heat exchangers. 3D simulation-based analysis of multiple pile heat exchanger foundations is highly impractical due to excessive computation times and simpler models are required for real applications. From a practical point of view, it is relevant to further investigate the potential of utilising semi-empirical models for analysing the thermal performance of energy pile foundations.

This paper continues the work presented in Alberdi-Pagola et al. (2018a) and Loveridge and Powrie (2013 and 2014a) and aims to analyse the applicability and

accuracy of semi-empirical g-functions for calculating fluid temperatures in energy pile foundation based GSHP systems.

The average energy pile foundation fluid temperatures are calculated with a full 3D finite element model (FEM) and semi-empirical models, respectively. Firstly, single pile 3D FEM modelled fluid and soil temperatures are compared to corresponding field observations which include thermal response test data and simultaneous temperature measurements at a distance. The validated 3D model is then extended to include multiple piles. Secondly, polynomial g-functions are fitted to dimensionless temperatures calculated with the single pile 3D model. To obtain the temperature field for an ensemble of piles assuming a dynamic thermal load, we carry out temporal and spatial superposition of single pile g-functions and compare it to corresponding full 3D modelled multi-pile temperatures.

2. Experimental data

The thermal response test (TRT) is a field test developed for borehole heat exchangers (Gehlin, 2002; Javed et al., 2011; Mogensen P., 1983), which can also be adapted to pile heat exchangers (Alberdi-Pagola et al., 2018a; Loveridge et al., 2014b; Vieira et al., 2017). The analysis of the TRT data yields the undisturbed soil temperature T_0 [°C], the thermal conductivity of the soil λ_s [W/m/K] and the thermal resistance of the pile R_c [K·m/W]. During the TRT, the heat carrier fluid is circulated in the ground heat exchanger while being continuously heated at a constant rate. As heat dissipates to the ground the fluid inlet- and outlet temperatures and the fluid flow rate are recorded in 10-minute intervals, for, at least, 60-70 hours in the case of precast pile heat exchangers (Alberdi-Pagola et al., 2018a).
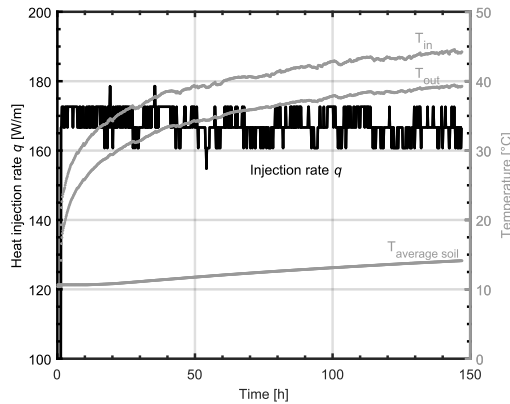
Figure 2: Thermal response testing (TRT) field data of pile heat exchanger LM3 (16.8 m active length and W-shape pipe arrangement) and average soil temperatures after Alberdi-Pagola (2018) and Alberdi-Pagola et al. (2017a).

The data used in this paper is shown in Figure 2 and it corresponds to the pile heat exchanger named LM3 analysed in Alberdi-Pagola (2018). The fluid and heat rate measurements are supplemented with soil temperatures measured simultaneously at a distance of 0.90 m from the pile centre (Alberdi-Pagola et al., 2017a). The soil temperatures comprise a weighted average of five temperature sensors placed at depths of 2, 6, 10, 14 and 18 m from the ground surface. The data serve to verify the models described below.

3. Methods

The 3D FEM models are described, and pile g-functions are presented subsequently. Finally, the analysed energy pile patterns are described.

3.1. 3D finite element models

3.1.1. Single pile 3D finite element model

The software COMSOL Multiphysics (COMSOL Multiphysics, 2017) is utilised for calculating the subsurface temperature response in and around the pile heat exchanger. In the model, the ground is assumed to be thermally isotropic and homogeneous. The thermal interaction between the energy pile and the surrounding soil is modelled by conduction and advection in the heat exchanger pipes, in a similar way to the models developed in Alberdi-Pagola et al. (2018a). The 3D model contains three domains (Figure 3): the soil, the concrete pile and the heat exchanger pipe, cast into the concrete. The cross section of the modelled pile is given in Figure 1b. Advective heat transfer due to groundwater flow is not considered.
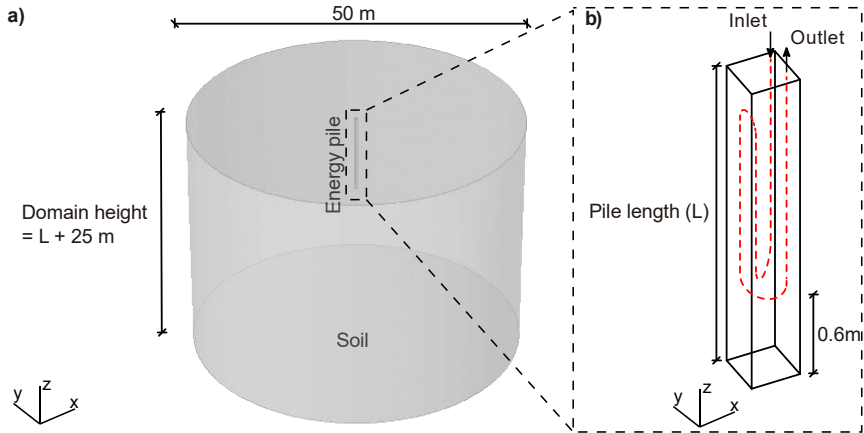
Figure 3: Description of the 3D finite element model simulated in COMSOL: a) simulated meshed domains; b) schematic of the W-shape pile heat exchanger (figure not scaled).

Alberdi-Pagola et al. (2018a) validated the single pile 3D FEM model utilised in this study by demonstrating excellent agreement between measured and simulated fluid and soil TRT temperatures. Given the greater time scales considered in this study relative to the ones in Alberdi-Pagola et al. (2018a), the model domain is enlarged and extends 50 m horizontally and from top pile to 25 m below the pile. Model tests have been conducted to ensure that modelled temperatures are independent of the chosen level of temporal and spatial discretisation.

The initial temperature in the model domain is set to 10 °C, based on the observed initial average undisturbed soil temperature shown in Figure 2. The temperature at the domain boundaries is fixed and equal to the initial temperature

To ensure the maintenance of a specific heat injection rate [W/m], a synthetic inlet temperature history was generated during the time dependent numerical simulation by coupling it to the outlet temperature of the previous time step. The fluid (water in this study) flow imposed in the heat exchanger pipes is 0.000136 m^3/s and it yields a turbulent regime. The materials and corresponding thermal properties in the model are listed in Table 1.

Table 1. Thermal properties of the materials in the model.

Parameters	Value
Volumetric heat capacity concrete ρc_{pc} [MJ/m^3/K]	2
Thermal conductivity concrete λ_c [W/m/K]	2
Volumetric heat capacity soil ρc_{ps} [MJ/m^3/K]	2
Thermal conductivity soil λ_s [W/m/K]	1, 2, 4
Thermal conductivity pipe λ_p [W/m/K]	0.42

3.1.2. Multiple pile 3D finite element models

To assess the thermal interaction between piles, the model described in the previous section is extended to include multiple energy piles. The thermal load is implanted in two ways depending on the considered scenario. For a constant thermal load over time, non-isothermal heat transport and fluid advection in the heat exchanger pipes are considered. However, for a time varying thermal load, a uniform heating rate is applied on the outer pipe wall, excluding fluid flow and heat transport inside the pipe which saves computational efforts. The maximum difference in the average fluid temperature from applying a uniform heating rate on the pipe wall is 0.2 °C which is considered acceptable for this study. The pipe thermal resistance of the pipe wall is considered as described in the following section.

3.2. Pile g-functions

The average fluid temperature T_f [°C] in the energy pile is:

$$T_f = T_0 + \frac{q}{2\pi\lambda_s} G_g + qR_c G_c + qR_{pipe} \tag{1}$$

where T_0 [°C] is the undisturbed soil temperature, q [W/m] is the heat transfer rate per metre length of energy pile, λ_s [W/m/K] is the thermal conductivity of the soil, G_g is the g-function for the ground temperature response, R_c [K·m/W] is the steady state concrete thermal resistance, G_c is the concrete G-function for the transient response of the pile and R_{pipe} [K·m/W] is the thermal resistance of the pipes.

G-functions are dimensionless curves of the change in temperature in the ground over time from applying a thermal load on the pile (Eskilson, 1987). The dimensionless temperature Φ and time Fo are:

$$\Phi = \frac{2\pi\lambda_s\Delta T}{q} \tag{2}$$

$$Fo = \frac{\alpha_s t}{r_b^2} \tag{3}$$

where ΔT [°C] is the temperature change relative to the undisturbed soil temperature T_0 [°C] and the average pile wall temperature T_b [°C], α_s [m²/s] is the thermal diffusivity, t [s] is the time and r_b [m] is the pile equivalent radius. The pile radius is defined as the equivalent circumference to the square perimeter. For a single pile, the pile wall temperature depends on time and its aspect ratio (AR = $L/2r_b$):

$$T_b = T_g + \frac{q}{2\pi\lambda_s} \cdot G(Fo, \frac{L}{2r_b}) \tag{4}$$

The pile g-functions in this study are derived from 3D temperature modelling of a single energy pile. The valid time ranges are 0.1 < Fo < 10000. The temperature response of the pile depends on the length of the energy pile. Thus, typical aspect ratios of 15, 30 and 45 are considered.

The multiple pile g-functions are derived from 3D FEM calculated temperatures for a single pile. The simulations yield soil temperatures at specified radial distances in addition to the pile wall temperatures. The multiple pile g-functions serve to compute the average pile wall temperature over time for all piles (Spitler and Bernier, 2016):

$$T_{bm} = T_0 - \frac{q}{2\pi\lambda_s} \cdot G_g(Fo, \frac{L}{2r_b}, \frac{S}{2r_b}) \tag{5}$$

where T_{bm} [°C] is the average pile wall temperature for an ensemble of piles and G_g is the multiple pile g-function, which depend on the dimensionless time Fo, the pile aspect ratio AR and the foundation aspect ratio $S/2r_b$, S being the pile spacing, as defined in Loveridge and Powrie (2014a).

To account for the thermal interaction between piles, the g-function is calculated by applying temporal (Spitler and Bernier, 2016) and spatial superposition (Cimmino et al., 2013) of the single pile G-function and radial temperatures. It is further assumed that the total heat load is distributed equally on the piles.

The pile G-function, as defined by Loveridge and Powrie (2013 and 2014b), accounts for the temporal development of pile thermal resistance which depends on the shape of the pile cross section, the position of the pipes and the thermal conductivity of the concrete λ_c. The full temperature response (Equation 1) includes the proportion of steady state pile thermal resistance that is realised at a given time Fo which is estimated with the 3D FEM model. The pile thermal resistance is:

$$R_c = \frac{T_p - T_b}{q} \qquad (6)$$
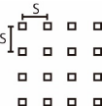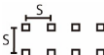
where T_p [°C] is the average temperature on the outer wall of the pipe.

The pipe thermal resistance R_{pipe} [K·m/W] includes the integrated convective and conductive resistances between the fluid and the concrete. Heat transport in the pipes reaches steady state quickly and, consequently, the pipe thermal resistance is considered constant. R_{pipe} is estimated as suggested by Al-Khoury (2011) and Diersch (2014), using Gnielinski's correlation to obtain the corresponding heat transfer coefficients. A detailed explanation of the method is given in Alberdi-Pagola et al. (2018b).

3.3. Energy pile patterns

Average fluid temperatures are calculated for six regular patterns (listed in Table 2). One irregular pattern is also analysed, based on a realistic geometrical arrangement of nine piles. The aspect ratio is 45 in all computations.

Table 2. Selected pile heat exchanger field configurations for present model comparisons.

Pattern		Spacing S [m]	Pattern		Spacing S [m]
1x2		1, 3, 5	3x3		3, 5
1x3		1, 3, 5	4x4		3, 5
2x3		3, 5			
2x4		3, 5	Irregular		(2.6, 12.4)

4. Results and discussion

Firstly, the single pile 3D model is compared to experimental TRT data to demonstrate its validity. The multiple pile g-functions are applied to simulation of two long periods of thermal loading. G-function temperatures are then compared to corresponding 3D FEM simulations.

4.1. Short term, single pile 3D FEM

Single pile 3D FEM modelled temperatures were computed for the TRT calibrated thermal parameters listed in Table 3, after Alberdi-Pagola et al. (2018a). The measured inlet temperature serves as a boundary condition for the pipe inlet in the 3D FEM model. Figure 4 shows a close match between measured and 3D FEM modelled average fluid and soil temperatures.

Table 3. Thermal properties used in the models for the forward runs, from calibration results of pile LM3 in Alberdi-Pagola et al. (2018a).

λ_s [W/m/K]	λ_c [W/m/K]	ρc_{ps} [MJ/m^3/K]	ρc_{pc} [MJ/m^3/K]
2.25	2.40	2.60	2.00
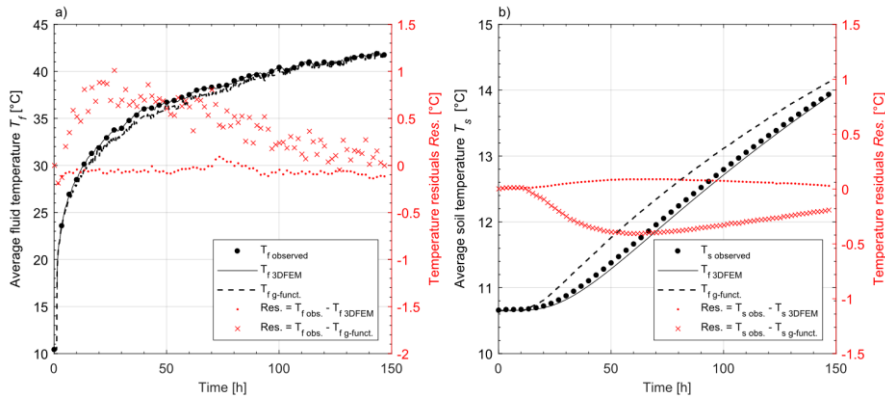
Figure 4: TRT and soil temperatures measured at a distance of 0.90 m from the pile centre. a) Observed and modelled average fluid temperatures and residuals. b) Observed and modelled average soil temperatures and residuals. The residuals are defined as the difference between observed and simulated temperatures.

4.2. Pile thermal interaction

The 3D FEM simulations serve to investigate whether concrete thermal resistance Rc is altered due to the thermal disturbance from nearby energy piles. The steady state concrete thermal resistance is calculated for two interacting piles spaced 1, 3 and 5 m

apart and then compared to the corresponding single pile concrete thermal resistance R_c (Table 4).

The presence of an additional pile has no clear effect on the steady state thermal resistance. The maximum change is 5.6% which is considered insignificant. This is in agreement with findings by Loveridge and Powrie (2014a), and therefore, it is considered appropriate to assume that the steady state pile resistance is independent of external thermal disturbances from nearby energy piles.

Table 4. Steady state pile concrete resistances R_c for single piles and two interacting piles at different pile spacings S.

		$\lambda_c = 2$ W/m/K $\lambda_s = 4$ W/m/K	$\lambda_c = 2$ W/m/K $\lambda_s = 2$ W/m/K
	Single pile	0.053	0.056
R_c [K·m/W]	2 piles, S = 1 m	0.055	0.059
	2 piles, S = 3 m	0.054	0.058
	2 piles, S = 5 m	0.054	0.057

As a further step, the temporal development in concrete thermal resistances R_c is calculated for a single pile and interacting piles, respectively. Figure 5 shows proportion of steady state concrete thermal resistances for the case of a single pile and two piles spaced 1, 3 and 5 m apart. At early times Fo < 0.1, the discrepancies are within a few percent and the lines for the two-pile models converge rapidly. Since Fo = 0.1 is less than 1 hour, it suffices to use single pile curves which is in accordance with Loveridge and Powrie (2014a).
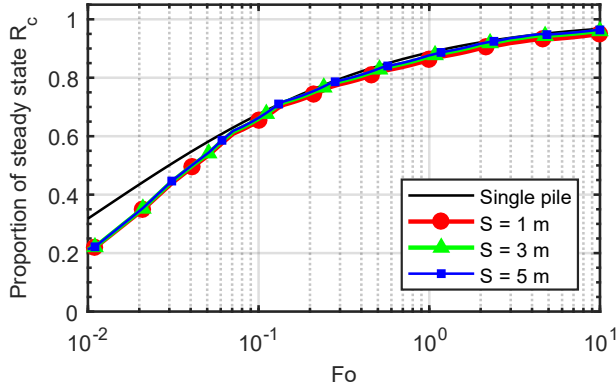
Figure5: Concrete G-functions for individual and pairs of interacting piles at different spacings S. Curves for $\lambda_s = 4$ W/m/K and $\lambda_c = 2$ W/m/K.

4.3. Pile g-functions

4.3.1. Single pile ground temperature g-functions

Single pile g-functions G_g with dimensionless ground temperature Φ and time Fo are plotted in Figure 6 for a range of aspect ratios and assuming identical thermal conductivity of the soil and concrete. The presented G-functions are fitted with 9th order polynomials. The coefficients are given in Alberdi-Pagola et al. (2018b).
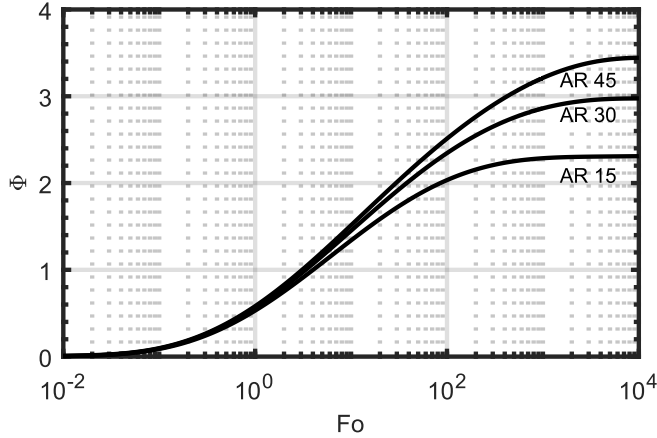
Figure 6: Pile G-functions for different aspect ratios (AR) 45, 30 and 15.

4.3.2. Single pile concrete g-functions

Alberdi-Pagola et al. (2018a) demonstrated that 96% of the steady state thermal resistance of the pile is reached by 100 hours (Fo ≈ 10). Consequently, it is assumed that the steady state pile thermal resistance is fully realised at Fo = 1000. Similar to the methodology presented in Alberdi-Pagola et al. (2018a) and Loveridge and Powrie (2014b), the pile thermal resistance is calculated for different ratios between soil and concrete thermal conductivity, λ_c/λ_s (Figure 7a).

The temporal development in the proportion of steady state pile thermal resistance R_c is shown in Figure 7b for ratios $\lambda_c/\lambda_s = 0.5$, 1 and 2. The curves differ at very short times and converge for Fo < 1, i.e., approximately 8 hours. R_c G-function curve fits are presented in Alberdi-Pagola et al. (2018b).
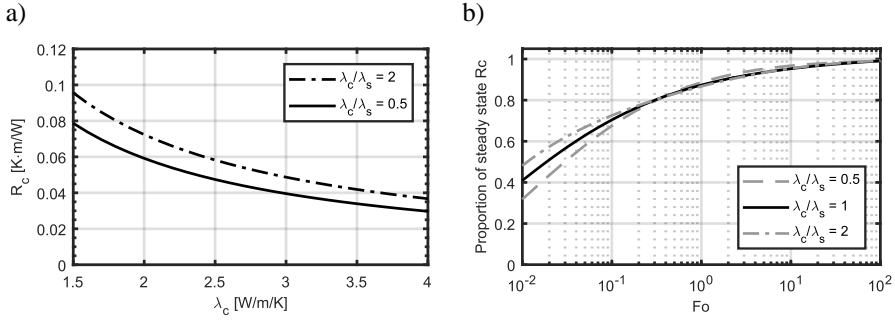
Figure 7: a) 3D model estimated upper and lower bounds for the concrete thermal resistance R_c, (Alberdi-Pagola et al. (2018a). b) Proportion of steady state R_c.

4.3.3. Pile g-functions

The single pile g-function and the corresponding 3D model was computed, respectively, with the thermal parameters provided in Table 3 (Figure 4). Relative to the simulated TRT, the residuals for the g-functions are larger than those of the 3D model. However, in both cases residuals are less than 3% relative to the observed average fluid temperature and 4% relative to the observed soil temperature, which are considered acceptable.

4.4. Modelled long-term behaviour

To illustrate the performance of the pile g-functions for simulating long-term operation, a comparison between the multiple pile 3D model and the multiple pile g-function computed temperatures given a constant heat injection rate and time-dependent heating, respectively.

4.4.1. Constant thermal load

Figure 8 shows the dimensionless temperatures curves computed with the multiple pile 3D model and the multiple pile g-functions, for the regular patterns listed in Table 2.

The temperatures calculated for different patterns are similar at short times, up to Fo = 700 at which point the curves diverge for the 2x3, 2x4, 3x3 and 4x4 patterns. Temperatures increase for larger foundations which is due to the thermal interaction between piles. Moreover, the difference between the computed multiple pile g-function and 3D modelled temperatures is greater for larger foundations. For the case of the 4x4 grid, the g-functions overestimate the 3D modelled temperatures by 20% for the case of 3 m pile spacing. The errors are larger for small pile spacings. This might be because the proposed model does not adequately capture the thermal dynamics in the nearest pile surrounding.
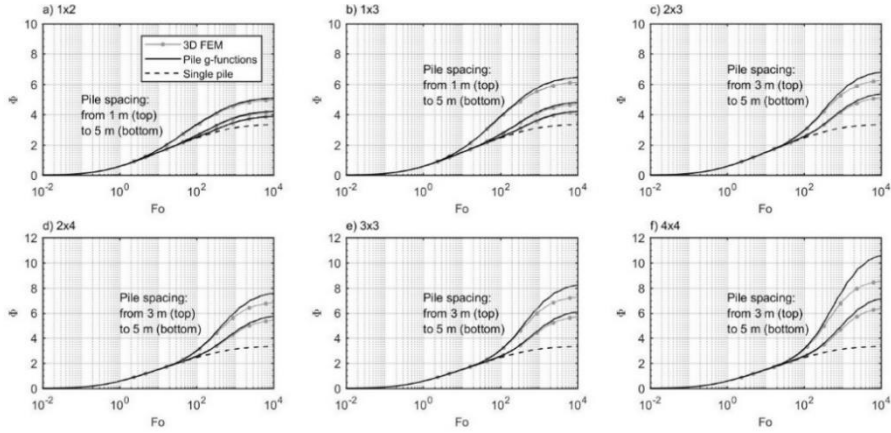
Figure 8: Regular pattern multiple pile g-functions and corresponding multiple pile 3D dimensionless temperatures assuming a constant thermal load. The single pile g-function corresponds to the curve for infinite pile spacing. Common legend for all subplots in a).

To understand the discrepancies between the proposed pile g-functions and the 3D model reference, non-dimensional soil temperature fields were contoured for the case of two piles spaced 1 m apart at times corresponding to 1 day, 1 year, 10 years and 25 years (Figure 9).
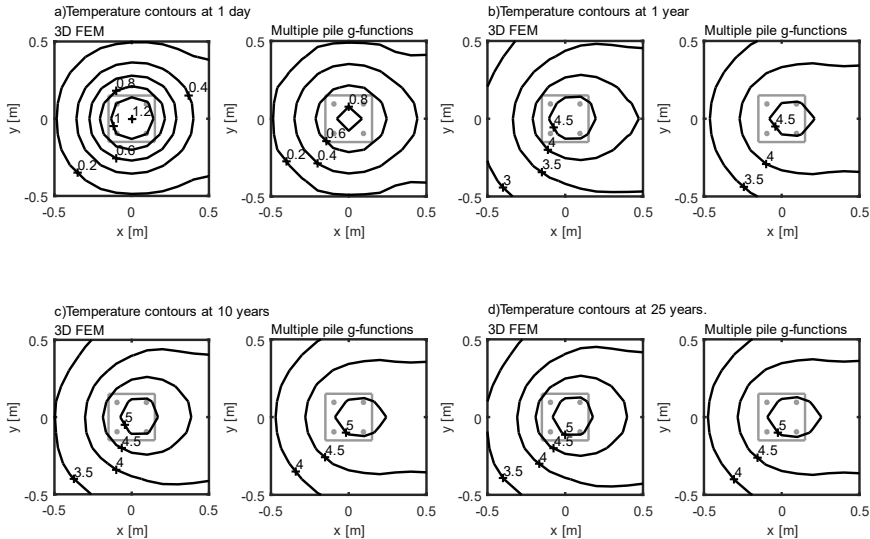
Figure 9: Temperature fields for two interacting piles with 1 m pile spacing, computed with the 3D FEM and the multiple pile g-functions at different times: a) 1 day; b) 1 year; c) 10 years and d) 25 years.

For times up to days, 3D modelled temperatures exceed corresponding g-functions, while for longer times, i.e., from 1 year on, g-functions exceed corresponding 3D model temperatures at the pile wall. The difference in g-function and 3D model computed temperatures (Figure 8) become larger as more piles are added. Error accumulation resulting from superposition methods have been reported before (Alberdi-Pagola et al., 2018b; Fossa, 2011; Fossa and Rolando, 2014) and studies have proposed correction functions, which depend on the number of boreholes and the form of the pattern, to overcome these issues (Capozza et al., 2012).

4.4.2. Time varying thermal load

Under operational conditions, the ground-loop is subjected to time varying thermal loads, due to the different heating/cooling needs of the buildings over the seasons. An annual sine-wave power profile based on operational temperatures is chosen, identical to that presented in Alberdi-Pagola et al. (2017b) (shown in Figure 10). The simulated, operational period is 10 years utilising daily averages of the thermal load.
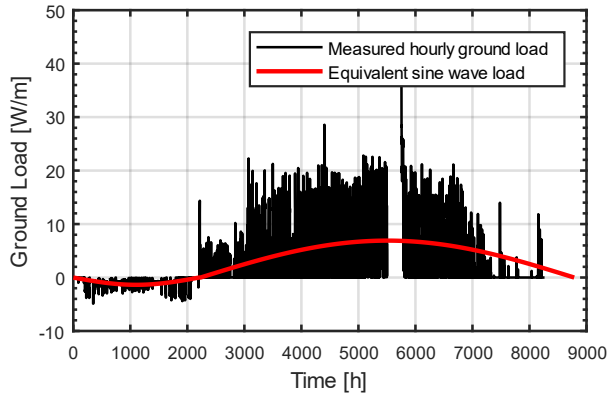
Figure 10: Equivalent sine wave for the measured one-year ground thermal load (positive = heat extraction; negative = heat injection) from Alberdi-Pagola et al. (2017b).

To assess the applicability of the pile g-functions simulations of the foundation patterns specified in Table 2 were performed for different soil and concrete thermal conductivity ratios k (where $k = \lambda_c/\lambda_s$): 0.5, 1 and 2.

Figure 11 shows computed temperatures for the 4x4 pattern with a 3-m pile spacing and the irregular pattern, respectively. A closer inspection of the initial 5 years of operation reveals a satisfactory match between g-function and 3D modelled temperatures. The maximum discrepancy is 0.5 °C (around 7%) for the case of the 4x4 pattern in which $k = 2$.
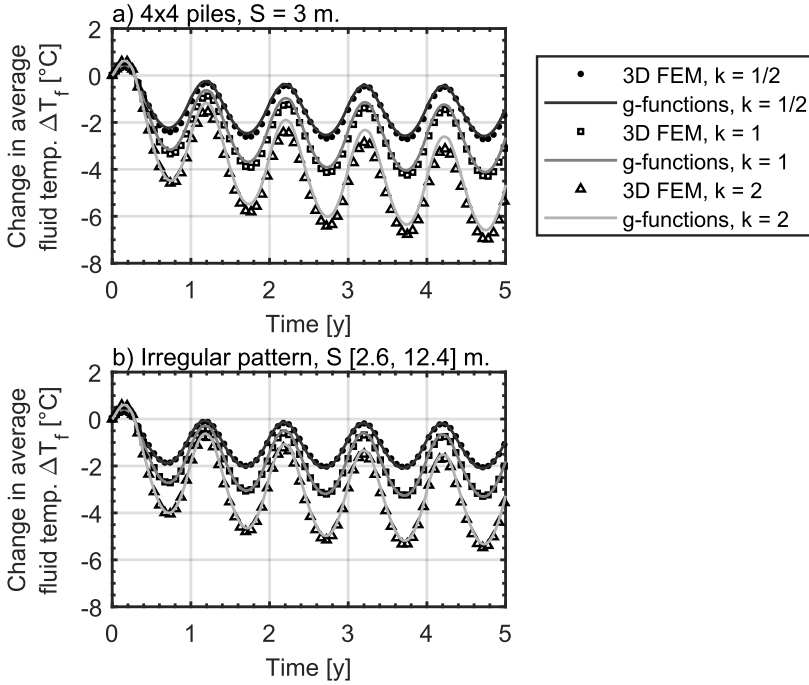
Figure 11: 3D modelled and g-function temperatures for 5 years of operation in the following cases: a) 4x4 pattern with a 3 m pile separation S (yields the highest average residual in Figure 12); b) irregular pattern. k = λ$_c$/λ$_s$. Common legend for both subplots.

Figure 12 summarizes the difference in temperatures computed with g-functions and 3D modelling for the analysed cases, normalised with the 3D FEM temperatures. The difference in computed temperatures increases for small pile spacing; when the number of pile heat exchangers increases; and for increasing k. As the number of piles increases, the need to interpolate between g-functions increases, hence, introducing additional errors in computed temperatures. As pile spacing increases, the error decreases since the contribution of each pile to the total g-function is smaller as the thermal influence decreases with distance.

It is concluded that the proposed multiple pile g-functions do not perfectly capture the heat transfer phenomena for short times. This is apparent in Figure 9a, where pile wall temperatures are slightly lower for the semi-empirical g-functions, and in Figure 4, where the average fluid temperatures simulated with the proposed g-functions fall below the 3D FEM temperatures. In any case, the differences are small and are considered acceptable for the purpose of this study.
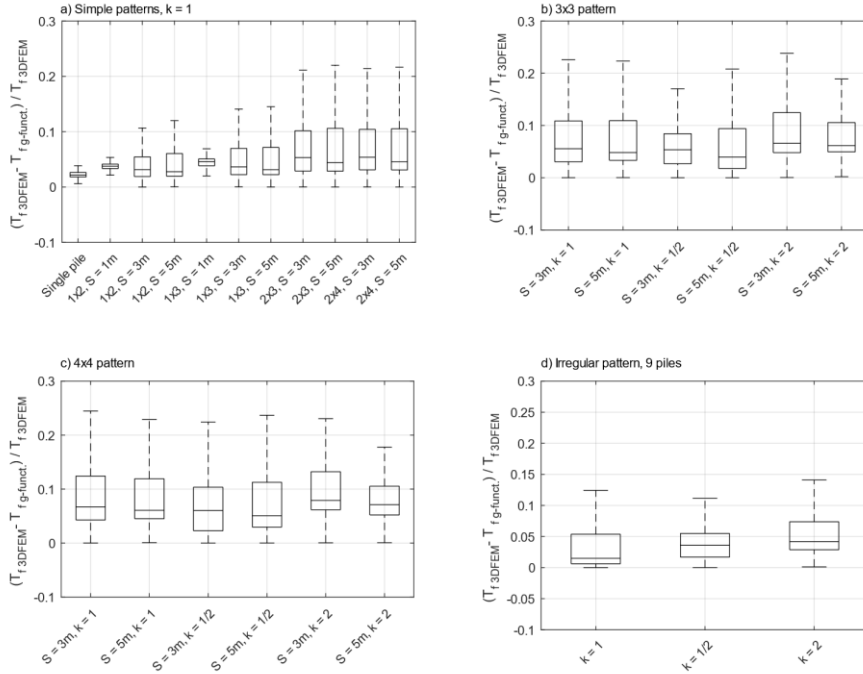
Figure 12: Normalised temperature difference boxplot where the central mark indicates the median. The bottom and top box edges indicate the 25th and 75th percentiles, respectively. S = pile spacing; k = λ_c/λ_s.

5. Conclusions

We apply 3D finite element modelling (FEM) and superposition methods for obtaining type curves for the dimensionless temperature response of multiple quadratic, precast foundation pile heat exchangers, under constant and time varying thermal loads.

The 3D FEM model accurately reproduces measured thermal response test fluid and soil temperatures. However, the computational burden of 3D FEM simulation of hundreds of energy piles is immense and certainly impractical. To that end, we employ 3D FEM to derive dimensionless type curves for the temperature response of a single energy pile and the ground, respectively (otherwise referred to as semi-empirical g-functions). To compute the thermal response for an ensemble of thermally interacting piles, we carry out spatial and temporal superposition of single pile responses, and thus obtain the corresponding g-function. The derived multiple pile g-functions account for the transient behaviour of the piles, their aspect ratio and the pile spacing. The pile and ground g-functions and the steady-state concrete thermal resistance are tabulated to ease the implementation.

The multiple pile g-functions yield reliable average fluid temperatures when compared to corresponding full 3D FEM simulations, however, they appear to not fully capture the short time thermal response. The largest deviation between 3D FEM and multiple pile g-functions under a time-varying thermal load is 7% and occurs for the 4x4 pattern when the thermal conductivity of the concrete is twice that of the soil. The error committed from using multiple pile g-functions rather than full 3D FEM is acceptable for practical use. As such, semi-empirical g-functions offer a fast and reliable basis for feasibility studies and for the dimensioning of the considered energy pile foundations.

Acknowledgements

References

Acuña, J., Fossa, M., Monzó, P. and Palm, B., 2012. Numerically Generated g-functions for Ground Coupled Heat Pump Applications, In *Proceedings of the COMSOL Conference in Milan*.

Ahmad, M., 2017. *Operation and Control of Renewable Energy Systems*. John Wiley & Sons. ISBN:9781119281689

Al-Khoury, R., 2011. *Computational modeling of shallow geothermal systems*, CRC Press; ISBN 0415596270.

Alberdi-Pagola, M., 2018. Thermal response test data of five quadratic cross section precast pile heat exchangers. Data Br. 18, 13–15. https://doi.org/10.1016/j.dib.2018.02.080

Alberdi-Pagola, M., Jensen, R.L., Madsen, S., Poulsen, S.E., 2018b. Method to obtain g-functions for multiple precast quadratic pile heat exchangers. DCE Technical Report No. 243, Aalborg University, Aalborg, Denmark. Available online: http://vbn.aau.dk/files/274763046/Method_to_obtain_g_functions_for_multiple_precast_quadratic_pile_heat_exchangers.pdf

Alberdi-Pagola, M., Madsen, S., Jensen, R.L., Poulsen, S.E., 2017b. Numerical investigation on the thermo-mechanical behavior of a quadratic cross section pile heat exchanger, in: Proceedings of the IGSHPA Technical/Research Conference and Expo.

Denver, USA, March 14-16. https://doi.org/http://dx.doi.org/10.22488/okstate.17.000520

Alberdi-Pagola, M., Poulsen, S.E., Jensen, R.L., Madsen, S., 2017a. Thermal response testing of precast pile heat exchangers: fieldwork report. DCE Technical Report No. 234, Aalborg University, Aalborg, Denmark.

Alberdi-Pagola, M., Poulsen, S.E., Loveridge, F., Madsen, S., Jensen, R.L., 2018a. Comparing heat flow models for interpretation of precast quadratic pile heat exchanger thermal response tests. Energy 145, 721–733. https://doi.org/10.1016/j.energy.2017.12.104

ASHRAE, 2009. 2009 ASHRAE Handbook. Fundamentals. American Society of Heating, Refrigerating and Air-Conditioning Engineers, Inc., 1791 Tullie Circle, N.E., Atlanta, GA 30329.

Bandos, T. V, Campos-Celador, Á., López-González, L.M., Sala-Lizarraga, J.M., 2014. Finite cylinder-source model for energy pile heat exchangers: Effects of thermal storage and vertical temperature variations. Energy 78, 639–648. https://doi.org/http://dx.doi.org/10.1016/j.energy.2014.10.053

Baudoin, A., 1988. Stockage intersaisonnier de chaleur dans le sol par batterie d'échangeurs baïonnette verticaux modèle de prédimensionnement. ANRT, Grenoble.

Bernier, M.A., Chahla, A., Pinel, P., 2008. Long-Term Ground-Temperature Changes in Geo-Exchange Systems. ASHRAE Trans. 114.

Bernier, M.A., Pinel, P., Labib, R., Paillot, R., 2004. A Multiple Load Aggregation Algorithm for Annual Hourly Simulations of GCHP Systems. HVAC&R Res. 10, 471–487. https://doi.org/10.1080/10789669.2004.10391115

Bourne-Webb, P., Bernard, J.-B., Friedemann, W., von der hude, N., Pralle, N., Uotinen, V.M., Widerin, B., 2013. Delivery of Energy Geostructures, in: *Energy Geostructures*. John Wiley & Sons, Inc., pp. 229–263. https://doi.org/10.1002/9781118761809.ch12

Brettman, T.P.E., Amis, T., Kapps, M., 2010. Thermal conductivity analysis of geothermal energy piles. Proc. Geotech. Challenges Urban Regen. Conf.

Buildingphysics, 2008. Earth Energy Designer EED 3.

Capozza, A., De Carli, M., Zarrella, A., 2012. Design of borehole heat exchangers for ground-source heat pumps: A literature review, methodology comparison and analysis

on the penalty temperature. Energy Build. 55, 369–379. https://doi.org/10.1016/J.ENBUILD.2012.08.041

Cimmino, M., Bernier, M., 2014. A semi-analytical method to generate g-functions for geothermal bore fields. Int. J. Heat Mass Transf. 70, 641–650. https://doi.org/10.1016/j.ijheatmasstransfer.2013.11.037

Cimmino, M., Bernier, M., Adams, F., 2013. A contribution towards the determination of g-functions using the finite line source. Appl. Therm. Eng. 51, 401–412. https://doi.org/http://dx.doi.org/10.1016/j.applthermaleng.2012.07.044

COMSOL Multiphysics, 2017. Introduction to COMSOL Multiphysics version 5.3. Burlington.

Diersch, H.-J.G., 2014. *FEFLOW Finite Element Modeling of Flow, Mass and Heat Transport in Porous and Fractured Media*. Springer Science & Business Media. https://doi.org/10.1007/978-3-642-38739-5

Eskilson, P., 1987. Thermal Analysis of Heat Extraction. PhD thesis, University of Lund, Sweden, Lund, Sweden.

Fossa, M., 2011. A fast method for evaluating the performance of complex arrangements of borehole heat exchangers. HVAC&R Res. 17, 948–958. https://doi.org/10.1080/10789669.2011.599764

Fossa, M., Cauret, O., Bernier, M., 2009. Comparing the thermal performance of ground heat exchangers of various lengths, in: Proceedings from the 11th International Conference on Energy Storage, EFFSTOCK.

Fossa, M., Rolando, D., 2015. Improving the Ashrae method for vertical geothermal borefield design. Energy Build. 93, 315–323. https://doi.org/https://doi.org/10.1016/j.enbuild.2015.02.008

Fossa, M., Rolando, D., 2014. Fully analytical finite line source solution for fast calculation of temperature response factors in geothermal heat pump borefield design, in: Proceedings, IEA Heat Pump Conference, 12-16 May, Montreal (Québec) Canada.

Gehlin, S., 2002. Thermal Response Test. Method Development and Evaluation. PhD thesis, Dep. Environ. Eng. Div. Water Resour. Eng. Luleå University of Technology, Sweden.

GSHP Association, 2012. Thermal Pile: Design, Installation & Materials Standards.

Hellström, G., 1991. Ground Heat Storage: Thermal Analyses of Duct Storage Systems. I.Theory. Department of Mathematical Physics.

Jalaluddin, A.M., Tsubaki, K., Inoue, S., Yoshida, K., 2011. Experimental study of several types of ground heat exchanger using a steel pile foundation. Renew. Energy 36, 764–771. https://doi.org/http://dx.doi.org/10.1016/j.renene.2010.08.011

Javed, S., Spitler, J.D., Fahlén, P., 2011. An experimental investigation of the accuracy of thermal response tests used to measure ground thermal properties. ASHRAE Trans. 117, 13–21.

Katsura, T., Nagano, K., Takeda, S., 2008. Method of calculation of the ground temperature for multiple ground heat exchangers. Appl. Therm. Eng. 28, 1995–2004. https://doi.org/http://dx.doi.org/10.1016/j.applthermaleng.2007.12.013

Kelvin, T.W., 1882. Mathematical and physical papers. Cambridge Univ. Press. London.

Laloui, L., Nuth, M., 2009. Investigations on the mechanical behaviour of a Heat Exchanger Pile, Deep Foundations on Bored and Auger Piles, Proceedings. Crc Press-Taylor & Francis Group, Boca Raton.

Lamarche, L., Beauchamp, B., 2007. A new contribution to the finite line-source model for geothermal boreholes. Energy Build. 39, 188–198. https://doi.org/10.1016/J.ENBUILD.2006.06.003

Li, M., Lai, A.C.K., 2012. New temperature response functions (G functions) for pile and borehole ground heat exchangers based on composite-medium line-source theory. Energy 38, 255–263. https://doi.org/http://dx.doi.org/10.1016/j.energy.2011.12.004

Loveridge, F., Olgun, C.G., Brettmann, T., Powrie, W., 2014a. The Thermal Behaviour of Three Different Auger Pressure Grouted Piles Used as Heat Exchangers. Geotech. Geol. Eng. 1–17. https://doi.org/https://doi.org/10.1007/s1070

Loveridge, F., Powrie, W., 2014a. G-Functions for multiple interacting pile heat exchangers. Energy 64, 747–757. https://doi.org/http://dx.doi.org/10.1016/j.energy.2013.11.014

Loveridge, F., Powrie, W., 2014b. 2D thermal resistance of pile heat exchangers. Geothermics 50, 122–135. https://doi.org/http://dx.doi.org/10.1016/j.geothermics.2013.09.015

Loveridge, F., Powrie, W., 2013. Temperature response functions (G-functions) for single pile heat exchangers. Energy 57, 554–564. https://doi.org/http://dx.doi.org/10.1016/j.energy.2013.04.060

Loveridge, F., Powrie, W., Nicholson, D., 2014b. Comparison of two different models for pile thermal response test interpretation. Acta Geotech. 9, 367–384. https://doi.org/https://doi.org/10.1007/s11440-014-0306-3

Maragna, C., 2016. Development of a numerical Platform for the Optimization of Borehole Heat Exchanger Fields, in: European Geothermal Congress 2016. pp. 19–24.

Maragna, C., Rachez, X., 2015. Innovative Methodology to Compute the Temperature Evolution of Pile Heat Exchangers, in: World Geothermal Congress 2015.

Mogensen P., 1983. Fluid to Duct Wall Heat Transfer in Duct System Heat Storage, in: Proc. Int. Conf. On Subsurface Heat Storage in Theory and Practice. Swedish Council for Building Research, Stockholm. Sweden, June 6–8, 1983, p. PP: 652-657.

Oklahoma State University, 1988. Closed-loop/ground source heat pump systems. Installation guide.

Olgun, C.G., McCartney, J.S., 2014. Outcomes from international workshop on thermoactive geotechnical systems for near-surface geothermal energy: from research to practice. DFI Journal-The J. Deep Found. Inst. 8, 59–73. https://doi.org/https://doi.org/10.1179/1937525514Y.0000000005

Pahud, D., 2002. Geothermal energy and heat storage. SUPSI – DCT – LEEE. Scuola Universitaria Professionale della Svizzera Italiana, Cannobio.

Pahud, D., Fromentin, A., costruito, D. ambiente costruzioni e design I. sostenibilità applicata all'ambiente, 1999. PILESIM - LASEN. Simulation Tool for Heating/Cooling Systems with Heat Exchanger Piles or Borehole Heat Exchangers. User Manual.

Pahud, D., Hubbuch, M., 2007. Measured thermal performances of the energy pile system of the Dock Midfield at Zürich Airport, in: Proceedings European Geothermal Congress.

Park, H., Lee, S.-R., Yoon, S., Choi, J.-C., 2013. Evaluation of thermal response and performance of PHC energy pile: Field experiments and numerical simulation. Appl. Energy 103, 12–24. https://doi.org/http://dx.doi.org/10.1016/j.apenergy.2012.10.012

Park, S., Lee, D., Choi, H.-J., Jung, K., Choi, H., 2015. Relative constructability and thermal performance of cast-in-place concrete energy pile: Coil-type GHEX (ground heat exchanger). Energy 81, 56–66. https://doi.org/http://dx.doi.org/10.1016/j.energy.2014.08.012

Philippe, M., Bernier, M., Marchio, D., 2009. Validity ranges of three analytical solutions to heat transfer in the vicinity of single boreholes. Geothermics 38, 407–413. https://doi.org/https://doi.org/10.1016/j.geothermics.2009.07.002

Philippe, M., Bernier, M., Marchio, D., 2010. Sizing calculation spreadsheet: Vertical geothermal borefields. Ashrae J. 52, 20.

Rees, S.J., 2016. An introduction to ground-source heat pump technology, in: *Advances in Ground-Source Heat Pump Systems*. Woodhead Publishing, pp. 1–25. https://doi.org/http://dx.doi.org/10.1016/B978-0-08-100311-4.00001-7

Signorelli, S., Bassetti, S., Pahud, D., Kohl, T., 2007. Numerical evaluation of thermal response tests. Geothermics 36, 141–166. https://doi.org/http://dx.doi.org/10.1016/j.geothermics.2006.10.006

Spitler, J.D., 2000. GLHEPRO-A design tool for commercial building ground loop heat exchangers, in: Proceedings of the Fourth International Heat Pumps in Cold Climates Conference. Citeseer.

Spitler, J.D., Bernier, M., 2016. Vertical borehole ground heat exchanger design methods. Rees, Simon J, in: *Advances in Ground-Source Heat Pump Systems*. Woodhead Publishing, pp. 29–61. https://doi.org/http://dx.doi.org/10.1016/B978-0-08-100311-4.00002-9

VDI, 2001. VDI 4640 Thermal use of the underground. Part 2: Ground source heat pump systems. The Association of German Engineers (VDI).

Vieira, A., Alberdi-Pagola, M., Christodoulides, P., Javed, S., Loveridge, F., Nguyen, F., Cecinato, F., Maranha, J., Florides, G., Prodan, I., Lysebetten, G. Van, Ramalho, E., Salciarini, D., Georgiev, A., Rosin-Paumier, S., Popov, R., Lenart, S., Poulsen, S.E., Radioti, G., 2017. Characterisation of Ground Thermal and Thermo-Mechanical Behaviour for Shallow Geothermal Energy Applications. Energies 2017, 10(12), 2044. https://doi.org/10.3390/en10122044

Zanchini, E., Lazzari, S., 2014. New g-functions for the hourly simulation of double U-tube borehole heat exchanger fields. Energy 70, 444–455. https://doi.org/https://doi.org/10.1016/j.energy.2014.04.022

Zanchini, E., Lazzari, S., 2013. Temperature distribution in a field of long Borehole Heat Exchangers (BHEs) subjected to a monthly averaged heat flux. Energy 59, 570–580. https://doi.org/https://doi.org/10.1016/j.energy.2013.06.040

Zeng, H.Y., Diao, N.R., Fang, Z.H., 2002. A finite line-source model for boreholes in geothermal heat exchangers. Heat Transf. Res. 31, 558–567. https://doi.org/https://doi.org/10.1002/htj.10057.

5.2. LESSONS LEARNT

Paper B has demonstrated that semi-empirical methods to simulate multiple energy piles comprise a valuable tool for feasibility studies and sizing of GSHP systems based on energy piles.

As a further step, the suitability of the computed g-functions to yield TRT estimates, comparable to the ones obtained in Paper A, has been checked. The analysed precast pile heat exchanger TRT data are available in [159] (Paper D) and the inverse modelling approach is the same as described in Paper A. Five TRTs have been analysed: LM1 corresponds to a single-U pile heat exchanger while the other four have a W-shape pipe arrangement. The results are compared to the 3D FEM calibration estimates reported in Table 5 in Paper A and Figure 5-1 shows the parameter estimates normalised with the 3D FEM results.
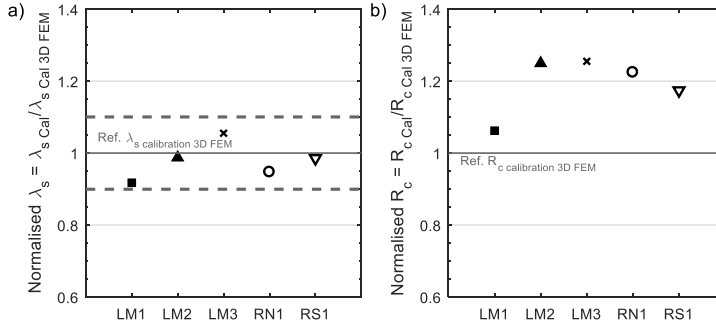
Figure 5-1: Parameter estimates from calibration of the semi-empirical models normalised with the 3D FEM based estimates. a) Thermal conductivity of soil λ_s [W/m/K]; b) Concrete thermal resistance R_c [Km/W]. LM1: single-U. LM2, LM3, RN1 and RS1: W-shape.

The semi-empirical models provide a reliable estimation of the thermal conductivity of the soil λ_s. However, they tend to overestimate the concrete thermal resistance R_c by 20% and 6% for the W-shape and single-U piles, respectively. The proposed models show acceptable estimates for soil thermal conductivity and can be used for TRT interpretation. However, the "simple" g-functions do not completely capture the complex thermal dynamics and interactions occurring within the W-shape pipe. Hence, the concrete thermal resistance estimates are slightly biased.

Regarding the type curves, instead of polynomials, "Shape-Preserving Piecewise Cubic Interpolations", proposed in [160,161] could be more convenient. To finish, more aspect ratios and radial distances should be computed to prevent unnecessary interpolation and to cover a wider range of energy pile aspect ratios.

For further information, please refer to Appendix V.

CHAPTER 6. VERIFICATION OF THERMAL DESIGN METHOD

6.1. SCOPE AND MOTIVATION

Here, the method developed in the previous chapter is applied to a real case. First, a case study in Denmark is introduced, where operational data from 2015 is analysed (Conference Paper I). Then, Paper C is introduced, where we apply the multiple pile method developed in Paper B to the case study and we propose an optimisation strategy for the ground loop sizing. Paper B focused on identifying the limitations of the method and analysed rather small energy pile groups (up to 16 piles). Paper C analyses larger groups, above 200 piles.

6.1.1. CONFERENCE PAPER I

The following paper, denoted Conference paper I, was presented in the REHVA World Congress Clima2016, in Aalborg, Denmark.

Alberdi-Pagola, M., Poulsen, S.E. & Jensen, L.J., 2016. "A performance case study of energy pile foundation at Rosborg Gymnasium (Denmark)", in *Proceedings of the 12th REHVA World Congress Clima2016*, May 2016, Aalborg, Denmark. Vol. 3, pp. 10. Aalborg University, Department of Civil Engineering.

http://vbn.aau.dk/files/233716932/paper_472.pdf.

Reprinted by permission from REHVA.

A performance case study of energy pile foundation at Rosborg Gymnasium (Denmark)

Maria Alberdi-Pagola[#1], Rasmus Lund Jensen[*2], Søren Erbs Poulsen[#3]

[#1, *2] *Department of Civil Engineering, Aalborg University*
Sofiendalsvej 11, 9200 Aalborg SV, Denmark
[#1]mapa@civil.aau.dk
[*2]rlj@civil.aau.dk
[#3] *Department of Civil Engineering, Research and Development, VIA University College*
Chr. M. Østergaards Vej 4, 8700 Horsens, Denmark
[#3]soeb@via.dk

Abstract

The Rosborg Gymnasium building in Vejle (Denmark) is partially founded on 200 foundation pile heat exchangers (energy piles). The thermo-active foundation has supplemented the heating and free cooling needs of the building since 2011 (4,000 m² living area). Operational data from the ground source heat pump installation has been compiled since the beginning of 2015. The heating requirement of the building supplied by the ground source heat pump exceeds the free cooling covered by ground heat exchange. The asymmetric utilisation of the soil should in principle, imply a decrease in the long-term ground temperatures. However, operational data show that the temperatures of the heat-carrier fluid do not fall below +4.2ºC during the heating season (winter) and that the soil recovers to undisturbed conditions during the summer when heat demand is low. In addressing the consequences of an imbalanced ground heat extraction/injection activity, this paper provides a performance study of the energy pile-based ground source heat pump installation utilising operational data. The study demonstrates that the measured seasonal performance factors so far are lower than expected: 2.7 in heating mode and 4.2 in cooling mode. Nevertheless, there is room for improvement if novel energy management strategies are applied. This highlights the relevance of considering the daily heating/cooling requirements of the building during the design phase of the heating and cooling system. Moreover, this study demonstrates the feasibility of ground source heat pump systems based on energy foundations in heating-dominant buildings.

Keywords - Shallow geothermal energy, GSHP, energy foundation, energy pile, case study, performance factors, performance.

1. Introduction

The Danish government has set two main environmental targets: to reduce a 40 % the greenhouse gas emissions by the year 2020 relative to 1990 and to cover the total domestic energy consumption by renewable energy sources by 2050 [1]. In combination with other renewable energies, shallow geothermal energy storage and abstraction has a great potential for realizing these two objectives.

As a new alternative to borehole heat exchangers (BHE) the construction industry developed the foundation pile heat exchanger (energy pile) in the 1980s [2]. Energy piles are thermally active building foundation elements with embedded geothermal pipes fixed to the steel reinforcement in which a circulating fluid exchanges heat with the pile and the surrounding soil. As such, the foundation of the building both serves as a structural component and a heating/cooling supply.

Extensive research has been reported by [3, 4, 5, 6] on the performance of ground source heat pump (GSHP) systems based on traditional BHE. [7] demonstrate that the thermal performance of the system is maintained over five years due to the applied energy management strategies. Typically, GSHP systems require a run-in period of one to two years before a satisfactory system performance is obtained.

Energy foundations are usually associated with high initial costs, but the literature give indications to the economic feasibility relative to traditional heating and cooling systems reported in case studies [8-10], experimental investigations [11, 12] and numerical models [13]. Current knowledge about energy management obtained from existing BHE installations can be applied to thermo-active geostructures which potentially improves both user acceptance and the cost-effectiveness of the system. However, the scarcity of actual published operational data hampers the dissemination of GSHP systems which mainly relates to uncertainty about long-term structural performance under different thermal loading regimes.

In Denmark, there are currently three energy pile foundations that utilise relatively small precast rectangular pile heat exchangers produced by Centrum Pæle A/S. This study is limited to the energy pile foundation at Rosborg Gymnasium (high-school) in Vejle, Denmark. Previous research indicates that the foundation is over-dimensioned in terms of thermal performance [14]. The system is fully operational yet there is a need to better understand its performance and to consider the operation of the GSHP system.

This paper aims to provide a performance study of the energy pile based GSHP system at Rosborg Gymnasium utilising measured, operational data. The paper is organized as follows. Firstly, the test site is described. Secondly, the methods section describes the analysis applied to the operational data. Thirdly, the operational data are analysed, and the performance study is presented and discussed before conclusions are drawn.

2. Description of the Site

An extension of Rosborg Gymnasium is founded on 200 energy piles that have supplied the heating of a 3,949 m^2 living area since 2011. The study area consists of two storeys and a large open canteen area which is situated in the south-west part of the building complex.

The pile foundation was dimensioned taking into account only the mechanical load from the building. That is, the thermal load from the geothermal use of the piles was neglected, as were the thermo-mechanical implications hereof.

The quadratic cross section (0.30 x 0.30 m^2) 15 meter long energy pile has a W-shape PE-X pipe arrangement heat exchanger fixed to the steel reinforcement [14]. The minimum distance between the piles is 1.5 m.

The GSHP system supplies heating in winter while in the summer, the heating circuit is closed. This permits the heat-carrier fluid to flow through the refrigeration circuit, thereby bypassing the heat pump, thus supplementing "free cooling" of the southern rooms in the building. In this way, the heat from the building is utilised for recharging the ground. The actual cooling demand of the building exceeds that which can be supplied by the GSHP system. Figure 1 shows a conceptual diagram of the GSHP system operating in heating mode. It is important to note that the ground-coupled system does not supply the domestic hot water.
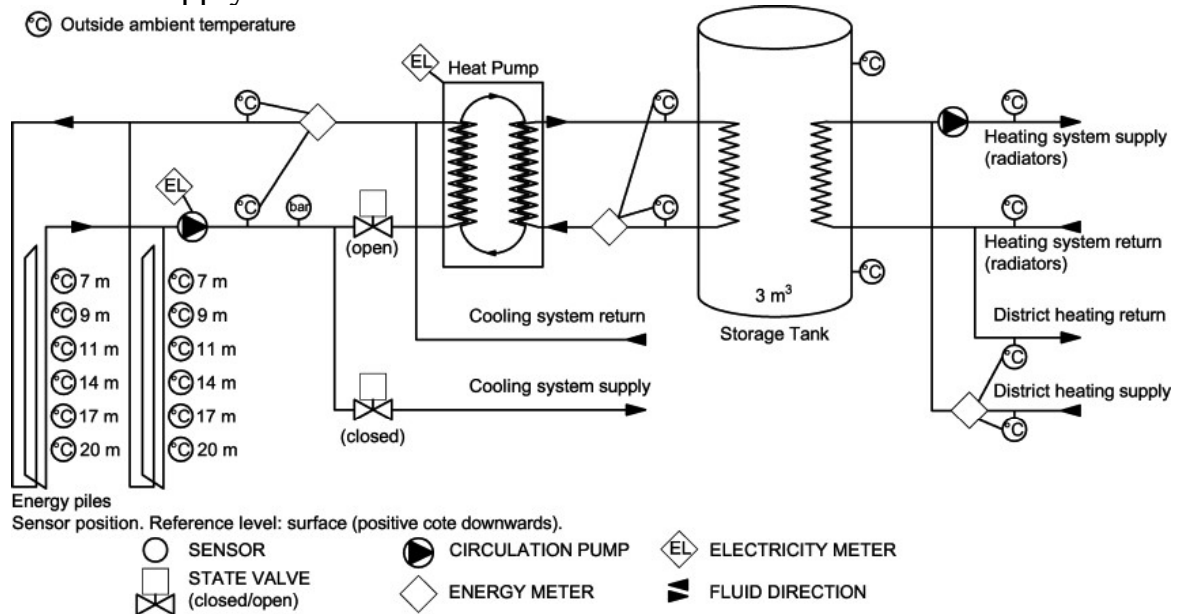
Fig. 1 Schematic of the GSHP systems with energy piles in heating mode and the sensor network.

The 200 pile heat exchangers are divided in 16 groups and within each group, the energy piles are connected in parallel. 2 of the 200 energy piles are instrumented with Pt100 temperature sensors positioned as shown on the left side in Fig. 1. The ground loop utilises a 20 % ethylene glycol based water solution as heat-carrier fluid.

The heat pump consists of a water-to-water unit with a nominal heating capacity of 200 kW and two compressors. The heat pump heats/charges a water accumulation tank from which a traditional radiator-based heating system is supplied. The district heating network serves as an auxiliary heating system. Free cooling utilises ventilation fan-coils coupled to the pile system.

Figure 1 illustrates the control and monitoring system and the relevant parameters for the GSHP system including: inlet and outlet temperatures and flow rates in different loops, local temperature measurements, electricity consumptions and heat pump status (on/off).

The foundation is situated 70 cm below terrain, below the primary groundwater table (any future vertical reference pertains to terrain elevation) with energy piles founded in glacial sand and gravel situated at 5 to 6 meters depth. The glacial sediments are topped by postglacial organic mud. Groundwater is artificially drained from the area. Groundwater flow is expected but it has not been investigated further. Prior soil investigations yield an estimated bulk soil thermal conductivity, λ_s, of 2.4 W/m/K and a volumetric heat capacity, S_{vc}, of 2.4 MJ/m^3/K [14].

All measurements were recorded for a period of 345 days starting on January 18th 2015 in an interval of 60 minutes for the temperatures in the energy piles, the temperatures in the top and bottom of the tank and the on/off state of the heat pump, while the rest of the readings were recorded in 1-minute interval. The district heating data was only available from March the 27th and just two of the Pt100 sensors placed in the instrumented energy piles have worked, malfunctioning from October 2015.

3. Methods

GSHP system performance evaluation consists of data collection and analysis. The methodology applied to the observed data includes an estimation of the heating and free cooling consumptions of the building and an analysis of the energy efficiency of the GSHP system.

3.1. Heating and Free Cooling Consumptions of the Building

The radiator loop was not monitored. Therefore, the heating consumption of the building has been quantified by adding the following two contributions: the energy extracted from the tank and the energy added from the district heating network. The sum of the two contributions yields the thermal energy supplied by the radiators to the living area (Fig. 1). The energy extracted from the tank has been determined by calculating the energy balance from charge and discharge cycles with the top and bottom (tank) temperature records (Fig. 1). The thermal losses of the tank have been considered in accordance with ASHRAE [15].

The free cooling delivered has been established from the temperature and flow readings from the ground loop.

3.2. Efficiency of the GSHP System

The analysis of the energy efficiency of the GSHP installation is based on thermal energy production. The records of inlet, T_{in} [°C], and outlet, T_{out} [°C], temperatures and flows, f [m³/s], facilitate computation of the instantaneous thermal power outputs, Q [kW], for heating or cooling, using (1):

$$Q = \rho c_p \cdot f \cdot (T_{in} - T_{out})$$ (1)

where ρc_p is the volumetric heat capacity of the heat-carried fluid.

Three main thermal power outputs are determined and analysed on the basis of the compiled, operational data. The following data, pertaining the closed circuits depicted in (Fig. 1), is collected :

- The energy extracted/rejected from/to the soil by the energy piles.
- The energy delivered to the storage tank by the heat pump.
- Energy supply from the district heating network, i.e., the energy added to the energy which is extracted from the storage tank.

Equation (1) is integrated with respect to time to obtain the accumulated energy during a specified time interval. The electricity consumption of the system, W_{SYS}, is also quantified by integrating the sum of the electricity consumptions of the compressors, W_{HP}, and the circulation pumps, W_{CP}, over time.

The energy efficiency of the system in heating mode is characterized by the coefficient of performance (COP) which is defined as the ratio between the heat output of the heat pump [kW] and the electricity consumption of the compressors and the circulation pumps [kW].

In heating mode, the total thermal energy delivered to the tank is the sum of the thermal energy abstracted from the ground and the measured electricity consumption of the compressors. The same expression is used to determine the energy efficiency ratio (EER) in free cooling mode. In this case, the electricity power consumption corresponds only to the usage of the circulation pumps, while the heat output is the thermal load rejected/injected from/to the ground. The aggregated COP for the entire heating season is defined as the seasonal performance factor (SPF) which includes total power consumption in the system operation over the heating season.

4. Results and Discussion

In the following, the performance of the GSHP system is analysed for the 345-days period.

4.1. Heating and Free Cooling Consumptions of the Building

The total heating consumption for the studied period is 106.57 MWh and the free cooling supplied is 4.44 MWh, which is very low compared to the heating requirements. The GSHP heating system was active for 3400 hours (6072 hours of heating period) while free cooling was utilised for 800 hours during the summer (2208 hours). The asymmetric utilisation of the soil where the net heat flow into the ground between discharge and charge fluxes is not balanced, should in principle, imply a decrease in the long-term ground temperature.

The heating delivered by the heat pump during the period of study is 100.79 MWh, which corresponds to 95% of the total heating requirement (see monthly breakdown in Fig. 2). The district heating contribution was 5.78 MWh, corresponding to 5 % of the total heating consumption. That is, the additional heat required from the district heating was insignificant.

4.2. Efficiency of the GSHP System

Figure 2 shows the monthly energy extracted from the ground compared to the heat delivered by the heat pump. The energy supplied in August is due to the accumulation tank being charged and not actual heating consumption by the building.

Figure 3 shows the monthly performance factors of the GSHP installation. The average of the instantaneous COP values is around 3.0, which is acceptable considering the heat pump manufacturer's estimated COP of 3.49 for fluid temperatures between +7 ℃ and +12 ℃. The COP provided by the manufacturer is based on experimental data obtained in steady state heat pump characterization tests.

The SPF for heating is relatively low following the summer despite an increase from 2.0 to 2.7 from spring/summer to autumn. The circulation pumps were continuously working until August 2015, which substantially increased the corresponding electricity consumption, adversely affecting the overall performance of

the installation. In September 2015, the external circulation pumps were programed to activate only at every compressor cycle. Subsequently, the electricity consumption has decreased (see Fig. 3). The cooling SPF is 4.2 with a standard deviation of 2.1, which indicates that the monthly average EERs are highly unstable. Hence, the system operation needs to be adjusted.

Fig. 2 Key figures for the thermal use of the energy piles in 2015.
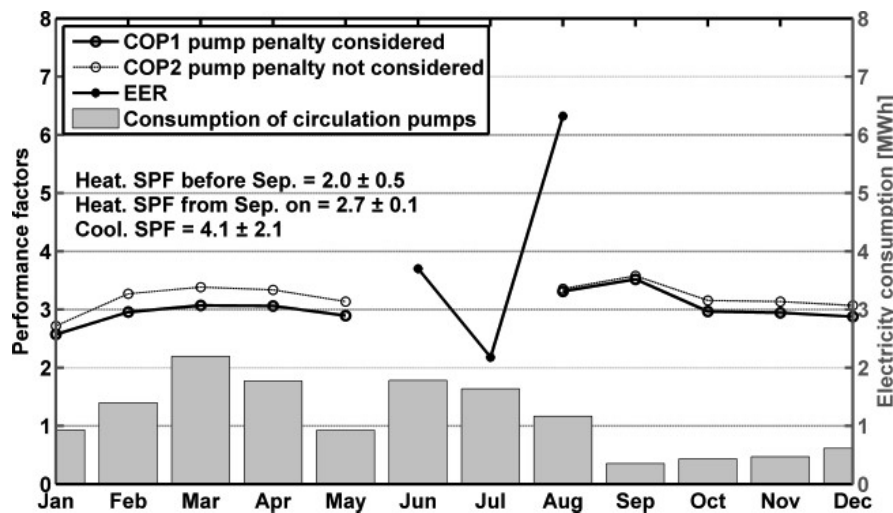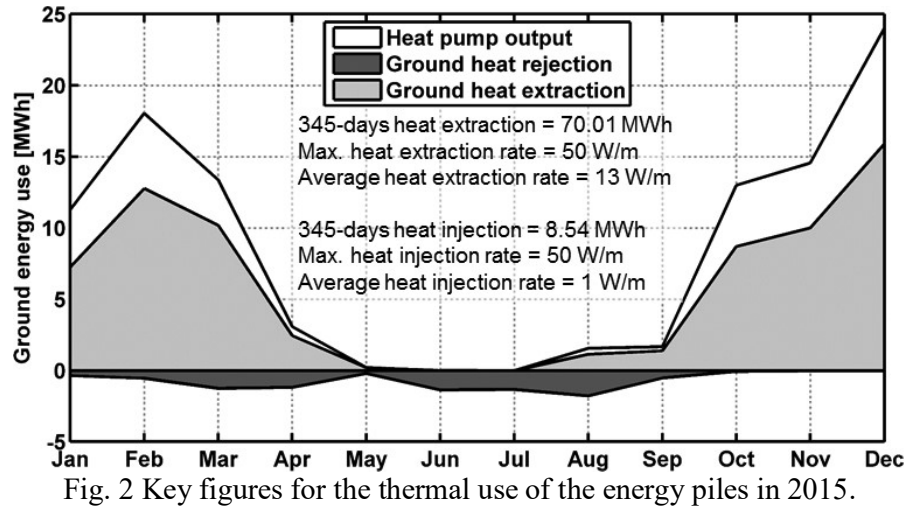
Fig. 3 Monthly performance factor for the GSHP system in heating and free cooling mode, respectively. SPFs: the electricity consumption of the secondary elements is considered also over the periods where the heat pump is not running, as it affects the overall performance.

Figure 4 illustrates measurements during a single day in January 2015 (A) and in December 2015 (B), respectively, of fluid inlet- and outlet temperatures to the heat pump, outdoor air temperatures, fluid supply temperatures to the storage tank and electricity consumption of the compressor.

The temperature of the return fluid to the energy piles does not decrease below 6 °C. When the compressor activates (spikes to 60 kW in January and to 30 kW in December in Fig. 4) the temperature difference between inlet and outlet is around 3 °C. The water supplementing the accumulation tank peaks at 55 °C. Notice that the power consumed by the circulation pumps in January is continuously 3 kW while it

approaches 0 kW in December. From the 22nd of December (B in Fig. 4) just one compressor is active and the ground loop flow rate has been halved, which implies longer heat pump cycles, in the order of hours instead of minutes, to supply identical heating with lower heat pump capacity and flow rates.
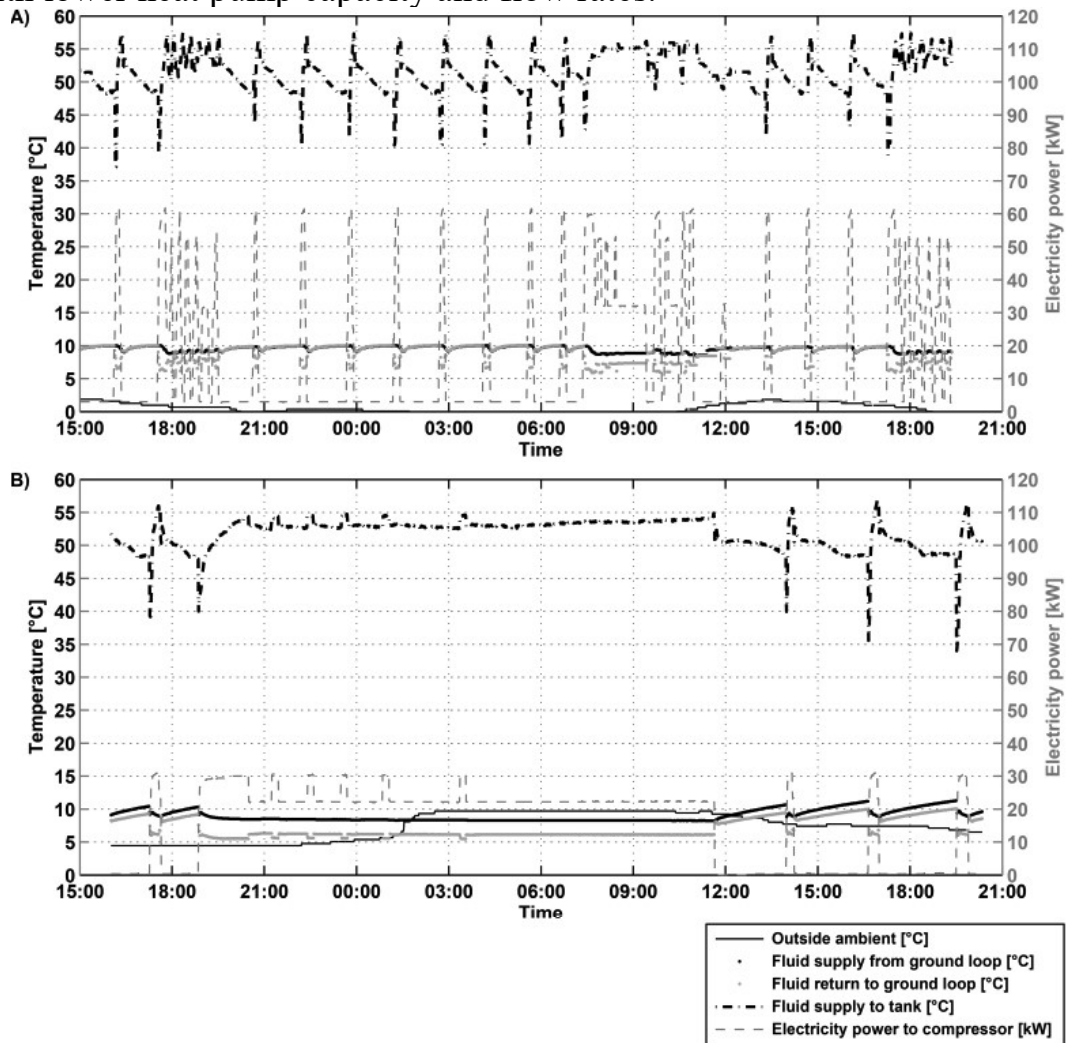
Fig. 4 30-hour performance A) on the 20/01/2015 and B) on the 27/12/2015.

4.3. Ground Energy Balance

Figure 2 shows the monthly extracted and injected thermal energy from and to the ground. The injected energy corresponds to the free cooling production which amounts to 8.54 MWh, corresponding to 12% of the 70.01 MWh extracted by the heat pump. The disagreement with the 4.44 MWh of free cooling consumption mentioned earlier is due to the involuntary free cooling registered from January to May 2015 which recharges the ground as the circulation pumps transfer heat from the building to the ground during heat pump standby. Figure 2 also provides the heat extraction rates per meter length of energy pile, during heating and cooling (50 W/m in both cases) which agree well with reported literature values for "normal underground and water-saturated sediments" given by BS-EN-15450-2007 [16].

4.4. Ground Loop Temperatures and Flow

Lower entering fluid temperature entails lower performance of the system. Figure 5 shows the daily average of the supply and return glycol temperatures for the ground loop. The unusual temperature increase in May and June is potentially due to the change in operation from heating to free cooling.
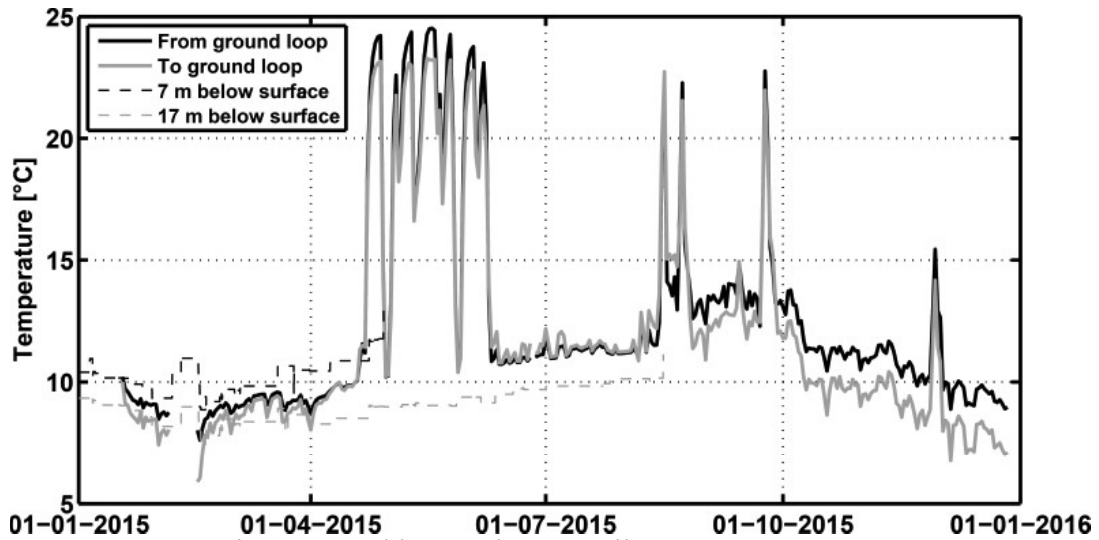
Fig. 5 Ground loop and energy pile temperatures.

In heating mode, the entering fluid temperature is greater than the leaving fluid temperature. While in cooling mode, the heat absorbed from the building increases the leaving fluid temperature, which can be seen to occur from and following June. Due to the decrease in the heating consumption in April and May and ground thermal recharge due to free cooling during summer, the initial ground temperature is recovered and surpassed prior to October according to the brine temperatures in the ground loop.

The expected groundwater flow in the area could bring a continuous load of heat, regardless of the heat injection by free cooling, which may disturb the temperature of the ground, affecting the energy budget of the thermal reservoir. This will be quantified in future research.

The lack of continuous circulation and the associated involuntary recharge of the ground cause the temperature difference between the inlet and outlet of the ground loop to increase following summer (Fig. 5).

Long-term space heating operation measurements indicate that the minimum temperature of the brine entering the heat pump is approximately 6.5 °C whereas the minimum leaving fluid temperature is 4.2°C. The measured brine temperatures are significantly higher than the +2 °C limitation recommended by [17].

The two pumps circulating the brine in the ground loop operate in parallel at 15 m^3/h each. The heat pump, however, operates at either 10 m^3/h or 20 m^3/h depending on whether one or two compressors are active. The resulting flow per energy pile yields a Reynolds number of 1400, which is not sufficient for ensuring turbulent flow conditions. Therefore, the total thermal resistance of the energy pile is higher which negatively affects the heat transport to and from the pile. To ensure turbulence the flow

rate must be increased by at least 45 % although its implications on the running costs could be counter-productive.

The energy pile temperatures were monitored approximately 7 m and 17 m below terrain (Fig. 5). The pile temperature measurements reflect the variation in the ground loop temperatures. Pile temperatures are relatively high throughout the year, implying that heat extraction from the ground can be further increased. Moreover, this indicates that the energy foundation is over-dimensioned in terms of thermal capacity.

4.5. New Strategies

Optimizing the energy performance of GSHP system can be achieved by managing its operation. The following proposals potentially improve the GSHP performance:

- Reduce the electricity consumption of the circulation pumps by synchronising properly their cycles and the compressors.
- Increase the ground loop flow in order to decrease the pile thermal resistance.
- Adapt the thermal energy generated by the system with the thermal load, increasing heat extraction from the ground. To this end, the ventilation can be supplied with the GSHP system instead of with the district heating network.
- Adjust the activation indoor temperature and flow conditions for the circulation pumps to improve the free cooling performance and increase its use by ventilation of additional rooms during the summer.

5. Conclusions

The Rosborg Gymnasium building in Vejle (Denmark) is partially founded on 200 energy piles. The thermo-active foundation has supplemented the heating and cooling of the gymnasium since 2011 (4,000 m^2 living area). This paper provides a performance study of the energy pile-based ground source heat pump installation utilising operational data compiled since the beginning of 2015.

The results indicate that the GSHP system is a viable option. However, an overall heating seasonal performance factor (SPF) of 2.7 and a mean coefficient of performance (COP) value of 2.9 in December 2015 indicate that the electricity consumption of the circulation pumps is relatively high and that it can be further reduced. Future investigation will encompass a comparison with traditional energy sources in terms of economy and CO2 emissions.

Ground loop temperatures are high during all seasons, implying that the GSHP system is over-sized in terms of thermal performance and capacity. As such higher heat extraction rates (from the ground) can be applied. Free cooling significantly improves the thermal recovery of the soil during the summer.

If the heating and cooling demands of the building are known, an optimal sizing of the heat pump and a more accurate estimation of the required number of energy piles are possible. To that end, the dimensioning needs to be based on ground thermal response test analysis and thermal dynamic simulations of the building and of the energy pile system.

Further research on Rosborg Gymnasium case study will include longer operational data periods, groundwater flow implications in the energy recharge and

withdrawal processes of the ground and thermal influences between activated and non-activated piles in irregular foundation patterns.

Acknowledgments

References

[1] Danish Energy Agency. Energy Policy in Denmark (2012), Danish Energy Agency: Amaliegade 44, 1256 Copenhagen K, Denmark.

[2] Brandl, H. Energy foundations and other thermo-active ground structures. Geotechnique (2006). 56(2): p. 81-122.

[3] Ardehali, M. Energy performance monitoring and examination of electrical demand and consumption of a geothermal heat pump system. Energy Engineering (2008). 105(5): p. 44-54.

[4] Urchueguía, J.F., et al. Comparison between the energy performance of a ground coupled water to water heat pump system and an air to water heat pump system for heating and cooling in typical conditions of the European Mediterranean coast. Energy Conversion and Management (2008). 49(10): p. 2917-2923.

[5] Ground Energy Support LLC. Ground Source Heat Pumps System Performance: Monitoring, Measuring, and Metering (2013).

[6] Olgun, C., Abdelaziz, S. and Martin, J. Long-Term Performance and Sustainable Operation of Energy Piles. In: ICSDEC 2012 (2013). p. 534-542.

[7] Montagud, C., et al. Analysis of the energy performance of a ground source heat pump system after five years of operation. Energy and Buildings (2011). 43(12): p. 3618-3626.

[8] Bockelmann, F., et al. Evaluation and optimization of underground thermal energy storage systems of Energy Efficient Buildings (WKSP) - A project within the new German R&D-framework EnBop. In: Proceedings of the Eighth International Conference for Enhanced Building Operations (2008) Berlin, Germany.

[9] Pahud, D. and Hubbuch, M. Measured thermal performances of the energy pile system of the Dock Midfield at Zürich Airport. in Proceedings European geothermal congress (2007).

[10] Hamada, Y., et al. Field performance of an energy pile system for space heating. Energy and Buildings (2007). 39(5): p. 517-524.

[11] Wood, C.J., Liu, H. and Riffat, S.B. An investigation of the heat pump performance and ground temperature of a piled foundation heat exchanger system for a residential building. Energy (2010). 35(12): p. 4932-4940.

[12] Wood, C.J., Liu, H. and Riffat, S.B. Comparison of a modelled and field tested piled ground heat exchanger system for a residential building and the simulated effect of assisted ground heat recharge. International Journal of Low-Carbon Technologies (2010). 5(3): p. 137-143.

[13] Gao, J., et al. Thermal performance and ground temperature of vertical pile-foundation heat exchangers: A case study. Applied Thermal Engineering (2008). 28(17–18): p. 2295-2304.

[14] Alberdi-Pagola, M. and Poulsen, S.E. Thermal response testing and performance of quadratic cross section energy piles (Vejle, Denmark). In XVI European Conference on Soil Mechanics and Geotechnical Engineering (2015). 2015: Edinburgh, United Kingdom. p. 2469-2474.

[15] ASHRAE, 2009. ASHRAE Handbook. Fundamentals (2009). 1791 Tullie Circle, N.E., Atlanta, GA 30329: American Society of Heating, Refrigerating and Air-Conditioning Engineers, Inc.

[16] BS EN 15450:2007. Heating systems in buildings - Design of heat pump heating systems (2007). British Standards.

[17] GSHP Association. Thermal Pile: Design, Installation & Materials Standards (2012). Ground Source Heat Pump Association: National Energy Centre, Davy Avenue, Knowlhill, Milton Keynes.

6.1.2. UPDATED OPERATIONAL DATA (2015-2018)

The data acquisition and control system of the case study building continuously records data. Data corresponding to 2015 has been analysed in the previous section. In the following some updated values are provided, corresponding to the 2015-2018 period.

The heating need of the building supplied by the energy pile installation has increased to an average of 135 MWh/year and the installation has hardly been used in free cooling mode. The return fluid temperature hardly goes below 5 °C, while the maximum temperature in the ground loop remains below 15 °C. This means that the temperature change that the pile soil system has been subjected to falls below 5 °C, relative to initial conditions. Figure 6-1 shows the ground loop temperatures between 2015 and 2018.
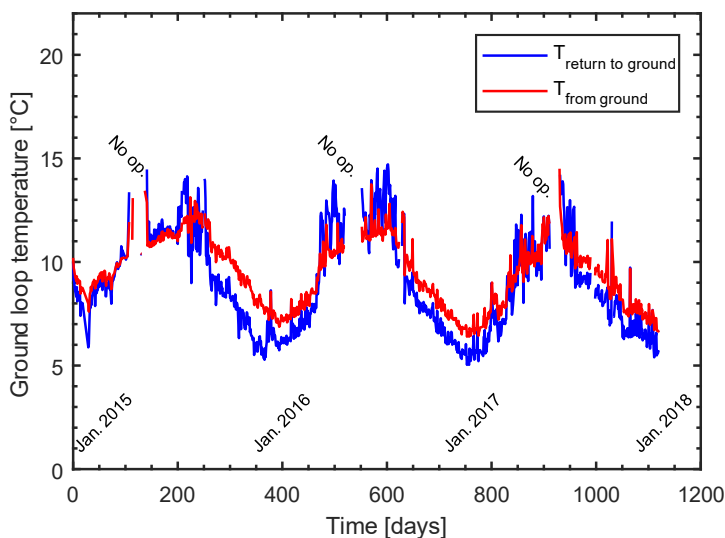
Figure 6-1: Daily aggregated ground loop temperatures between 2015 and 2018 at Rosborg Gymnasium.

After the paper presented in section 6.1.1. was written, we learned that there are 219 energy piles instead of 200 and that the operation started in autumn 2012 instead of in 2011. A thorough analysis of the operational data is ongoing since its coefficient of performance has dropped from 3 to 2.7 after some changes were completed in the system. An upcoming publication will illustrate and analyse the operational data between 2015 and 2018 and it will also look into the cooling potential of the system. Table 6-1 summarises the main parameters.

Table 6-1: Main operational parameters in Rosborg Gymnasium case study, data corresponding to 2015-2018 period.

Heating area supplied	3950 m^2
Beginning of operation	Autumn 2012
Heating need supplied	135 MWh
Proportion of heating need supplied	95-100%
Backup system	District heating
Number of energy piles	219
Length and square cross section size	15 m; 0.3 m
Fluid temperature in ground loop min	4.5 °C
Fluid temperature in ground loop max	15.0 °C
Heat pump capacity	200 kW
COP	2.6 - 3.0
Heat extraction rate max	43 W/m
Heat extraction rate average	12 W/m
Temperature out from heat pump	50-55 °C
Temperature supply radiatiors	50 °C
Pressure in system	2 bar
Volume storage tank	3 m^3

6.1.3. PAPER C

The following manuscript, denoted Paper C, has been submitted to Renewable Energy. The paper has been reviewed and minor revisions were required. Here, the revised manuscript is reproduced.

Alberdi-Pagola, M., Poulsen, S.E., Jensen, L.J. & Madsen, S., (under consideration). "A case study of the sizing and optimisation of an energy pile foundation (Rosborg, Denmark)", *Renewable Energy*.

Reprinted by permission from Elsevier.

A case study of the sizing and optimisation of an energy pile foundation (Rosborg, Denmark)

Maria Alberdi-Pagola [a, *], Søren Erbs Poulsen [b],

Rasmus Lund Jensen [a], Søren Madsen [c]

[a] *Department of Civil Engineering, Aalborg University, Denmark.*

[b] *VIA Building, Energy & Environment, VIA University College, Denmark.*

[c] *COWI A/S, Denmark.*

* Corresponding author. Department of Civil Engineering, Thomas Manns Vej 23, 9220 Aalborg Øst, Denmark. E-mail address: mapa@civil.aau.dk (M. Alberdi-Pagola).

_____

Abstract

    This paper applies previously validated multiple pile g-functions, for estimating operational average fluid temperatures in an actual energy pile foundation in Rosborg, Denmark. We find that the multiple pile g-functions yield fluid temperatures similar to what is observed, at minimal computational cost. The temperature model is then utilised in an optimisation algorithm that yields the minimum number of energy piles required by simultaneously maximising the pile spacing and taking into consideration the thermal load of the building. The optimisation shows that the thermal needs of the building can be fully supplied by 148 rearranged energy piles, instead of the current 219. The optimisation tool is also applied to a full-factorial design sweep which shows a large sensitivity of the number of energy piles on the thermal conductivity of the ground.

1. Introduction

Ground source heat pump (GSHP) systems produce renewable thermal energy that offer high levels of efficiency for space heating and cooling [1]. GSHP systems have a significant impact on the direct use of geothermal energy, accounting for 70% of the worldwide installed capacity [2].

Foundation pile heat exchangers (henceforth referred to as energy piles) are an alternative to borehole heat exchangers (BHE) when deep foundation is required in a building [3]. Figure 1 presents an example of precast energy piles.

Figure 1: a) Demonstration model of the precast pile heat exchanger with built in geothermal pipes. b) Pile heat exchanger field after driving. c) Pipe work.

Relative to BHEs, energy piles have lower initial costs [4,5], their potential to minimise the overall environmental impact of a structure has been demonstrated [6] and their contribution towards zero energy buildings has been suggested too [7].

The thermal dimensioning of energy pile foundations is typically addressed by methods developed for borehole heat exchangers which are implemented in commercial software such as GLHEPro [8], EED [9], LoopLink PRO [10] or GLD [11]. Optimisation strategies for sizing GSHP systems have also been reported in the literature. De Paly et al. [12] minimise the soil temperature change over time by adjusting the individual heat extraction rate in each borehole; Beck et al. [13] adjust the position of each borehole individually and Maragna [14] uses multi objective optimisation to find a balance between the borehole field configuration and economic parameters.

The thermal design of energy pile foundations should follow a similar approach, in an attempt to balance performance and costs: the number of pile heat exchangers must cover the thermal requirements of the building without compromising the sustainability of the installation and without incurring excessive expenses. However, in energy foundations, unlike borehole heat exchanger fields, the available area, the length and position of the pile heat exchanger are determined by the structural requirements which renders optimisation tools that allows rearrangement of the heat exchanger field improper [15].

Despite the large potential in the field of energy foundations, their implementation is limited. Some of the causes for the low spread are the low cost of other energy

sources - such as district heating [16], natural gas grid or fossil fuels [1] - the lack of financial incentives [1], the higher cost associated to the additional pipe works opposed to the standard foundations [5], as illustrated in Figure 1, and the lack of information regarding the technology in early stage decision making. Specific tools and guidelines that account for the particularities of energy foundations would ease their utilisation.

PILESIM [17] is an experimentally validated commercial software for energy piles, however it does not take irregular patterns into consideration. Makasis et al. [18] uses machine learning to find the maximum energy that can be provided by a specified energy pile foundation, yet the method has not yet been applied to irregular pile patterns.

Foundation piles may be placed in irregular grids, since their position is subject to the mechanical load distribution received from the building. Precast piles are thinner and, usually, shorter than in-situ piles and, therefore, under comparable conditions, a higher amount of precast piles is needed to compensate their smaller size, reducing the pile spacing. Precast piles are occasionally placed irregularly in clusters, from singles to fours, spaced less than 1 m apart. The small pile spacing causes significant thermal interaction between neighbouring energy piles. This increases the required number of piles and entails higher costs during construction and operation. Hence, it appears reasonable to equip only a subset of the foundation piles as ground source heat exchangers so long the foundation is able to meet the thermal requirements of the building [19]. This trade-off leads to an optimisation problem in which the number of energy piles and which piles to pick as ground source heat exchangers are constrained by a need to maintain long term sustainable ground temperatures and to meet the thermal requirements of the building.

Previous research on precast pile heat exchangers [20] has shown that semi-empirical multiple pile g-functions yield reliable estimates of fluid temperatures for relatively small, irregular pile arrays. This paper continues the work presented in [20] and aims to analyse the applicability of the multiple pile g-functions in a case study of Rosborg Gymnasium, Denmark, which is founded on energy piles and to propose an optimisation strategy based on the desirability function approach [21] to minimise the number of energy piles.

2. Methods

The fluid temperatures to the heat pump for the energy pile foundation in Rosborg is modelled with semi-empirical g-functions that are described briefly in the following (we refer the reader to [20,22] for additional information). The optimisation procedure is then described.

2.1. Multiple pile g-functions

The average fluid temperature T_f [°C] for a group of pile heat exchangers is:

$$T_f = T_0 + \frac{q}{2\pi\lambda_s}G_g + qR_cG_c + qR_{pipe} \qquad (1)$$

where T_0 [°C] is the undisturbed soil temperature, q [W/m] is the heat transfer rate per metre length of energy pile, λ_s [W/m/K] is the thermal conductivity of the soil, G_g is the multiple pile g-function for the ground temperature response, R_c [K·m/W] is the steady state concrete thermal resistance, G_c is the concrete G-function for the transient response of the pile and R_{pipe} [K·m/W] is the thermal resistance of the pipes.

G-functions are dimensionless curves of the change in temperature in the ground over time from applying a thermal load on the pile [23]. The pile g-functions in this study are derived from 3D temperature modelling of single energy piles for different pile length to diameter ratios (aspect ratio), which yield pile and soil temperatures at specified radial distances.

G_g depends on the aspect ratio of the pile heat exchanger, the number of piles and the pile spacing. To account for the interaction between piles, the multiple pile g-function G_g is calculated by temporal and spatial superposition of single pile g-function temperatures. G_c and R_c depend on the position of the pipes and the ratio between the thermal conductivity of the concrete and the soil. R_{pipe} depends on the thermal properties and flow rate of the heat carrier fluid and the thermal conductivity of the pipe. The dimensionless temperatures and curves are fitted with polynomials, to ease implementation. A detailed explanation of the method, comprising the dimensionless type curves and the coefficients for G_g, G_c and R_c, is given in [20,22] and a summary of the equations and coefficients applied in this study is provided in Appendix A.

2.2. Optimisation of pile heat exchanger design

The geometrical arrangement of foundation piles is determined solely by the structural requirements of the building. However, it is important that the spatial arrangement of the energy piles is as uniform as possible to avoid significant local changes in the soil temperature, which potentially have implications for the structural integrity of the piles, and ensure homogeneous thermal settlements or uplifts, if any [24]. Once an energy pile pattern is chosen from the predefined grid of foundation piles, corresponding fluid temperatures are estimated with the multiple pile g-functions. The energy pile pattern is then adjusted until the desired temperatures are achieved while honouring the thermal requirements of the building.

2.2.1. Optimisation of pile arrangement

The ideal way to place ground heat exchangers in a field is by minimising the influence between them which corresponds to maximising the pile spacing. To provide the energy pile arrangement that maximises the pile spacing, given the structural constraints, a constrained optimisation scheme is proposed. The scheme accepts as input the coordinates of the foundation piles, the number of required energy piles and a minimum initial pile spacing. The MATLAB "*patternsearch*" non-continuous subroutine [25] is utilised for determining the arrangement of the required

energy piles, while maximising pile spacing. For every computation, the local optimisation algorithm distributes n_p piles by maximising their spacing. Therefore, the optimiser finds the maximum pile spacing that can accommodate n_p piles in the provided grid, i.e., leading to a uniform pile distribution covering as much free space as possible.

Figure 2 shows an example of a foundation pattern with 11 piles of which 7 are aimed to be energy piles. An initial guess for the desired energy pile spacing is also chosen, e.g., 4 m. Now, the optimisation scheme attempts to find the best distribution for the required 7 energy piles. However, due to the predefined position of the piles, it is not possible to pick 7 energy piles because the condition to keep a 4-m pile spacing (dotted grey line) cannot be fulfilled. Hence, the optimisation scheme reduces the pile spacing to 3 m (solid grey line) and tries again to select among the existing piles, successfully now, the ones that should be equipped as energy piles. The prevailing condition is to keep the number of energy piles initially imposed and the algorithm will adapt the energy pile spacing, to keep it as high as possible, given the geometric restrictions.
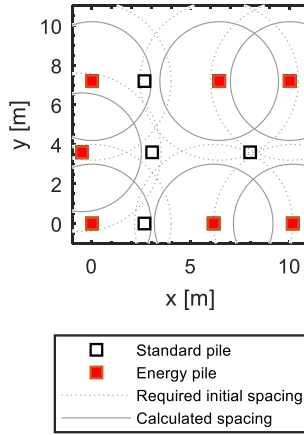
Figure 2: Optimum arrangement of 7 energy piles in a foundation with 11 foundation piles.

2.2.2. Desirability function approach

The multiple pile g-function model is applied to the pile arrangement determined by the optimisation scheme outlined in the previous subsection (2.2.1) to yield average fluid temperatures in the ground loop (Equation 1). Now, the optimum number of pile heat exchangers required to supply a given building demand is determined by maximising a so-called desirability function. The desirability function approach [21], also described in [26,27], is used for optimisation of multiple response processes by assigning a desirability function $d_i(Y_i)$ value between 0 and 1 to each response $Y_i(x)$, where $d_i(Y_i) = 0$ and $d_i(Y_i) = 1$ represent unacceptable and ideal responses,

respectively. The individual desirabilities are combined using the geometric mean, to give the overall desirability D (hereon the notation used in [27] is adopted):

$$D = (d_1(Y_1)d_2(Y_2)\dots d_k(Y_k))^{1/k} \tag{2}$$

where k is the number of responses. Clearly, if any response Y_i is completely undesirable, i.e., $di(Yi) = 0$, then the overall desirability is zero.

Different desirability functions $d_i(Y_i)$ are defined, depending on whether a response Y_i is to be maximised, minimised or assigned a target value. Let define L_i, U_i and T_i as lower, upper and target values, respectively. According to this, the desired response Y_i needs to fall within $L_i \leq T_i \leq U_i$.

When a specific value needs to be assigned to a response (a.k.a. target is best), its desirability functions is defined as:

$$d_i(Y_i) = \begin{cases} 0 & \text{if } Y_i(x) < L_i \\ \left(\dfrac{Y_i(x) - L_i}{T_i - L_i}\right)^s & \text{if } L_i \leq Y_i(x) \leq T_i \\ \left(\dfrac{Y_i(x) - U_i}{T_i - U_i}\right)^t & \text{if } T_i \leq Y_i(x) \leq U_i \\ 0 & \text{if } Y_i(x) > U_i \end{cases} \tag{3}$$

where s and t determine the importance to hit the target value. When $s = t = 1$, the desirability function increases linearly towards the target value T_i.

When a response needs to be maximised, its desirability function is defined as:

$$d_i(Y_i) = \begin{cases} 0 & \text{if } Y_i(x) < L_i \\ \left(\dfrac{Y_i(x) - L_i}{T_i - L_i}\right)^s & \text{if } L_i \leq Y_i(x) \leq T_i \\ 1 & \text{if } Y_i(x) > T_i \end{cases} \tag{4}$$

where T_i is understood as a large enough value for the response.

Lastly, when a response needs to be minimised, its desirability function is defined as:

$$d_i(Y_i) = \begin{cases} 1 & \text{if } Y_i(x) < T_i \\ \left(\dfrac{Y_i(x) - U_i}{T_i - U_i}\right)^s & \text{if } T_i \leq Y_i(x) \leq U_i \\ 0 & \text{if } Y_i(x) > U_i \end{cases} \tag{5}$$

where T_i is understood as a small enough value for the response.

The desirability approach penalises the values that differ from the target values or admissible limits and allows the assignment of weights to the different responses. In this study, the desirability function is defined by adjusting three responses simultaneously:

i) The number of energy piles, which needs to be minimised. It is limited between 1 (ideally, a single pile would need to be an energy pile) and the total number of foundation piles, i.e., thermally activating all the standard piles.

ii) The return temperature to the ground loop. The minimum allowed temperature in the ground loop must exceed 0 °C [28], with a target value of 2 °C ("target is best"), to minimise thermal effects on the mechanical response of the pile. The upper limit is set to 20 °C.

iii) The long-term average fluid temperature must be as close as possible to the initial soil temperature to ensure stable performance of the heat pump over time and to mitigate the environmental impact of the system ("target is best").

The three responses have been assigned equal weights. The practical implementation of the method is divided into the steps shown in Figure 3. Once an optimum configuration for n_p piles is determined, the global optimisation algorithm calculates the corresponding fluid temperatures. In the proposed scheme, the energy pile pattern is updated until the temperature requirements defined in the desirability function are satisfied. The optimisation scheme is also applied to a full-factorial design sweep of the case study where the thermal conductivity of the soil λ_s [W/m/K] and the thermal load Q [kW] are varied to analyse the sensitivity of the energy foundation to varying conditions.
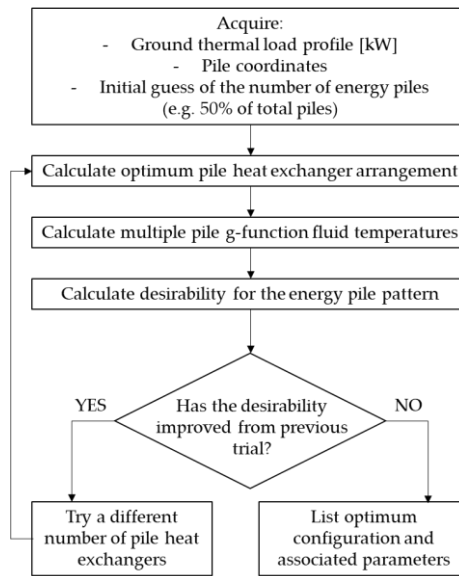
Figure 3: Workflow for obtaining the optimum number and arrangement of energy piles.

3. Case study

The southern extension of Rosborg Gymnasium high school in Vejle, Denmark, is founded on 269 piles, 219 of which are energy piles (Figure 4). All 269 piles were scheduled to serve as energy piles, however, 50 piles were cut as the desired foundation depth could not be reached by hammering. The driven, quadratic cross section (30 cm by 30 cm), precast 15 m energy piles are fitted with W-shaped heat exchanger piping (Figure 1). In Denmark, 90% of the piles are precast [29] and between 85-90% of the production is addressed to the building industry [30]. Standard dimensions are square sections with dimension from 25 cm to 45 cm (Figure 1).
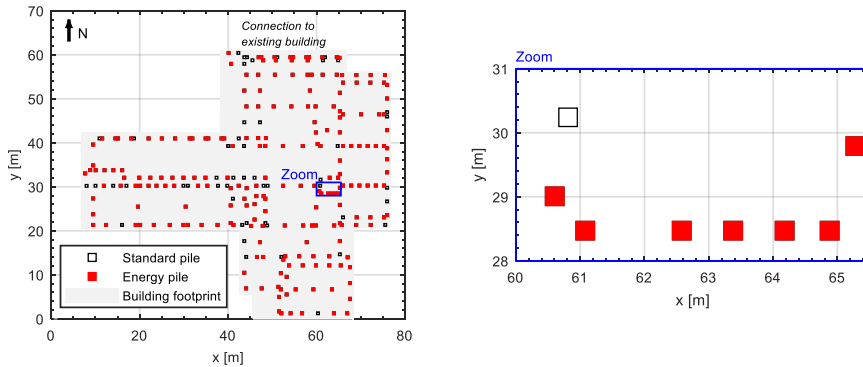
Figure 4: Top view of foundation pattern of the case study. a) Overview; b) Zoom to a high pile density area. The legend is common for both subplots.

The ground source heat pump system has supplied the space heating need of the 3950 m^2 living area since autumn 2012 which amounts to approximately 135 MWh/year. The system is capable of supplying free cooling to the southern rooms (approx. 900 m^2), however, this option is rarely used and the cooling amounts to just 2 MWh/year (Figure 5). The ground thermal load is also provided in Figure 5 (81 MWh/year).
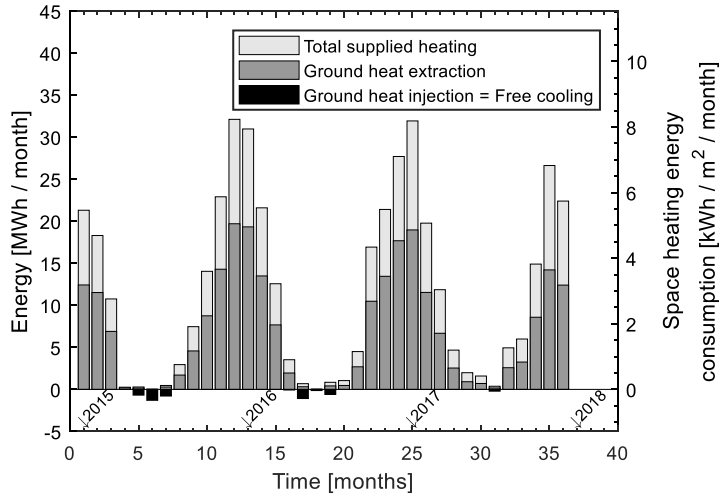
Figure 5: Supplied heating and cooling at Rosborg Gymnasium, Denmark.

The pile heat exchangers are connected in parallel. The ground loop utilises a 20% ethylene glycol-based water solution as heat carrier fluid. The heat pump consists of a water-to-water unit with a heating capacity of 200 kW and two compressors. The heat pump charges a water accumulation tank (55 °C) from which a traditional radiator-based heating system is supplied. The district heating network serves as an auxiliary heating system. Free cooling uses ventilation fan-coils coupled to the ground loop.

The foundation is situated 70 cm below terrain, just below the primary groundwater table. The foundation piles are placed in glacial sand and gravel sediments situated at 5-6 m below terrain, topped by postglacial organic clay [31–33]. Figure 6 shows the density, thermal conductivity and volumetric heat capacity profiles for the site. The case study is further described in [31,32].
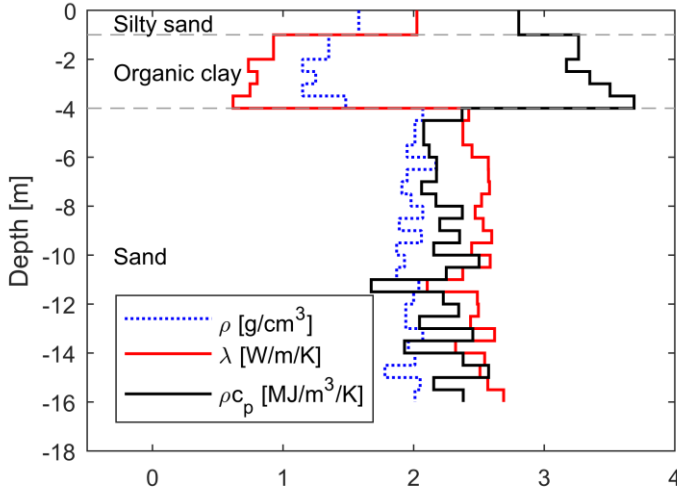
Figure 6: Density ρ [g/cm³], thermal conductivity λ [W/m/K] and volumetric heat capacity ρcₚ [MJ/m³/K] profile at the Rosborg test site, after [33]. Depth is relative to the ground surface.

3.1. Data processing

The inlet and outlet temperature time series as well as the total flow rate and the energy to/from the ground loop have been extracted from the building control and monitoring system. The raw data consist of 5-minute averages recorded between 2015 and 2017 (Figure 7). The measured thermal power and temperature time series are aggregated to hourly, daily and monthly averages (Figure 7), ensuring conservation of energy.

For the computations, the operational data from 2015 and 2017 are extrapolated back in time to autumn 2012. During the first 3 years of operation, system start up implied reduced supplied heating and cooling and therefore, only 50% of the extrapolated demand is considered for the period 2012-2015. The studied energy pile foundation works mainly in heating mode, i.e., an unbalanced heat extraction over time is expected. In principle, this will lower long-term soil temperatures.
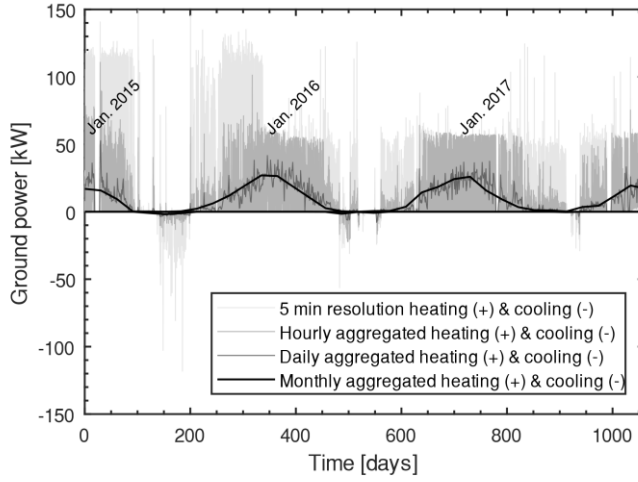
Figure 7: Measured ground thermal power (2015-2017) at 5-minute resolution and hourly, daily and monthly aggregated powers, respectively.

3.2. Model parameters

The model parameters utilised in the case study are listed in Table 1. Each of the parameters influences the overall thermal performance of the system and more about the implications can be learned in [34,35].

The undisturbed soil temperature T0 is determined by field measurements prior to thermal response test (TRT) [33,36]. The thermal conductivities of the soil λ_s and the concrete λ_c are estimated from field TRT measurements, presented in [33]. The volumetric heat capacities of the soil ρc_{ps} and the concrete ρc_{pc}, are estimated from laboratory testing, also presented in [33]. The total flow circulating in the ground loop was recorded by the data acquisition and control system of the building [31]. The flow in each pile is the total flow divided by the number of energy piles. The fluid and pipe properties were obtained from manufacturer brochures [37,38].

Table 1. Parameters for the case study.

Undisturbed soil temperature	T_0 [°C]	10.20
Thermal conductivity of soil	λ_s [W/m/K]	2.21
Volumetric heat capacity of soil*	ρc_{ps} [MJ/m³/K]	2.47
Thermal conductivity of concrete	λ_c [W/m/K]	3.05
Volumetric heat capacity of concrete	ρc_{pc} [MJ/m³/K]	2.37
Thermal conductivity of fluid	λ_f [W/m/K]	0.54
Volumetric heat capacity of fluid	ρc_{pf} [MJ/m³/K]	4.01
Density of fluid	ρ_f [kg/m³]	1048
Dynamic viscosity heat carrier fluid	μ_f [Pa·s]	0.002
Thermal conductivity of pipe	λ_p [W/m/K]	0.42
Total flow in ground loop	f_{total} [m³/s]	0.0083
Number of pile heat exchangers	n_p [-]	219
Circulating flow per pile	f [m³/s]	$3.39 \cdot 10^{-5}$
Pile active length	L [m]	15
Cross section size	S [m]	0.30 x 0.30
Energy pile aspect ratio	AR [-]	39
Number of pipes in cross section	n [-]	4
Pipe outer diameter	$\emptyset_{out}$ [m]	0.020
Pipe inner diameter	$\emptyset_{in}$ [m]	0.016

* Layer thickness-weighted arithmetic mean.

4. Results and discussion

Firstly, the model is compared to operational data to demonstrate its validity. The optimisation method is then applied to the case study pile arrangement and the parameter sweep analyses the influence of variations in the soil thermal properties and building requirements on the required size of the energy foundation.

4.1. Model verification

To evaluate the predictive capabilities of the model, simulated average fluid temperatures have been compared to corresponding observations during the three years of collected data (Figure 8).
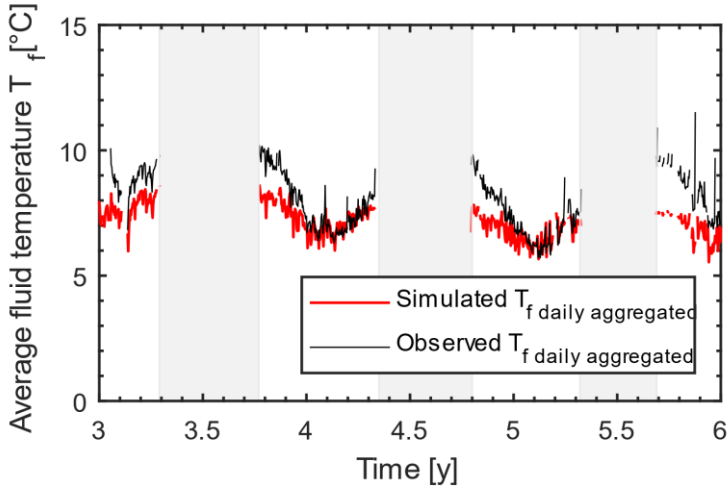
Figure 8: Observed and modelled average fluid temperatures. The periods where heat extraction is non-existing are hidden.

The model reproduces the shape of the observed temperatures for heat extraction periods. When the heat removal from the ground dominates, the phenomena is mainly governed by conduction in the soil which is well captured by the model. The model reproduces the lowest temperatures which is critically important for ground source heat pump system.

The simulations diverge from the observations as the heating need decreases, i.e., in low activity or stand-by periods. In these stages, other factors, which are not considered by the model, begin to play a role: possible groundwater flow, heat island effect from the building, heat gains through the building standing on top of the foundation, seasonal surface temperature variations and indoor temperature sensors measuring on standing fluid in pipes.

4.1.1. Influence of load aggregation

To analyse the implication of using hourly, daily, weekly or monthly thermal loads, a comparison of computed temperatures with different levels of aggregation has been performed. The thermal load assumed in the comparison, corresponds to the average applied power in the period 2015-2017. Figure 9 shows the residuals for the computed average fluid temperatures, relative to the hourly simulation.
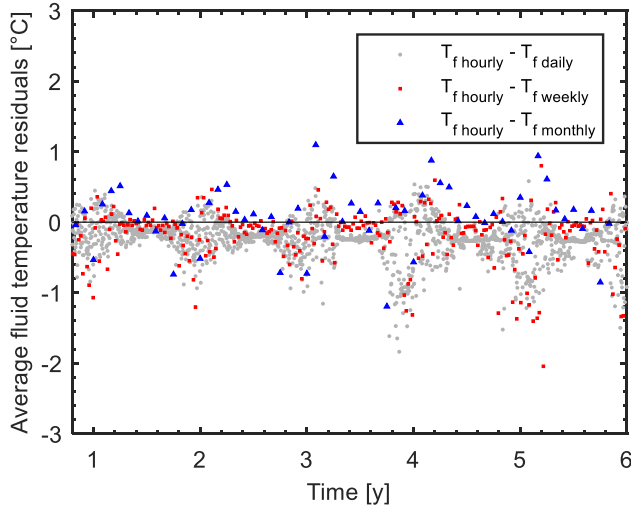
Figure 9: Average fluid temperature T_f residuals for different time resolutions, relative to the hourly simulation.

When aggregated values are used, a loss of accuracy can be expected, as the temperatures calculated with the simplified thermal loads might not capture the peak temperatures. When a daily aggregation of the heat power is used, the most frequent difference with the hourly most critical temperatures is around 1 °C. Even though the occurrence of those critical low temperature does not extend over time, it is important to be aware of this fact during design and to consider the duration of the peak needs in the thermal load, as suggested in [9]. Unfortunately, this information is not available for the case study.

Weekly and monthly loads yield similar magnitude of residuals. Thus, as mentioned, a method to consider peak needs, their duration and permits the analysis of weekly or monthly loads will be beneficial since computation times can be shorten considerably, as shown in Table 2.

Table 2: Computation times.

Simulated time	Resolution	Time-steps	Computation time [s]
	Hourly	87600	450
25 years	Daily	3650	95
	Weekly	522	2.75
	Monthly	120	0.88

The accuracy and resolution of the simulations shall depend on the information available at every stage of the process and the resources, namely: feasibility study, dimensioning or operational optimisation. The higher the quality of the thermal

profiles of the building, the more accurate will be the ground loop temperature predictions. It is important to refine the thermal loads as information is gathered so that the accuracy of the simulations can be improved.

The thermal response of the soil occurs on a timescale of hours. Previous research [20] has shown that the thermal disturbance at approximately 1 m distance from the pile begins after 1 day. Therefore, it is considered that the effect of the daily simplification on the model accuracy is minimal and, in the following, a daily thermal load will be analysed.

4.2. Long-term ground temperature prediction

Figure 10 shows the computed average fluid temperature following 25 years of operation, extrapolating existing heating and cooling loads. Computed temperatures are above 4 °C and steady-state average ground temperature conditions are established after 15 years of operation.
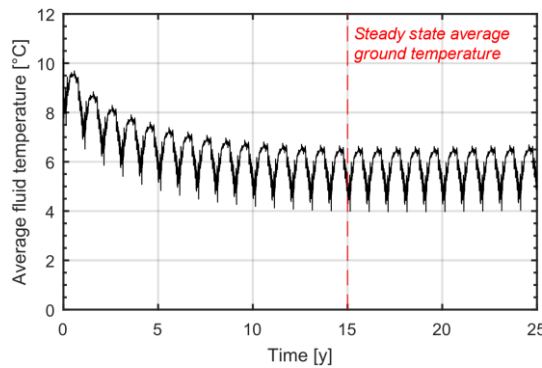
Figure 10: Predicted long-term temperatures for Rosborg Gymnasium.

4.3. Optimisation of pile heat exchanger design

The dimensioning of the energy pile foundation in Rosborg was done conservatively by replacing all traditional foundation piles with energy piles. At this time, there were no guidelines nor tools available for dimensioning energy pile foundations. Consequently, the construction costs were potentially elevated from using an excess number of energy piles. In this section, we aim to properly dimension the energy pile foundation at Rosborg, by minimising the number of energy piles while still being able to supply the required heating and cooling loads and to ensure the long-term sustainability of ground temperatures.

The parameters for the optimisation are listed in Table 1. The Reynolds number of the ground loop flow rate is ca. 2500, indicating a transient regime between laminar and turbulent flow conditions. Previous research [20] has shown that there is not a

significant reduction in the pipe thermal resistance when applying fully turbulent flow relative to high transient. 15-year simulations are carried out.

Figure 11 shows the dependence of the minimum temperature return to the ground loop and the desirability function on the number of energy piles. At least 105 energy piles are required for maintaining fluid temperatures above 0 °C. Since the desirability condition regarding sub-zero temperatures is not fulfilled, the overall desirability is zero. As the minimum fluid temperature increases, the desirability increases until the addition of additional energy piles is outweighed by the condition that ensures minimisation of the number of energy piles. Thus, as the number of energy piles increases, the desirability progressively falls to zero for the maximum number of energy piles.
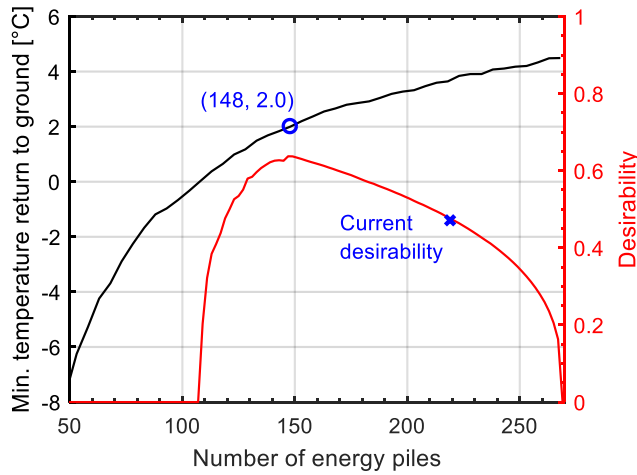
Figure 11: Minimum return fluid temperature the ground loop and desirability for different numbers of energy piles.

The optimal arrangement, at which desirability is maximised, counts 148 energy piles, distributed as shown in Figure 12. Figure 12 also provides the optimum energy pile arrangements for 110 and 220 energy piles. The results imply that Rosborg Gymnasium can supply the current thermal demand with 32% less energy piles. The desirability of the current setup is also provided in Figure 11. It falls practically on top of the desirability curve, meaning that when 219 piles are needed, the optimisation of the pile position gets harder and its influence is not significant. This is visible in Figure 12c, where the higher amount of energy piles required, hardly leaves room for optimisation within the constraints. Therefore, the fluid temperatures that the model yields with the arrangement in Figure 12c are similar to the ones obtained with the pile arrangement presented in Figure 4.
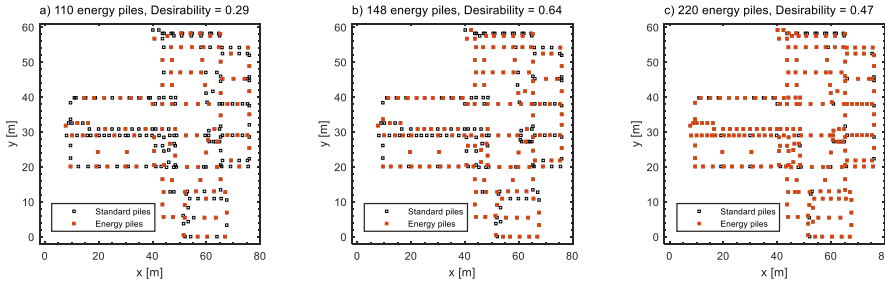
Figure 12: Optimal location of energy piles for different desirabilities: 110, 148 and 220 pile heat exchangers for a), b) and c), respectively.

Deciding upon the number of energy piles, depends, ultimately, on the engineer's judgement. Besides, the desirability function can be defined in an alternative way, assigning different weights or adding more responses, such as costs. Additional constraints and conditions modifies the shape of the desirability function, and, thus, potentially impacting the outcome of the optimisation.

4.4. Parametric study

The optimisation tool is applied in a full-factorial parameter sweep where the thermal conductivity of the soil λ_s [W/m/K] and the thermal load Q [kW] are varied to analyse the sensitivity of the performance of the energy pile foundation to varying conditions. The thermal conductivity of the soil varies from 1.0 to 3.5 W/m/K, based on typical soils in Denmark, whereas the thermal load requirements range between 0.5 to 1.5 times the current need of the building, i.e., between 40.5 MWh and 121.5 MWh of heat extraction per year. The remaining variables are kept as given in Table 1. The optimum pile arrangement is calculated for each parameter combination (10^2) and contour plots of desirability, the number of required energy piles, the minimum temperature in the ground loop and the average fluid temperature are shown in Figure 13.
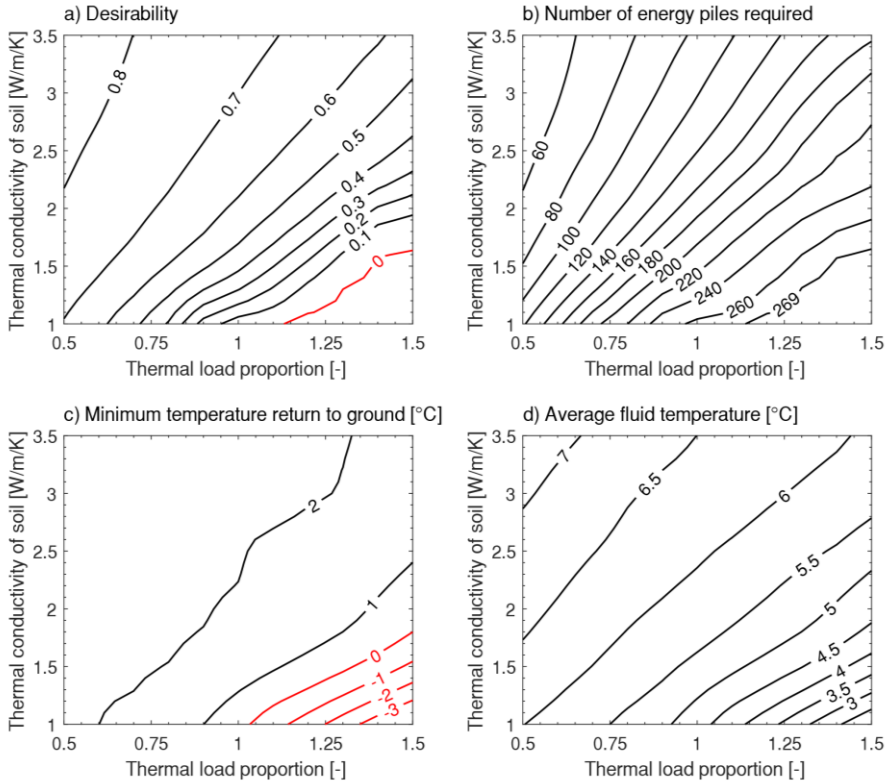
Figure 13: a) Desirability, b) number of required energy piles, c) minimum temperature return to the ground loop and d) average fluid temperature, for the optimal pile arrangement.

The four subplots in Figure 13 need to be read simultaneously. Figure 13a shows the desirability contours for each parameter combination. The higher desirability contour lines approaching 1 on the left top part indicate that the three conditions that define the desirability are close to be simultaneously fulfilled. Meaning that, obviously, the higher the thermal conductivity of the soil and the lower the proportion of thermal load, the higher will be the desirability, the lower will be the required number of energy piles and the more satisfactory will be the temperature conditions.

The null desirability, highlighted in red, indicates an unacceptable boundary. This means that for high thermal load proportions (above 1.1) and low thermal conductivities of soil (below 1.6 W/m/K), even the maximum number of energy piles (269 in Figure 13b) yields unacceptable minimum temperature of the return fluid to the ground (red lines in Figure 13c).

Figure 13c also indicates that acceptable minimum fluid temperatures are reached as the thermal conductivity of the soil increases. Figure 13b shows a large sensitivity

of the number of energy piles to the thermal conductivity of the ground. The thermal conductivity of the soil cannot be engineered and must be determined by appropriate field or laboratory measurements such as thermal response testing during the geotechnical investigations where piles are driven to assess the depth of the foundation [33].

It is common practice to design ground source heat pump installations to cover 80% of the heating load, given that peaks in demand are supplied by a complementary source [14]. Obtaining an accurate energy demand profile for a planned building is not always possible. In that case, parameter sweeps are useful for quantifying the uncertainty on the number of energy piles from having insufficient knowledge of the thermal load of the building. To that end, it must be stipulated, that obtaining accurate estimates of the heating and cooling requirements of a building in the planning phase is essential when applying the method presented in this paper.

5. Conclusions

We apply dimensionless temperature type curves (g-functions) and superposition techniques for estimating the fluid temperatures in energy pile foundations. The temperature model is applied in an optimisation scheme, based on the desirability function approach, in which the minimum number and arrangement of energy piles required for supplying the thermal needs of the building is estimated, while maintaining sustainable long-term temperatures.

The multiple pile g-functions yield reliable average fluid temperatures when compared to corresponding observed temperatures during heat extraction.

The optimisation tool shows that the number of pile heat exchangers needed for this case study could have been reduced by 32%.

The parameter sweep carried out provides practical design charts that support the dimensioning when the thermal load of the building and/or the soil thermal properties are uncertain.

The desirability function approach and the flexibility of the proposed method allow more conditions and features to be considered in future improvements, such as costs and complementary energy sources. As such, the multiple pile g-function based temperature model combined with the proposed optimisation strategy offers a reliable basis for feasibility studies and for the dimensioning of energy pile foundations.

Acknowledgements

Appendix A

As previously stated in Section 2, the average fluid temperature T_f [°C] for a group of pile heat exchangers is:

$$T_f = T_0 + \frac{q}{2\pi\lambda_s} G_g + qR_cG_c + qR_{pipe} \tag{A.1}$$

where T_0 [°C] is the undisturbed soil temperature, q [W/m] is the heat transfer rate per metre length of energy pile, λ_s [W/m/K] is the thermal conductivity of the soil, G_g is the multiple pile g-function for the ground temperature response, R_c [K·m/W] is the steady state concrete thermal resistance, G_c is the concrete G-function for the transient response of the pile and R_{pipe} [K·m/W] is the thermal resistance of the pipes. In the following, the equations for the various functions in Equation A.1 are described. The following content is further described in [20,22] and, hence, this appendix comprises a summary.

The inlet and outlet temperatures in the ground loop can be calculated by solving the two-equation system:

$$q = f \cdot \rho c_{pf} \cdot \frac{(T_{in} - T_{out})}{n_p \cdot L} \tag{A.2}$$

$$T_f = \frac{(T_{in} + T_{out})}{2} \tag{A.3}$$

where f [m^3/s] is the circulating flow in the ground loop, ρc_{pf} [J/m^3/K] is the volumetric heat capacity of the heat carried fluid, T_{in} [°C] and T_{out} [°C] are the inlet and outlet temperatures in the ground loop, respectively, np is the number of energy piles comprising the energy foundation and L [m] is the active length per energy pile.

G-functions are dimensionless response factors that describe the change in temperature in the ground around a heat exchanger with time as a result of an applied thermal load q [23]. In this study, the normalised temperature changes Φ and time Fo are defined as:

$$\Phi = \frac{2\pi\lambda_s\Delta T}{q} \tag{A.4}$$

$$Fo = \frac{\alpha_s t}{r_b^2} \tag{A.5}$$

where ΔT [K] is the temperature change between the undisturbed soil temperature T_0 [°C] and the average pile wall temperature T_b [°C], α_s [m^2/s] is the thermal diffusivity, i.e., the ratio between the thermal conductivity λ_s [W/m/K] and the volumetric heat capacity of the soil ρc_{ps} [J/m^3/K], t [s] is the time and r_b [m] is the pile equivalent radius. The pile radius is the radius that provides an equivalent circumference to the square perimeter.

The pile g-functions in this study are derived from 3D temperature modelling of single energy piles for different pile length to diameter ratios (aspect ratio AR), as proposed in [19,39] and developed in [20,22], which yield pile and soil temperatures at specified radial distances. Figure 14 shows the dimensionless temperature curves resulted from simulations of single energy piles with AR 30 and AR 45, at normalised distances $S/2r_b$.

a)   AR 30   b)   AR 45
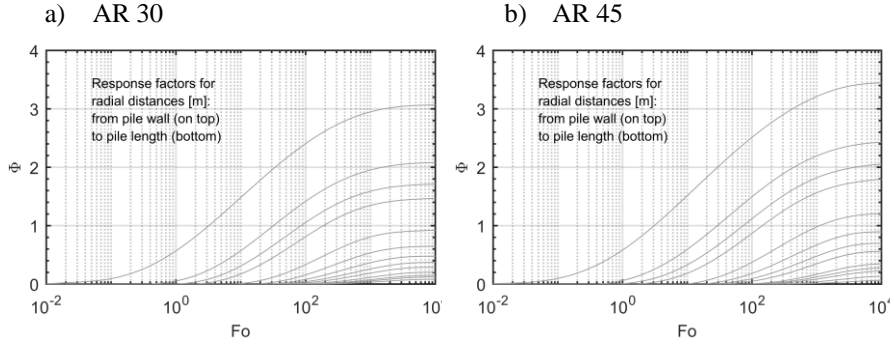
Figure 14: Dimensionless temperature responses for soil temperature changes at normalised distances $S/2r_b = T_b$, 1.3, 2, 2.6, 5.2, 7.9, 10.5, 13.1, 19.6, 26: a) aspect ratio 30; b) aspect ratio 45 [22].

The temperatures are fitted with polynomials, to ease implementation. The ground temperature response functions for each distance are valid for min (Fo) < Fo < 10000. For Fo < min (Fo), G_g should be set to zero. G_g can be described as:

$$G_g = a \cdot \ln(Fo)^9 + b \cdot \ln(Fo)^8 + c \cdot \ln(Fo)^7 + d \cdot \ln(Fo)^6 + e \\ \cdot \ln(Fo)^5 + f \cdot \ln(Fo)^4 + g \cdot \ln(Fo)^3 + h \\ \cdot \ln(Fo)^2 + i \cdot \ln(Fo) + j \tag{A.6}$$

The curve fitting parameters are provided below in Tables 3 and 4, for selected radial distances. For intermediate values not considered in the tables of coefficients, a linear interpolation needs to be applied. Linear interpolations are considered sufficient precise and quick [40].

Table 3: Spatial G-function coefficients for AR 30 [22].

S/2r	∞	1.3	2.6	7.8	10.5	13.1	19.6	31.2
Distance from pile edge [m]	0.00	0.50	1.00	3.00	4.00	5.00	7.50	11.90
a	-6.133E-09	1.592E-08	3.032E-09	-2.950E-08	-1.835E-08	-8.193E-09	4.478E-09	5.694E-09
b	1.568E-07	-3.884E-07	-2.610E-07	6.249E-07	4.464E-07	2.521E-07	-2.753E-08	-9.627E-08
c	-1.134E-06	1.065E-06	3.712E-06	-8.417E-07	-1.408E-06	-1.386E-06	-7.791E-07	-1.265E-07
d	-2.850E-06	3.737E-05	8.788E-06	-4.916E-05	-3.272E-05	-1.717E-05	3.368E-06	7.355E-06
e	1.151E-04	-1.932E-04	-3.290E-04	1.488E-04	1.576E-04	1.253E-04	4.287E-05	-7.582E-06
f	-7.257E-04	-1.620E-03	1.088E-05	1.312E-03	8.230E-04	4.161E-04	-7.755E-05	-1.598E-04
g	-4.868E-03	6.314E-03	9.692E-03	-2.005E-03	-2.544E-03	-2.093E-03	-6.775E-04	1.941E-04
h	4.514E-02	5.190E-02	1.794E-02	-8.278E-03	-5.495E-03	-2.838E-03	4.586E-04	9.959E-04
i	3.243E-01	9.452E-02	-5.962E-03	6.321E-03	8.970E-03	7.734E-03	2.646E-03	-7.663E-04
j	5.689E-01	5.337E-02	-8.649E-03	7.817E-03	6.984E-03	4.715E-03	5.910E-04	-9.730E-04
RMSE*	1.138E-05	9.286E-06	8.402E-06	5.272E-06	5.359E-06	5.164E-06	1.858E-06	1.107E-07
R²**	1.000E+00	9.997E-01	9.999E-01	9.999E-01	1.000E+00	1.000E+00	1.000E+00	9.998E-01
min Fo [-]	0.01	0.43	2.10	20.00	26.00	33.50	58.00	175.00
min time [h]	0.10	4.36	21.28	202.67	263.47	339.48	587.75	1773.38
max Φ [-]	3.07	2.07	1.46	0.65	0.48	0.37	0.21	0.09
max Fo [-]	10000	10000	10000	10000	10000	10000	10000	10000

*RMSE: Root Mean Squared Error
**R²: Coefficient of Determination

Table 4: Spatial G-function coefficients for AR 45 [22].

S/2r_b	∞	1.3	2.6	7.9	10.5	13.1	19.6	45.6
Distance from pile edge [m]	0.00	0.50	1.00	3.00	4.00	5.00	7.50	17.40
a	4.199E-09	2.392E-09	-1.052E-08	-1.870E-09	3.169E-09	5.693E-09	6.248E-09	6.536E-10
b	-3.525E-08	-9.048E-08	7.076E-08	8.660E-08	3.149E-08	-5.976E-09	-4.042E-08	-1.085E-08
c	-8.541E-07	3.281E-07	2.267E-06	1.246E-08	-8.020E-07	-1.156E-06	-1.115E-06	-1.007E-07
d	8.311E-06	1.546E-05	-1.062E-05	-1.446E-05	-6.407E-06	-7.995E-07	4.745E-06	1.493E-06
e	6.477E-05	-8.856E-05	-1.926E-04	2.152E-06	5.308E-05	7.320E-05	6.764E-05	6.226E-06
f	-8.423E-04	-1.116E-03	3.158E-04	7.615E-04	4.225E-04	1.714E-04	-1.086E-04	-5.328E-05
g	-3.519E-03	4.209E-03	7.437E-03	1.341E-03	-2.729E-04	-1.015E-03	-1.256E-03	-1.418E-04
h	4.648E-02	4.981E-02	1.806E-02	-6.134E-03	-4.251E-03	-2.209E-03	5.635E-04	4.997E-04
i	3.245E-01	1.100E-01	4.341E-03	-1.030E-02	-1.528E-03	3.378E-03	6.238E-03	8.745E-04
j	5.817E-01	6.060E-02	-7.559E-03	3.802E-03	4.919E-03	4.112E-03	1.336E-03	-4.694E-04
RMSE*	1.658E-05	1.609E-05	1.374E-05	1.943E-05	1.491E-05	9.313E-06	2.111E-06	3.081E-07
R²**	9.999E-01	1.000E+00	1.000E+00	9.998E-01	1.000E+00	9.997E-01	9.971E-01	9.972E-01
min Fo [-]	0.01	0.43	1.7	20	25	32	78	350
min time [h]	0.10	4.36	17.23	202.67	253.34	324.28	790.42	3546.76
max Φ [-]	3.45	2.43	1.79	0.90	0.70	0.56	0.35	0.06
max Fo [-]	10000	10000	10000	10000	10000	10000	10000	10000

*RMSE: Root Mean Squared Error
**R²: Coefficient of Determination

The curves provided in Figure 14 and described by equation A.6 can be superimposed in time and space to account for multiple piles. This principle relies on the heat conduction equation and boundary conditions on being linear [41]. In the spatial superposition the temperature distributions around every ground heat

exchanger are added in order to calculate the overall temperature variation at the pile walls [42]:

$$\Delta T_b(t) = \frac{1}{n_p} \sum_{i=1}^{n_p} \sum_{j=1}^{n_p} \Delta \overline{T_b}(d_{ij}, t) \tag{A.7}$$

$$d_{ij} = \begin{cases} r_b, & i = j \\ \sqrt{(x_i - x_j)^2 + (y_i - y_j)^2}, & i \neq j \end{cases} \tag{A.8}$$

where ΔT_b [K] is the average temperature variation at the pile heat exchanger wall, (x_i, y_i) [m] are the coordinates of the ith pile heat exchanger, n_p is the number of pile heat exchangers in the foundation and d_{ij} [m] is the pile distance.

Time variations can be applied by deconvolution of the time varying heat transfer rate [41]. The temperature at discrete time step in the pile heat exchanger foundation is computed as:

$$\Delta T_n = \sum_{i=1}^{i=n} \frac{q_i}{2\pi\lambda_s} \left(G(Fo_n - Fo_{(i-1)}) - G(Fo_n - Fo_i) \right) \tag{A.9}$$

where n is the point in normalised time in which the superposition is evaluated.

The steady state concrete thermal resistance R_c [K·m/W] and the concrete G-function for the transient response of the pile G_c [39,43] depend on the shape of the pile cross section, the position of the pipes and the ratio between the thermal conductivity of the concrete and the soil. The transient response of the pile concrete is calculated as the proportion of the steady state thermal resistance that has been achieved in the 3D FEM simulations at a given value of time Fo:

$$R_c = \frac{T_p - T_b}{q} \tag{A.10}$$

where T_p [°C] is the average temperature on the outer wall of the pipe.

Alberdi-Pagola et al. [33] provided the pile thermal resistance for different ratios between soil and concrete thermal conductivity, λ_c/λ_s (Figure 15a). The temporal development in the proportion of steady state pile thermal resistance R_c for W-shape pipe arrangements is shown in Figure 15b for ratios $\lambda_c/\lambda_s = 0.5$, 1 and 2 [20].

a)

b)
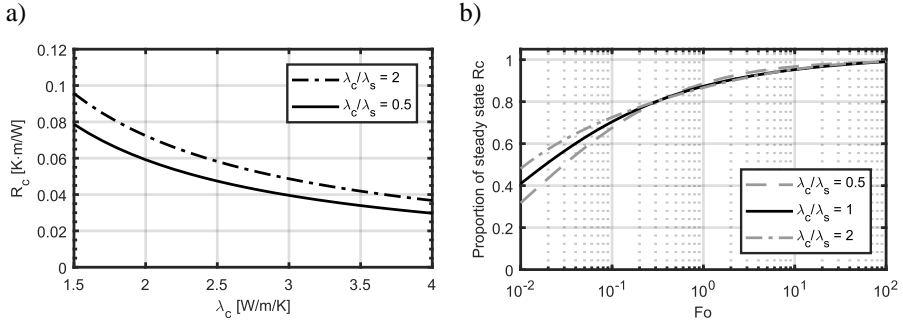
Figure 15: a) 3D model estimated upper and lower bounds for the concrete thermal resistance R_c [33]. b) Proportion of steady state R_c [20]. Both subplots correspond to W-shape pipe arrangements.

The curves are fitted with polynomials, to ease implementation. The upper and lower bounds for the concrete thermal resistance R_c for square precast pile heat exchangers with W-shape pipes for a range of thermal conductivities of concrete ($1 < \lambda_c < 4$) take the form of Equation A.11, while the concrete temperature response G-function G_c, valid for $0.01 < Fo < 100$, takes the form of Equation A.12:

$$R_c = a \cdot \lambda_c^5 + b \cdot \lambda_c^4 + c \cdot \lambda_c^3 + d \cdot \lambda_c^2 + e \cdot \lambda_c + f \tag{A.11}$$

$$\begin{aligned} G_c = a \cdot \ln(Fo)^6 + b \cdot \ln(Fo)^5 + c \cdot \ln(Fo)^4 + d \cdot \ln(Fo)^3 \\ + e \cdot \ln(Fo)^2 + f \cdot \ln(Fo) + g \end{aligned} \tag{A.12}$$

The curve fitting parameters for R_c and G_c are defined in Tables 5 and 6, respectively. As before, linear interpolation is suggested for non-computed values.

Table 2: Curve fitting parameters for upper and lower bounds for the concrete thermal resistance R_c [22].

	W-shape	
λ_c/λ_s	2	0.5
a	-0.00105	-0.00096
b	0.01557	0.01422
c	-0.09284	-0.08438
d	0.28459	0.25660
e	-0.47303	-0.42066
f	0.40727	0.35237

Table 3: Curve fitting parameters for concrete G-functions G_c [22].

λ_c/λ_s	2U		
	0.5	1	2
a	7.4143E-07	3.2209E-06	-6.8329E-07
b	-1.6587E-05	3.5142E-05	1.2454E-05
c	6.6686E-05	-2.3294E-04	-4.7563E-05
d	1.0464E-03	-1.0900E-04	3.1674E-05
e	-1.2676E-02	-5.0508E-03	-4.8439E-03
f	5.8398E-02	5.3798E-02	4.9111E-02
g	8.8640E-01	8.6614E-01	8.6694E-01
RMSE*	0.0039	0.0025	0.00003
R^2**	0.9991	0.9997	0.99992

*RMSE: Root Mean Squared Error
**R^2: Coefficient of Determination

The pipe thermal resistance R_{pipe} [K·m/W] is defined in Equation A.13 as the sum of the pipe convective (first term on right hand side) and conductive (second term on right hand side) resistances:

$$R_{pipe} = \frac{1}{2n\pi r_i h_i} + \frac{\ln(r_o/r_i)}{2n\pi\lambda_{pipe}} \qquad (A.13)$$

where n is the number of pipes in the pile heat exchanger cross section, r_i [m] is the inner radius of the pipe, r_o [m] is the outer radius of the pipe, h_i [W/m^2/K] is the heat transfer coefficient and λ_{pipe} [W/m/K] is the thermal conductivity of the pipe material. h_i can be calculated using the Gnielinski correlation as described in [44,45].

References

[1]   S.J. Rees, An introduction to ground-source heat pump technology, in: Adv. Ground-Source Heat Pump Syst., Woodhead Publishing, 2016: pp. 1–25. doi: http://dx.doi.org/10.1016/B978-0-08-100311-4.00001-7.

[2]   J.W. Lund, T.L. Boyd, Direct utilization of geothermal energy 2015 worldwide review, Geothermics. 60 (2016) 66–93. https://doi.org/10.1016/j.geothermics.2015.11.004.

[3]   H. Brandl, Energy foundations and other thermo-active ground structures, Geotechnique. 56 (2006) 81–122. https://doi.org/10.1680/geot.2006.56.2.81.

[4]   L. Laloui, A. Di Donna, Energy Geostructures: Innovation in Underground

Engineering, John Wiley & Sons, Inc., 2013. ISBN 978-1-84821-572-6.

[5]   A. Di Donna, B. Marco, A. Tony, Energy Geostructures: Analysis from research and systems installed around the World, (2017). In DFI 2017: 42nd Annual Conference on Deep Foundations, USA.

[6]   D. Nicholson, P. Smith, G.A. Bowers, F. Cuceoglu, C.G. Olgun, J.S. McCartney, K. Henry, L.L. Meyer, F.A. Loveridge, Environmental impact calculations, life cycle cost analysis, DFI J. - J. Deep Found. Inst. 8 (2014) 130–146. doi:10.1179/1937525514Y.0000000009.

[7]   J. Gao, A. Li, X. Xu, W. Gang, T. Yan, Ground heat exchangers: Applications, technology integration and potentials for zero energy buildings, Renew. Energy. 128 (2018) 337–349. doi:10.1016/J.RENENE.2018.05.089.

[8]   J.D. Spitler, GLHEPRO-A design tool for commercial building ground loop heat exchangers, in: Proc. Fourth Int. Heat Pumps Cold Clim. Conf., Citeseer, 2000.

[9]   Building Physics, Earth Energy Designer EED 4, 2017. https://www.buildingphysics.com/manuals/EED4.pdf.

[10]   Geo Connections, Loop Link PRO, (2018). https://looplinkpro.com/features/.

[11]   Gaia Geothermal, GLD Overview, (2016). http://www.gaiageo.com/products.html.

[12]   M. de Paly, J. Hecht-Méndez, M. Beck, P. Blum, A. Zell, P. Bayer, Optimization of energy extraction for closed shallow geothermal systems using linear programming, Geothermics. 43 (2012) 57–65. doi:http://dx.doi.org/10.1016/j.geothermics.2012.03.001.

[13]   M. Beck, P. Bayer, M. de Paly, J. Hecht-Méndez, A. Zell, Geometric arrangement and operation mode adjustment in low-enthalpy geothermal borehole fields for heating, Energy. 49 (2013) 434–443. doi:http://dx.doi.org/10.1016/j.energy.2012.10.060.

[14]   C. Maragna, Development of a numerical Platform for the Optimization of Borehole Heat Exchanger Fields, in: Eur. Geotherm. Congr. 2016, 2016: pp. 19–24.

[15]   J. Fadejev, R. Simson, J. Kurnitski, F. Haghighat, A review on energy piles design, sizing and modelling, Energy. 122 (2017) 390–407. doi:10.1016/j.energy.2017.01.097.

[16] H. Bjorn, Shallow geothermal energy from a Danish standpoint, Geotherm. Energ. (2018), press note.

[17] D. Pahud, A. Fromentin, D. ambiente costruzioni e design I. sostenibilità applicata all'ambiente costruito, PILESIM - LASEN. Simulation Tool for Heating/Cooling Systems with Heat Exchanger Piles or Borehole Heat Exchangers. User Manual., 1999. http://repository.supsi.ch/id/eprint/3047.

[18] N. Makasis, G.A. Narsilio, A. Bidarmaghz, A machine learning approach to energy pile design, Comput. Geotech. 97 (2018) 189–203. doi:10.1016/J.COMPGEO.2018.01.011.

[19] F. Loveridge, W. Powrie, G-Functions for multiple interacting pile heat exchangers, Energy. 64 (2014) 747–757. doi:http://dx.doi.org/10.1016/j.energy.2013.11.014.

[20] M. Alberdi-Pagola, S. E. Poulsen, R. L. Jensen, S. Madsen, Design methodology for precast quadratic pile heat exchanger-based shallow geothermal ground-loops: multiple pile g-functions, Geothermics. (under review).

[21] G. Derringer, R. Suich, Simultaneous Optimization of Several Response Variables, J. Qual. Technol. 12 (1980) 214–219. doi:10.1080/00224065.1980.11980968.

[22] M. Alberdi-Pagola, R.L. Jensen, S. Madsen, S.E. Poulsen, Method to obtain g-functions for multiple precast quadratic pile heat exchangers., Aalborg University, Aalborg, Denmark, (2018). http://vbn.aau.dk/files/274763046/Method_to_obtain_g_functions_for_multiple_precast_quadratic_pile_heat_exchangers.pdf.

[23] P. Eskilson, Thermal Analysis of Heat Extraction, PhD thesis, University of Lund, Sweden, 1987.

[24] F. Dupray, L. Laloui, A. Kazangba, Numerical analysis of seasonal heat storage in an energy pile foundation, Comput. Geotech. 55 (2014) 67–77. doi:http://dx.doi.org/10.1016/j.compgeo.2013.08.004.

[25] The MathWorks Inc., MATLAB R2017a and Global Optimization Toolbox, (2017).

[26] N.R. Costa, J. Lourenço, Z.L. Pereira, Desirability function approach: A review and performance evaluation in adverse conditions, Chemom. Intell. Lab. Syst. 107 (2011) 234–244. doi:10.1016/J.CHEMOLAB.2011.04.004.

[27]   Nist Sematech, Engineering statistics handbook. Multiple responses: The desirability approach, (2013). https://www.itl.nist.gov/div898/handbook/pri/section5/pri5322.htm (accessed May 11, 2018).

[28]   VDI, VDI 4640 Thermal use of the underground. Part 2: Ground source heat pump systems, The Association of German Engineers (VDI), 2001.

[29]   Møller, O., Frederiksen, J.K., Augustesen, A.H., Okkels, N. and Sorensen, K.G., 2016. Design of piles – Danish practice, in Proceedings of ISSMGE - ETC 3 International Symposium on Design of Piles in Europe.

[30]   Centrum Pæle A/S, Personal Communication, (2018).

[31]   M. Alberdi-Pagola, R.L. Jensen, S.E. Poulsen, A performance case study of energy pile foundation at Rosborg Gymnasium (Denmark), in: 12th REHVA World Congr. Clima2016, Department of Civil Engineering, Aalborg University, Aalborg, Denmark, 2016: p. 10. http://vbn.aau.dk/files/233716932/paper_472.pdf.

[32]   M. Alberdi-Pagola, R.L. Jensen, S. Madsen, S.E. Poulsen, Measurement of thermal properties of soil and concrete samples, Aalborg University, Aalborg, Denmark, 2017. http://vbn.aau.dk/files/266378485/Measurement_of_thermal_properties_of_ soil_and_concrete_samples.pdf.

[33]   M. Alberdi-Pagola, S.E. Poulsen, F. Loveridge, S. Madsen, R.L. Jensen, Comparing heat flow models for interpretation of precast quadratic pile heat exchanger thermal response tests, Energy. 145 (2018) 721–733. doi:10.1016/j.energy.2017.12.104.

[34]   F. Cecinato, F.A. Loveridge, Influences on the thermal efficiency of energy piles, Energy. 82 (2015) 1021–1033. doi:http://dx.doi.org/10.1016/j.energy.2015.02.001.

[35]   M. Faizal, A. Bouazza, R.M. Singh, Heat transfer enhancement of geothermal energy piles, Renew. Sustain. Energy Rev. 57 (2016) 16–33. doi:http://dx.doi.org/10.1016/j.rser.2015.12.065.

[36]   S. Gehlin, Thermal Response Test. Method Development and Evaluation, PhD thesis, Luleå University of Technology, 2002.

[37]   M. Global, Ethylene Glycol Product Guide, 2008. http://www.meglobal.biz/media/product_guides/MEGlobal_MEG.pdf.

[38]   Engineering Toolbox, Ethylene Glycol Heat-Transfer Fluid, (2003). https://www.engineeringtoolbox.com/ethylene-glycol-d_146.html (accessed March 30, 2018).

[39]   F. Loveridge, W. Powrie, Temperature response functions (G-functions) for single pile heat exchangers, Energy. 57 (2013) 554–564. doi:http://dx.doi.org/10.1016/j.energy.2013.04.060.

[40]   E. Zanchini, S. Lazzari, Temperature distribution in a field of long Borehole Heat Exchangers (BHEs) subjected to a monthly averaged heat flux, Energy. 59 (2013) 570–580. doi:https://doi.org/10.1016/j.energy.2013.06.040.

[41]   J.D. Spitler, M. Bernier, 2 - Vertical borehole ground heat exchanger design methods, Rees, S.J., in: Adv. Ground-Source Heat Pump Syst., Woodhead Publishing, 2016: pp. 29–61. doi:http://dx.doi.org/10.1016/B978-0-08-100311-4.00002-9.

[42]   M. Cimmino, M. Bernier, F. Adams, A contribution towards the determination of g-functions using the finite line source, Appl. Therm. Eng. 51 (2013) 401–412. doi:http://dx.doi.org/10.1016/j.applthermaleng.2012.07.044.

[43]   F. Loveridge, W. Powrie, 2D thermal resistance of pile heat exchangers, Geothermics. 50 (2014) 122–135. doi:http://dx.doi.org/10.1016/j.geothermics.2013.09.015.

[44]   R. Al-Khoury, Computational modeling of shallow geothermal systems, CRC Press, 2011.

[45]   H.-J.G. Diersch, FEFLOW Finite Element Modeling of Flow, Mass and Heat Transport in Porous and Fractured Media, Springer Science & Business Media, 2014. doi:10.1007/978-3-642-38739-5.

6.1.4. LESSONS LEARNT

The simulations carried out in Paper C are utilised now to analyse the temperature changes that the pile foundation will be subject to in the long term. Figure 6-2 shows the average fluid temperature in the ground loop and the average pile wall temperature for the optimal energy pile configuration calculated for the case study in Paper C, corresponding to the 14th year of operation.

a)
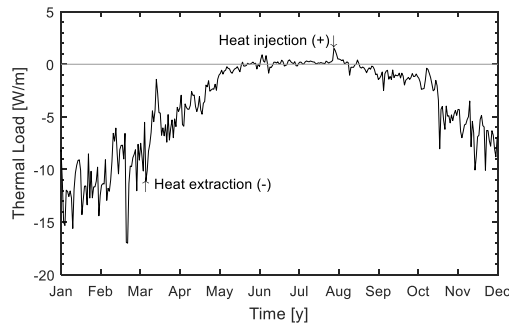
b)
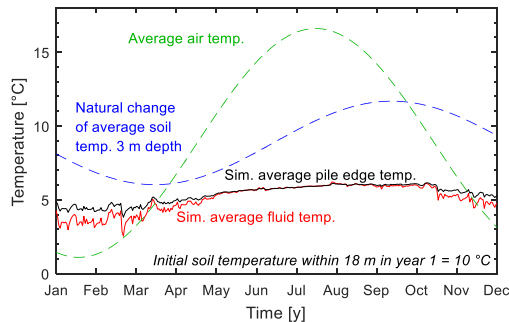
Figure 6-2: Predictions for Rosborg Gymnasium with optimum energy pile foundation configuration, corresponding to the 14th year of operation. Daily data is shown. a) Applied thermal load; b) temperatures.

The lowest temperature during the year measures an average fluid temperature of 2.5 °C, which corresponds to 4 °C in the pile edge, while the fluid and pile temperatures balance up in 6.5 °C by the beginning of next winter. The relative variation in the pile temperature over the year is 4 °C while the total temperature decrease from the initial condition is 7.5 °C. Hence, the temperature change in the ground is of rather low and follows a seasonal period, as reported in [45]. The pile edge temperatures in this study show a more rapid variation than the one reported by [45]. This occurs because, in the piles analysed in this PhD thesis, the pipes are placed closer to the edge. For

informative purposes, Figure 6-2 also shows the natural temperature changes that would occur in the ground at 3 m depth, resulted only from air temperature variations.

6.2. DESIGN CHECKLIST AND CONCLUSION

To ensure the success of a project, the energy pile foundation needs to be considered in early stage planning. When the geotechnical engineer decides that, due to the poor mechanical properties of the soil at the site, a pile foundation is required for a new building, the option to use an energy pile foundation needs to be taken into account. Ref. [45] reviews further information and parameters required for energy pile foundations, additional to those determined from standard geotechnical site investigation routines.

The design of energy foundations requires a multidisciplinary approach that accounts for interacting thermal and mechanical aspects that cannot be ignored [86]. The scheme shown in Figure 6-3, based on the work by [86], lists the main steps to carry out in parallel towards an integrated design. I.e., it shows how the geotechnical (and structural) and thermal designs interact.

The proposed workflow considers the possibility to perform a TRT during site investigation works (in the thermal design stream). The tests should be carried out during the geotechnical investigations where a trial pile or a few preliminary piles, depending on the size of the works, are driven to assess the choice of the type of pile and the driving equipment [12].

When the thermal loads of the building are known, and the foundation has been designed, in terms of pile length, cross section and position, the thermal design can begin and the expected temperature changes, determined. These additional temperature changes resulted from the shallow geothermal use can be calculated with the method developed in this PhD thesis. Then, those thermal variations are introduced in the geotechnical design side where the additional thermal stresses and strains can be assessed with, e.g., the load transfer method or a tailored numerical tool such as the one developed in this thesis.

The energy pile foundation design can be adapted to fulfil the structural and geotechnical constraints, by reducing the supplied share of the building thermal needs or by redefining the desirability function establishing more restricting upper and lower temperature limits. If the energy foundation cannot cover the complete thermal needs of the building, then, a back-up system is required.
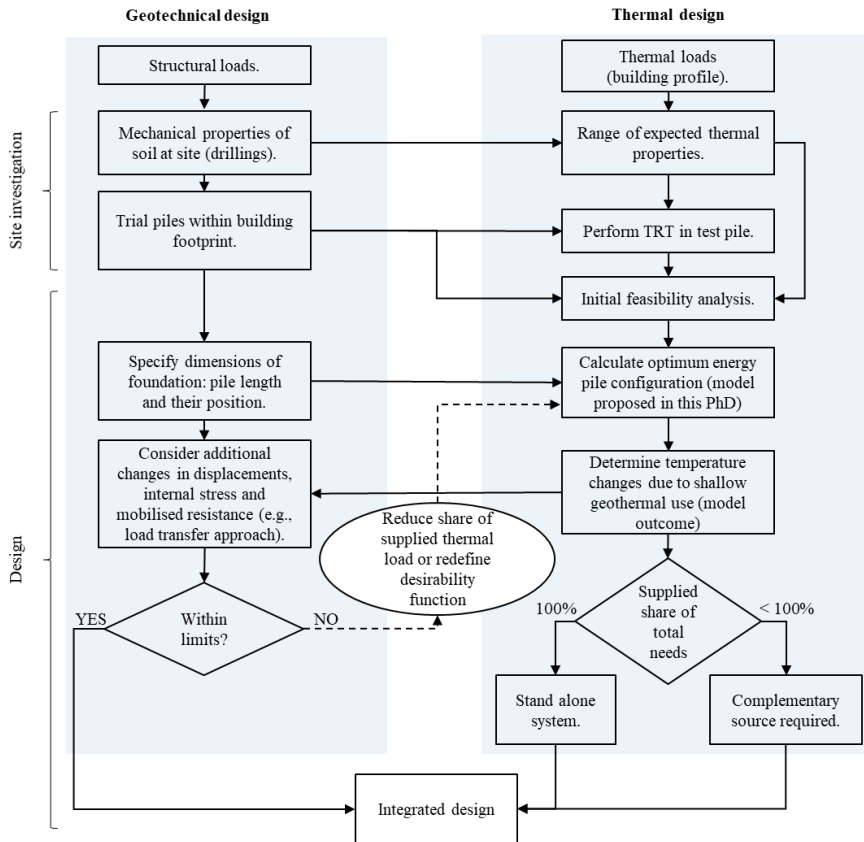
Figure 6-3: Workflow and interaction between the geotechnical and thermal aspects to reach a successful integrated design of a GSHP system based on energy piles. Modified after [86].

CHAPTER 7. DISCUSSION AND CONCLUSION

This chapter provides first a short discussion about the limitations and advantages of the methods applied in this PhD thesis and it concludes with a summary of the results.

7.1. DISCUSSION

The work completed with the TRT in Paper A provides a significant amount of experimental data which allows to carry out inverse modelling yielding consistent results with the independent laboratory measurements. However, the inverse modelling of 3D finite element models for TRT data interpretation is not recommended in practical applications and more simple models, such as semi-empirical models that consider the geometry of the energy piles are recommended.

Paper B proposes a design method based on semi-empirical models of multiple energy piles. The experimental data in this aspect is more limited. Further soil temperature data at several radial distances would assist a more thorough assessment of the accuracy of the models. Even though the development of semi-empirical models is simple, the model does not account for groundwater flow and, therefore, its applicability is limited, and it must be used with care when seasonal thermal storage needs to be considered.

Aggregation of errors derived from spatial superposition techniques found in Paper B have also been reported in literature. Nevertheless, it has been demonstrated that for time varying thermal loads (non-constant thermal pulses in the long term), the semi-empirical models yield average fluid temperatures similar to corresponding full 3D FEM and the errors are within acceptable limits for design purposes.

In Paper C, the multiple pile g-functions are used to reproduce operational average fluid temperatures for heat extraction periods in an actual energy pile foundation in Denmark. Regarding the proposed optimisation strategy based on the desirability function approach has strong features: it is flexible and allows new conditions to be easily implemented, such as more restrictive upper and lower temperature limits. For design purposes, the proposed tool seems very practical. More case studies should be tried to for further validation of the model.

To analyse the thermo-mechanical implications, a tailored finite element model has been developed considering a time varying thermal load in an energy pile, where the soil was considered homogeneous and isotropic. However, according to the latest literature, models that account for the different mechanical properties of the soil layers

are more convenient. Besides, the analysis of a monotonic thermal load, i.e., the temperature change calculated from the multiple energy pile model here proposed, should suffice for design. For this purpose, the load transfer method [44,76,77] seems appropriate since it allows the tuning of the soil-pile and pile-structure interaction parameters.

7.2. CONCLUSION

The main objective of this PhD thesis is to create a framework for the analysis and design of GSHP systems based on precast quadratic pile heat exchangers to cover the heating and/or cooling needs of a building, without compromising the structural role of the piles.

To analyse the thermo-mechanical implications of the geothermal use of energy piles, a numerical study has been carried out. The results show that a typical geothermal utilisation of the energy foundation does not generate significant structural implications on the geotechnical capacity of a single energy pile. However, ground thermal loads need to be considered in the design phase to account for potential extreme temperature changes. These findings are in line with the literature.

The temperature disturbance in the pile-soil system, resulted from the heating and cooling of the piles, depends on the thermal properties of the concrete, the surrounding soil and the pile arrangement. Hence, an assessment of the induced temperature changes with respect to the initial undisturbed temperature needs to be carried out in order to estimate the induced thermal stresses and strains. Therefore, there was a need to develop a tool that considers the peculiarities of precast energy piles and that calculates the temperature changes occurring in the energy piles given a thermal load of a building.

First, the suitability of different heat flow models to interpret thermal response test data of pile heat exchangers is investigated. Interpretations based on semi-empirical pile models yield soil thermal conductivity estimates similar to those obtained from the 3D finite element inverse modelling, given minimum testing times of 60 hours. It is highlighted the relevance of using appropriate models to describe the thermal behaviour of precast energy piles in the short and long term.

Semi-empirical models show a promising potential to account for thermal interactions between piles due to its simple implementation. Hence, semi-empirical dimensionless temperature g-functions for multiple piles are developed by utilising 3D finite element model heat transport simulations with temporal and spatial superposition techniques. Multiple pile g-functions yield fluid temperatures similar to those obtained with full 3D modelling, at minimal computational cost.

As a further step, the multiple pile g-functions are applied for estimating operational average fluid temperatures in an existing energy pile foundation in Denmark. The multiple pile g-functions reproduce fluid temperatures similar to what is observed. The thermal model is then utilised in an optimisation algorithm that yields the minimum number of energy piles required by simultaneously maximising the pile spacing (constrained by the foundation pattern) and taking into consideration the thermal load of the building. The optimisation tool shows that the number of pile heat exchangers needed for this case study could have been reduced by 32%. The model can also be used to create design charts that would support the early design process. Additionally, the tool facilitates the implementation of additional conditions for the optimisation, that can be tailored for specific cases.

Energy piles comprise a real option for space conditioning. Their design needs to consider thermal and geotechnical aspects and this PhD has developed a frame to ease this holistic design. The multiple pile g-function based temperature model combined with the proposed optimisation strategy offers a reliable basis for feasibility studies and for the safe dimensioning of energy pile foundations.

CHAPTER 8. FUTURE WORK

This PhD thesis has presented a frame for the design of energy pile foundations for heating and cooling applications. Yet, further work must be conducted.

A thorough analysis of all the operational data of the case study presented will be carried out. Recent findings suggest that there is room for improvement for some operational parameters. Documentation work will be developed, considering recommendation for end users. From here, best practice guidelines will be developed, which will assist dimensioning, construction and operation of future projects.

The importance of receiving a reliable building profile for the correct dimensioning of the GSHP installation has been identified. Besides, the proposed design method does not account for groundwater flow influences, required to dimension seasonal thermal energy storage. Therefore, it would be very helpful to extend the design method to a holistic model that encompasses those aspects.

The analysed case study uses the energy pile foundation for heating; however, the building has a cooling need and the installation is prepared to supply a share of that demand with free cooling. Unfortunately, to date, the end users have not made the most of it. Initial investigations show a big potential to use the soil as a heat sink for the cooling system of the building. Hence, further work will focus on analysing the cooling potential of energy pile foundations. This will make the technology more competitive since it will be endorsed as heating and cooling supply system.

Currently, an EUDP project (Danish program for energy technology development and demonstration), running until 2020, looks into two aspects of energy pile foundations: i) calculating the cooling potential and ii) investigating the geothermal potential of a district that could be supplied by energy pile foundations. The project relies on the foreseen role of heat pumps in the district heating networks of the future, not just in the traditional district heating grid, as stated in the introduction of this thesis, but also in the coming 4th generation district heating networks [162,163].

The main step forward for energy geostructures will occur when they are treated in the regulations, e.g., Eurocodes and country or local legislations. Soon, "green" certifications and Life Cycle Analyses will be required, applicable not just to individual products or elements but also to complete installations and buildings. Thus, decisions will be based on shared interests between costs and sustainability aspects.

On this matter, energy pile foundations own a huge potential to minimise the overall environmental impact of a structure, based on the dual role of the piles, and GSHP installations can be 100% renewable, where electricity is generated from renewable sources such as wind or sun.

REFERENCES IN SUMMARY

[1]   Rogelj, J., Den Elzen, M., Höhne, N., Fransen, T., Fekete, H., Winkler, H., Schaeffer, R., Sha, F.; Riahi, K. and Meinshausen, M. (2016). 'Paris Agreement climate proposals need a boost to keep warming well below 2 C', *Nature, 534*, pp. 631–639.

[2]   Danish Energy Agency (2017). *Denmark's Energy and Climate Outlook*, ISBN 978-87-93180-28-4.

[3]   Harris, M. (2011). 'Thermal energy storage in Sweden and Denmark. Potentials for technology transfer', Master thesis, Lund University, Lund, Sweden.

[4]   Pavlov, G. K. and Olesen, B. W. (2011). 'Seasonal Ground Solar Thermal Energy Storage – Review of Systems and Applications', in *Proceedings ISES Sol. World Congress*, pp. 515–525. doi:10.18086/swc.2011.29.24.

[5]   Midttømme, K., Banks, D., Ramstad, R. K., Sæther, O. M. and Skarphagen, H. (2008). 'Ground-Source Heat Pumps and Underground Thermal Energy Storage - Energy for the future', *NGU Special Publication*, *11*, pp. 93-98.

[6]   Danish Energy Agency (2018). *Basisfremskrivning 2018*, ISBN 978-87-93180-33-8.

[7]   Fødevareministeriet (2017). 'M. BEK nr 240 af 27/02/2017 Bekendtgørelse om jordvarmeanlæg'.

[8]   Haehnlein, S., Bayer, P. and Blum, P. (2010). 'International legal status of the use of shallow geothermal energy', *Renewable Sustainable Energy Reviewes, 14*, pp. 2611–2625. https://doi.org/10.1016/j.rser.2010.07.069.

[9]   Røgen, B., Ditlefsen, C. and Vangkilde-Pedersen, T. (2015). 'Geothermal energy use, 2015 country update for Denmark', in *Proceedings World Geothermal Congress 2015*.

[10]   Bjorn, H. (2018). 'Shallow geothermal energy from a Danish standpoint', *Geothermal Energy,* press publication.

[11]   Lund, J. W. and Boyd, T. L. (2016). 'Direct utilization of geothermal energy 2015 worldwide review', *Geothermics, 60*, pp. 66–93. https://doi.org/10.1016/j.geothermics.2015.11.004.

[12]   Møller, O., Frederiksen, J.K., Augustesen, A.H., Okkels, N. and Sorensen,

K.G. (2016). 'Design of piles – Danish practice', in *Proceedings of ISSMGE - ETC 3 International Symposium on Design of Piles in Europe.*

[13]   Rees, S. J. 'An introduction to ground-source heat pump technology', in *Advances in Ground-Source Heat Pump Systems*; Woodhead Publishing, 2016. ISBN 978-0-08-100311-4.

[14]   Banks, D. *An Introduction to Thermogeololy. Ground Source Heating and Cooling*, Blackwell Publishing, Oxford, 2008. ISBN 9780470670347.

[15]   Farouki, O. T. (1981). 'Thermal properties of soils', *Cold Regions Research and Engineering Laboratory,* Hanover*,* The Netherlands.

[16]   Danmarks Meteorologiske Institut (2018). 'Vejrarkiv'. Available online: http://www.dmi.dk/vejr/. [Accessed on Jun 1, 2018].

[17]   VDI (2001). 'VDI 4640 Thermal use of the underground. Part 2: Ground source heat pump systems', The Association of German Engineers (VDI), Germany.

[18]   Geotrainet (2011). 'Geotrainet Training Manual for Design of Shallow Geothermal Systems', Geotrainet: Geo-Education for sustainable geothermal heating and cooling market.

[19]   Rees, S. W., Adjali, M. H., Zhou, Z., Davies, M. and Thomas, H. R. (2000). 'Ground heat transfer effects on the thermal performance of earth-contact structures', *Renewable Sustainable Energy Reviews, 4*, pp. 213–265. https://doi.org/10.1016/S1364-0321(99)00018-0.

[20]   Brandl, H. (2006). 'Energy foundations and other thermo-active ground structures', *Geotechnique*, 56, pp. 81–122. https://doi.org/10.1680/geot.2006.56.2.81

[21]   Di Donna, A., Marco, B. and Tony, A. (2017). 'Energy Geostructures: Analysis from research and systems installed around the World'. In *DFI 2017: 42nd Annual Conference on Deep Foundations*, USA.

[22]   Laloui, L. and Di Donna, A. (2013). *Energy Geostructures: Innovation in Underground Engineering*, John Wiley & Sons, Inc., 2013; ISBN 978-1-84821-572-6.

[23]   Nicholson, D., Smith, P., Bowers, G. A., Cuceoglu, F., Olgun, C. G., McCartney, J. S., Henry, K., Meyer, L. L. and Loveridge, F. A. (2014). 'Environmental impact calculations, life cycle cost analysis', *DFI Journal –*

The Journal of the Deep Foundations Institute, 8, pp. 130–146, https://doi.org/10.1179/1937525514Y.0000000009

[24] Park, S., Lee, D., Choi, H. J., Jung, K. and Choi, H. (2015). 'Relative constructability and thermal performance of cast-in-place concrete energy pile: Coil-type GHEX (ground heat exchanger)', *Energy*, *81*, pp. 56–66. https://doi.org/10.1016/j.energy.2014.08.012.

[25] Loveridge, F., Olgun, C. G., Brettmann, T. and Powrie, W. (2014). 'The Thermal Behaviour of Three Different Auger Pressure Grouted Piles Used as Heat Exchangers', *Geotechnical and Geoogical. Engineering*, pp. 273-289. https://doi.org/10.1007/s10706-014-9757-4

[26] Brettman, T. P. E., Amis, T. and Kapps, M. (2010). 'Thermal conductivity analysis of geothermal energy piles', in *Proceedings of the Geotechnical Challenges in Urban Regeneration Conference,* pp. 26–28.

[27] Laloui, L. and Nuth, M. (2009). 'Investigations on the mechanical behaviour of a Heat Exchanger Pile', *In Deep Foundations on Bored and Auger Piles*, VanImpe, W. F., VanImpe, P. O., Eds.; Crc Press-Taylor & Francis Group: Boca Raton; ISBN 978-0-415-47556-3.

[28] De Groot, M., De Santiago, C., and Pardo de Santayana, F. (2014). 'Heating and cooling an energy pile under working load in Valencia', in *23rd European Young Geotechncal Engineers Conference.*

[29] Alberdi-Pagola, M. and Poulsen, S. E. (2015). 'Thermal response testing and performance of quadratic cross section energy piles (Vejle, Denmark)', in *XVI European Conference for Soil Mechanics and Geotechnical Engineering 2015.*

[30] Pahud, D. (2002). 'Geothermal energy and heat storage', SUPSI – DCT – LEEE. Scuola Universitaria Professionale della Svizzera Italiana, Cannobio.

[31] Balfour Beatty Ground Engineering (2016). 'Geothermal driven piles'. Available online: http://www.balfourbeatty.com/media/29535/geothermal-driven-piles.pdf. [Accessed on March 2016].

[32] Park, H., Lee, S.R., Yoon, S. and Choi, J.C. (2013). 'Evaluation of thermal response and performance of PHC energy pile: Field experiments and numerical simulation', *Applied Energy*, *103*, pp. 12–24. https://doi.org/10.1016/j.apenergy.2012.10.012

[33] Jalaluddin, A. M., Tsubaki, K., Inoue, S. and Yoshida, K. (2011).

'Experimental study of several types of ground heat exchanger using a steel pile foundation'. *Renewewable Energy, 36*, pp. 764–771, https://doi.org/10.1016/j.renene.2010.08.011

[34] Lennon, D. J., Watt, E. and Suckling, T. P. (2009). 'Energy piles in Scotland', in *Proceedings of the Fifth International Conference on Deep Foundations on Bored and Auger Piles*; (Eds), V. I. & V. I., Ed.; Taylor & Francis Group, London: Frankfurt.

[35] Alberdi-Pagola, M., Poulsen, S. E., Loveridge, F., Madsen, S. and Jensen, R. L. (2018). 'Comparing heat flow models for interpretation of precast quadratic pile heat exchanger thermal response tests', *Energy, 145*, pp. 721–733. https://doi.org/10.1016/j.energy.2017.12.104

[36] Alberdi-Pagola, M., Madsen, S., Jensen, R. L. and Poulsen, S. E. (2018). 'Thermo-mechanical aspects of pile heat exchangers: background and literature review', Aalborg: Department of Civil Engineering, Aalborg University. DCE Technical Reports, nr. 250, pp. 37. Available online: http://vbn.aau.dk/files/281634409/Thermo_mechanical_aspects_of_pile_heat_exchangers_background_and_literature_review.pdf

[37] Danish Standard (2010). 'DS/EN 1997-1/AC:2010 Eurocode 7: Geotechnical design - Part 1: General rules'.

[38] GSHP Association (2012). 'Thermal Pile: Design, Installation & Materials Standards'. http://www.gshp.org.uk/pdf/GSHPA_Thermal_Pile_Standard.pdf

[39] Alberdi-Pagola, M., Madsen, S., Jensen, R. L. and Poulsen, S. E. (2017). 'Numerical investigation on the thermo-mechanical behavior of a quadratic cross section pile heat exchanger', in *Proceedings of the IGSHPA Technical/Research Conference and Expo*; Denver, USA, March 14-16, 2017. http://dx.doi.org/10.22488/okstate.17.000520

[40] Laloui, L., Moreni, M. and Vulliet, L. (2003). 'Comportement d'un pieu bi-fonction, fondation et échangeur de chaleur', *Canadian Geotechnical Journal*, *40*, pp. 388–402. doi:10.1139/t02-117.

[41] Mimouni, T. and Laloui, L. (2014). 'Towards a secure basis for the design of geothermal piles', *Acta Geotechnica, 9*, pp. 355–366. https://doi.org/10.1007/s11440-013-0245-4

[42] Bourne-Webb, P. J., Amatya, B., Soga, K., Amis, T., Davidson, C. and Payne, P. (2009). 'Energy pile test at lambeth college, London: Geotechnical and

thermodynamic aspects of pile response to heat cycles', *Geotechnique*, *59*, pp. 237–248. https://doi.org/10.1680/geot.2009.59.3.237

[43]   Amatya, B. L., Soga, K., Bourne-Webb, P. J., Amis, T. and Laloui, L. (2012). 'Thermo-mechanical behaviour of energy piles', *Geotechnique*, *62*, pp. 503–519. https://doi.org/10.1680/geot.10.P.116

[44]   Knellwolf, C., Peron, H and; Laloui, L. (2011). 'Geotechnical analysis of heat exchanger piles', *Journal of Geotechnical and Geoenvironmental Engineering*, *137*, pp. 890–902. https://doi.org/10.1061/(ASCE)GT.1943-5606.0000513.

[45]   Loveridge, F., Low, J. and Powrie, W. (2017). 'Site investigation for energy geostructures', *Quarterly Journal of Engineering Geology and Hydrogeology*, *50*, pp. 158–168. doi.org/10.1144/qjegh2016-027

[46]   Olgun, C. G., Ozudogru, T. Y. and Arson, C. F. (2014). 'Thermo-mechanical radial expansion of heat exchanger piles and possible effects on contact pressures at pile–soil interface', *Géotechnique Letters*, *4*, pp. 170–178. https://doi.org/10.1680/geolett.14.00018

[47]   Campanella, R. G. and Mitchell, J. K. (1968). 'Influence of temperature variations on soil behavior', *Journal of the Soil Mechanics and Foundations Division*, *94*, Issue 3, pp. 609-734.

[48]   Boudali, M., Leroueil, S. and Srinivasa Murthy, B. R. (1994). 'Viscous behaviour of natural clays', in *13th International Conference Soil Mechanics and Foundation Engineering ICSMFE,* New Delhi, India.

[49]   Hueckel, T., François, B. and Laloui, L. (2009). 'Explaining thermal failure in saturated clays', *Geotechnique*, *59*, pp. 197–212. https://doi.org/10.1680/geot.2009.59.3.197

[50]   Cekerevac, C. and Laloui, L. (2004). 'Experimental study of thermal effects on the mechanical behaviour of a clay', *International Journal for Numerical Analysis Methods in Geomechanics*, *28*, pp. 209–228, https://doi.org/10.1002/nag.332

[51]   Bodas Freitas, T. M., Cruz Silva, F. and Bourne-Webb, P. J. (2013). 'The response of energy foundations under thermo-mechanical loading', in *Proceedings of the 18th International Conference on Soil Mechanics and Geotechnical Engineering*.

[52]   Laloui, L. and François, B. (2009). 'ACMEG-T: soil thermoplasticity model',

Journal of Engineering Mechanics, *135*. https://doi.org/10.1061/(ASCE)EM.1943-7889.0000011

[53] Vieira, A., Alberdi-Pagola, M., Christodoulides, P., Javed, S.; Loveridge, F., Nguyen, F., Cecinato, F., Maranha, J., Florides, G., Prodan, I., Lysebetten, G. Van, Ramalho, E., Salciarini, D., Georgiev, A., Rosin-Paumier, S., Popov, R., Lenart, S., Poulsen, S. E. and Radioti, G. (2017). 'Characterisation of Ground Thermal and Thermo-Mechanical Behaviour for Shallow Geothermal Energy Applications', *Energies*, *10*(12), 2044. https://doi.org/10.3390/en10122044

[54] Laloui, L., Olgun, C. G., Sutman, M., McCartney, J. S., Coccia, C. J., Abuel-Naga, H. M. and Bowers, G. A. (2014). 'Issues involved with thermoactive geotechnical systems: characterization of thermomechanical soil behavior and soil-structure interface behavior'. *DFI Journal – Journal of Deep Foundation Institute*, *8*, pp.108–120. https://doi.org/10.1179/1937525514Y.0000000010

[55] Amis, T. and Bourne-Webb, P. J. (2008). 'The effects of heating and cooling energy piles under working load at Lambeth College', in *33rd Annual and 11th International DFI Conference UK*.

[56] Mimouni, T. (2014). 'Thermomechanical Characterization of Energy Geostructures with Emphasis on Energy Piles', PhD thesis, École Polytechnique Fédérale de Lausanne EPFL, Lausanne, Switzerland.

[57] Laloui, L., Nuth, M. and Vulliet, L. (2006). 'Experimental and numerical investigations of the behaviour of a heat exchanger pile', *International Journal of Numerical Analysis Methods for Geomechanics*, *30*, pp. 763–781. https://doi.org/10.1016/S1571-9960(05)80040-0

[58] Di Donna, A., Rotta Loria, A. F. and Laloui, L. (2016). 'Numerical study of the response of a group of energy piles under different combinations of thermo-mechanical loads', *Computers and Geotechnics, 72*, pp. 126–142. https://doi.org/10.1016/j.compgeo.2015.11.010

[59] De Santayana, F. P., de Santiago, C., de Groot, M., Uchueguía, J., Arcos, J. L. and Badenes, B. (2018). 'Effect of Thermal Loads on Precast Concrete Thermopile', *Environmental Geotechnics*. https://doi.org/10.1680/jenge.17.00103

[60] Faizal, M., Bouazza, A. and Singh, R. M. (2016). 'An experimental investigation of the influence of intermittent and continuous operating modes on the thermal behaviour of a full scale geothermal energy pile', *Geomechanics for Energy and the Environment*, *8*, pp. 8–29. https://doi.org/10.1016/j.gete.2016.08.001

[61]   Rotta Loria, A. F. and Laloui, L. (2016). 'The interaction factor method for energy pile groups'. *Computers and Geotechnics, 80*, pp. 121–137. https://doi.org/10.1016/j.compgeo.2016.07.002

[62]   Rotta Loria A. F. and Laloui, L. (2017). 'Impact of Thermally Induced Soil Deformation on the Serviceability of Energy Pile Groups'. In: Ferrari A., Laloui L. (eds) *Advances in Laboratory Testing and Modelling of Soils and Shales (ATMSS).* ATMSS 2017. Springer Series in Geomechanics and Geoengineering. Springer, Cham.

[63]   Rotta Loria, A. F. (2018). 'Thermo-mechanical performance of energy pile groups', PhD thesis, École Polytechnique Fédérale de Lausanne EPFL, Lausanne, Switzerland. doi:10.5075/EPFL-THESIS-8138.

[64]   Loria, A. F. R. and Laloui, L. (2016). 'The equivalent pier method for energy pile groups', *Geotechnique*, *67*, pp. 691-702. http://dx.doi.org/10.1680/jgeot.16.P.139

[65]   Rotta Loria, A. F. and Laloui, L. (2017). 'Group action effects caused by various operating energy piles', *Géotechnique.* https://doi.org/10.1680/jgeot.17.P.213.

[66]   Suryatriyastuti, M. E., Mroueh, H. and Burlon, S. (2012). 'Understanding the temperature-induced mechanical behaviour of energy pile foundations', *Renewable and Sustainable Energy Reviews, 16*, pp. 3344–3354. https://doi.org/10.1016/j.rser.2012.02.062

[67]   Hassani Nezhad Gashti, E., Malaska, M. and Kujala, K. (2014). 'Evaluation of thermo-mechanical behaviour of composite energy piles during heating/cooling operations'. *Engineering Structures, 75*, pp. 363–373. https://doi.org/10.1016/j.engstruct.2014.06.018

[68]   Olgun, C. G., Ozudogru, T. Y., Abdelaziz, S. L. and Senol, A. (2015). 'Long-term performance of heat exchanger piles', *Acta Geotechnica*, *10*, pp. 553–569. https://doi.org/10.1007/s11440-014-0334-z

[69]   Abdelaziz, S. L. A. M. (2013). 'Deep energy foundations: geotechnical challenges and design considerations', PhD thesis, Virginia Polytechnic Institute and State University, Blacksburg, Virginia.

[70]   Coyle, H. M. and Reese, L. C. (1966). 'Load transfer for axially loaded piles in clay', *Journal of Soil Mechanics & Foundations Division.*

[71]   Péron, H., Knellwolf, C. and Laloui, L. (2011). 'A method for the

geotechnical design of heat exchanger piles'. In *Proceedings of the geo-frontiers 2011 conference*, *211*, pp. 470–479.

[72]   Burlon, S., Habert, J., Szymkievicz, F., Suryatriyastuti, M. and Mroueh, H. (2013). 'Towards a design approach of bearing capacity of thermo-active piles', in *European Geothermal Congress*.

[73]   Suryatriyastuti, M. E., Mroueh, H. and Burlon, S. (2014). 'A load transfer approach for studying the cyclic behavior of thermo-active piles'. *Computers and Geotechnics, 55*, pp. 378–391. https://doi.org/10.1016/j.compgeo.2013.09.021

[74]   Mimouni, T. and Laloui, L. (2013). 'Thermo-Pile: A Numerical Tool for the Design of Energy Piles', in *Energy Geostructures*; John Wiley & Sons, Inc., 2013; pp. 265–279. ISBN 9781118761809.

[75]   Oasys (2014). 'Pile Version 19.5. Pile Oasys Geo Suite for Windows. User manual'; Ltd., O., Ed.; London, UK.

[76]   Suryatriyastuti, M. (2013). 'Numerical study of the thermoactive piles behavior in cohesionless soils', PhD thesis, Université Lille, France.

[77]   Sutman, M. (2016). 'Thermo-Mechanical Behavior of Energy Piles: Full Scale Field Testing and Numerical Modeling', PhD thesis, Virginia Polytechnic Institute and State University, USA.

[78]   Suryatriyastuti, M. E., Mroueh, H., Burlon, S. and Habert, J. (2013). 'Numerical analysis of the bearing capacity in thermo-active piles under cyclic axial loading'. In *Energy geostructures: Innovation in Underground Engineering*, Hoboken, ISTE Ltd. and John Wiley and Sons, 2013.

[79]   Murphy, K. D. and McCartney, J. S. (2015). 'Seasonal response of energy foundations during building operation', *Geotechnical and Geological Engineering, 33*, pp. 343–356. https://doi.org/10.1007/s10706-014-9802-3

[80]   SIA (2005). 'Utilisation de la chaleur du sol par des ouvrages de fondation et de soutènement en béton: guide pour la coneption, la réalisation et la maintenance'; SIA, Société suisse des ingénieurs et des architectes. ISBN 9783908483595.

[81]   NHBC Foundation (2010). 'Efficient Design of Piled Foundations for Low-Rise Housing: Design Guide', Building Research Establishment. ISBN 9781848061064.

[82]   Loveridge, F., Amis, T. and Powrie, W. (2012). 'Energy pile performance and preventing ground freezing', in I*nternational Conference on Geotechnical Engineering and Geomechanics.*

[83]   Bourne-Webb, P., Pereira, J.-M., Bowers, G. A., Mimouni, T., Loveridge, F. A., Burlon, S., Olgun, C. G., McCartney, J. S. and Sutman, M. (2014). 'Design tools for thermoactive geotechnical systems'. *DFI Journal - The Journal of Deep Foundation Institute*, *8*, pp. 121–129. https://doi.org/10.1179/1937525514Y.0000000013

[84]   Rotta Loria, A. F., Bocco, M., Garbellini, C., Muttoni, A. and Laloui, L. (2018). 'The role of thermal loads in the performance-based design of energy piles', *Géotechnique (under-review).*

[85]   Laloui, L. and Rotta Loria, A. F. (2018). 'Energy geostructures analysis and design. Intensive course in EPFL, Lausanne, Switzerland.

[86]   Bourne-Webb, P., Burlon, S., Javed, S., Kürten, S. and Loveridge, F. (2016). 'Analysis and design methods for energy geostructures', *Renewable Sustainable Energy Reviews, 65*, pp. 402–419, https://doi.org/10.1016/j.rser.2016.06.046.

[87]   Olgun, C. G. and McCartney, J. S. (2014). 'Outcomes from international workshop on thermoactive geotechnical systems for near-surface geothermal energy: from research to practice', DFI Journal - The Journal of Deep Foundation Institute, 8, pp. 59–73, https://doi.org/10.1179/1937525514Y.0000000005.

[88]   Spitler, J. D. (2000). 'GLHEPRO-A design tool for commercial building ground loop heat exchangers', in *Proceedings of the fourth international heat pumps in cold climates conference*, Citeseer.

[89]   Building Physics (2017). 'Earth Energy Designer EED 4'.

[90]   Geo Connections Loop. 'Link PRO'. Available online: https://looplinkpro.com/features/ [Accessed March 2016].

[91]   Gaia Geothermal. 'GLD Overview'. Available online: http://www.gaiageo.com/products.html. [Accessed May 2018].

[92]   ASHRAE 2007 (2007). 'ASHRAE Handbook - Heating, Ventilating, and Air-Conditioning Applications (I-P Edition)'.

[93]   Cecinato, F. and Loveridge, F. A. (2015). 'Influences on the thermal

efficiency of energy piles'. *Energy*, *82*, pp. 1021–1033. https://doi.org/10.1016/j.energy.2015.02.001

[94]   Loveridge, F. and Powrie, W. (2013). 'Temperature response functions (G-functions) for single pile heat exchangers'. *Energy*, *57*, pp. 554–564, https://doi.org/10.1016/j.energy.2013.04.060

[95]   Bandos, T. V, Campos-Celador, Á., López-González, L. M. and Sala-Lizarraga, J. M. (2014). 'Finite cylinder-source model for energy pile heat exchangers: Effects of thermal storage and vertical temperature variations', *Energy*, *78*, pp. 639–648. https://doi.org/10.1016/j.energy.2014.10.053.

[96]   Loveridge, F. and Powrie, W. (2014). 'G-Functions for multiple interacting pile heat exchangers', *Energy*, *64*, pp. 747–757, https://doi.org/10.1016/j.energy.2013.11.014.

[97]   Loveridge, F., Powrie, W. and Nicholson, D. (2014). 'Comparison of two different models for pile thermal response test interpretation', *Acta Geotechnica*, *9*, pp. 367–384. https://doi.org/10.1007/s11440-014-0306-3

[98]   Loveridge, F. (2012). 'The thermal performance of foundation piles used as heat exchangers in ground energy systems', PhD thesis, University of Southampton, UK.

[99]   Javed, S., Fahlén, P. and Claesson, J. (2009). 'Vertical ground heat exchangers: A review of heat flow models'. In *Effstock 2009-Stockholm*.

[100]   Eskilson, P. (1987). 'Thermal Analysis of Heat Extraction', PhD thesis, University of Lund, Sweden.

[101]   Katsura, T., Nagano, K. and Takeda, S. (2008). 'Method of calculation of the ground temperature for multiple ground heat exchangers'. *Applied Thermal Engineering*, *28*, pp. 1995–2004. https://doi.org/10.1016/j.applthermaleng.2007.12.013

[102]   Fossa, M., Cauret, O. and Bernier, M. (2009). 'Comparing the thermal performance of ground heat exchangers of various lengths', in *Proceedings from the 11th International Conference on Energy Storage, EFFSTOCK*.

[103]   Fossa, M. (2011). 'A fast method for evaluating the performance of complex arrangements of borehole heat exchangers'. *HVAC&R Research*, *17*, pp. 948–958. doi:10.1080/10789669.2011.599764.

[104]   Fossa, M. and Rolando, D. (2014). 'Fully analytical finite line source solution

for fast calculation of temperature response factors in geothermal heat pump borefield design', In *Proceedings, IEA Heat Pump Conference, 12-16 May, Montreal (Québec), Canada.*

[105] Cimmino, M., Bernier, M. and Adams, F. (2013). 'A contribution towards the determination of g-functions using the finite line source', *Applied Thermal Engineering*, *51*, pp. 401–412. https://doi.org/10.1016/j.applthermaleng.2012.07.044

[106] Cimmino, M. and Bernier, M. (2014). 'A semi-analytical method to generate g-functions for geothermal bore fields'. *International Journal of Heat Mass Transfer*, *70*, pp. 641–650. https://doi.org/10.1016/j.ijheatmasstransfer.2013.11.037

[107] Bernier, M. A., Chahla, A. and Pinel, P. (2008). 'Long-Term Ground-Temperature Changes in Geo-Exchange Systems', *ASHRAE Transactions*, *114*.

[108] Bernier, M. A., Pinel, P., Labib, R. and Paillot, R. (2004). 'A Multiple Load Aggregation Algorithm for Annual Hourly Simulations of GCHP Systems', *HVAC&R Research, 10*, pp. 471–487. doi:10.1080/10789669.2004.10391115.

[109] Philippe, M., Bernier, M. and Marchio, D. (2010). 'Sizing calculation spreadsheet: Vertical geothermal borefields'. *Ashrae Journal,52*, 20.

[110] Fossa, M. and Rolando, D. (2015). 'Improving the Ashrae method for vertical geothermal borefield design', *Energy and Buildings*, *93*, pp. 315–323. https://doi.org/10.1016/j.enbuild.2015.02.008

[111] Acuña, J., Fossa, M., Monzó, P. and Palm, B. (2012). 'Numerically Generated g-functions for Ground Coupled Heat Pump Applications', In *Proceedings of the COMSOL Conference in Milan*.

[112] Monzó, P. (2018). 'Modelling and monitoring thermal response of the ground in borehole fields', PhD thesis, KTH Stockholm, Sweden.

[113] Hellström, G. (1991). 'Ground Heat Storage: Thermal Analyses of Duct Storage Systems I. Theory', Lund University, Department of Mathematical Physics, Sweden.

[114] Pahud, D. and Fromentin (1991). 'PILESIM - LASEN. Simulation Tool for Heating/Cooling Systems with Heat Exchanger Piles or Borehole Heat Exchangers. User Manual.', Available in: http://repository.supsi.ch/3047/

[115]   Pahud, D. and Hubbuch, M. (2007). 'Measured thermal performances of the energy pile system of the Dock Midfield at Zürich Airport', in *Proceedings European geothermal congress 2007*.

[116]   Zanchini, E., Lazzari, S. and Priarone, A. (2012). 'Long-term performance of large borehole heat exchanger fields with unbalanced seasonal loads and groundwater flow', *Energy*, *38*, pp. 66–77, https://doi.org/10.1016/j.energy.2011.12.038

[117]   Zanchini, E. and Lazzari, S. (2014). 'New g-functions for the hourly simulation of double U-tube borehole heat exchanger fields', *Energy*, *70*, pp. 444–455. https://doi.org/10.1016/j.energy.2014.04.022

[118]   de Paly, M., Hecht-Méndez, J., Beck, M., Blum, P., Zell, A. and Bayer, P. (2012). 'Optimization of energy extraction for closed shallow geothermal systems using linear programming', *Geothermics*, *43*, pp. 57–65, https://doi.org/10.1016/j.geothermics.2012.03.001

[119]   Beck, M., Bayer, P., de Paly, M., Hecht-Méndez, J. and Zell, A. (2013). 'Geometric arrangement and operation mode adjustment in low-enthalpy geothermal borehole fields for heating', *Energy*, *49*, pp. 434–443, https://doi.org/10.1016/j.energy.2012.10.060

[120]   Teza, G., Galgaro, A. and De Carli, M. (2012). 'Long-term performance of an irregular shaped borehole heat exchanger system: Analysis of real pattern and regular grid approximation', *Geothermics*, *43*, pp. 45–56, https://doi.org/10.1016/j.geothermics.2012.02.004.

[121]   Maragna, C. (2016). 'Development of a numerical Platform for the Optimization of Borehole Heat Exchanger Fields', in *European Geothermal Congress 2016*, pp. 19–24.

[122]   Mogensen P. (1983). 'Fluid to Duct Wall Heat Transfer in Duct System Heat Storage', In *Proceedings of the International Conference On Subsurface Heat Storage in Theory and Practice*; Swedish Council for Building Research: Stockholm. Sweden, June 6–8, 1983; pp. 652-657.

[123]   Loveridge, F., Brettmann, T., Olgun, C. G. and Powrie, W. (2014). 'Assessing the applicability of thermal response testing to energy piles', in *At global perspectives on the sustainable execution of foundation works, Sweden, May 2014*.

[124]   Hu, P., Zha, J., Lei, F., Zhu, N. and Wu, T. (2014). 'A composite cylindrical model and its application in analysis of thermal response and performance for

energy pile', *Energy and Buildings*, *84*, pp. 324–332, https://doi.org/10.1016/j.enbuild.2014.07.046.

[125] Yu, K. L., Singh, R. M., Bouazza, A. and Bui, H. 2015). 'Determining soil thermal conductivity through numerical simulation of a heating test on a heat exchanger pile'. *Geotechnical and Geological Engineering*, *33*, pp. 239–252. https://doi.org/10.1007/s10706-015-9870-z

[126] Badenes, B., de Santiago, C., Nope, F., Magraner, T., Urchueguía, J., de Groot, M., Pardo de Santayana, F., Arcos, J. L. and Martín, F. (2016). 'Thermal characterization of a geothermal precast pile in Valencia (Spain)', in *European Geothermal Congress 2016*; Strasbourg, France, 19-24 Sept 2016.

[127] Zarrella, A., Emmi, G., Zecchin, R. and De Carli, M. (2017). 'An appropriate use of the thermal response test for the design of energy foundation piles with U-tube circuits', *Energy and Buildings*, *134*, pp. 259–270, https://doi.org/10.1016/j.enbuild.2016.10.053

[128] Claesson, J. and Hellström, G. (2000). 'Analytical Studies of the Influence of Regional Groundwater Flow by on the Performance of Borehole Heat Exchangers', in *Proceedings TERRASTOCK 2000, 8th International Conference on Thermal Energy Storage*. University of Stuttgart, Germany.

[129] Xiaolong, M. and Jürgen, G. (2010). 'Efficiency Increase of Soil Heat Exchangers due to Groundwater Flow and Air Injection', in *Proceedings World Geothermal Congress 2010*; Bali, Indonesia, 25-29 April 2010.

[130] Pardo, N., Montero, Á., Sala, A., Martos, J. and Urchueguía, J. F. (2011). 'Efficiency improvement of a ground coupled heat pump system from energy management', *Applied Thermal Engineering*, *31*, pp. 391–398, https://doi.org/10.1016/j.applthermaleng.2010.09.016

[131] Magraner, T., Montero, Á., Quilis, S. and Urchueguía, J. F. (2010). 'Comparison between design and actual energy performance of a HVAC-ground coupled heat pump system in cooling and heating operation', *Energy and Buildings*, *42*, pp. 1394-1401. https://doi.org/10.1016/j.enbuild.2010.03.008.

[132] Montagud, C., Corberán, J. M., Montero, Á. and Urchueguía, J. F. (2011). 'Analysis of the energy performance of a ground source heat pump system after five years of operation', *Energy and Buildings*, *43*, pp. 3618–3626, https://doi.org/10.1016/j.enbuild.2011.09.036

[133] Schnürer, H., Sasse, C. and Fisch, M. N. (2005). 'Thermal Energy Storage in Office Buildings Foundations'. Available online: https://businessdocbox.com/Green_Solutions/70941158-Thermal-energy-storage-in-office-buildings-foundations.html [Accessed on 15-June 2016]

[134] Schröder, B., Hanschke, T. (2003). 'Energiepfähle - umweltfreundliches Heizen und Kühlen mit geothermisch aktivierten Stahlbetonfertigpfählen', *Bautechnik*, *80*, pp. 925–927. https://doi.org/10.1002/bate.200306210

[135] Centrum Paele A/S (2016). 'Energipæle'. Available online: http://www.centrumpaele.dk/paele/energipaele.html. [Accessed 14-February 2016].

[136] Geelen, C., Krosse, L., Sterrenburg, P., Bakker, E.-J. and Sijpheer, N. (2003). 'Handboek Energiepalen', TNO Milieu, Energie en Procesinnovatie: Laan van Westenenk 501, Postbus 342, 7300 AH Apeldoorn, The Netherlands.

[137] Kelvin, T. W. (1982). 'Mathematical and physical papers'. *Cambridge University Press. London.*

[138] Ingersoll, L. R. (1954). 'Heat Conduction - With Engineering and Geological Application', The Univer.; Read Books, 1954; ISBN 9781443730747.

[139] Loveridge, F. and Powrie, W. (2014). '2D thermal resistance of pile heat exchangers', *Geothermics*, *50*, pp. 122–135, https://doi.org/10.1016/j.geothermics.2013.09.015

[140] Al-Khoury, R. (2011). *Computational modeling of shallow geothermal systems*, CRC Press; ISBN 0415596270.

[141] Diersch, H.-J. G. (2014). 'FEFLOW Finite Element Modeling of Flow, Mass and Heat Transport in Porous and Fractured Media', Springer Science & Business Media; ISBN 364238739X.

[142] Alberdi-Pagola, M., Poulsen, S. E., Jensen, R. L. and Madsen, S. (2017). 'Thermal response testing of precast pile heat exchangers: fieldwork report' Aalborg: Department of Civil Engineering, Aalborg University. DCE Technical Reports, nr. 234, pp. 43. Available online: http://vbn.aau.dk/files/266379225/Thermal_response_testing_of_precast_pile_heat_exchangers_fieldwork_report.pdf

[143] Gehlin, S. (2002). 'Thermal Response Test. Method Development and Evaluation', PhD thesis, Luleå University of Technology, Sweden.

[144] Alberdi-Pagola, M., Poulsen, S.E., Jensen, R.L., and Madsen, S. (2018). 'Design methodology for precast quadratic pile heat exchanger-based shallow geothermal ground-loops: multiple pile g-functions' *Geothermics (under-review)*.

[145] Hot Disk AB (2014). 'Hot Disk Thermal Constants Analyser TPS 1500 unit, Instruction Manual'.

[146] Dansk Standard (2015). 'DS/EN ISO 22007-2 (2015): Plastics – Determination of the thermal conductivity and thermal diffusivity – Part 2: Transient plane heat source (hot disc) method'.

[147] Alberdi-Pagola, M., Jensen, R. L., Madsen, S. and Poulsen, S. E. (2017). 'Measurement of thermal properties of soil and concrete samples'. Aalborg: Department of Civil Engineering, Aalborg University. DCE Technical Reports, nr. 235, pp. 30. Available online: http://vbn.aau.dk/files/266378485/Measurement_of_thermal_properties_of_soil_and_concrete_samples.pdf

[148] Doherty, J. (2010). 'PEST Model-Independent Parameter Estimation. User Manual'; Computing, W. N., Ed.; 5th Edition.

[149] Shonder, J. A. and Beck, J. V. (2000). 'Field test of a new method for determining soil formation thermal conductivity and borehole resistance', *ASHRAE Transactions*, *106*, pp. 843–850.

[150] Spitler, J. D. and Bernier, M. (2016). 'Vertical borehole ground heat exchanger design methods', Rees, S. J., in *Advances in Ground-Source Heat Pump Systems*; Woodhead Publishing, pp. 29–61 ISBN 978-0-08-100311-4.

[151] Zanchini, E. and Lazzari, S. (2013). 'Temperature distribution in a field of long Borehole Heat Exchangers (BHEs) subjected to a monthly averaged heat flux', *Energy*, *59*, pp. 570–580, https://doi.org/10.1016/j.energy.2013.06.040

[152] Alberdi-Pagola, M., Jensen, L.J., Madsen, S. And Poulsen, S.E. (2018). Method to obtain g-functions for multiple precast quadratic pile heat exchangers. Aalborg: Department of Civil Engineering, Aalborg University. DCE Technical Reports; nr. 243, pp. 34. Available online: http://vbn.aau.dk/files/274763046/Method_to_obtain_g_functions_for_multiple_precast_quadratic_pile_heat_exchangers.pdf

[153] Alberdi-Pagola, M., Poulsen, S. E., Jensen, L. J. and Madsen, S. (2018). 'A case study of the sizing and optimisation of an energy pile foundation (Rosborg, Denmark). *Renewable Energy (under-review)*.

[154]   The MathWorks Inc. (2017). 'MATLAB R2017a and Global Optimization Toolbox'.

[155]   Derringer, G. and Suich, R. (1980). 'Simultaneous Optimization of Several Response Variables', *Journal of Quality Technology*, *12*, pp. 214–219, doi:10.1080/00224065.1980.11980968.

[156]   Costa, N. R., Lourenço, J. and Pereira, Z. L. (2011). 'Desirability function approach: A review and performance evaluation in adverse conditions', *Chemometrics and Intelligent Laboratory Systems, 107*, pp. 234–244, https://doi.org/10.1016/j.chemolab.2011.04.004

[157]   Nist Sematech (2018). 'Engineering statistics handbook. Multiple responses: The desirability approach'. Available online: https://www.itl.nist.gov/div898/handbook/pri/section5/pri5322.htm [Accessed on 11-May 2018].

[158]   Philippe, M., Bernier, M. and Marchio, D. (2009). 'Validity ranges of three analytical solutions to heat transfer in the vicinity of single boreholes', *Geothermics*, *38*, pp. 407–413, https://doi.org/10.1016/j.geothermics.2009.07.002

[159]   Alberdi-Pagola, M. (2018). 'Thermal response test data of five quadratic cross section precast pile heat exchangers', *Data in Brief*, *18*, pp. 13–15, https://doi.org/10.1016/j.dib.2018.02.080

[160]   The MathWorks Inc. (2017). 'MATLAB R2017a'.

[161]   Fritsch, F. N. and Carlson, R. E. (1980). 'Monotone Piecewise Cubic Interpolation', *SIAM Journal on Numerical Analysis*, *17*, pp. 238–246, https://doi.org/10.1137/0717021

[162]   Lund, H., Werner, S., Wiltshire, R., Svendsen, S., Thorsen, J. E., Hvelplund, F. and Mathiesen, B. V. (2014). '4th Generation District Heating (4GDH): Integrating smart thermal grids into future sustainable energy systems', *Energy*, *68*, https://doi.org/10.1016/j.energy.2014.02.089

[163]   Danish Energy Agency (2017). 'Regulation and planning of district heating in Denmark'. URL: https://ens.dk/sites/ens.dk/files/Globalcooperation/regulation_and_planning_of_district_heating_in_denmark.pdf

APPENDICES

Notice each appendix follows its own page numbering.

Appendix I.   Published TRT data (Paper D)

The data of five TRTs is made available.

Alberdi-Pagola, M., 2018. "Thermal Response Test data of five quadratic cross section precast pile heat exchangers", *Data in Brief*, 18, pp. 13-15.

https://doi.org/10.1016/j.dib.2018.02.080.

Reprinted by permission from Elsevier.

Data Article

Thermal response test data of five quadratic cross section precast pile heat exchangers

Maria Alberdi-Pagola

Department of Civil Engineering, Aalborg University, Denmark

ARTICLE INFO

ABSTRACT

This data article comprises records from five Thermal Response Tests (TRT) of quadratic cross section pile heat exchangers. Pile heat exchangers, typically referred to as energy piles, consist of traditional foundation piles with embedded heat exchanger pipes. The data presented in this article are related to the research article entitled *"Comparing heat flow models for interpretation of precast quadratic pile heat exchanger thermal response tests"* (Alberdi-Pagola et al., 2018) [1]. The TRT data consists of measured inlet and outlet temperatures, fluid flow and injected heat rate recorded every 10 min. The field dataset is made available to enable model verification studies.

Specifications Table

Subject area	Engineering, Renewable energies
More specific subject area	Shallow geothermal energy applications and soil investigation techniques.
Type of data	Tables in Excel sheets.
How data was acquired	The field data was acquired with a Kamstrup Multical ® 801.
Data format	Raw.
Experimental factors	Five tests were performed in different pile heat exchangers, i.e., different length and pipe configurations.

Experimental features	During the TRT, the heat carrier fluid (water) is circulated in the ground heat exchanger while being continuously heated at a specified rate. Heat dissipates to the ground heat exchanger and subsequently to the ground. The test records fluid inlet- and outlet temperatures, the fluid flow rate and energy consumption and logs them in 10-min intervals for at least 48 h. The tables also provide the accumulated energy and volume.
Data source location	The data analysed have been collected in two different locations in Denmark: Langmarksvej test site in Horsens (55° 51′ 43″ N, 9° 51′ 7″ E), where energy piles LM1, LM2 and LM3 have been tested. Rosborg test site in Vejle (55° 42′ 30″ N, 9° 32′ 0″ E), where energy piles RN1 and RS1 have been tested.
Data accessibility	The data are available with this article.

Value of the data

- Each TRT is presented in an individual Excel sheet.
- These data can be used to validate thermal models of pile heat exchangers.
- There are not publicly available full-scale TRT datasets for pile heat exchangers.
- Sharing data will support the development of this type of ground heat exchangers.
- These data can supplement other data sets to assist the development of thermal dimensioning guidelines for pile heat exchanger foundations.

1. Data

Dimensioning of Ground Source Heat Pump installations typically relies on thermal response testing (TRT) of one or more ground heat exchangers. The dataset of this article provides raw TRT data of several precast pile heat exchangers, described in [1]. Fig. 1 shows the setup for one of the tests.

2. Experimental design, materials and methods

During the TRT, the heat carrier fluid (water) is circulated in the ground heat exchanger while being continuously heated at a specified rate. Heat dissipates to the ground heat exchanger and subsequently to the ground. The test records fluid inlet- and outlet temperatures, the fluid flow rate and energy consumption and logs them in 10-min intervals for at least 48 h.

The shared data consists of five TRTs of square cross section precast pile heat exchangers. The five energy piles have different lengths and pipe configurations. The tests have been carried out at two different locations in Denmark.

Model interpretation of the measured TRT temperatures yield estimates of the undisturbed soil temperature T_0 [°C], the average soil thermal conductivity λ_s [W/m/K] over the length of the heat exchanger and the thermal resistance the ground heat exchanger R_b [K m/W] [3–5].

The TRT sets are compiled in a single Excel file, separated in sheets named by the pile IDs (refer to Table 2 in [1]). Each sheet is divided in seven columns, namely: date, accumulated heat energy [kWh], accumulated volume [m^3], inlet temperature T1 [°C], outlet temperature T2 [°C], flow [l/h] and injection heat rate or effect [kW]. Notice the data is given from the closest in time to the most distant.

The TRT equipment is produced by UBeG, Ref. [6]. The temperature sensors are Pt 500 and Pt 1000 type and the flow-meter is an ultrasonic flowmeter Ultraflow® type by Kamstrup. The records are compiled by a Kamstrup Multical 801 logger. The equipment is further described in Ref. [2].

Fig. 1. Ongoing TRT at Langmarksvej. Inlet- and outlet pipes are insulated to prevent disturbances from ambient temperature conditions [2].

Acknowledgements

Transparency document. Supplementary material

Transparency document associated with this article can be found in the online version at doi:10.1016/j.dib.2018.02.080.

Appendix A. Supplementary material

Supplementary data associated with this article can be found in the online version at doi:10.1016/j.dib.2018.02.080.

References

[1] M. Alberdi-Pagola, S.E. Poulsen, F.A. Loveridge, S. Madsen, R.L. Jensen, Comparing heat flow models for interpretation of precast quadratic pile heat exchanger thermal response tests, Energy 145 (2018) 721–733. http://dx.doi.org/10.1016/j.energy.2017.12.

[2] M. Alberdi-Pagola, S.E. Poulsen, R.L. Jensen, S. Madsen, Thermal Response Testing of Precast Pile Heat Exchangers: Field-work Report, Aalborg University. Department of Civil Engineering, Aalborg (2017) 43 (Available online) ⟨http://vbn.aau.dk/files/266379225/Thermal_response_testing_of_precast_pile_heat_exchangers_fieldwork_report.pdf⟩.

[3] P. Mogensen, Fluid to duct wall heat transfer in duct system heat storage, in: Proc. Int. Conf. on Subsurface Heat Storage in Theory and Practice, 1983 Stockholm. Swedish Council for Building Research, Sweden, June 6–8, 1983, pp. 652–657.

[4] S. Gehlin, Thermal Response Test. Method Development and Evaluation (Ph.D. Thesis), Luleå University of Technology, Luleå, Sweden, 2002.

[5] J.D. Spitler, S.E.A. Gehlin, Thermal response testing for ground source heat pump systems - an historical review, Renew. Sustain. Energy Rev. 50 (2015) 1125–1137. http://dx.doi.org/10.1016/j.rser.2015.05.061.

[6] UBEG Umwelt Baugrund Geothermie Geotechnik, Thermal Response Test Equipment Data, Germany, 2013.

Appendix II. Analysis of thermo-mechanical behaviour (Conference paper II)

Alberdi-Pagola, M., Madsen, S., Jensen, L.J. & Poulsen, S.E., 2017. "Numerical investigation on the thermo-mechanical behavior of a quadratic cross section pile heat exchanger", in *Proceedings of the IGSHPA Technical/Research Conference and Expo Denver*, USA, March 14-16, 2017. http://dx.doi.org/10.22488/okstate.17.000520. Available online:

https://shareok.org/bitstream/handle/11244/49304/oksd_igshpa_2017_Alberdi-Pagola.pdf?sequence=1&isAllowed=y

Reprinted by permission from IGSHPA.

Numerical investigation on the thermo-mechanical behavior of a quadratic cross section pile heat exchanger

Maria Alberdi-Pagola, Søren Madsen, Rasmus Lund Jensen, Søren Erbs Poulsen

ABSTRACT

Pile heat exchangers are traditional foundation piles with built in heat exchangers. As such, the footing of the building both serves as a structural component and a heating/cooling supply element. The existing geotechnical design standards do not consider the nature of thermo-active foundations and, therefore, there is a need to develop guidelines to design them properly. This paper contributes by studying the thermo-mechanical behavior of the precast piles which are 15-meter long and have a quadratic cross section and a W-shape pipe heat exchanger. This article aims to numerically assess the additional changes in the pile load transfer generated by its heating and cooling. In addressing this objective, a preliminary multi-physical finite element analysis is conducted which serves as a tool for exploring: i) the thermally induced mechanical stresses within the concrete and on the pile-soil axial and shaft resistances; ii) the maximum upward/downward displacements. A one-year time span is considered under operational and extreme thermal boundary conditions. The results show that a typical geothermal utilization of the energy foundation does not generate significant structural implications on the geotechnical capacity of a single energy pile. However, ground thermal loads need to be considered in the design phase to account for potential extreme temperature changes, which could generate thermal stresses that equalize the mechanically generated ones.

INTRODUCTION

The Danish government aims to reduce 40% the greenhouse gas emissions by 2020 relative to 1990 and to cover the total domestic energy requirements by renewable resources by 2050 (Danish Energy Agency, 2012). In this matter, ground source heat pump systems cooperate in the transition towards sustainable energy sources.

Pile heat exchangers, also known as energy piles, are thermo-active ground structures that utilize reinforced concrete foundation piles as vertical closed-loop heat exchangers, developed as an alternative to borehole heat exchangers (Brandl, 2006). As such, the foundation of the building both serves as a structural and a heating and/or cooling component and as a result, their dimensioning becomes a coupled thermo-hydro-mechanical challenge. Pile heat exchangers can vary in length from 10 to 50 meters and in width from 0.3 to 1.5 meters. Besides, the geothermal pipes can be placed in the central part or closer to the pile edge (Brandl, 2006). Due to this variety, several experimental and numerical studies attempt to develop novel approaches that

Maria Alberdi Pagola (mapa@civil.aau.dk) is a Ph.d. student at the Department of Civil Engineering at Aalborg University where Rasmus Lund Jensen is an associate professor and Søren Madsen is an assistant professor. Søren Erbs Poulsen is a docent at VIA University College, Horsens.

characterize the heat transfer in and around such structures (Cecinato and Loveridge, 2015, Park et al., 2013, Loveridge and Powrie, 2013, Bandos et al., 2014).

Pile design approaches in Europe are based on the determination of the ultimate and serviceability limit states according to Eurocode 7 (DS/EN 1997-1/AC, 2010). Yet the regulations do not consider the geothermal use in the foundation design process with regards to structural requirements. Thermal piles can be subject to a net change of the temperature relative to the initial condition over time, which causes thermal stresses and head displacements. Under thermo-elastic conditions, if the pile is a free body, i.e. it has no restraints, it will expand while heating and contract during cooling to yield a thermal free strain. In reality, a pile will not expand or contract freely as it will be confined by the structure on top and the surrounding soil, at different levels of degrees of freedom (Figure 1). As a result, the measured strain change due to temperature changes will be less than the free axial thermal strain and the constrained strains will develop thermal stresses (GSHP Association, 2012).
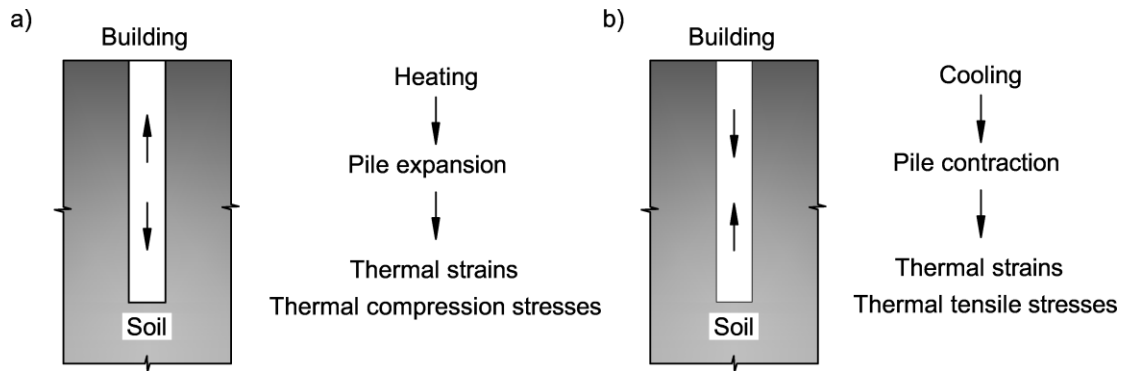
Figure 1   Response mechanism of a pile heat exchanger to thermal loading, a) for heating and b) for cooling.

The structural implications of the thermal loading in the service life of energy piles is still uncertain (Pahud and Hubbuch, 2007). The study of the effect of the mechanical loads in the long term is still an issue for practitioners and, therefore, energy foundations carry the same difficulties exacerbated by the cyclic (seasonal) thermal load effects in the soil and pile-soil interface. It has not been investigated whether the long-term bearing capacity of thermo-active piles is affected by the thermal cycles even though no operational failures have been reported to date. To ensure that the geotechnical performance of the pile is not negatively affected, conservative safety procedures are applied: the fluid temperature in the ground loop is not allowed to go below 2°C and there is a tendency to place more energy piles than required (VDI, 2001, VDI, 2010, SIA, 2005, NHBC Foundation, 2010, GSHP Association, 2012, Loveridge, 2012, Mimouni and Laloui, 2014).

The temperature range imposed by the geothermal exploitation of the foundations falls between 2°C to 30°C or higher and their nature depends on the needs of the building (Laloui and Di Donna, 2013). These temperature changes can affect the stress state at the pile-soil interface and the shear strength of the soil that affects the tip resistance (Olgun et al., 2014). Recent studies on the impact of thermal loading at pile-soil interface indicate that the bearing capacity of the pile is not significantly affected (Suguang et al., 2014, Di Donna, 2014, GSHP Association, 2012, Mimouni, 2014, Olgun et al., 2014). Xiao et al. (2014) and Di Donna (2014) have analyzed monotonic temperature variations in the range from 6°C to 50°C-60°C and have concluded that higher temperatures increase the strength of the clay-concrete contact and that the sand-concrete interface is not affected by the monotonic temperature changes.

Two main full-scale performance studies of energy piles lead the state of the art in the field: the Lambeth College, London (Bourne-Webb et al., 2009) and the École Polytechnique Fédérale de Lausanne EPFL (Laloui et al., 2006, Mimouni, 2014). Both studies conclude: 1) short-term plastic response of soils has not been observed due to the geothermal use since effective stresses typically are within yield surfaces, i.e., within the thermo-elastic domain; 2) the additional stresses produced in the energy pile due to thermal loads depend on the degrees of freedom of the pile. Therefore, the pile-soil interaction under working mechanical and thermal loads provokes systems that depend on soil conditions, level of pile confinement and magnitude of thermal loads, making hard to establish general rules. Fortunately, simple descriptive mechanistic frameworks have been established from observed behaviors (Bourne-Webb et al., 2009, Amatya et al., 2012, Knellwolf et al., 2011, Laloui and Di Donna, 2011).

Numerical tools are used to analyze not just experimental conditions but also potential scenarios, supporting the understanding of the physics behind the problem and assisting the development of behavior rules. Several numerical studies explore the thermo-mechanical phenomena of energy piles in different soil conditions. Regarding load transfer mechanisms, Suryatriyastuti et al. (2012), Hassani Nezhad Gashti et al. (2014)and Laloui et al. (2006) encompass good examples validated against experimental data.

The understanding of the behavior of the thermo-active foundations is still fundamental for their optimization during the design phase and under operational conditions. This paper presents a preliminary attempt to describe the thermo-mechanical implications, additional to those due to static axial loading, disturbing the thermally active version of a single precast quadratic cross section pile under operational and extreme situations for a specific case study, described in Alberdi-Pagola et al. (2016).

This paper is organized as follows: firstly, three ground thermal demand scenarios are defined based on measured data. Secondly, a three dimensional finite element model is described where the thermal loads are used as boundary conditions. Then, the Results and Discussion section analyzes the structural implications under the different thermal circumstances on a 1-year time span and, finally, conclusions are drawn.

ANALYZED DATA

The equivalent energy wave technique has been developed by Abdelaziz et al. (2015) to analyze the long-term performance of ground coupled heat exchangers. It generates a realistic annual sine curve based on measured operational ground thermal loads. The ground load is defined as the power measured through the ground loop of the ground source heat pump installation, divided by the number of energy piles and the length of the piles [W/m].
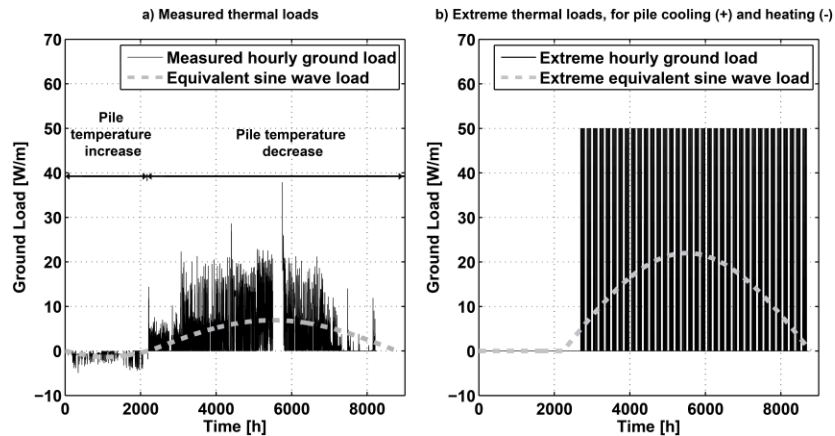
Figure 2 a) Measured ground thermal load and its equivalent wave; b) Generated ground thermal load and its equivalent wave, valid for extreme cooling of the pile (when heat extraction) and extreme heating of the pile (when heat injection).

An equivalent wave has been generated for a year of operational data available from Rosborg Gymnasium reported in Alberdi-Pagola et al. (2016) (Figure 2a). The treated ground source heat pump installation is mainly used for heating yet some free-cooling partially recharges the ground in summer (Figure 2a). This situation imitates the current working conditions and it will be referred as "Measured thermal loads". Two more scenarios account for extreme thermal load conditions (Figure 2b), making the heat pump work in peak capacity conditions during 8 hours per day, 5 days a week. The extreme heat extraction from the ground represents an extreme heating need of the building during winter with no recharge in summer. The extreme heat injection to the ground mimics an extreme cooling need of the building. The extreme cases equal in magnitude but own opposite sign.

METHODOLOGY

Three dimensional finite element modelling has been used to analyze the coupled thermo-mechanical problem of a single quadratic cross section thermal pile. The model aims to reflect the geotechnical and operational conditions at the mentioned case study.

Finite element model characteristics

The finite element software COMSOL Multiphysics 5.2 (COMSOL Multiphysics, 2015) has been used to calculate the subsurface temperature response and the stress and strain domains in and near the pile heat exchanger under heating and cooling loads. A linear-elastic behavior was imposed to all the model domain, based on the observed thermo-elastic structural behavior of an energy pile under normal working in-situ conditions reported in Bourne-Webb et al. (2009) and Laloui et al. (2006). The thermal interaction of the pile heat exchanger with the surrounding soil is modelled by pure conduction. The presence of groundwater flow is ignored in the calculations. The soil is assumed to be isotropic and homogeneous.
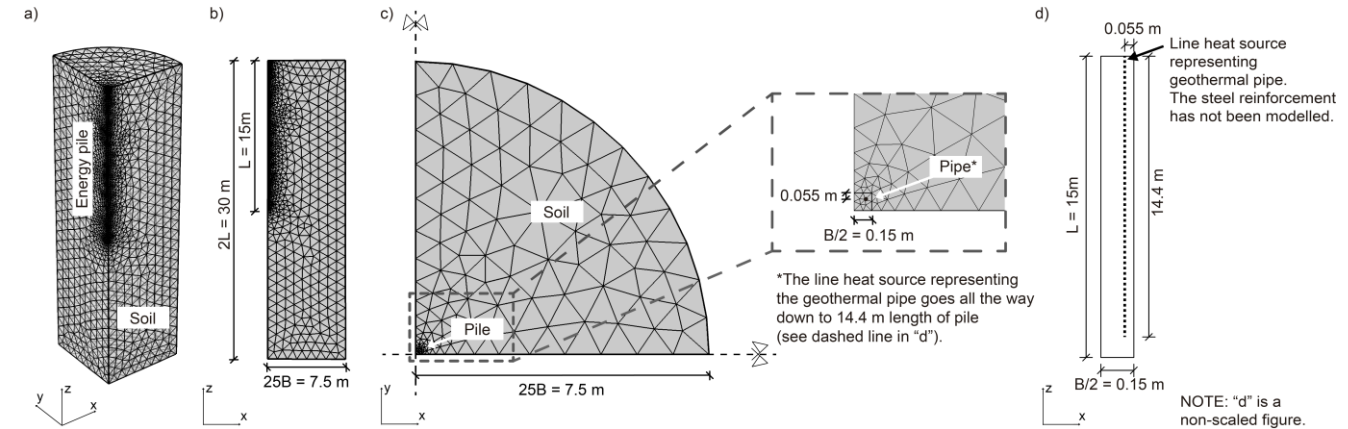
Figure 3 a) Illustration of the 3D finite element mesh, b) side view of the finite element model c) top view of the finite element model and zoomed detail of the position of the simplified geothermal pipe d) Non-scaled side view of the pile heat exchanger and the simplified geothermal pipe.

The 3D model contains two domains (Figure 3a): the soil and the concrete pile, which contains a line heat source mimicking the PE-X pipe (Figure 3c). The model dimensions were established following the suggestions by Suryatriyastuti et al. (2012): lateral extension 25B, being B = 0.3 m (pile side), and vertical height for the soil volume

2L, being L = 15 m (pile length). A quarter of the domain has been simulated taking advantage of symmetries (Figure 3b). No interface elements between the pile and the soil have been considered, allowing a perfect contact between them. This has been considered a conservative scenario since Suryatriyastuti et al. (2012) and Hassani Nezhad Gashti et al. (2014) reported that simulated thermal stresses are larger in perfect contact. The finite element model uses a mesh with 34,505 tetrahedral elements, more refined around the pile and it gets coarser with distance (Figure 3a).

Material properties

Table 1 summarizes the parameters for the pile and the soil (sand) used in the model. These values are taken from performed measurements and literature. The steel reinforcement has not been considered as it means less than 5% of the total weight of the pile.

Table 1. Properties of the materials used in the model.

Parameter	Value
Young modulus pile	41,900.00 MPa
Young modulus rigid sand (Geotechdata.info, 2013)	30.00 MPa*
Poisson ratio pile	0.30
Poisson ratio soil	0.30
Thermal expansion coefficient pile	3.00E-05 1/K
Thermal expansion coefficient soil	1.50E-05 1/K
Density concrete	2370.00 kg/m³
Density soil	1900.00 kg/m³
Thermal conductivity concrete	1.80 W/m/K
Thermal conductivity soil	2.30 W/m/K
Volumetric heat capacity concrete	1.98 MJ/m³/K
Volumetric heat capacity soil	2.60 MJ/m³/K

*Considered constant with depth.

Initial- and boundary conditions

Rolled displacement boundary conditions fix the horizontal movement on the side borders while pinned conditions restrict both the horizontal and vertical movement on the bottom boundary of the soil domain. To account for the gravity effect and the mechanical load, a two-step stationary run has been performed. These steps provoke stresses and strains, both in the concrete and in the soil that should be added to the thermally-induced ones. The initial soil vertical effective stress is 0.25 MPa at the bottom of the pile and the horizontal stresses of the soil are neglected for the hereon analysis. The bearing capacity of the 15 meter pile is 1510 kN in compression (non factored), estimated from data from Dansk Geoteknik A/S (1973). The pile head displacement under geostatic conditions, meaning no mechanical load added, is 16 mm (1.1 mm/m of pile length).

The pile is restrained at the toe allowing the free movement during pile cooling and prohibiting the expansion while heating, mimicking an end-bearing pile. The mechanical load applied at the top of the pile is 600 kN (factoring the bearing capacity 2.5 times), which gives a ratio of 0.1 between the applied load and the compressive strength of concrete (68 MPa). The application of this load resulted in a pile top settlement of 1 mm (0.06 mm/m of pile length).

Regarding the thermal boundary conditions, an initial temperature of 10°C, similar to the observed average undisturbed ground temperature at the represented case, is assumed in the whole domain. A constant temperature boundary of 10°C is also applied to the ground level and the side boundaries of the soil block are selected as open boundaries to mimic the infinite soil (Hassani Nezhad Gashti et al., 2014).

The fluid circulating inside the pipes has been represented as a line heat source (Figure 3c) subjected to a

transient and uniform heat rate [W/m] over its length (described in section "Analyzed data"). There was no external mechanical load applied during the transient models to ease the estimation of the uncoupled thermal stresses and strains.

RESULTS AND DISCUSSION

The pile-soil system has been modelled, subjected to transient thermal loads over a year. The time span is limited to the available data. The analysis aims to quantify the maximum thermal stresses and the maximum thermal displacements generated in the pile-soil system due to the geothermal use. Therefore, two types of mechanical boundary conditions have been applied to the pile extremes, as described in Table 2. Besides, the provided naming code will assist the identification of each simulated case in the analysis hereby.

Table 2. Applied boundary conditions and identification of simulations.

	Maximum thermal stresses	Maximum thermal displacements at pile head
Boundary conditions	Rigid connection at head and end-bearing condition at toe.	Free head movement and restrained toe.
Measured thermal loads	1A	1B
Extreme heat extraction	2A	2B
Extreme heat injection	3A	3B

The axial thermal stresses generated in the center of the pile for the three scenarios are shown in Figure 4a, uncoupled from the stresses generated by the mechanical load. Table 3 summarizes the main results of the transient simulations. The contour of the profiles in Figure 4 are comparable to previous literature (Hassani Nezhad Gashti et al., 2014), with a stabilized zone along the middle and two transient zones at the extremes indicating the uniform nature of the thermal effects.

For heat injection cases (simulations 1A in summer and 3A), the upper zones with higher compression stresses, occur due to the influence of the constant temperature boundary condition imposed at the soil surface and the restrained movement of the pile head. The second region at the bottom might be influenced by the thermal gradients generated below the end of the heat line source and the restrained toe movement. The maximum compression stress as a result of the thermal loads reaches 6.5 MPa (simulation 3A, Table 3). For this case, the magnitude of the temperature-induced load is very close to the purely mechanical load, increasing the solicitation of the toe, resulting on a combined load of 1185 kN, almost 80% of the pile capacity, corresponding to failure. This would not be allowed for design, as it is above the design bearing capacity (including safety factors) and it indicates that thermal loads need to be considered in the design of the energy foundations. For operational circumstances, on the other hand, the combined load in summer hardly increases 2%.

A temperature increment of 1°C results in an additional temperature-induced vertical force of 100 kN approximately, very similar to the values reported by Laloui et al. (2006) and Amatya et al. (2012). However, in terms of stresses, the studied pile suffers considerable increases, in the order of 1000 kPa/°C, due to the small cross section of the pile.

The cooling of the pile provokes a constrained contraction, generating a maximum tensile stress of -2.2 MPa and -0.7 MPa for simulations 2A and 1A in winter, respectively (Figure 4a). The tensile stresses dissipate with depth as the upwards movement of the pile toe is permitted.

Regarding the mechanical properties of concrete, the maximum compressive stresses developed means 10%

of the ultimate compression strength. Hence, the combined thermal and mechanical load would reach 20% of the compression resistance. The tensile strength of the concrete, without reinforcement, has been estimated as 5 MPa from Neville (1995). It is still twice higher than the computed maximum tensile stress.

The maximum shaft shear stress estimated is 160 kPa at the pile toe for the extreme heat injection case (simulation 3A) even though over the pile length the shear stresses were negligible. The constrained pile expansion at the pile toe induce an increase of shear stresses concentrated in the bottom region of the pile (Figure 4b). On the other hand, during pile cooling, the perfect contact in the interface increases the shaft stress component, creating a higher mobilized shear stress over the pile length for the extreme heat extraction (simulation 2A). As highlighted by Hassani Nezhad Gashti et al. (2014), the mobilization of the shaft loads when the bottom movement is allowed rises concern on the behavior of floating thermal piles.
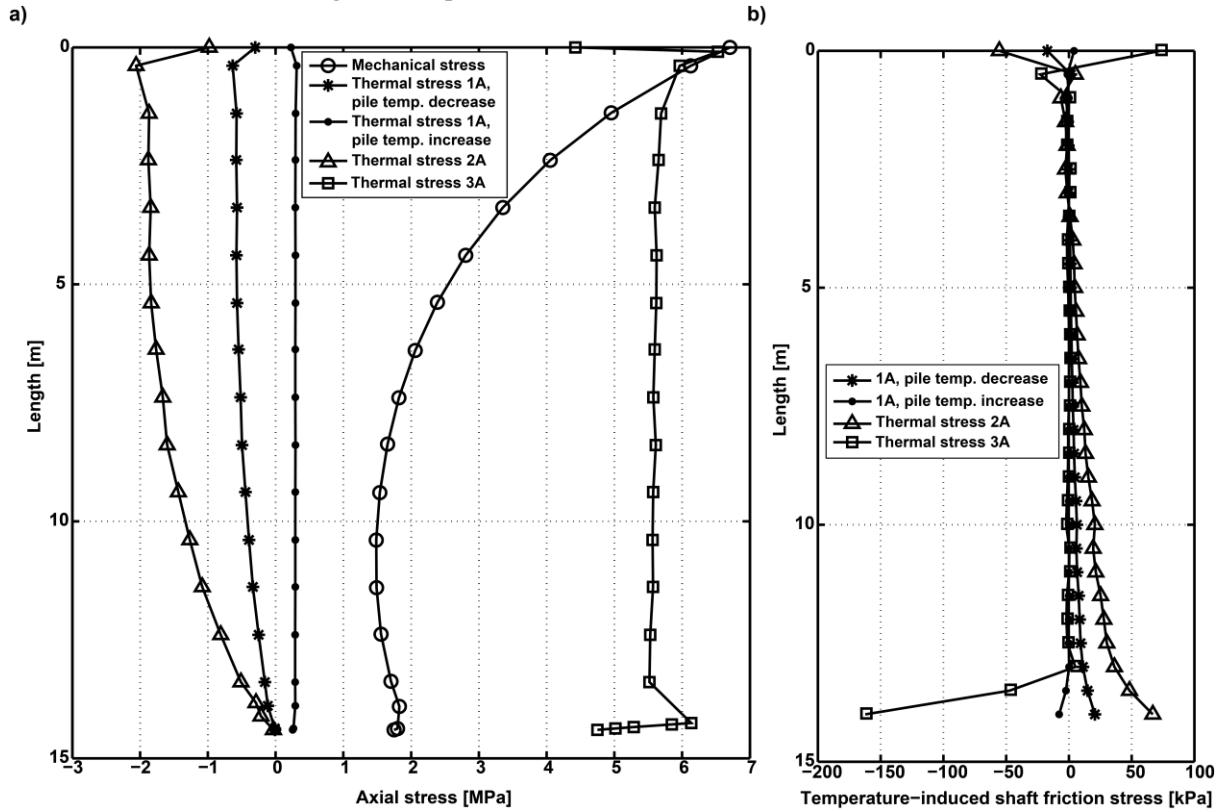
Figure 4   a) Thermally induced axial stresses over the pile length at the its center and the axial stresses mobilized by the static mechanical load. Negative sign states for tensile stresses. b) Mobilized thermally-induced shear stresses.

According to DS/EN 1997-1/AC (2010), the pile fails when it settles 10% of the pile base diameter (i.e., 0.023 mm/m). For the considered cases, the displacements are insignificant (Table 3). The maximum predicted deformation belongs to the combined effects of a temperature decrease that generates the pile contraction (simulation 2B) and the mechanical load, providing a head settlement of 0.17 mm/m, i.e., 7.5% of the allowed settlement. This agrees with the conclusions from Xiao et al. (2016) who reported that the cooling cycle can dominate the serviceability limit state design of pile heat exchangers. It is concluded that the deformations resulted from the geothermal exploitation are very low, probably due to the high rigidity of the pile.

Table 3. Maximum thermal stresses and displacements predicted for a one-year study.

	Maximum temperature change from initial condition	Maximum thermal-induced axial stress	Maximum thermal-induced displacement of pile head relative to pile length
Measured thermal loads			
Heat injection in summer	0.5°C	0.3 MPa [1A]	-0.01 mm/m [1B]
Heat extraction in winter	2.0°C	-0.7 MPa [1A]	0.03 mm/m [1B]
Extreme heat extraction	-6.0°C	-2.2 MPa [2A]	0.11 mm/m [2B]
Extreme heat injection	6.0°C	6.5 MPa [3A]	-0.11 mm/m [3B]

Sign criteria: for displacements, positive means downwards and for stresses, positive means compression.

This paper investigates the additional thermal stresses and displacements generated in a pile heat exchanger due to its geothermal use over a year. The time span was limited by the available data. This rough study indicates i) orders of magnitude of the thermally induced stresses and displacements and potential temperature changes under certain thermal conditions and ii) relevant aspects that require more refining in coming studies.

The analyzed thermal loads do not produce the thermal quasi steady state situation required to dimension the long-term performance of the ground source heat pump installations. This condition would allow to quantify the total temperature change that the pile-soil system would be subjected to in the long term. Therefore, the present study underestimates the net temperature change. I.e., for heat extraction cases, higher tensile stresses and higher pile head settlements than the simulated ones would be predicted in the long term, while compression stresses would increase when heat injection is required. On the other hand, the mechanically restrained toe and head boundary conditions and the perfect contact between pile and soil are conservative measures that give rise to overestimated stress states.

CONCLUSIONS

This paper presents a preliminary approach to quantify the additional thermal stresses and displacements generated in a pile heat exchanger due to its geothermal use. For that, measured and extreme thermal loads have been applied to a linear thermo-elastic 3D finite element model of a single precast energy pile and the surrounding soil.

Transient simulations over a year show that a typical utilization of the energy foundation does not generate significant structural implications on a single thermal pile in terms of axial and mobilized shaft stresses and generated displacements. However, for extreme heating conditions, meaning a temperature increase of 6°C, the combined thermal and mechanical loads can reach 80% of the bearing capacity of the pile in compression, which would not be acceptable in design. Besides, the stress state conditions could worsen in the long term, highlighting the importance of proper structural analysis in the design phase of the pile heat exchangers.

Future attempts should account for more complex phenomena (pile-soil friction, thermo-mechanical constitutive laws of soils, pile group effects, etc.). Besides, the thermal influence between neighboring piles, the effect of the natural temperature variations of the soil and the impact of the building on top of the geothermal reservoir domain should be emphasized as they will affect the amount of usable thermal energy in the long-term.

ACKNOWLEDGMENTS

REFERENCES

ABDELAZIZ, S. L., OLGUN, C. G. & MARTIN II, J. R., 2015. *Equivalent energy wave for long-term analysis of ground coupled heat exchangers.* Geothermics, 53, 67-84.

ALBERDI-PAGOLA, M., JENSEN, R. L. & POULSEN, S. E., 2016. *A performance case study of energy pile foundation at Rosborg Gymnasium (Denmark).* 12th REHVA World Congress Clima2016, 22-25 May 2016 Aalborg, Denmark. Department of Civil Engineering, Aalborg University, p. 10.

AMATYA, B. L., SOGA, K., BOURNE-WEBB, P. J., AMIS, T. & LALOUI, L., 2012. *Thermo-mechanical behaviour of energy piles.* Geotechnique, 62, 503-519.

BANDOS, T. V., CAMPOS-CELADOR, Á., LÓPEZ-GONZÁLEZ, L. M. & SALA-LIZARRAGA, J. M., 2014. *Finite cylinder-source model for energy pile heat exchangers: Effects of thermal storage and vertical temperature variations.* Energy, 78, 639-648.

BOURNE-WEBB, P. J., AMATYA, B., SOGA, K., AMIS, T., DAVIDSON, C. & PAYNE, P., 2009. *Energy pile test at lambeth college, London: Geotechnical and thermodynamic aspects of pile response to heat cycles.* Geotechnique, 59, 237-248.

BRANDL, H., 2006. *Energy foundations and other thermo-active ground structures.* Geotechnique, 56, 81-122.

CECINATO, F. & LOVERIDGE, F. A., 2015. *Influences on the thermal efficiency of energy piles.* Energy, 82, 1021-1033.

COMSOL MULTIPHYSICS, 2015. *COMSOL Multiphysics version 5.1: user's guide.* In: COMSOL (ed.). Burlington.

DANISH ENERGY AGENCY, 2012. *Energy Policy in Denmark.* Solid Media Solutions ed. Amaliegade 44, 1256 Copenhagen K, Denmark: Danish Energy Agency.

DANSK GEOTEKNIK A/S, 1973. *Geoteknisk rapport. Grundundersøgelser for Amtsgymnasium i Vejle, Vestre Engvej, Vejle.*

DI DONNA, A., 2014. *Thermo-mechanical aspects of energy piles.* PhD Thesis, École polytechnique fédérale de Lausanne EPFL.

DS/EN 1997-1/AC, 2010. *Eurocode 7: Geotechnical design - Part 1: General rules.* Dansk Standard.

GEOTECHDATA.INFO., 2013. *Soil elastic Young's modulus* [Online]. Available: http://www.geotechdata.info/parameter/soil-young's-modulus.html.

GSHP ASSOCIATION, 2012. *Thermal Pile: Design, Installation & Materials Standards.* National Energy Centre, Davy Avenue, Knowlhill, Milton Keynes: Ground Source Heat Pump Association.

HASSANI NEZHAD GASHTI, E., MALASKA, M. & KUJALA, K., 2014. *Evaluation of thermo-mechanical behaviour of composite energy piles during heating/cooling operations.* Engineering Structures, 75, 363-373.

KNELLWOLF, C., PERON, H. & LALOUI, L., 2011. *Geotechnical analysis of heat exchanger piles.* Journal of Geotechnical and Geoenvironmental Engineering, 137, 890-902.

LALOUI, L. & DI DONNA, A., 2011. *Understanding the behaviour of energy geo-structures.* Proceedings of the Institution of Civil Engineers-Civil Engineering, 2011. Thomas Telford Ltd, 184-191.

LALOUI, L. & DI DONNA, A., 2013. *Energy Geostructures: Innovation in Underground Engineering,* John Wiley & Sons, Inc.

LALOUI, L., NUTH, M. & VULLIET, L., 2006. *Experimental and numerical investigations of the behaviour of a heat exchanger pile.* International Journal for Numerical and Analytical Methods in Geomechanics, 30, 763-781.

LOVERIDGE, F., 2012. *The thermal performance of foundation piles used as heat exchangers in ground energy systems.* PhD Thesis, University of Southampton.

LOVERIDGE, F. & POWRIE, W., 2013. *Temperature response functions (G-functions) for single pile heat exchangers.* Energy, 57, 554-564.

MIMOUNI, T., 2014. *Thermomechanical Characterization of Energy Geostructures with Emphasis on Energy Piles.* PhD Thesis, École polytechnique fédérale de Lausanne EPFL.

MIMOUNI, T. & LALOUI, L., 2014. *Towards a secure basis for the design of geothermal piles.* Acta Geotechnica, 9, 355-366.

NHBC FOUNDATION, 2010. *Efficient design of piled foundations for low-rise housing, design guide.*

OLGUN, C. G., OZUDOGRU, T. Y. & ARSON, C., 2014. *Thermo-mechanical radial expansion of heat exchanger piles and possible effects on contact pressures at pile-soil interface.*

PAHUD, D. & HUBBUCH, M., 2007. *Measured thermal performances of the energy pile system of the Dock Midfield at Zürich Airport.* Proceedings European geothermal congress, 2007.

PARK, H., LEE, S.-R., YOON, S. & CHOI, J.-C., 2013. *Evaluation of thermal response and performance of PHC energy pile: Field experiments and numerical simulation.* Applied Energy, 103, 12-24.

SIA, 2005. *Utilisation de la chaleur du sol par des ouvrages de fondation et de soutènement en béton: guide pour la coneption, la réalisation et la maintenance,* SIA, Société suisse des ingénieurs et des architectes.

SUGUANG, X., SULEIMAN, M. T. & MCCARTNEY, J. S., 2014. *Shear Behavior of Silty Soil and Soil-Structure Interface under Temperature Effects.* Geo-Congress 2014. Atlanta, Georgia, USA: American Society of Civil Engineers.

SURYATRIYASTUTI, M. E., MROUEH, H. & BURLON, S., 2012. *Understanding the temperature-induced mechanical behaviour of energy pile foundations.* Renewable and Sustainable Energy Reviews, 16, 3344-3354.

VDI, V. D. I., 2001. VDI 4640 Thermal Use of the Underground. Part 3: *Utilization of the Subsurface for Thermal Purposes.* Underground Thermal Energy Storage. Berlin: VDI-Gessellschaft Energie und Umwelt (GEU).

VDI, V. D. I., 2010. *VDI 4640 Thermal Use of the Underground. Part 1: Fundamentals, approvals, environmental aspect.* Berlin: VDI-Gessellschaft Energie und Umwelt (GEU).

XIAO, J., LUO, Z., MARTIN II, J. R., GONG, W. & WANG, L., 2016. *Probabilistic geotechnical analysis of energy piles in granular soils. Engineering Geology,* 209**,** 119-127.

Appendix III.   Description of fieldwork (Technical report I)

Alberdi-Pagola, M., Poulsen, S.E., Jensen, L.J. & Madsen, S., 2017. "Thermal response testing of precast pile heat exchangers: fieldwork report". Aalborg: Department of Civil Engineering, Aalborg University. DCE Technical Reports, nr. 234, pp. 43. Available online:

http://vbn.aau.dk/files/266379225/Thermal_response_testing_of_precast_pile_heat_exchangers_fieldwork_report.pdf

Aalborg Universitet

AALBORG UNIVERSITY

DENMARK

Thermal response testing of precast pile heat exchangers

Pagola, Maria Alberdi; Poulsen, Søren Erbs; Jensen, Rasmus Lund; Madsen, Søren

[Link to publication from Aalborg University](#)

DEPARTMENT OF CIVIL ENGINEERING
AALBORG UNIVERSITY

Thermal response testing of precast pile heat exchangers: fieldwork report.

Maria Alberdi-Pagola
Søren Erbs Poulsen (VIA University College, Horsens, DK)
Rasmus Lund Jensen
Søren Madsen

Aalborg University
Department of Civil Engineering

DCE Technical Report No. 234

Thermal response testing of precast pile heat exchangers: fieldwork report.

by

Maria Alberdi-Pagola
Søren Erbs Poulsen (VIA University College)
Rasmus Lund Jensen
Søren Madsen

December 2017

Scientific Publications at the Department of Civil Engineering

Technical Reports are published for timely dissemination of research results and scientific work carried out at the Department of Civil Engineering (DCE) at Aalborg University. This medium allows publication of more detailed explanations and results than typically allowed in scientific journals.

Technical Memoranda are produced to enable the preliminary dissemination of scientific work by the personnel of the DCE where such release is deemed to be appropriate. Documents of this kind may be incomplete or temporary versions of papers—or part of continuing work. This should be kept in mind when references are given to publications of this kind.

Contract Reports are produced to report scientific work carried out under contract. Publications of this kind contain confidential matter and are reserved for the sponsors and the DCE. Therefore, Contract Reports are generally not available for public circulation.

Lecture Notes contain material produced by the lecturers at the DCE for educational purposes. This may be scientific notes, lecture books, example problems or manuals for laboratory work, or computer programs developed at the DCE.

Theses are monograms or collections of papers published to report the scientific work carried out at the DCE to obtain a degree as either PhD or Doctor of Technology. The thesis is publicly available after the defence of the degree.

Latest News is published to enable rapid communication of information about scientific work carried out at the DCE. This includes the status of research projects, developments in the laboratories, information about collaborative work and recent research results.

Table of contents

List of figures

List of tables

List of acronyms

AR: Aspect Ratio
BHE: Borehole Heat Exchanger
DAQ: Data Acquisition System
EP: Energy Pile
GHE: Ground Heat Exchanger
LM: Langmarksvej
RN: Rosborg Gymnasium North extension
RS: Rosborg Gymnasium South extension
TRT: Thermal Response Test
TSA: Temperature Sensors Array

1. Introduction

Centrum Pæle A/S, Aalborg University, VIA University College and INSERO Horsens are partners in an industrial PhD project dealing with quadratic cross section pile heat exchangers. This document presents the fieldwork undertaken in the project at two test sites in Denmark: one in Horsens and another in Vejle. The tasks have been carried out between January 2014 and February 2016.

The fieldwork consists mainly of several thermal response tests (TRT) of precast pile heat exchangers. Pile heat exchangers, also known as energy piles, are thermo-active ground structures that utilize reinforced concrete foundation piles as vertical closed-loop heat exchangers. The interpretation of the in-situ TRT yields the effective thermal conductivity of the ground λ_s [W/m/K] and the borehole or pile thermal resistance R_b [K·m/W]. These estimated thermal parameters form the basis for dimensioning a planned ground source heat pump installation based on closed loop vertical ground heat exchangers. However, this report does not cover topics related to the interpretation of TRT data.

The report is organized as follows: first, the concept of TRT is explained. Second, the test sites are described. Third, the field work is presented and a summary of the future work regarding the methodology to treat the data from the tests is provided. Finally, further documentation of the fieldwork, the pile heat exchangers and the TRT equipment is extended in diverse appendices.

2. Thermal response testing

Thermal response testing (TRT) is a widely used field method for estimating soil thermal conductivity λ_s [W/m/K] and thermal resistance of traditional borehole heat exchangers (BHE) R_b [K·m/W] (Mogensen P., 1983, Gehlin, 2002). In the TRT, the heat carrier fluid (water) is circulated in the GHE at a specified rate while being continuously warmed by a heater. Heat dissipates to the GHE and subsequently to the ground, and records of the fluid inlet- and outlet temperatures, the fluid flow rate and energy consumption are compiled every 10 minutes during the test (for at least 48 hours). Ambient temperatures inside and outside the TRT equipment are also recorded during the test. Figure 1 illustrates the TRT set-up.

The thermal conductivity of the ground λ_s and the GHE thermal resistance R_b are estimated in the interpretation of the measured heat carrier fluid inlet and outlet temperatures. The thermal conductivity of the ground λ_s is a measure of the ease with which the soil conducts heat. Heat is more easily extracted from highly conductive soils and such soils recuperate more rapidly from thermal depletion. The interpretation of the TRT yields an average soil thermal conductivity over the length of the GHE. It is not possible, in the interpretation, to distinguish individual soil layers unless a Distributed TRT is performed (Acuña et al., 2009). The presence of groundwater flow increases the effective thermal conductivity of the ground. The GHE thermal resistance R_b is the integrated thermal resistance between the heat carrier fluid and the ground. As such, the piping, the flow rate and regime, heat exchanger configuration, grout and GHE diameter influence the GHE thermal resistance R_b. It should be as low as possible to facilitate the heat transfer.

The analytical infinite line source approach is a standard method for analysing TRT of traditional vertical borehole heat exchangers (ASHRAE, 2011). However, there is a lack of scientifically supported guidelines for analysing TRT data from energy piles (Loveridge, 2012, GSHP Association, 2012). The quadratic cross section precast piles do not fulfil the basic geometrical assumptions for vertical ground heat exchangers and, therefore, novel approaches that better characterize the heat transfer in and around such structures are required.
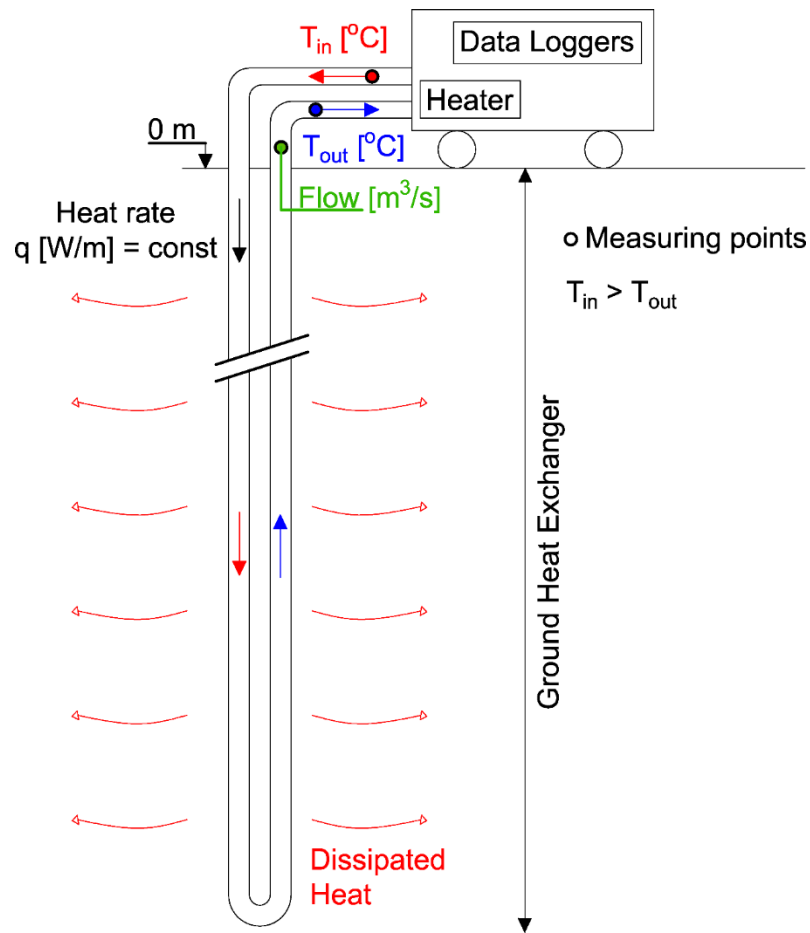
Figure 1: Thermal response test set-up, after Gehlin (2002). The figure represents the TRT in heating mode, i. e., when the inlet temperature T_{in} overcomes the outlet T_{out}.

3. Test sites

In the following, the two test sites will be described in terms of geology and types of GHEs.

3.1. Langmarksvej

The test site is situated at Langmarksvej 84 (street address), 8700 Horsens, Denmark (55° 51′ 43″ N, 9° 51′ 7″ E), 800 m from the VIA University College campus (Figure 2). The test site was established in 2010 as part of a research collaboration between Centrum Pæle A/S, Horsens A.M.B.A. district heating company and VIA University College. After 4 years without operation, the test site is currently used in the present PhD project.

Figure 2: The Langmarksvej test site, Langmarksvej 84, 8700 Horsens, Denmark.

3.1.1. Geology

A monitoring drilling was executed on the 2/11/2015 by Franck Geoteknik A/S and a stratigraphic profile was compiled. Soil samples were collected every 0.5 m and for each sample the following properties were measured in the laboratory: bulk density ρ [g/cm^3], water content in weight [%], thermal conductivity λ_s [W/m/K] and volumetric heat capacity ρc_p [MJ/m^3/K]. The geological setting and thermal parameter measurements are listed in Figure 3 (see Appendix A for further details). The thermal properties have been measured with a Hot Disk apparatus, Transient Plane Source (Hot Disk AB, 2014). The lab measurements are further described in Alberdi-Pagola et al. (2017). As depicted, 4-5 m of fillings emerge on top of glacial clay till.

10
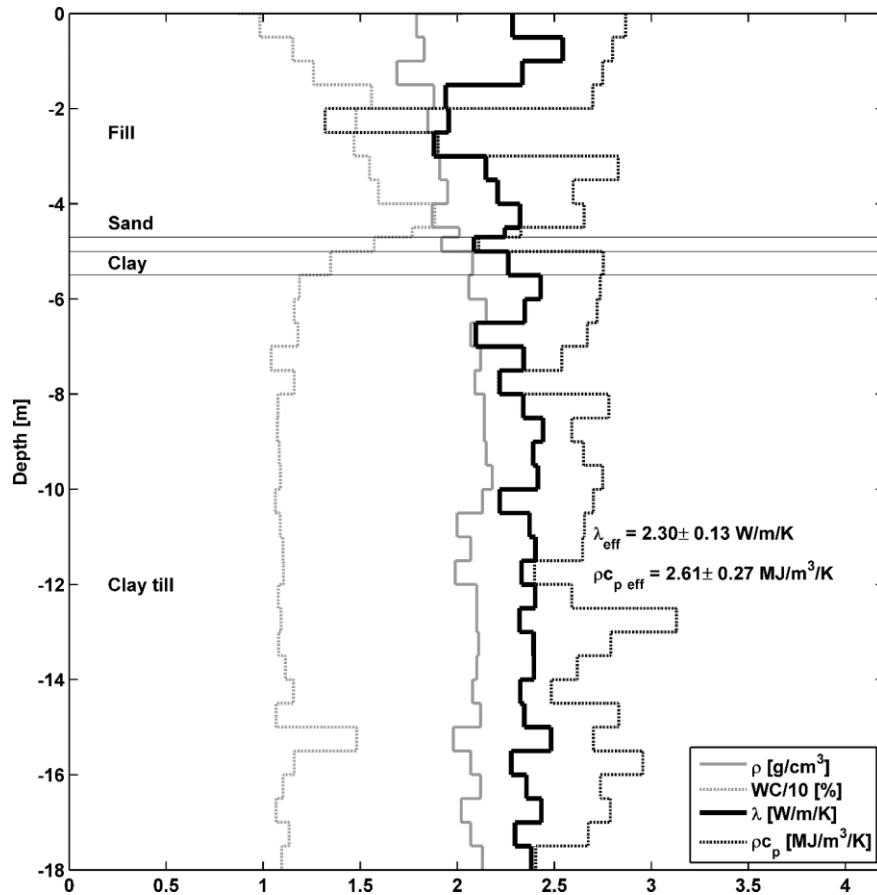
Figure 3: Stratigraphic profile at the Langmarksvej test site. Bulk density ρ, water content, thermal conductivity λ_s and volumetric heat capacity ρc_p measured in the laboratory using the Hot Disk apparatus are also provided. ρc_p eff and λ_s eff are weighted average estimates over the length of the drilling.

3.1.2. Ground heat exchangers

The test site comprises four energy piles, a BHE and a drilling instrumented with a temperature sensor array (TSA). The GHEs are located as shown in Figure 4. Additional pictures of the test site are provided in Appendix A. Table 1 lists key information for the tested GHEs and Figure 5 depicts the cross section of the energy pile, which applies to all energy piles described in this document.

These pile heat exchangers have a length between 12 to 18 m, a quadratic cross section (0.30 m x 0.30 m) and a W-shape pipe configuration heat exchanger fixed to the steel reinforcement. Appendix B provides technical drawings of the energy piles. A vertical profile for the TSA showing the location of the temperature sensors is provided in Figure 6. The temperature sensors are Pt100 type, described in Appendix C, and they are placed inside a pipe (2 cm diameter). The annulus between the pipe and the ground is filled with quartz sand. The sensors are connected to LabView software (National Instruments, 2015a), working on a nearby computer, which collects the ground temperature records every second during the TRT.

11

Table 1: Properties of tested GHE at the Langmarksvej (LM) test site (information provided by Centrum Pæle A/S and VIA University College).

Test Site	Langmarksvej 84, 8700 Horsens				
GHE name	LM-BHE	LM-EP8	LM-EP7	LM-EP4	LM-EP3
GHE pipe type	Double U [2U]	Single U [1U]	Single U [1U]	W-shape [W]	W-shape [W]
GHE length [m]	18	12	18	12	18
GHE active length [m]	16.5	10.8	16.8	10.8	16.8
Aspect Ratio (AR = length / width)	82	28	44	28	44
Pipe length [m]	68.0	20.8	33.6	42.0	65.0
Pipe material	PEX-A	PEX-A	PEX-A	PEX-A	PEX-A
Pipe outer diameter [mm]	20	20	20	20	20
Pipe inner diameter [mm]	16.2	16.2	16.2	16.2	16.2
Pipe thermal conductivity [W/m/K]	0.42	0.42	0.42	0.42	0.42
Use of spacers	Yes	No	No	No	No
Shank spacing [m]	0.15	0.27	0.27	0.27	0.27
Grout material	Quartz sand	Concrete	Concrete	Concrete	Concrete
GHE shape	Circular, 0.2 m diameter	Square, 0.3m x 0.3m	Square, 0.3 m x 0.3 m	Square, 0.3 m x 0.3 m	Square, 0.3 m x 0.3 m
Installation method	Auger drilling	Driven pile	Driven pile	Driven pile	Driven pile
Supplementary instrumentation	No	No	No	No	Pt100 temperature sensors in the ground at different levels (Figure 4)
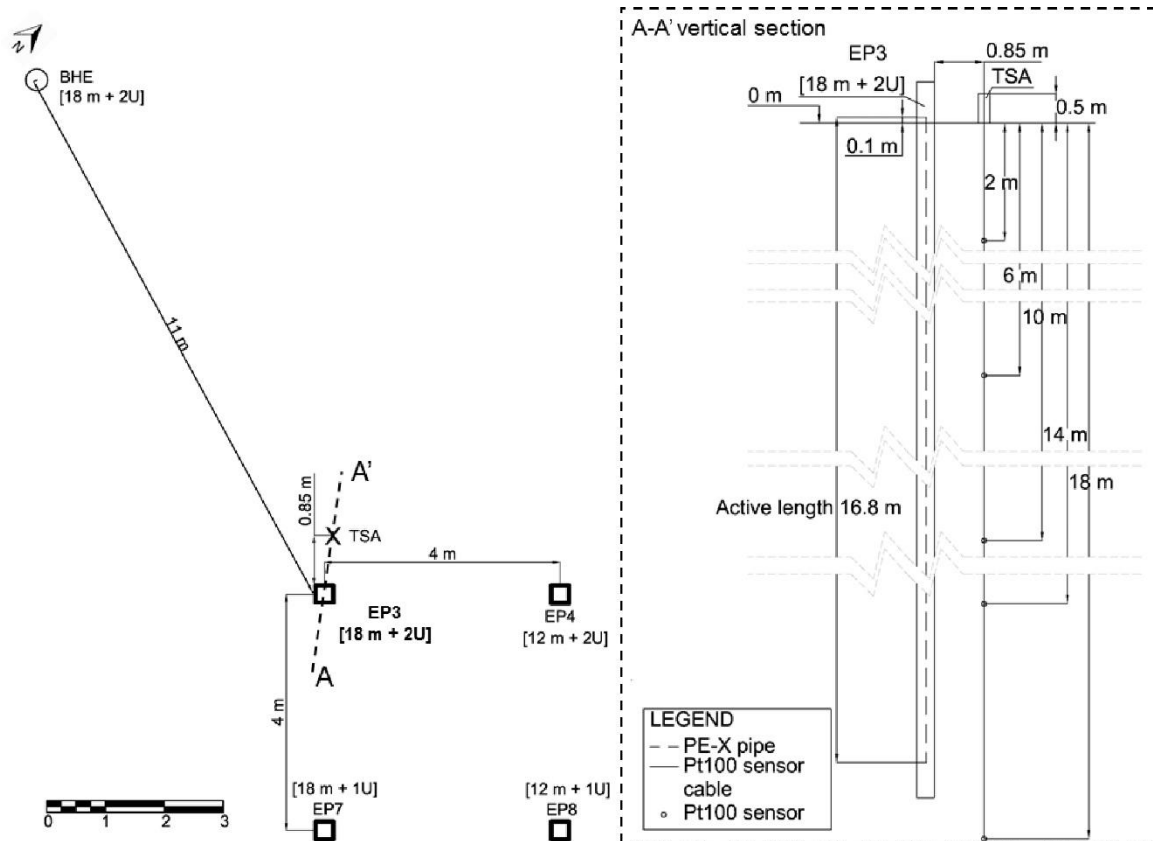
Figure 4: Ground heat exchanger location at Langmarksvej test site (Langmarksvej 84, 8700 Horsens): top view and vertical section. EP: Energy Pile; BHE: Borehole Heat Exchanger; TSA: Temperature Sensor Array; 1U: Single-U pipe arrangement; 2U: Double-U pipe arrangement.

a)

b.1)

b.2)
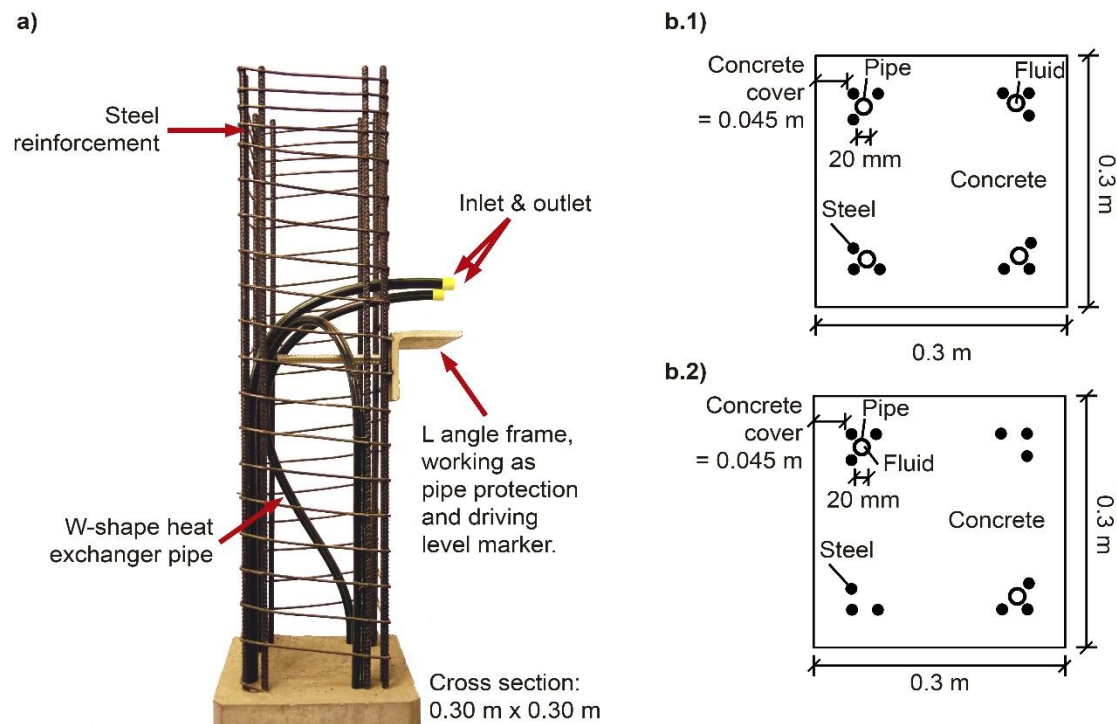
Figure 5: Demonstration model of the precast energy pile with W-shaped heat exchanger pipes fitted to the reinforcement bars; b.1) horizontal cross section of the W-shape energy pile and; b.2) horizontal cross section of the single-U energy pile.

*Cotes in mm
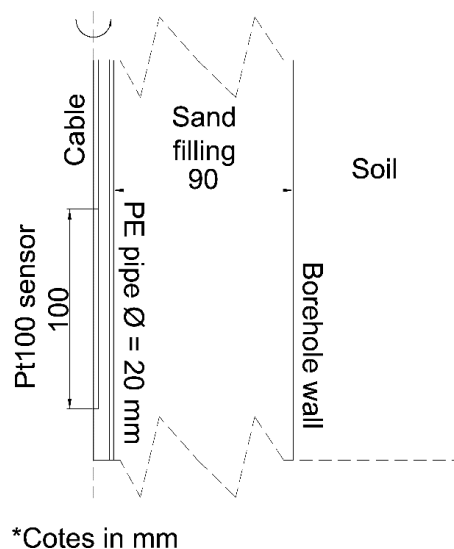
Figure 6: Vertical cross section of the location of a single Pt100 temperature sensor within the TSA drilling, located 0.85 m apart form EP3.

3.2. Rosborg Gymnasium

The test site is located at Vestre Engvej 61, 7100 Vejle, Denmark (55° 42′ 30″ N, 9° 32′ 0″ E) (Figure 7). The south extension of the Rosborg Gymnasium building is founded on 200 foundation pile heat

14

exchangers. The thermo-active foundation has supplemented the heating and free cooling requirements of the building since 2011 (4,000 m^2 heated area). More information about the performance of the installation can be found in Alberdi-Pagola et al. (2016). The north extension of the gymnasium complex is currently under construction. To date, the foundation that consists of 220 energy piles, has been constructed.
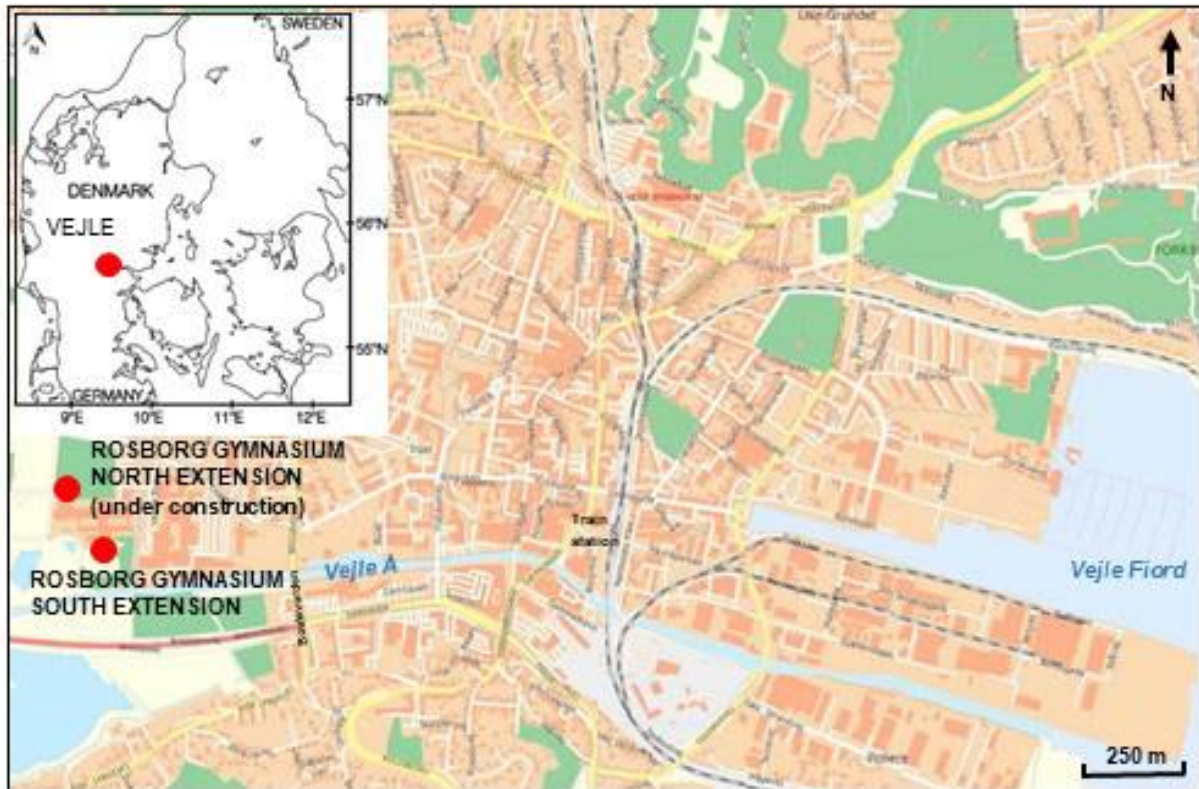
Figure 7: The Rosborg Gymnasium building at Vestre Engvej 61, 7100 Vejle, Denmark. The south and north extensions are founded on 200 and 220 energy piles, respectively.

3.2.1. Geology

A monitoring drilling was executed on the 21/02/2015 by Franck Geoteknik A/S and a stratigraphic profile was compiled. Soil samples were collected each 0.5 m and for each sample the following properties were measured in the laboratory, the same way as at Langmarksvej: bulk density ρ [g/cm^3], water content in weight [%], thermal conductivity λ_s [W/m/K] and volumetric heat capacity ρc_p [MJ/m^3/K]. The geological setting and thermal parameter measurements are listed in Figure 8 (see Appendix A for further details). The lab measurements are further described in Alberdi-Pagola et al. (2017).

The piles are founded in glacial sand 5-6 m below terrain, which is overlain by postglacial, organic mud (Table 2). The groundwater table is situated around 0.70 m below terrain (Dansk Geoteknik A/S, 1973, Franck Geoteknik A/S, 2013). A more detailed stratigraphic column is provided in Appendix A. Both buildings are founded on similar geology.

15
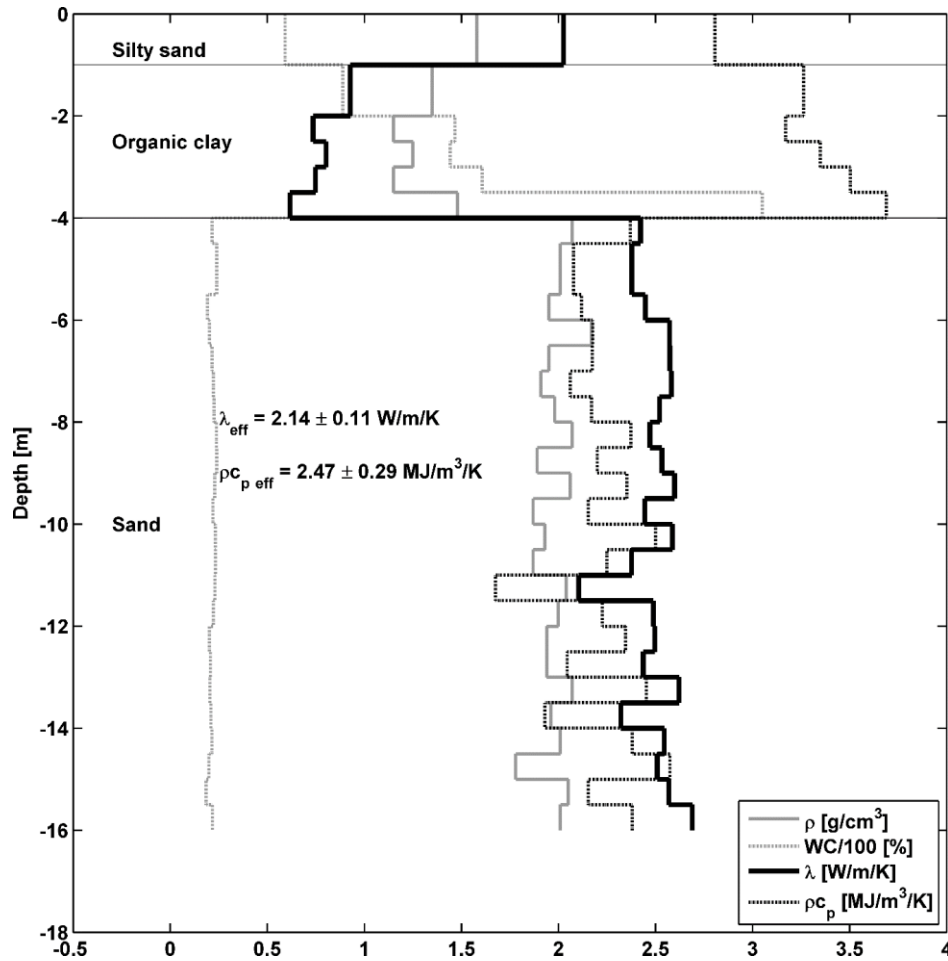
Figure 8: Stratigraphic profile at the Rosborg North test site. Bulk density ρ, water content, thermal conductivity λ_s and volumetric heat capacity ρc_p measured in the laboratory using the Hot Disk apparatus are also provided. $\rho c_{p\ eff}$ and $\lambda_{s\ eff}$ are weighted average estimates over the length of the drilling.

3.2.2. Pile heat exchangers

Figures 9 and 10 show the footprints of the north and south extensions at Rosborg Gymnasium, respectively. Two of the 220 energy piles at the north extension are instrumented and a TRT has been executed in the energy pile indicated in Figure 9. Two of the 200 energy piles at the south building extension are instrumented with Pt100 temperature sensors. Two additional piles, which are accessible from inside the building, are available for testing. One of these energy piles (marked in Figure 10) was tested and analysed in Alberdi-Pagola and Poulsen (2015).
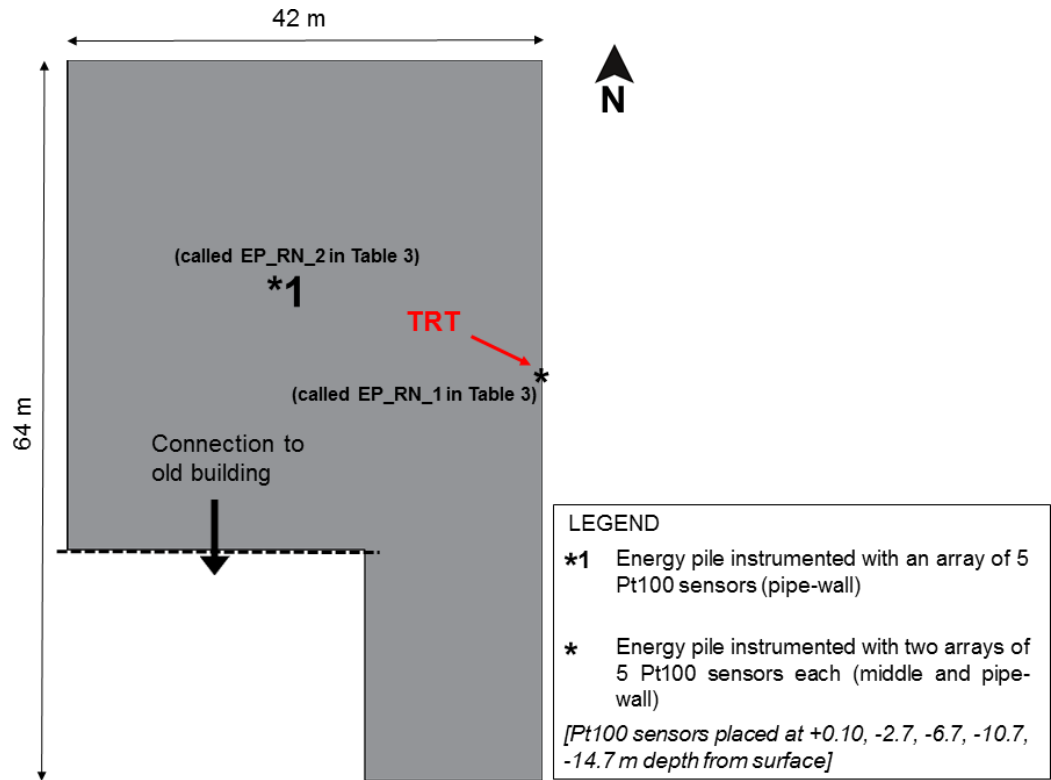
Figure 9: Footprint of the Rosborg Gymnasium's northern extension building. The location of instrumented piles and piles available for testing are also provided.
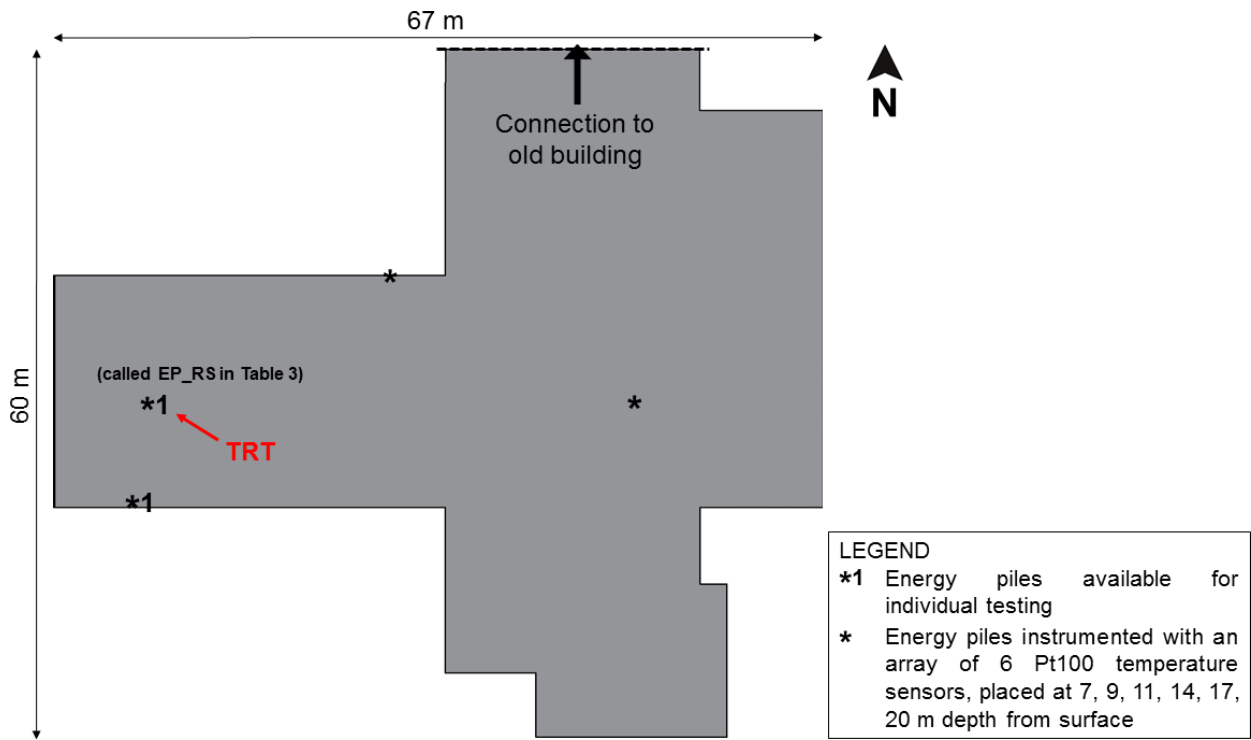
Figure 10: Footprint of the Rosborg Gymnasium's southern extension building. The location of instrumented piles and piles available for testing are also provided.

Table 2 lists key information about the tested energy piles at Rosborg Gymnasium and Figure 11 shows the depths of the Pt100 temperature sensors installed in the piles tested at the north extension. More details about the way the sensors were placed within the concrete is shown in Figure 20 (Appendix A).

Table 2: Properties of tested energy piles (EP) at Rosborg Gymnasium test site.

Test Site	Vestre Engvej 61, 7100 Vejle, Denmark		
	Rosborg Gymnasium South	Rosborg Gymnasium North	
Energy pile name	EP_RS	EP_RN_1	EP_RN_2
Energy pile pipe type	W-shape [W]	W-shape [W]	W-shape [W]
Energy pile length [m]	Unknown	16	16
Energy pile active length [m]	15.0	14.8	14.8
Pipe length [m]	54	58	58
Aspect Ratio (AR = length / width)	39	39	39
Pipe material	PEX-A	PEX-A	PEX-A
Pipe outer diameter [mm]	20	20	20
Pipe inner diameter [mm]	16.2	16.2	16.2
Pipe thermal conductivity [W/m/K]	0.42	0.42	0.42
Use of spacers	No	No	No
Shank spacing [m]	0.27	0.27	0.27
Grout material	Concrete	Concrete	Concrete
GHE shape	Square, 0.3 m x 0.3 m	Square, 0.3 m x 0.3 m	Square, 0.3 m x 0.3 m
Installation method	Driven pile	Driven pile	Driven pile
Supplementary instrumentation	No	2 Pt100 strings, 5 levels (Figure 11)	1 string Pt100, 5 levels, (Figure 11)

Vertical section EP_RN_1 & 2   Cross section EP_RN_1   Cross section EP_RN_2
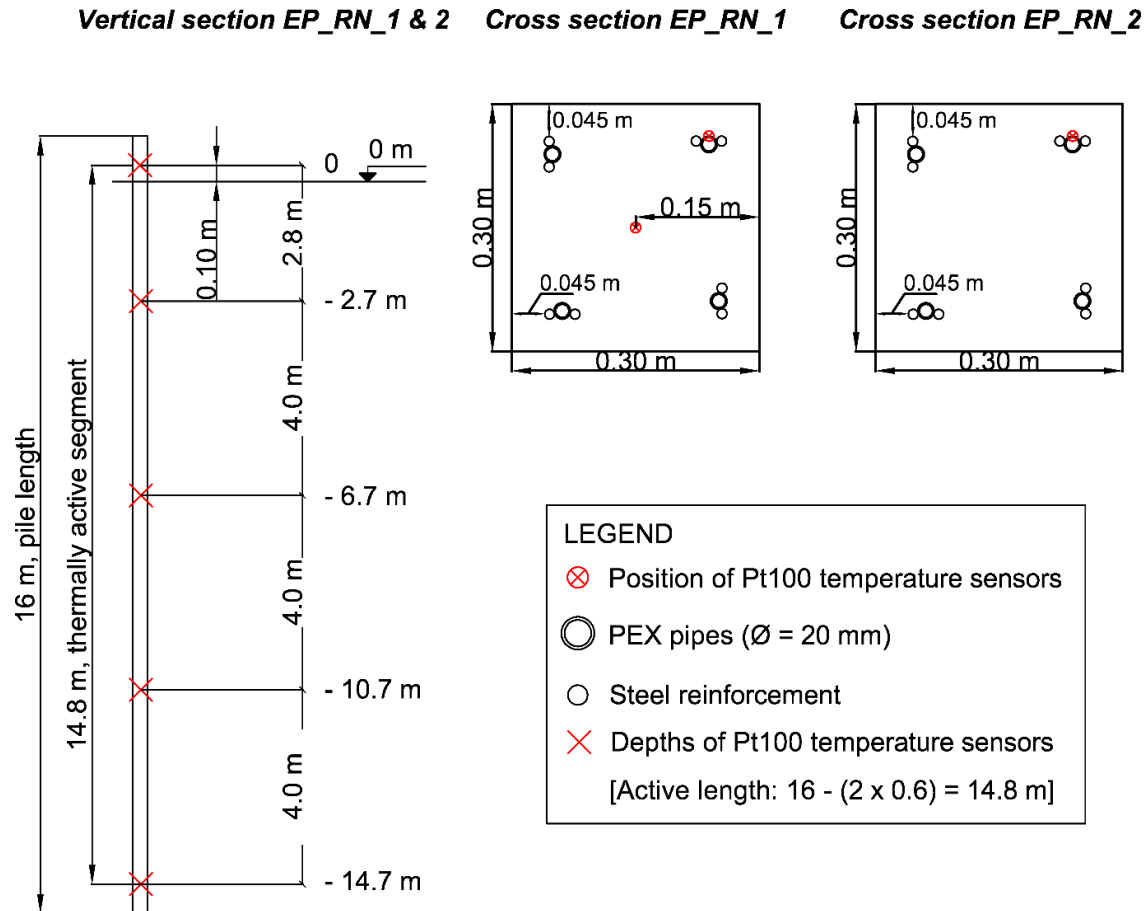
Figure 11: Schematic arrangement of Pt100 strings within the instrumented piles and their depths at Rosborg North, piles 1 and 2 (EP_RN_1 & 2): vertical section and cross sections.

4. TRT sets

In the TRTs presented in this study, the heat carrier fluid (water at 10 °C approx.) is circulated without heating for approximately 30 minutes while maintaining a fluid pressure of 2 bar prior to switching on the heater (and thus starting the test). According to the international standards the minimum duration of a TRT of a borehole heat exchanger is 48 hours (ASHRAE, 2011). The duration of the TRT is determined by the amount of early data that has to be discarded in order to determine soil thermal conductivity λ_s (approximately the first ten hours) in accordance with the assumptions of the standard line source-based method of interpretation (Hellström, 1998). Energy consumption, inlet- and outlet temperatures, fluid flow and the power dissipated are recorded during the test. A total of 8 TRT data sets have been collected which are described in the following. Further documentation of the fieldwork, the tests and the equipment is provided in Appendixes A, D and E.

4.1. Langmarksvej

Five TRTs were performed:
   a) Four TRTs of energy piles with different lengths and heat exchanger pipe arrangements (Figure 4 and Table 1). Key parameters for the TRTs are provided in Table 3.
   b) One TRT of a single BHE (Figure 4, Tables 1 and 2).
   c) Ground temperatures at different depths logged during a single TRT of EP3 at a temperature sensor array (Figure 4).

Table 3 summarises the main parameters of the TRT sets and it also compares the test conditions to the recommendations given by ASHRAE (ASHRAE, 2011). The discrepancies with the recommendations from ASHRAE regarding the late time difference between fluid inlet and outlet temperatures in TRTs of BHE and EP8, are due to: i) the flow rate set is too high in the TRT of the BHE and ii) the length of EP8 is 12 m and it contains a single U heat exchanger pipe. These reasons hamper the efficient dissipation of heat into the ground. The TRT of EP7 was interrupted for 10 hours. The data is available in Appendix C.

Table 3: Key parameters for the TRTs performed at the Langmarksvej test site.

TRT Date	13-08-2015	17-11-2015	24-11-2015	01-12-2015	27-01-2016	ASHRAE recommendations
GHE name	BHE	EP8	EP7	EP4	EP3	
Equipment used	UBeG	UBeG	UBeG	UBeG	UBeG	-
Average Undisturbed Soil Temperature [°C]	12.0	12.2	11.5	11.4	10.4	-
ρc_p from Hot Disk measurements [MJ/m^3/K]	2.6	2.6	2.6	2.6	2.6	-
λ_s from Hot Disk measurements [W/m/K]	2.3	2.3	2.3	2.3	2.3	-
Heat carrier fluid	Water	Water	Water	Water	Water	-
Measurement interval [min]	10	10	10	10	10	≤ 10
Volumetric flow rate [m^3/h]	0.89	0.50	0.48	0.56	0.51	-
Reynolds number	19349	10942	10468	12195	10998	-
Average heat injection rate [W/m]	60.3	101.4	115.9	159.4	167.6	> 50
Heat injection rate, standard deviation as % of average	1.83	4.33	-	4.70	3.74	Peaks < 10
TRT duration [h]	49.8	114.2	69.3	114.2	146.7	> 48
Average, late time $\Delta T = T_{in} - T_{out}$ [°C]	1.02	1.95	3.50	2.65	4.89	> 3.0
Recovery test?	Yes	No	No	No	Yes	-
Recovery test duration [h]	50.7	-	-	-	115.0	-

4.2. Rosborg Gymnasium

Table 4 summarises key parameters for the TRT sets and lists test conditions compared to recommendations given by ASHRAE (ASHRAE, 2011).

Table 4: Summary of main parameters of the TRTs performed at Rosborg Gymnasium test site.

TRT Date	13-01-2014	20-04-2015	09-02-2016	ASHRAE recommendations
GHE name	EP_RS	EP_RS	EP_RN	-
Equipment used	VIA	UBeG	UBeG	-
Average Undisturbed Soil Temperature [°C]	10.2	10.1	9.8	-
ρc_p from Hot Disk measurements [MJ/m³/K]	2.1	2.1	2.1	-
λ_s from Hot Disk measurements [W/m/K]	2.5	2.5	2.5	-
Heat carrier fluid	Water	Water	Water	-
Measurement interval [min]	10	10	10	≤ 10
Volumetric flow [m³/h]	0.38	0.54	0.54	-
Reynolds number	8519	11713	11981	-
Average heat injection rate [W/m]	152.5	183.3	157.8	> 50
Heat injection rate, standard deviation as % of average	4.29	5.39	3.06	Peaks < 10
TRT duration [h]	96.3	69.2	49.3	> 48
Average, late time $\Delta T = T_{in} - T_{out}$ [°C]	5.10	4.52	3.78	> 3.0
Recovery test?	No	No	No	-

4.3. Test comparison

The TRT data are plotted in Figure 12 as normalised temperature Φ (Equation 1) vs. the Fourier number Fo (Equation 2) for a constant rate of heat transfer q [W/m]:

$$\Phi = \frac{2\pi\lambda_s \Delta T}{q} \tag{1}$$

$$Fo = \frac{\alpha_s t}{r_b^2} \tag{2}$$

where ΔT is the change in temperature, λ_s is the soil thermal conductivity [W/m/K], α_s is the soil thermal diffusivity [m²/s], defined as the ratio between the thermal conductivity λ_s and the volumetric heat capacity ρc_p of the soil [J/m³/K] and t is the elapsed test time [s]. Figure 12 indicates a higher GHE thermal resistance for the single-U heat exchangers relative W-shape configurations, as expected. This can be deduced from the higher temperature increase measured in the single-U heat exchanger tests. Besides, the test performed in the borehole heat exchanger yields the highest temperature increments, which implies that the double-U heat exchanger pipe placed in the borehole is less efficient transferring heat to the soil relative to the tested energy piles.
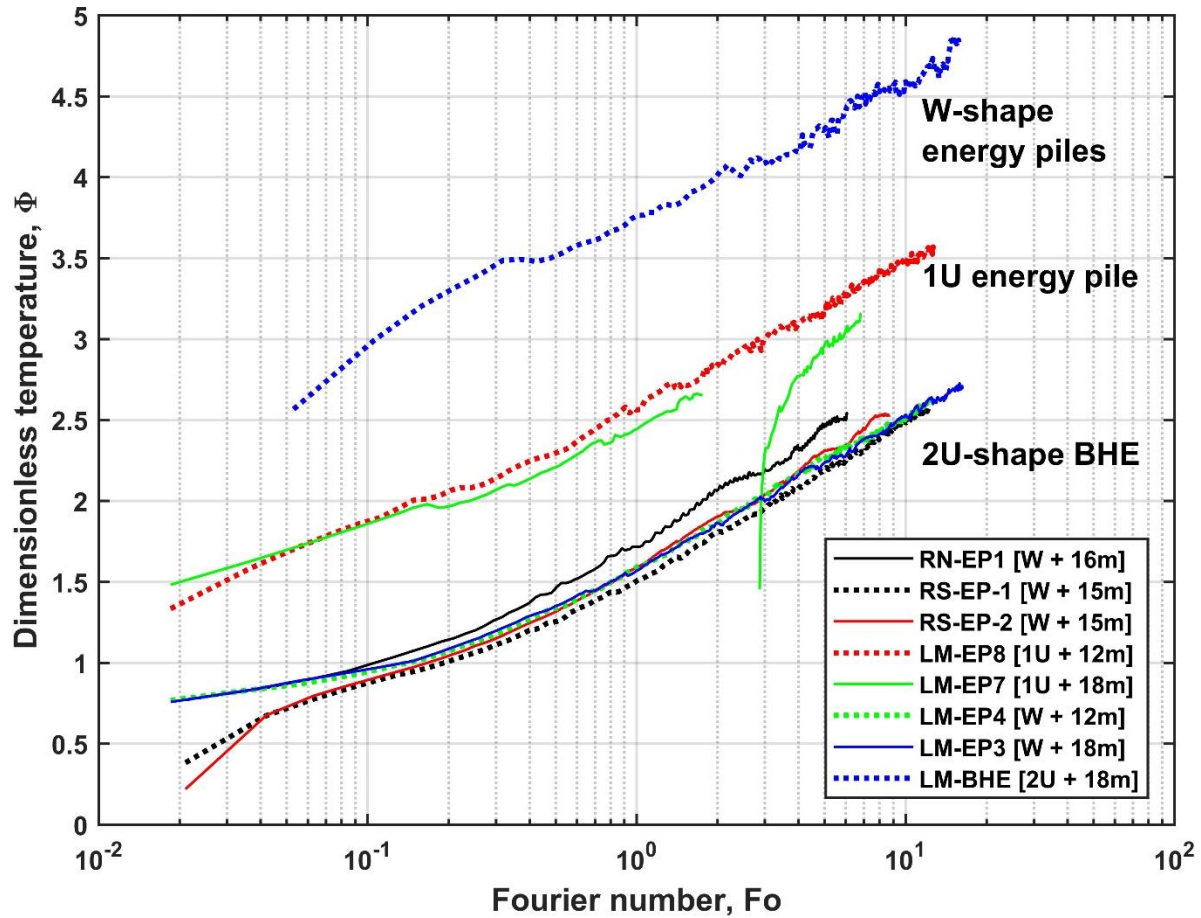
Figure 12: Short term GHE temperature responses in the TRTs. RS = Rosborg South, RN = Rosborg North, LM = Langmarksvej, BHE = Borehole Heat Exchanger

5. Summary

This document has presented the fieldwork undertaken in an Industrial PhD project at two test sites in Denmark (Horsens and Vejle). The project deals with quadratic cross section precast pile heat exchangers and it is a collaboration between Centrum Pæle A/S, Aalborg University, VIA University College and INSERO Horsens.

Pile heat exchangers, also known as energy piles, are thermo-active ground structures that utilize reinforced concrete foundation piles as vertical closed-loop heat exchangers. The fieldwork consists of several thermal response tests (TRT) of precast pile heat exchangers. The tests and its basis have been described, as well as the properties of each energy pile and the surrounding soil in both test sites, and supplementary instrumentation and equipment.

The interpretation of the in-situ TRT yields the effective thermal conductivity of the ground λ_s [W/m/K] and the borehole or pile thermal resistance R_b [K·m/W]. These thermal parameters form the basis for dimensioning a planned ground source heat pump installation based on closed loop vertical ground heat exchangers.

The future work will be focused on the analysis and interpretation of the recorded field data to verify models for quadratic cross section energy piles. The scientific objectives are:

- To validate existing and novel, short run-time analytical and numerical models of the thermal behaviour of quadratic heat exchanger pile (2D - 3D implications).
- Based on the validated models, to investigate the feasibility of TRT methods for energy pile applications. Particular attention will be paid to the estimation of soil thermal conductivity λ_s [W/m/K] and pile thermal resistance R_b [K·m/W].
- To provide recommendations regarding interpretation methods, testing times and likely uncertainties for quadratic pile TRTs.

6. Acknowledgements

7. References

ACUÑA, J., MOGENSEN, P. & PALM, B., 2009. Distributed thermal response test on a U-pipe borehole heat exchanger. Effstock 2009, 11th International Conference on Thermal Energy Storage, Stockholm, June 14-17 2009. Academic Conferences Publishing.

ALBERDI-PAGOLA, M., JENSEN, R. L., MADSEN, S. & POULSEN, S. E. 2017. Measurement of thermal properties of soil and concrete samples In: AALBORG UNIVERSITY, D. O. C. E. (ed.). Aalborg, Denmark: Aalborg University.

ALBERDI-PAGOLA, M., JENSEN, R. L. & POULSEN, S. E., 2016. A performance case study of energy pile foundation at Rosborg Gymnasium (Denmark). 12th REHVA World Congress Clima2016, 22-25 May 2016 Aalborg, Denmark. p. 10 (accepted).

ALBERDI-PAGOLA, M. & POULSEN, S. E., 2015. Thermal response testing and performance of quadratic cross section energy piles (Vejle, Denmark). XVI European Conference on Soil Mechanics and Geotechnical Engineering 2015. Edinburgh, United Kingdom: ICE Institution of Civil Engineers.

ASHRAE, 2011. 2011 ASHRAE Handbook - Heating, Ventilating, and Air-Conditioning Applications (SI Edition). American Society of Heating, Refrigerating and Air-Conditioning Engineers, Inc.

DANSK GEOTEKNIK A/S, 1973. Geoteknisk rapport. Grundundersøgelser for Amtsgymnasium i Vejle, Vestre Engvej, Vejle.

DANSK STANDARD, 2008. DS/EN 60751: Industrial platinum resistance thermometers and platinum temperature sensors.

FRANCK GEOTEKNIK A/S, 2013. Geoteknisk rapport, parameterundersøgelse. Rosborg Gymnasium, Vestre Engvej 61, Vejle. Ny Nordfløj.

GEHLIN, S., 2002. Thermal Response Test. Method Development and Evaluation. Doctor of Philosophy, Luleå University of Technology.

GSHP ASSOCIATION, 2012. Thermal Pile: Design, Installation & Materials Standards. National Energy Centre, Davy Avenue, Knowlhill, Milton Keynes: Ground Source Heat Pump Association.

HAMID, A., 2004. F200 Calibration Certificate. In: LABORATORIES, A. S.

HELLSTRÖM, G., 1998. Thermal Performance of Borehole Heat Exchangers. Swedish Council for Building Research (BFR).

HOT DISK AB, 2014. Hot Disk Thermal Constants Analyser TPS 1500 unit, Intruction Manual.

ISOTHERMAL TECHNOLOGY 2000. Venus 2140: Evaluation Report

LOVERIDGE, F., 2012. The thermal performance of foundation piles used as heat exchangers in ground energy systems. PhD Thesis, University of Southampton.

MOGENSEN, P., 1983. Fluid to Duct Wall Heat Transfer in Duct System Heat Storage. Proc. Int. Conf. On Subsurface Heat Storage in Theory and Practice. 1983 Stockholm. Sweden, June 6–8, 1983. Swedish Council for Building Research, PP: 652-657.

NATIONAL INSTRUMENTS, 2015a. LabVIEW User Manual.

NATIONAL INSTRUMENTS, 2015b. NI 9216 Datasheet.

UBEG UMWELT BAUGRUND GEOTHERMIE GEOTECHNIK, 2013. Thermal Response Test Equipment Data. Germany.

WHEELER, A. J. & GANJI, A. R., 2004. Introduction to Engineering Experimentation, Upper Saddle River, New Jersey 07458, USA, Pearson Education, Inc.

8. Appendices

A) Test site documentation

This section provides a detailed description of the geology at the field sites. Subsequently, pictures are provided (Figures 13 to 21).

i. Langmarksvej

Depth (m)	Geology	Sample	Number	Description
0.0 m		–	1	TOPSOIL/CLAY, slightly sandy, grayish brown (10YR 5/2), calcareous, Fl/Re
		–	2	FILL/SAND, clayey, slightly gravelly, dark brown yellowish (10YR 4/4), calcareous, Fl/Re
- 1.0 m		–	3	FILL/SAND, clayey, stones, dark brown yellowish (10YR 4/4), calcareous, Fl/Re
		–	4	FILL/SAND, fine, clayey, slightly gravelly, acid smell, dark olive gray (5Y 3/2), non-calcareous, Fl/Re
- 2.0 m		–	5	FILL/CLAY, sandy, acid smell, dark olive gray (5Y 3/2), non-calcareous, Fl/Re
		–	6	FILL/SAND, fine, clayey, acid smell, olive gray (5Y 5/2), non-calcareous, Fl/Re
- 3.0 m		–	7	FILL/CLAY, sandy, stones, acid smell, dark olive gray (5Y 3/2), non-calcareous, Fl/Re
		–	8	FILL/SAND, fine to medium, clay lumps, stones, brick remains, acid smell, dark olive gray (5Y 3/2), slightly calcareous, Fl/Re
- 4.0 m		–	9	FILL/CLAY, slightly sandy, slightly gravelly, "cable", gray (5Y 5/1), non-calcareous, Fl/Re
		–	10	FILL/CLAY, slightly sandy, slightly gravelly, "cable", dark gray (5Y 4/1), non-calcareous, Fl/Re
- 5.0 m		–	11	SAND, fine to medium, clay slumps, dark gray (5Y 4/1), non-calcareous, Fl/Re
		–	12	CLAY, sandy, yellowish brown (10YR 5/6), calcareous, GL/Gc
		–	13	CLAY TILL, lean, silty, sandy, gravelly, iron strips, yellowish brown (10YR 5/4), calcareous, GL/Gc
- 6.0 m		–	14	CLAY TILL, lean, silty, sandy, dark gray (5Y 4/1), calcareous, GL/Gc
		–	15	CLAY TILL, lean fat, silty, sandy, dark gray (5Y 4/1), calcareous, GL/Gc
- 7.0 m		–	16	CLAY TILL, lean, silty, sandy, gravelly, dark olive gray (5Y 3/2), calcareous, GL/Gc
		–	17	CLAY TILL, lean, silty, sandy, gravelly, dark olive gray (5Y 3/2), calcareous, GL/Gc
- 8.0 m		–	18	CLAY TILL, lean///looser not as compact as the others, very sandy, slightly gravelly, dark olive gray (5Y 3/2), calcareous, GL/Gc
		–	19	CLAY TILL, lean, sandy, slightly gravelly, very dark gray (10YR 3/1), calcareous, GL/Gc
- 9.0 m		–	20	CLAY TILL, lean, sandy, slightly gravelly, very dark gray (10YR 3/1), calcareous, GL/Gc
		–	21	CLAY TILL, lean, sandy, slightly gravelly, very dark gray (10YR 3/1), calcareous, GL/Gc
- 10.0 m		–	22	CLAY TILL, lean, sandy, slightly gravelly, very dark gray (10YR 3/1), calcareous, GL/Gc
		–	23	CLAY TILL, lean, sandy, slightly gravelly, very dark gray (10YR 3/1), calcareous, GL/Gc
- 11.0 m		–	24	CLAY TILL, lean, sandy, slightly gravelly, very dark gray (10YR 3/1), calcareous, GL/Gc
		–	25	CLAY TILL, lean, sandy, slightly gravelly, very dark gray (10YR 3/1), calcareous, GL/Gc
- 12.0 m		–	26	CLAY TILL, lean, sandy, slightly gravelly, very dark gray (10YR 3/1), calcareous, GL/Gc
		–	27	CLAY TILL, lean, sandy, slightly gravelly, very dark gray (10YR 3/1), calcareous, GL/Gc
- 13.0 m		–	28	CLAY TILL, slightly fatter than the previous, sandy, slightly gravelly, very dark gray (10YR 3/1), calcareous, GL/Gc
		–	29	CLAY TILL, lean, sandy, slightly gravelly, very dark gray (10YR 3/1), calcareous, GL/Gc
- 14.0 m		–	30	CLAY TILL, lean, sandy, slightly gravelly, very dark gray (10YR 3/1), calcareous, GL/Gc
		–	31	CLAY TILL, lean, sandy, slightly gravelly, very dark gray (10YR 3/1), calcareous, GL/Gc
- 15.0 m		–	32	CLAY TILL, lean, sandy, slightly gravelly, very dark gray (10YR 3/1), calcareous, GL/Gc
		–	33	CLAY TILL, slightly fat, sandy, slightly gravelly, shiny surfaces, very dark gray (10YR 3/1), calcareous, GL/Gc
- 16.0 m		–	34	CLAY TILL, lean, sandy, slightly gravelly, very dark gray (10YR 3/1), calcareous, GL/Gc
		–	35	CLAY TILL, lean, sandy, slightly gravelly, very dark gray (10YR 3/1), calcareous, GL/Gc
- 17.0 m		–	36	CLAY TILL, lean, sandy, slightly gravelly, very dark gray (10YR 3/1), calcareous, GL/Gc
		–	37	CLAY TILL, lean, sandy, slightly gravelly, very dark gray (10YR 3/1), calcareous, GL/Gc
- 18.0 m		–	38	CLAY TILL, lean, sandy, slightly gravelly, very dark gray (10YR 3/1), calcareous, GL/Gc

Figure 13: Soil description of the samples collected each 0.5 m in the drilling executed to host the temperature sensor array TSA.

Figure 14: Ongoing TRT at the 18 m deep BHE at Langmarksvej. Inlet- and outlet pipes are insulated to prevent disturbances from ambient temperature conditions.

Figure 15: A single EP at the Langmarksvej test site prior to connecting the TRT equipment.

Figure 16: Monitoring drilling work. The drilling is located 0.85 m from EP3 (see Figure 4).

Figure 17: View of the EP3, the TSA and the BHE at the Langmarksvej test site.

Figure 18: Ongoing TRT of the 18 m long EP3 at Langmarksvej. Inlet- and outlet pipes are insulated to prevent disturbances from ambient temperature conditions. The adjacent box, covered with black plastic bags, contains the computer and the modules to log the temperature data from the underground Pt100 TSA.

ii. Rosborg Gymnasium

Depth (m)	Geology	Sample	Number	Description
0.0 m			1	TOPSOIL, slightly sandy, 10YR 2/1, non-calcareous, O/Pg.
- 1.0 m			2	SAND, fine sized, very silty with stones and plant remainders, 2.5Y 2.5/1, non-calcareous, Ma/Pg.
- 2.0 m			3	ORGANIC CLAY/GYTTJA, slightly silty and sandy, plant remainders, high plasticity, shining surfaces, 2.5Y, 2.5/1, non-calcareous, Fe/Pg.
			4	ORGANIC CLAY/GYTTJA, shells and small calcareous grains, plant remainders, high plasticity and sticky, shining surfaces, 2.5Y, 2.5/1, calcareous, Fe/Pg.
- 3.0 m			5	ORGANIC CLAY/GYTTJA, high shell amount and small calcareous grains, plant remainders, high plasticity and sticky, shining surfaces, 2.5Y, 2.5/1, very calcareous, Fe/Pg.
			6	ORGANIC CLAY/GYTTJA, few shells, plant remainders, slangs of iron and few brown strips, high plasticity and sticky, shining surfaces, 2.5Y, 2.5/1, slightly calcareous, Fe/Pg.
- 4.0 m			7	ORGANIC CLAY/GYTTJA or PEAT, few shells, plant remainders, slangs of iron and few brown strips, high plasticity and sticky, shining surfaces, 2.5Y, 2.5/1, slightly calcareous, Fe/I
			8	SAND, medium sized, poorly sorted with numerous gravel grains and stones. 2.5Y 3/2, non-calcareous, Ma/Pg.
- 5.0 m				
			9	SAND, medium to coarse sized, poorly sorted, 2.5Y 3/2, non-calcareous, Ma/Pg.
- 6.0 m			10	SAND, medium to coarse sized, poorly sorted with gravel grains, 2.5Y 4/1, non-calcareous, Ma/Pg.
			11	SAND, medium to coarse sized, poorly sorted with gravel grains, 2.5Y 3/1, non-calcareous, Ma/Pg.
- 7.0 m			12	SAND, medium to coarse sized, poorly sorted with stones, 2.5Y 4/1, slightly calcareous, Fe/Sg.
			13	SAND, medium to coarse sized, poorly sorted with stones, 2.5Y 4/1, non-calcareous, Fe/Sg.
- 8.0 m			14	SAND, medium sized, poorly sorted with stones, 2.5Y 4/1, slightly calcareous, Fe/Sg.
			15	SAND, fine to medium sized, well sorted, 2.5Y 3/1, slightly calcareous, Fe/Sg.
- 9.0 m			16	SAND, medium sized, well sorted with few gravel grains, 2.5Y 3/1, calcareous, Fe/Sg.
			17	SAND, medium sized, well sorted, 2.5Y 4/1, calcareous, Fe/Sg.
10.0 m			18	SAND, medium sized, well sorted, 2.5Y 4/1, slightly calcareous, Fe/Sg.
			19	SAND, medium sized, well sorted, 2.5Y 4/1, slightly calcareous, Fe/Sg.
11.0 m			20	SAND, fine to medium sized, poorly sorted, 2.5Y 4/1, slightly calcareous, Fe/Sg.
			21	SAND, fine to medium sized, with gravel grains, 2.5Y 4/1, calcareous, Fe/Sg.
12.0 m			22	SAND, medium to coarse sized, with gravel grains, 2.5Y 3/1, calcareous, Fe/Sg.
			23	SAND, coarse sized, poorly sorted with gravel grains, 2.5Y 3/2, calcareous, Fe/Sg.
13.0 m			24	SAND, fine to medium sized, well sorted few with gravel grains, 2.5Y 3/2, calcareous, Fe/Sg.
			25	SAND, fine sized, well sorted, 2.5Y 3/2, calcareous, Fe/Sg.
14.0 m			26	SAND, fine sized, with clayey lumps, 2.5Y 4/1, calcareous, Fe/Sg.
			27	SAND, fine to medium sized, well sorted, 2.5Y 4/1, calcareous, Fe/Sg.
15.0 m			28	SAND, medium to fine sized, well sorted, 2.5Y 4/1, calcareous, Fe/Sg.
			29	SAND, medium sized, poorly sorted with gravel grains, 2.5Y 4/1, calcareous, Fe/Sg.
16.0 m			30	SAND, fine to medium sized, well sorted, 2.5Y 4/1, calcareous, Fe/Sg.

Figure 19: Soil description of the samples collected each 0.5 m in the monitoring drilling executed at Rosborg Gymnasium.

Location of the Pt100 temperature sensors within the pile reinforcement, before the concrete was casted.

Figure 20: Pile instrumentation with Pt100 temperature sensors.

Figure 21: A) Ongoing TRT of the 16 m long EP at Rosborg North. Inlet- and outlet pipes are insulated to prevent disturbances from ambient conditions. B) The adjacent box, covered with black plastic bags contains the computer and the modules to log the temperature data from the Pt100 temperature sensors casted into the pile (see Figures 11 and 20).

B) Energy pile drawings
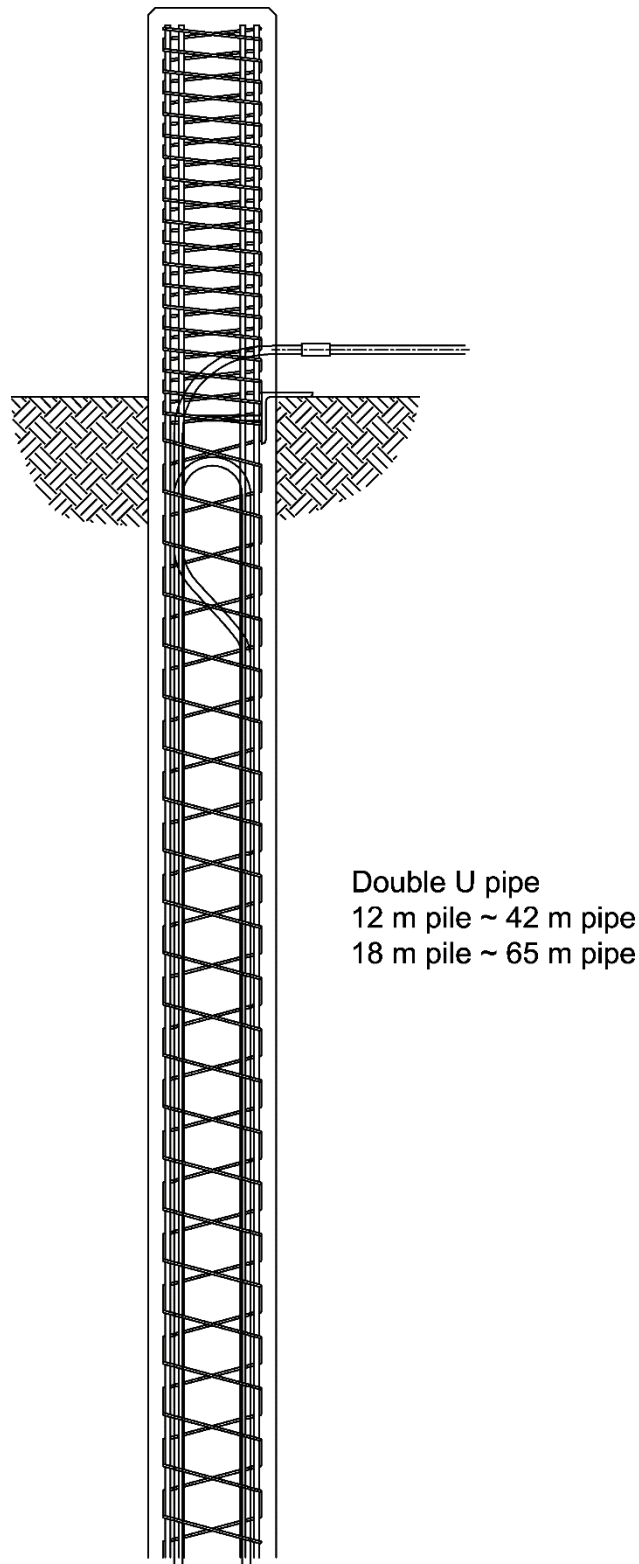
Double U pipe
12 m pile ~ 42 m pipe
18 m pile ~ 65 m pipe

Figure 22: Vertical cross section of a W-shape driven energy pile.
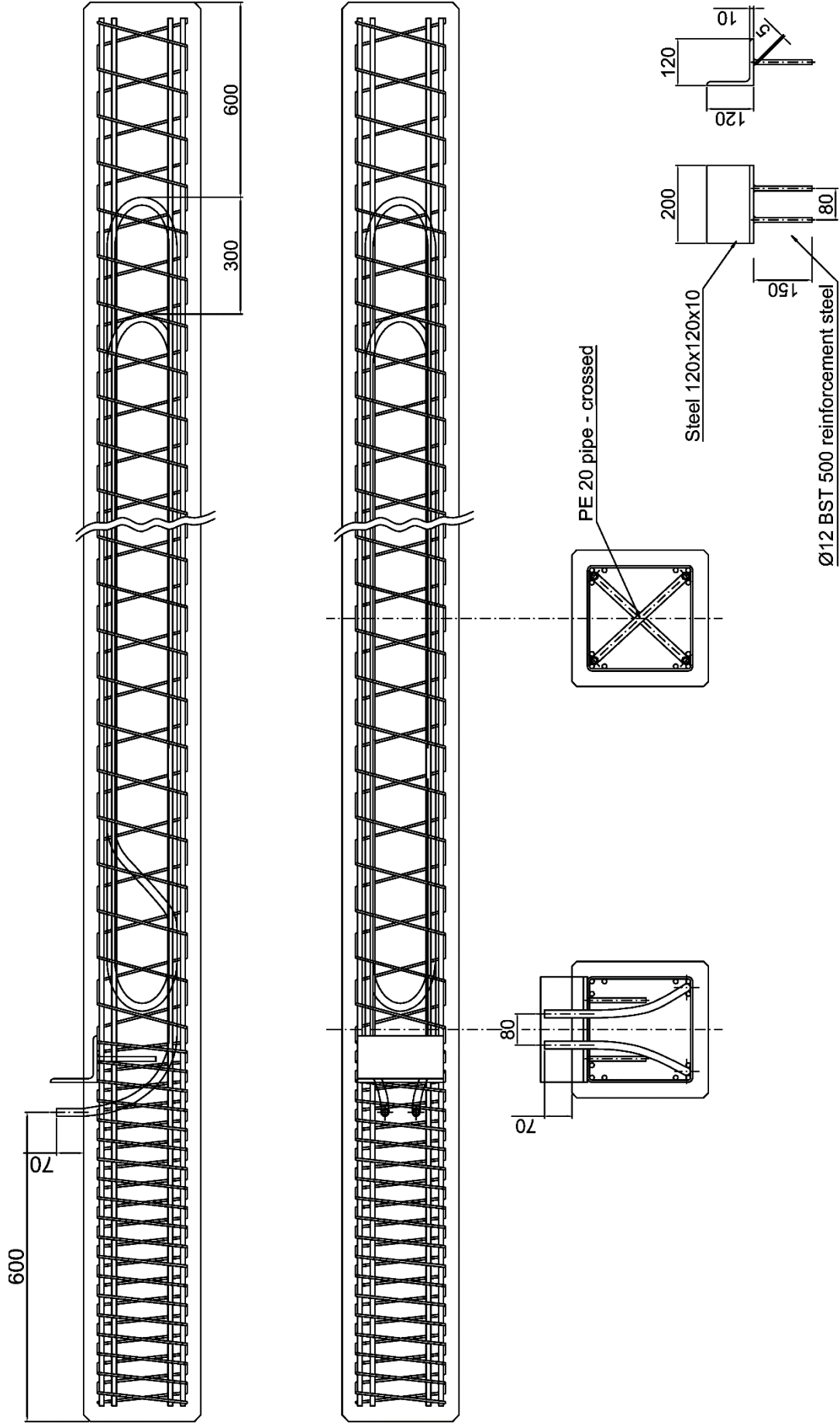
Figure 23: Geometry and dimensions in mm of a W-shape energy pile.

PE 20 pipe – crossed

Steel 120x120x10

Ø12 BST 500 reinforcement steel

C) Temperature measurements

Resistance-temperature detectors (PT100) have been used to measure the ground temperatures during the TRT of EP3 at Langmarksvej and the pile temperatures during the TRT of RN_EP_1 at Rosborg North. Resistance-temperature detectors are temperature sensors based on the change in the electrical resistance resulted from a temperature change in a metal, in this case, Platinum (Pt) (Wheeler and Ganji, 2004). For the tests, a 2-wire Pt100 type was chosen.

The Pt100 temperature sensors have been calibrated for the range of expected experimental temperatures (from 0 to 50°C) at Aalborg University the 8/01/2016. The process consists of quantifying the deviation of the resistance readings (and thereby, temperature measurements) of the Pt100 from the temperature measurements taken with the reference thermometer (considered as the true value). This way, the resistance readings can be corrected and the right temperature displayed during the experiments. Five cable lengths where used connected to the sensors: 3, 7, 11, 15 and 19 m. The setup schematic is provided in Figure 24 and the process breakdown is hereby described:
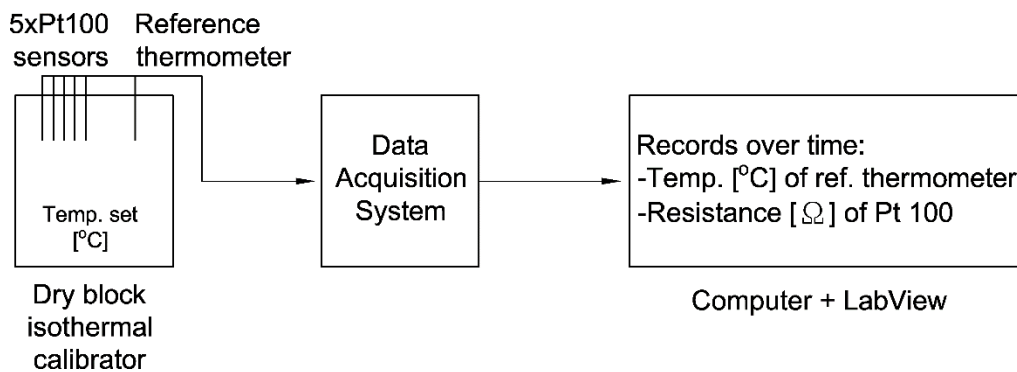
Figure 24: Schematic of the calibration setup.

1. The sensors (with the five cable lengths) and the reference thermometer are inserted into a dry block isothermal calibrator where the temperature can be selected.
2. A first temperature step at 50°C is set in the calibrator.
3. The sensors and the thermometer are connected to a data acquisition unit DAQ which addresses the readings to a nearby computer.
4. The computer has LabView software (National Instruments, 2015a) installed. Here the resistance measurements from the Pt100 and the temperature readings from the reference thermometer are logged every second.
5. Each temperature step lasts 30 minutes approximately. First, the sensors need 15 minutes to stabilise in the new temperature. Once they show constant readings, a 10-15 minutes period is recorded.
6. An average of the resistance readings corresponding to the 10-15 minutes period is plotted against the corresponding temperature reading from the reference thermometer (Point 1 in Figure 25).
7. The process is repeated for further temperature steps: 40, 30, 20, 10 and 0 °C. Therefore, the total number of points in Figure 25 is 6.
8. At this moment, a line is fitted to the 6 points (by linear regression).
9. The coefficients of the trend line (slope and y-intercept) will be used in LabView to correct the readings of the Pt100 sensors during the experiments.
10. The process was repeated for each cable length. In this case, there are five calibration curves, one per length. Figure 25 provides the calibration curve for a 3 m long cable.
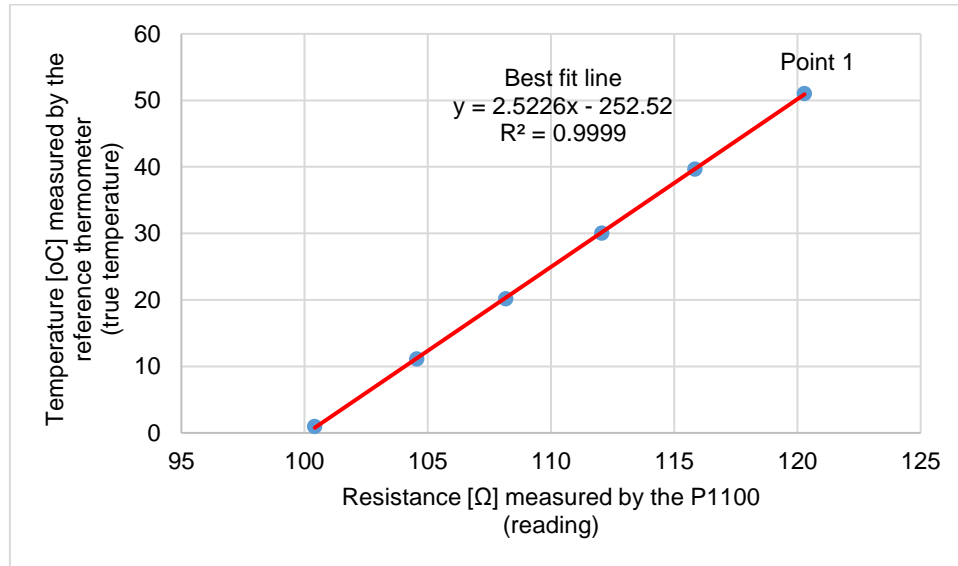
Figure 25: Calibration curve for the 3 m length cable. True temperature VS resistance reading.

Finally, an estimation of accuracy was executed. The "typical" uncertainty for a Pt 100 module is ± 0.20 °C (National Instruments, 2015b) and, therefore, the uncertainty resulted from the following analysis should be comparable. The accuracy of the temperature measurement is affected by many different factors. The sources of uncertainty are:

- Long term deviation of the reading. No information can be found about it and that, hence, a long term deviation equal to the long term deviation of the ASL F200 precision thermometer with Pt 100 sensor (the reference thermometer) is considered: ± 0.005 °C/year.

- Uncertainty from the reference thermometer (Hamid, 2004).
  The calibrated Pt 100 precision thermometer has an uncertainty of ± 0.006 °C**.**

- Uncertainty of the data acquisition system, NI 9216 module, to account for errors in the resistance readings.
  The module data sheet (National Instruments, 2015b) provides the following: an offset error of ± 0.012 Ω and a gain error of ± 0.007%.
  The change of resistance over 50 °C of span is 19.73 Ω (119.73 Ω at 50 °C – 100 Ω at 0 °C)(Wheeler and Ganji, 2004).
  The conversion from resistance uncertainty to temperature uncertainty is:
  50 °C / 19.73 Ω = 2.534 °C/Ω.
  Thus:
  Offset error: 0.012 · 2.534 °C = ± 0.030408 °C
  Gain error: 0.007% · 119.73 Ω · 2.534 °C/Ω = ± 0.02124 °C

- Uncertainty of the ambient temperature disturbance (stability) on the data acquisition module.
  A deviation of 10 °C in the ambient temperature is assumed (day-night variation during the TRT).
  The module data sheet (National Instruments, 2015b) provides the following: an offset drift of ± 0.0033 Ω and a gain drift of ± 0.000007/°C.
  Offset drift: 0.0033 Ω/°C · 10 °C · 2.534 °C/Ω = ± 0.083622 °C
  Gain drift: 0.000007/°C · 119.73 Ω · 2.534 °C/Ω = ± 0.0021238 °C

- Uncertainty of the isothermal calibrator Isocal Venus 2140 B (Isothermal Technology, 2000).
  According to the manufacturer, the maximum uncertainty on the temperature homogeneity of the isothermal metal block is ± 0.004 °C.

- Uncertainty derived from the cable length, i.e., the effect of the cable length in the measured temperature.
  An uncertainty in the measurement of the length of the cable of 0.02 m is assumed.
  The measurements from the calibration process allow to obtain the relation between the length of the cables and the resistance. An average value between the coefficients (slopes derived from the resistance VS length relation for each temperature step) has been taken: 0.0962 Ω/m.
  The uncertainty in the temperature reading resulted from the cable length:
  0.02 m · 0.0962 Ω/m · 2.534 °C/Ω = ± 0.0049 °C

- Uncertainty of the sensor itself. The following information has been taken from Dansk Standard (2008):
  Temperature coefficient resistance α: 0.00385 Ω/Ω/°C, which is defined as:

$$\alpha = \frac{R_{100} - R_0}{100 \cdot R_0}$$

Being R_0 the resistance of the sensor at 0°C and R_{100} the resistance of the sensor at 100 °C. This relation can be used to calculate the uncertainty of the resistance temperature detector:

$$\Delta R = R_0 \cdot \alpha \cdot \Delta T$$

To calculate the uncertainty within a range of 50 °C, from 0°C to 50 °C:

$$\Delta R_{50} = R_0 \cdot \alpha \cdot \Delta T$$

The resistance of the sensor at 0 °C is given by the standard for different type of sensors and a Class B sensor has been assumed, being: 100.00 Ω ± 0.12 Ω at 0 °C. Therefore, the uncertainty at 0 °C is ± 0.12 Ω.
The uncertainty in the resistance for a detector ranging temperatures from 0 °C to 50 °C is:
ΔR = 0.12 Ω · 0.00385 Ω/Ω/°C · 50°C = ± 0.0231Ω
Translating it to temperature units, the uncertainty of the Pt100 sensor is:
0.0231 Ω · 2.534 °C/Ω = ± 0.0585354 °C

Subsequently, the global uncertainty (U) of the calibrated Pt 100, estimated by quadrature addition and under a perfect calibration assumption, would be:

$$U = \sqrt{0.005^2 + 0.006^2 + 0.03041^2 + 0.02124^2 + 0.0836^2 + 0.0021^2 + 0.004^2 + 0.0049^2 + 0.0585^2}$$
$$= \pm 0.11°C$$

This uncertainty is slightly lower than the typical expected error.

D) Thermal response test data

This appendix provides the figures (from Figure 26 to Figure 36) of the data sets collected during the 8 TRTs performed at the Langmarksvej and Rosborg Gymnasium test sites.

i. Undisturbed ground temperature profiles

Prior to the execution of a TRT, the undisturbed temperature of the ground must be measured. Figures 26 and 27 show the undisturbed temperature profiles at Langmarksvej and at Rosborg, respectively.
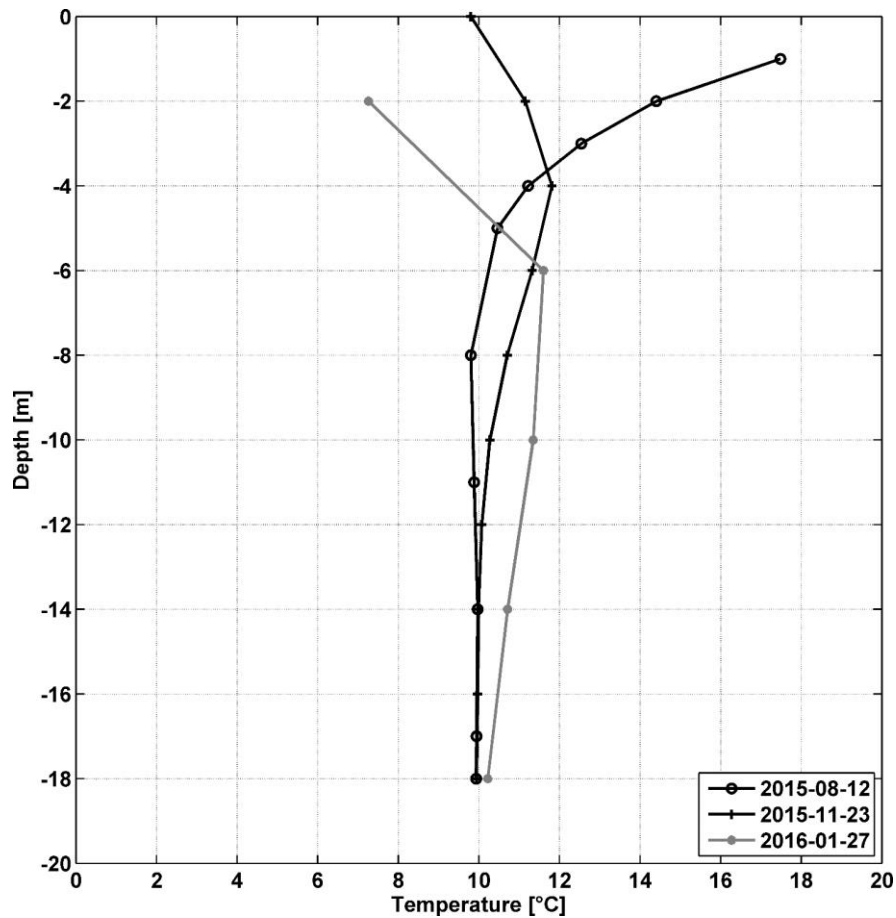
Figure 26: Undisturbed soil temperatures measured during the testing periods at the Langmarskvej test site.

Figure 27 shows the temperature profiles for the thermally active length of the heat exchanger. The average undisturbed soil temperature is 9.8 °C on the 9th of February 2016. It was not possible to measure a temperature profile prior to the TRT executed in January 2014 and April 2015 at the south extension.
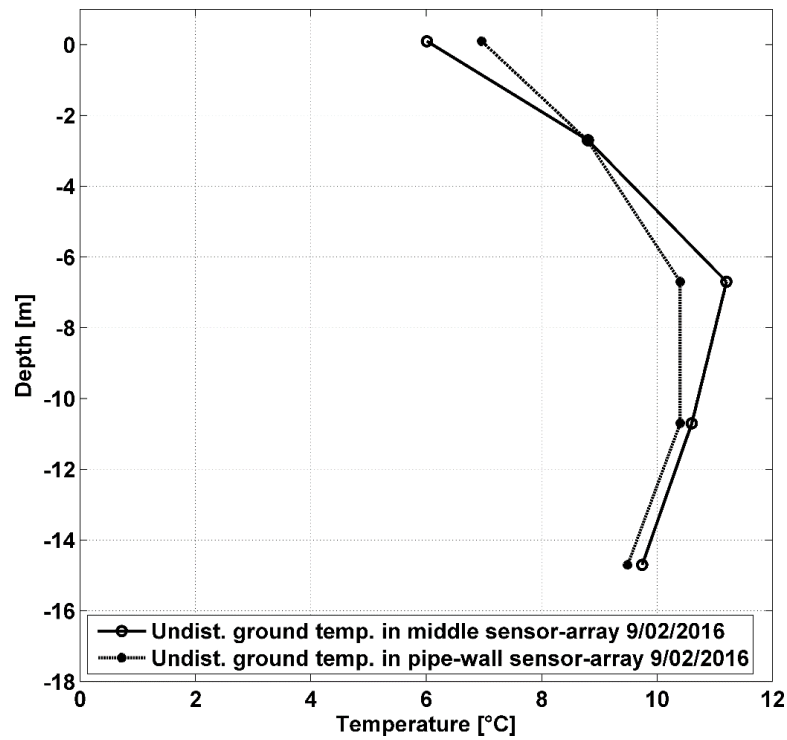
Figure 27: Undisturbed soil temperatures measured prior to the TRT of the energy pile at Rosborg North (EP_RN_1) the 9/02/2016.

ii.   Langmarksvej BHE [W + 18 m]
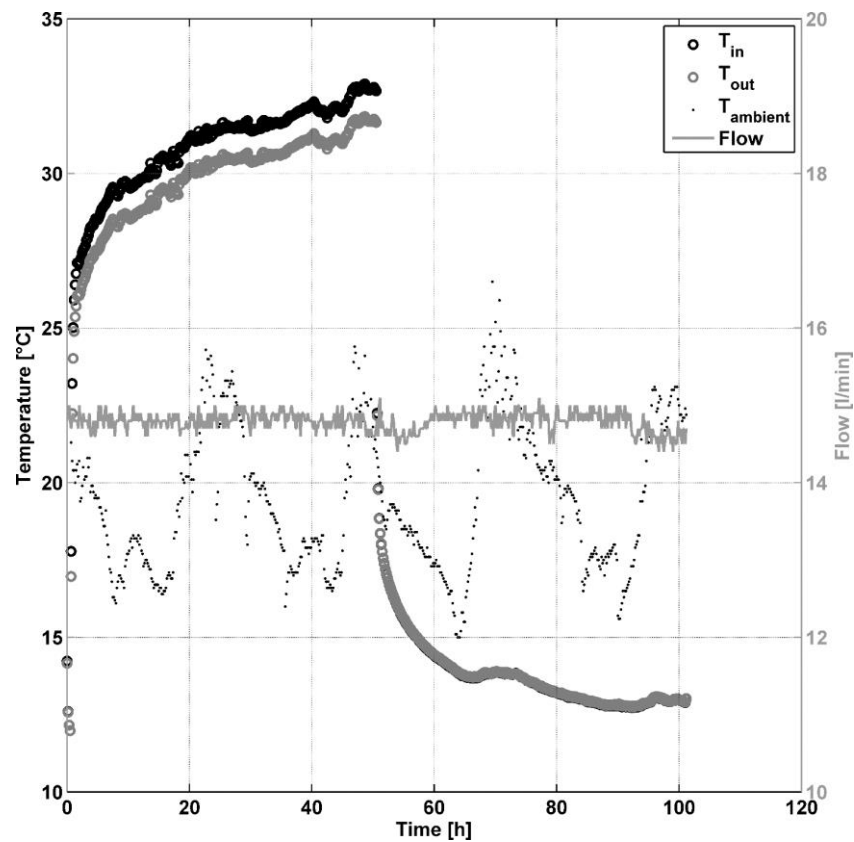
Figure 28: Measured temperature and fluid flow profiles during the TRT of the BHE at Langmarksvej test site. T_{in} and T_{out} are the inlet- and outlet fluid temperature, respectively. Notice that recovery data (water circulation without heating) was also collected for 50 hours following the test.

iii.   Langmarksvej EP8 [1U + 12 m]
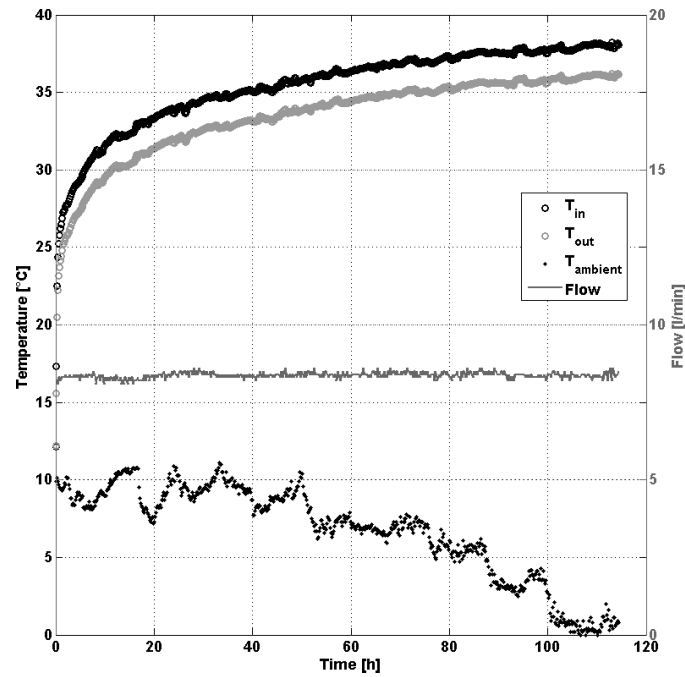
Figure 29: Measured temperature and fluid flow profiles during the TRT of EP8 at the Langmarksvej test site. T_{in} and T_{out} are the inlet- and outlet fluid temperature, respectively.

iv.   Langmarksvej EP7 [1U + 18 m]
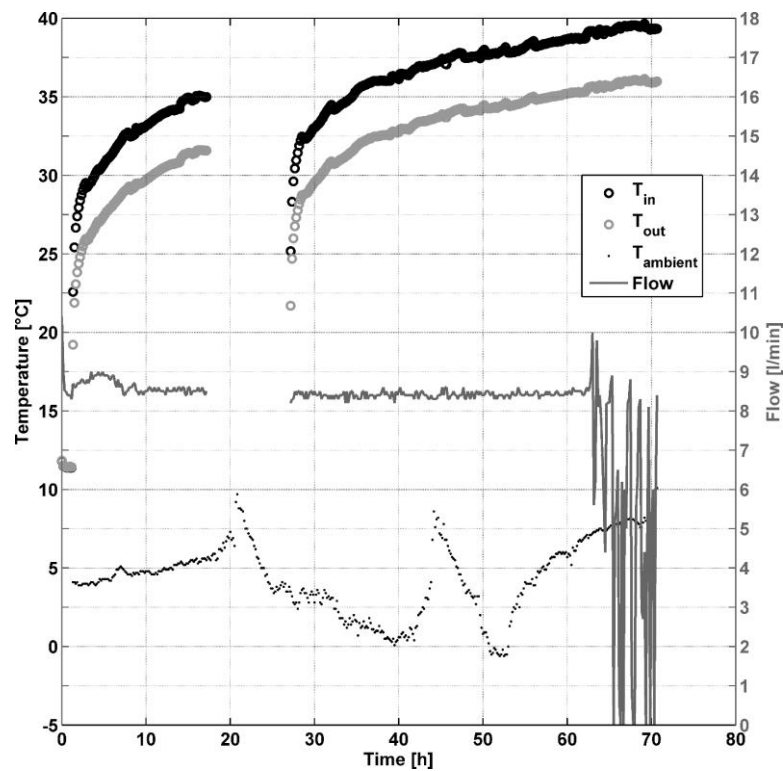
Figure 30: Measured temperature and fluid flow profiles during the TRT of EP7 at the Langmarksvej test site. T_{in} and T_{out} are the inlet- and outlet fluid temperature, respectively. Notice that the power was interrupted for 10 hours during the test.

v. Langmarksvej EP4 [W + 12 m]
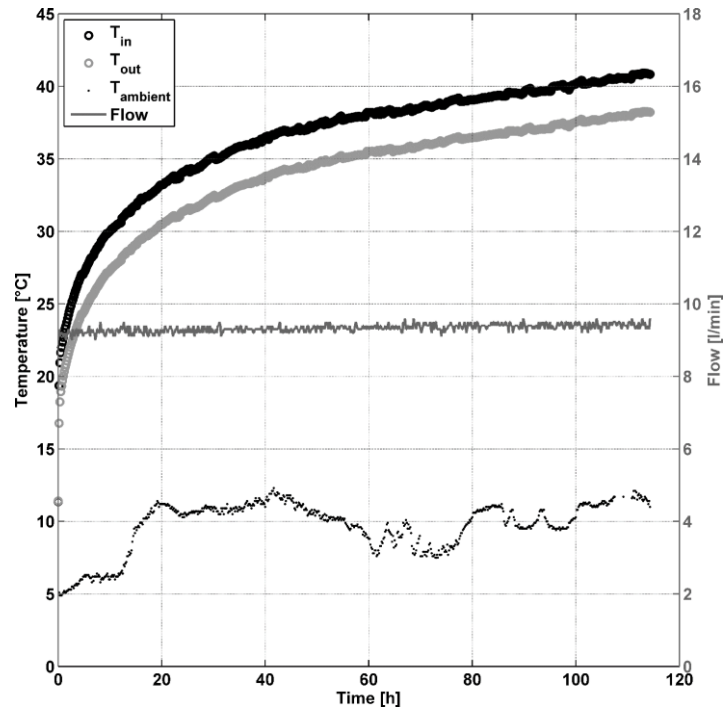
Figure 31: Measured temperature and fluid flow profiles during the TRT of EP4 at the Langmarksvej test site. T_{in} and T_{out} are the inlet- and outlet fluid temperature, respectively.

vi. Langmarksvej EP3 [W + 18 m]

The soil temperatures shown in Figure 33 imply that heating is observed at a distance of 0.85 m from the energy pile after approximately 25 hours of testing.
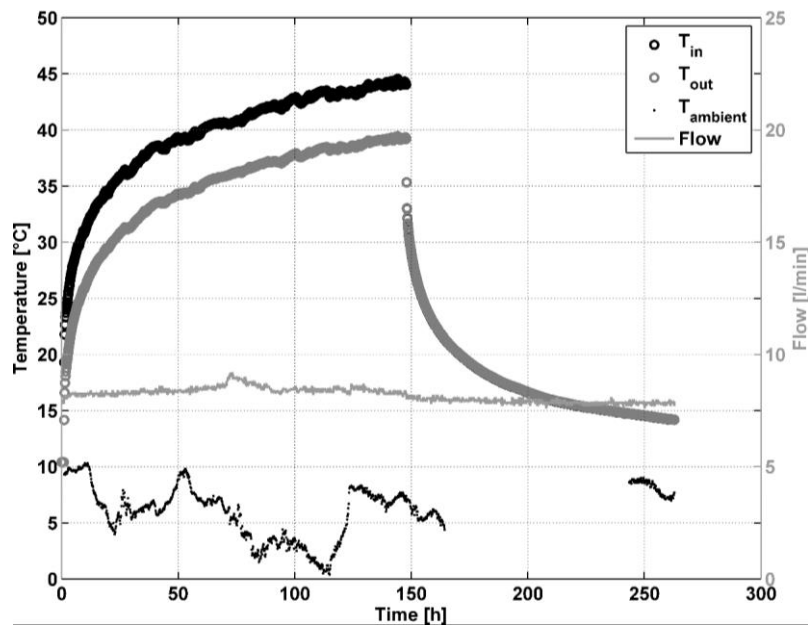
Figure 32: Measured temperature and fluid flow profiles during the TRT of EP3 at the Langmarksvej test site. T_{in} and T_{out} are the inlet- and outlet fluid temperature, respectively. Notice that recovery data (water circulation without heating) was also collected over 115 hours.
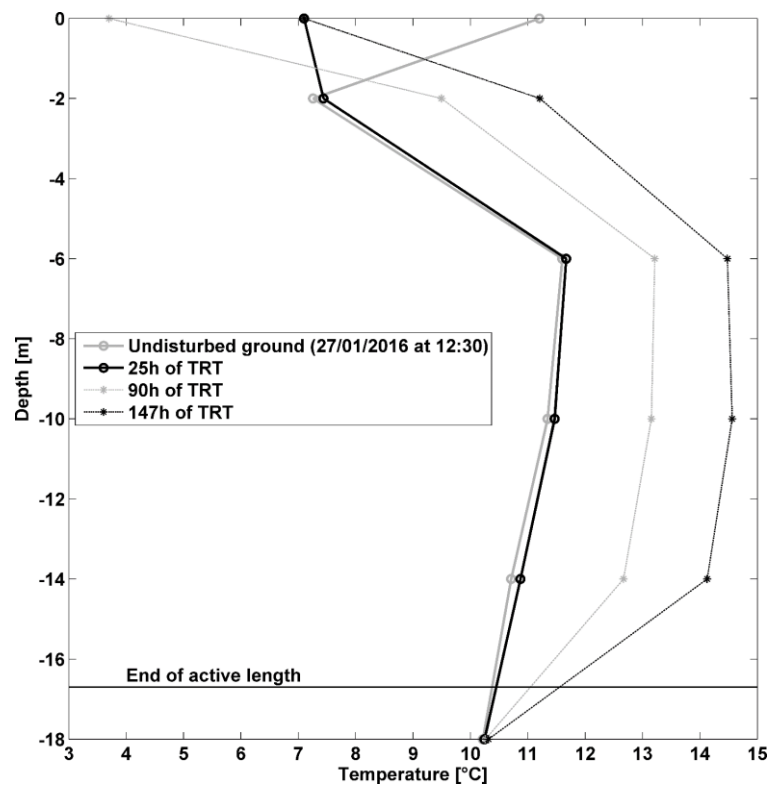
Figure 33: Measured ground temperature profiles from the TSA (0.85 m from EP3, Figure 4) at different levels (0, -2, -6, -10, -14, -18 m below terrain) and at different times (0, 25, 90, 147 hours) during the TRT of EP3 at the Langmarksvej test site.

vii.   Rosborg Gymnasium South: EP_RS

This test is analysed in Alberdi-Pagola and Poulsen (2015).
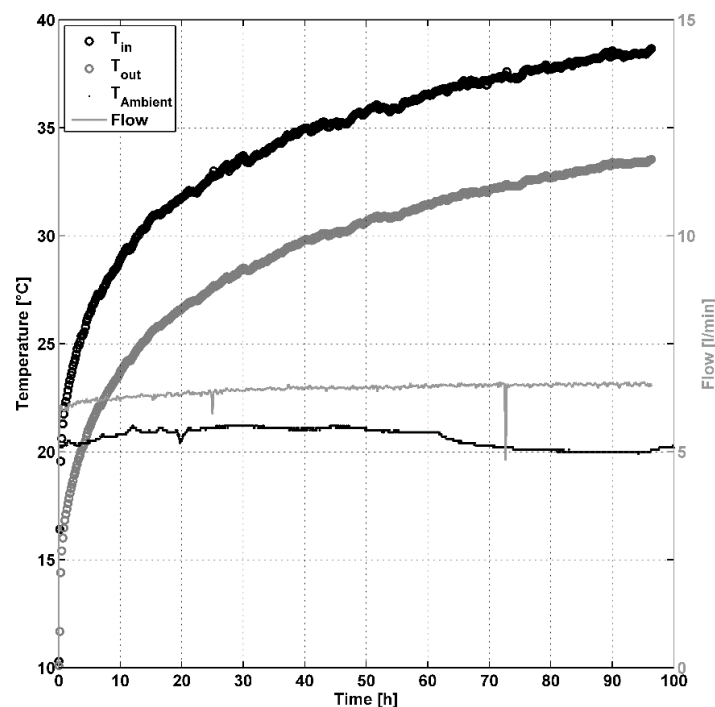
Figure 34: Measured temperature and fluid flow profiles during the TRT of EP_RS at the north extension of Rosborg Gymnasium. T_{in} and T_{out} are the inlet- and outlet fluid temperature, respectively.

viii. Rosborg Gymnasium North: EP_RN
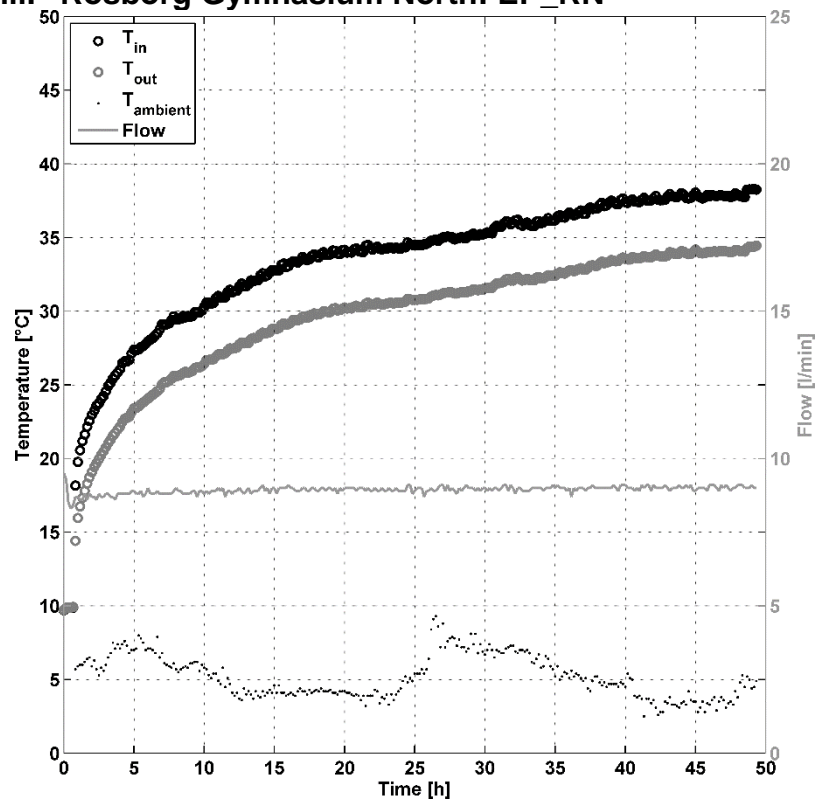
Figure 35: Measured temperature and fluid flow profiles during the TRT of EP_RN at the north extension of Rosborg Gymnasium. T_{in} and T_{out} are the inlet- and outlet fluid temperature, respectively.
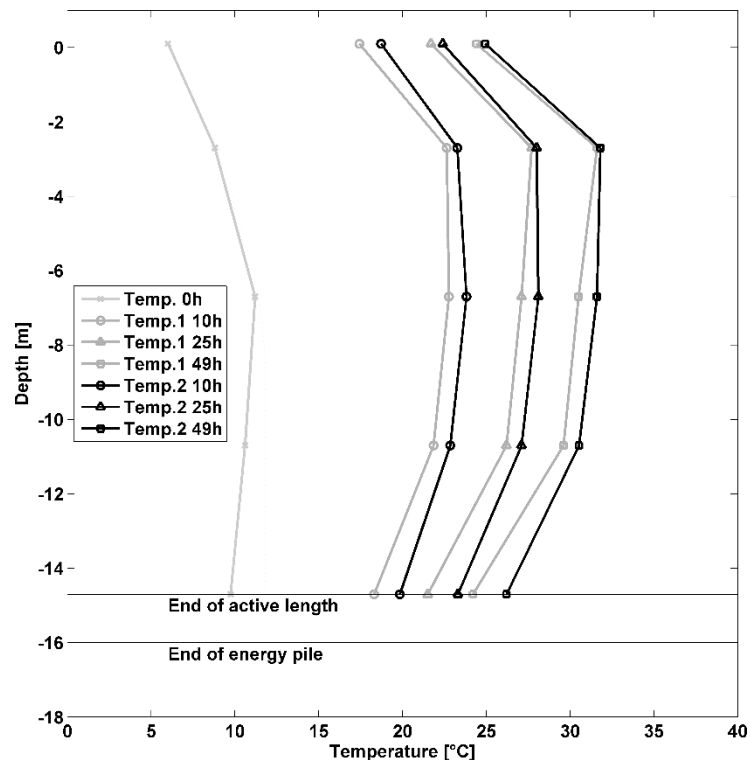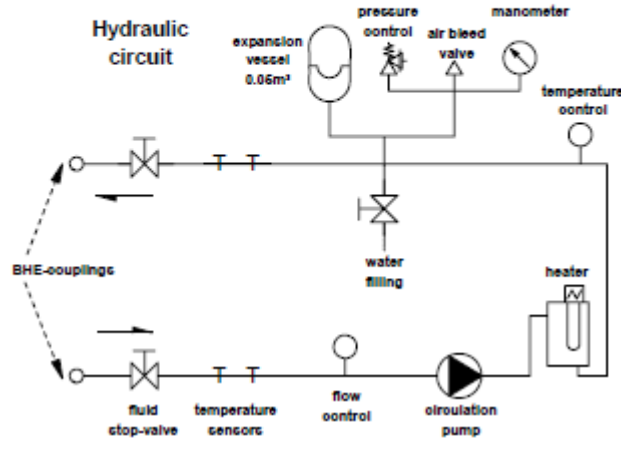
Figure 36: Pile temperatures measured with the Pt100 temperature sensors casted in the concrete at different levels (+0.1, -2.7, -6.7, -10.7, 14.7 m relative to the ground surface) and at different times (0, 10, 25, 49 hours) during the TRT of the energy pile EP_RN [W + 16 m] at the north extension of Rosborg Gymnasium. Temp.1 = middle sensor-string and Temp.2 = pipe-wall sensor-string (Figure 11).

E) TRT equipment data sheet

The TRT equipment is produced by UBeG Umwelt Baugrund Geothermie Geotechnik (2013).

Thermal Response Test Equipment Data

Country: Germany	
Contact Person: Marc Sauer	
Organisation/Company: UBeG Dr. E. Mands & Dipl.-Geol. M. Sauer GbR	
Address: Reinbergstraße 2 35580 Wetzlar	
Phone: +49 (0) 6441-212910	
Email: ubeg@ubeg.de	

General TRT data

Type: *Heat injection*	No TRTs: *6; 10 exported*	Size, weight: *1100x800x550, ca. 70 kg (only box)*
Aim: *commercial*		Pump: *~2m³/h*
Powered by: *Electricity*		Heater: *electrical, 9 kW step less*
Built on/in: *Caterpillar*		HP/Cooler: *without*

Hydraulic circuit

Temperature measurements: *inside box, at heat exchanger head, double PT 500 & PT 1000, direct installation and immersion sleeves ± 0,05°C*
Flow rate measurements: *direct installation as IDM or mechanical*
Voltage stabilization: *optional*
Electricity measurement: *Yes, ±0,1 kWh*
GPS: *No*
Remote Control: *optional*
Remote Data Collection: *optional*
Logger: *automatic*

TRT Experience

Years of operation: *10*

Number of performed measurements: *– 400 commercial*

Typical borehole depths: *tested up to 300m*

Applications: *BHE*

Typical collector type: *2U, sometimes U1 and coaxial pipe, any types of filling*

Typical fluid type: *water*

Typical groundwater temperature: *Ø 12,5°C, min. 8,8 – max. 19,8°C*

Geographical area: *Europe*

Analysis Method: *Numerical / Line source + parameter estimation (own software) / continuous temperature depth profiling (optional)*

Appendix IV.   Description of laboratory work (Technical report II)

Alberdi-Pagola, M., Jensen, L.J., Madsen, S. & Poulsen, S.E., 2017. "Measurement of thermal properties of soil and concrete samples". Aalborg: Department of Civil Engineering, Aalborg University. DCE Technical Reports, nr. 235, pp. 30. Available online:

http://vbn.aau.dk/files/266378485/Measurement_of_thermal_properties_of_soil_and_concrete_samples.pdf

AALBORG UNIVERSITY

DENMARK

Measurement of thermal properties of soil and concrete samples

Pagola, Maria Alberdi; Jensen, Rasmus Lund; Madsen, Søren; Poulsen, Søren Erbs

Measurement of thermal properties of soil and concrete samples

Maria Alberdi-Pagola
Rasmus Lund Jensen
Søren Madsen
Søren Erbs Poulsen (VIA University College, Horsens, DK)

Aalborg University
Department of Civil Engineering

DCE Technical Report No. 235

Thermal property measurements of soil and concrete samples

by

Maria Alberdi-Pagola
Rasmus Lund Jensen
Søren Madsen
Søren Erbs Poulsen (VIA University College)

December 2017

Scientific Publications at the Department of Civil Engineering

Technical Reports are published for timely dissemination of research results and scientific work carried out at the Department of Civil Engineering (DCE) at Aalborg University. This medium allows publication of more detailed explanations and results than typically allowed in scientific journals.

Technical Memoranda are produced to enable the preliminary dissemination of scientific work by the personnel of the DCE where such release is deemed to be appropriate. Documents of this kind may be incomplete or temporary versions of papers—or part of continuing work. This should be kept in mind when references are given to publications of this kind.

Contract Reports are produced to report scientific work carried out under contract. Publications of this kind contain confidential matter and are reserved for the sponsors and the DCE. Therefore, Contract Reports are generally not available for public circulation.

Lecture Notes contain material produced by the lecturers at the DCE for educational purposes. This may be scientific notes, lecture books, example problems or manuals for laboratory work, or computer programs developed at the DCE.

Theses are monograms or collections of papers published to report the scientific work carried out at the DCE to obtain a degree as either PhD or Doctor of Technology. The thesis is publicly available after the defence of the degree.

Latest News is published to enable rapid communication of information about scientific work carried out at the DCE. This includes the status of research projects, developments in the laboratories, information about collaborative work and recent research results.

Table of contents

List of figures

List of tables

List of acronyms

RN: Rosborg Gymnasium North extension
LM: Langmarksvej test site

1. Introduction

Centrum Pæle A/S, Aalborg University, VIA University College and INSERO Horsens are partners in an industrial PhD project within the field of shallow geothermal energy systems based on pile heat exchangers. Pile heat exchangers, also known as energy piles, are thermally active building foundation elements with embedded geothermal pipes fixed to the steel reinforcement in which a circulating fluid exchanges heat with the pile and the surrounding soil. As such, the foundation of the building both serves as a structural component and a heating/cooling supply element. The thermal properties of the pile-soil system, therefore, influence the operational performance of the ground source heat pump system.

This document aims to present the laboratory work undertaken to analyse the thermal properties of the soil at two test sites in Denmark and the concrete produced by Centrum Pæle A/S, used to produce the pile heat exchangers studied in the present PhD project. The tasks have been carried out between February 2016 and February 2017.

The presented work mainly consists of thermal property measurements. They become important as they form the basis for dimensioning a planned ground source heat pump installation based on closed loop vertical ground heat exchangers. This report complements the report "Thermal response testing of precast pile heat exchangers: fieldwork report" by (Alberdi-Pagola et al., 2017).

The report is organized as follows: first, the measurement methods and the test procedures are described. Second, the soils at both test sites are described, together with the measurements. Third, the measurements of the properties of the concrete are treated. The work is extended in appendixes.

2. Methods

Both soil and concrete samples are treated in a similar way. Each sample is properly described and its thermal properties, water content and bulk and dry densities are measured. The thermal expansion is not measured in this study. The thermal properties experimentally determined for the concrete are compared with the estimates from selected prediction models. To double-check the reliability of the measurements, the measurements are compared to literature values.

2.1. Thermal properties

The thermal properties have been measured by means of a Hot Disk apparatus (Figure 1). The Hot Disk equipment relies on the transient plane source method (Hot Disk AB, 2014) according to the Dansk Standard (2015) DS/EN ISO 22007-2 (2015). The transient plane source method yields estimations on the thermal conductivity λ [W/m/K], volumetric heat capacity ρc_p [MJ/m^3/K]. Thermal diffusivity α [m^2/s] is defined as the ratio between the thermal conductivity and volumetric heat capacity.

The Hot Disk sensor is an electrically conducting metallic double spiral (nickel), covered by two thin layers of insulating material (kapton). During the measurement, the sensor is placed between two pieces of sample. As the electrical current runs, the temperature of the sensor increases and at the same time, the temperature resistance as a function of time is measured. Hence, the sensor acts as a heat source and a dynamic temperature sensor. Hot Disk AB (2014) defines the accuracy of the thermal conductivity measurements as ± 5%, while the accuracy for the thermal diffusivity is defined between ± 5 and 10%. The uncertainty for the average value of the measurement $\bar{x}$ is defined as their root-sum-squared relation of the systematic and random errors for 95% confidence level:

$$w_{\bar{x}} = (B_{\bar{x}}^2 + P_{\bar{x}}^2)^{1/2} \tag{1}$$

Five repeated measurements have been taken for each sample at a room temperature between 19 to 21 °C.
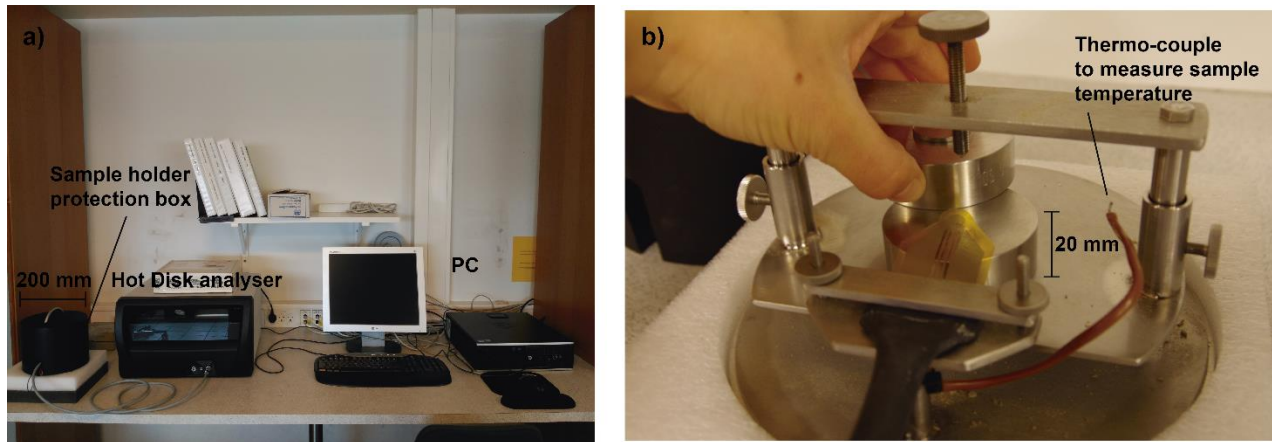
Figure 1: a) Hot Disk apparatus set up at the GeoLab at VIA University College, Horsens, DK; b) Sample holder for small samples, such as the shown steel standard cylinders.

2.2. Other physical properties affecting thermal properties

The soil specimens are characterised under "undisturbed" conditions. The water content has been measured following the DS/EN ISO/TS 17892-1: 2004 (2004) standard and the bulk and dry density determination follow the DS/EN ISO/TS 17892-2: 2004 (2004). The organic matter content has been measured following the ASTM Standards (1998).

Regarding the concrete, the determination of potential lower and upper bounds of its thermal properties are aimed. Under operational conditions, the pile heat exchanger will be driven into a medium that could have different moist content. This means that the saturation process is governed by the capillary domain. Therefore, the maximum water content that the material can acquire by suction, water pressure or condensation will be higher than the one absorbed by being in contact with air and it could reach 10 % in weight, depending on the concrete. Therefore, a range of thermal properties is targeted and the samples are measured in oven dry, saturated and normally dry (ambient air) conditions. The drying and the saturation processes and the density, absorption and voids in hardened concrete measurements are determined following the ASTM Standards (2013). The samples were allowed to "normally dry", from the saturated condition, under normal ambient surroundings for times extended over 6-7 days. The samples were oven dried again to determine the water content of the last measurement. The test are performed in samples with a curing time of more than a month.

2.3. Prediction models of thermal properties of concrete

As a further step, prediction models reported in the literature to determine the thermal properties of different materials are studied. Concrete is compounded of constituents with a wide variation in thermal properties. The thermal properties of the concrete are affected by: porosity (air and water content), humidity, mineral composition (aggregates and water/cement ratio), particle contact and temperature.

The specific heat of concrete is highly influenced by moisture content, aggregate type, cement type and density of concrete (Khaliq and Kodur, 2011). For composite materials, such as concrete, it can be calculated by the mixing theory (Bentz et al., 2011):

$$c_{p,\ concrete} = \sum_{i=1}^{n} c_{p,i} \cdot m_i \tag{2}$$

where $c_{p,i}$ is the heat capacity of each constituent (cement, water, fly ash, fine and coarse aggregates, etc.) and m_i refers to the mass fraction of each of those components. However, it has been demonstrated that this model is not applicable to concrete mixtures that contain phase change materials (Pomianowski et al., 2014).

The thermal conductivity is more complex to determine as it is influenced by the way the particles are arranged. Its maximum and minimum values for a two phase system (solid and fluid) with porosity ε, are provided by the series and parallel phase distributions, respectively, i.e., by the harmonic and the arithmetic means. As a third option, the geometric mean model assumes a random distribution of phases (Tavman, 1996, Khan, 2002).

For materials where the porosity is large, e.g., powders, granular materials and composites materials (randomly distributed and non-interacting particles in a homogeneous medium), Maxwell's model gives good results (Tavman, 1996).

To consider the influence of admixtures such as silica fume and fly ash on the cement paste, Demirboğa et al. (2007) provide some empirical correlations. Garboczi and Bentz (1992) provided advanced computer simulation models.

Several authors have suggested various thermal conductivity prediction models for traditional concrete mixes (Marshall, 1972, Khan, 2002). The first option was proposed by Campbell and Thorne, described in Marshall (1972) and Khan (2002):

$$\lambda_{concrete} = \lambda_m \cdot (2M - M^2) + \frac{\lambda_m \cdot \lambda_a \cdot (1-M)^2}{\lambda_a \cdot M + \lambda_m \cdot (1-M)} \tag{3}$$

$$M = 1 - \sqrt{1-p}$$

where, p is the volume of mortar per unit volume of concrete, λ the thermal conductivity and suffixes "m" and "a" refer to mortar and aggregate, respectively.

The second option is the composite model for conduction or the Hashin-Strikman model, used in Chan (2014), Wadsö L. (2012) and Mehta and Monteiro (2006):

$$\lambda_{concrete} = \lambda_c + \frac{v_d}{\dfrac{1}{\lambda_d - \lambda_c} + \dfrac{v_c}{3 \cdot \lambda_c}} \tag{4}$$

where, λ_c and λ_d are the thermal conductivities of the continuous and particle phases, respectively, and where v_c and v_d are the volume of the continuous and particle phases, respectively.

Kim et al. (2003) proposed an empirical relation that yields the thermal conductivity of concrete based on the relationship as functions of aggregate volume fraction AG, fine aggregate fraction S/A, water-cement ratio W/C, temperature T and moisture condition R_h in concrete. However, this expression requires a referenced thermal conductivity measured from specimens whose receipt is known:

$$\lambda_{concrete} = \lambda_{ref} \cdot [0.293 + 1.01 \cdot AG] \cdot \left[0.8 \cdot \left(1.62 - 154 \cdot \left(\frac{W}{C}\right)\right) + 0.2 \cdot R_h\right]$$
$$\cdot [1.05 - 0.0025 \cdot T] \cdot \left[0.86 + 0.0036 \cdot \left(\frac{S}{A}\right)\right] \tag{5}$$

In cases where the nature of the pores within the concrete is known, Khan (2002) compared the Campbell and Thorne model's estimations (Equation 3) to the ones obtained from models developed for porous materials, highlighting the importance of considering the porous state, specially, for mixtures where aggregate conductivity is high.

3. Thermal properties of soil

The soil samples are collected in two test sites in Denmark: one in Horsens and another in Vejle.

3.1. Langmarksvej

The test site is situated at Langmarksvej 84 (street address), 8700 Horsens, Denmark (55° 51′ 43″ N, 9° 51′ 7″ E), 800 m from the VIA University College campus (Figure 2). The test site was established in 2010 as part of a research collaboration between Centrum Pæle A/S, Horsens A.M.B.A. district heating company and VIA University College. After 4 years without operation, the test site is currently used in the present PhD project.

A monitoring drilling was executed 0.85 m apart from one of the pile heat exchangers on the 2/11/2015 by Franck Geoteknik A/S, using the auger drilling technique. Soil samples were collected each 0.5 m and they were kept in sealed plastic bags.

Figure 2: The Langmarksvej test site, Langmarksvej 84, 8700 Horsens, Denmark.

3.1.1. Soil description

A stratigraphic column was developed (Figure 3). As depicted, 5 m of fillings emerge on top of glacial clay till.

Depth (m)	Geology	Sample	Number	Description
0.0 m			1	TOPSOIL/CLAY, slightly sandy, grayish brown (10YR 5/2), calcareous, Fl/Re
			2	FILL/SAND, clayey, slightly gravelly, dark brown yellowish (10YR 4/4), calcareous, Fl/Re
-1.0 m			3	FILL/SAND, clayey, stones, dark brown yellowish (10YR 4/4), calcareous, Fl/Re
			4	FILL/SAND, fine, clayey, slightly gravelly, acid smell, dark olive gray (5Y 3/2), non-calcareous, Fl/Re
-2.0 m			5	FILL/CLAY, sandy, acid smell, dark olive gray (5Y 3/2), non-calcareous, Fl/Re
			6	FILL/SAND, fine, clayey, acid smell, olive gray (5Y 5/2), non-calcareous, Fl/Re
-3.0 m			7	FILL/CLAY, sandy, stones, acid smell, dark olive gray (5Y 3/2), non-calcareous, Fl/Re
			8	FILL/SAND, fine to medium, clay lumps, stones, brick remains, acid smell, dark olive gray (5Y 3/2), slightly calcareous, Fl/Re
-4.0 m			9	FILL/CLAY, slightly sandy, slightly gravelly, "cable", gray (5Y 5/1), non-calcareous, Fl/Re
			10	FILL/CLAY, slightly sandy, slightly gravelly, "cable", dark gray (5Y 4/1), non-calcareous, Fl/Re
			11	SAND, fine to medium, clay slumps, dark gray (5Y 4/1), non-calcareous, Fl/Re
-5.0 m			12	CLAY, sandy, yellowish brown (10YR 5/6), calcareous, GL/Gc
			13	CLAY TILL, lean, silty, sandy, gravelly, iron strips, yellowish brown (10YR 5/4), calcareous, GL/Gc
-6.0 m			14	CLAY TILL, lean, silty, sandy, dark gray (5Y 4/1), calcareous, GL/Gc
			15	CLAY TILL, lean fat, silty, sandy, dark gray (5Y 4/1), calcareous, GL/Gc
-7.0 m			16	CLAY TILL, lean, silty, sandy, gravelly, dark olive gray (5Y 3/2), calcareous, GL/Gc
			17	CLAY TILL, lean, silty, sandy, gravelly, dark olive gray (5Y 3/2), calcareous, GL/Gc
-8.0 m			18	CLAY TILL, lean///looser not as compact as the others, very sandy, slightly gravelly, dark olive gray (5Y 3/2), calcareous, GL/Gc
			19	CLAY TILL, lean, sandy, slightly gravelly, very dark gray (10YR 3/1), calcareous, GL/Gc
-9.0 m			20	CLAY TILL, lean, sandy, slightly gravelly, very dark gray (10YR 3/1), calcareous, GL/Gc
			21	CLAY TILL, lean, sandy, slightly gravelly, very dark gray (10YR 3/1), calcareous, GL/Gc
-10.0 m			22	CLAY TILL, lean, sandy, slightly gravelly, very dark gray (10YR 3/1), calcareous, GL/Gc
			23	CLAY TILL, lean, sandy, slightly gravelly, very dark gray (10YR 3/1), calcareous, GL/Gc
-11.0 m			24	CLAY TILL, lean, sandy, slightly gravelly, very dark gray (10YR 3/1), calcareous, GL/Gc
			25	CLAY TILL, lean, sandy, slightly gravelly, very dark gray (10YR 3/1), calcareous, GL/Gc
-12.0 m			26	CLAY TILL, lean, sandy, slightly gravelly, very dark gray (10YR 3/1), calcareous, GL/Gc
			27	CLAY TILL, lean, sandy, slightly gravelly, very dark gray (10YR 3/1), calcareous, GL/Gc
-13.0 m			28	CLAY TILL, slightly fatter than the previous, sandy, slightly gravelly, very dark gray (10YR 3/1), calcareous, GL/Gc
			29	CLAY TILL, lean, sandy, slightly gravelly, very dark gray (10YR 3/1), calcareous, GL/Gc
-14.0 m			30	CLAY TILL, lean, sandy, slightly gravelly, very dark gray (10YR 3/1), calcareous, GL/Gc
			31	CLAY TILL, lean, sandy, slightly gravelly, very dark gray (10YR 3/1), calcareous, GL/Gc
-15.0 m			32	CLAY TILL, lean, sandy, slightly gravelly, very dark gray (10YR 3/1), calcareous, GL/Gc
			33	CLAY TILL, slightly fat, sandy, slightly gravelly, shiny surfaces, very dark gray (10YR 3/1), calcareous, GL/Gc
-16.0 m			34	CLAY TILL, lean, sandy, slightly gravelly, very dark gray (10YR 3/1), calcareous, GL/Gc
			35	CLAY TILL, lean, sandy, slightly gravelly, very dark gray (10YR 3/1), calcareous, GL/Gc
-17.0 m			36	CLAY TILL, lean, sandy, slightly gravelly, very dark gray (10YR 3/1), calcareous, GL/Gc
			37	CLAY TILL, lean, sandy, slightly gravelly, very dark gray (10YR 3/1), calcareous, GL/Gc
-18.0 m			38	CLAY TILL, lean, sandy, slightly gravelly, very dark gray (10YR 3/1), calcareous, GL/Gc

Figure 3: Soil description of the samples collected each 0.5 m in the drilling executed at Langmarksvej. Legend according to DGF Bulletin 1 (Larsen, G., 1995).

3.1.2. Measurements

The samples were kept as intact as possible in sealed plastic bags and they were measured within the next 24 - 48 hours. Despite sample number 11 in Figure 3 (sand) which needed to be reconstituted to a realistic density to perform a single sided measurement (see Appendix A), the other samples were cohesive soils and a double side measurement of intact samples could be performed.

Figure 4 illustrates the depth dependence of the bulk density ρ [g/cm^3], water content [%], thermal conductivity λ_s [W/m/K] and volumetric heat capacity ρc_p [MJ/m^3/K] of the samples. The weighted average estimates over the length of the drilling give an effective thermal conductivity λ_s of 2.30 ± 0.13 W/m/K and an effective volumetric heat capacity ρc_p of 2.61 ± 0.27 MJ/m^3/K.
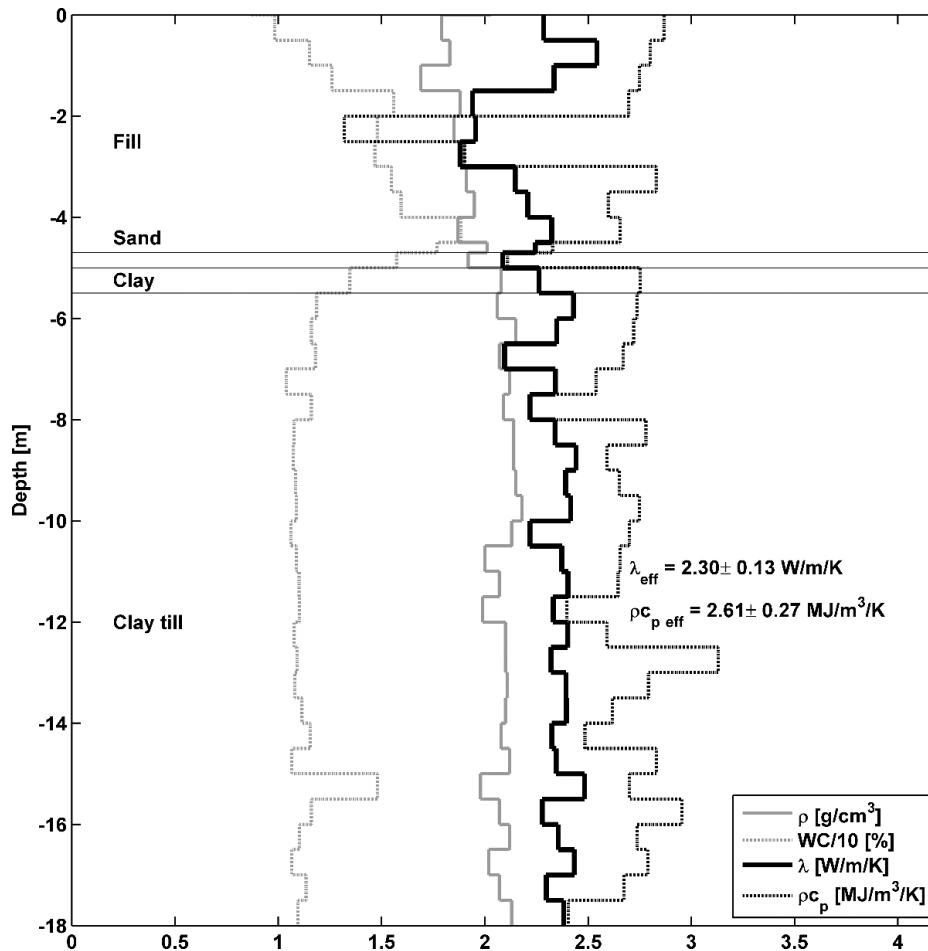
Figure 4: Stratigraphic profile at the Langmarksvej test site. Bulk density ρ, water content, thermal conductivity λ_s and volumetric heat capacity ρc_p measured in the laboratory using the Hot Disk apparatus are also provided. ρc_p eff and λ_s eff are weighted average estimates over the length of the drilling.

3.2. Rosborg Gymnasium

The test site is located at Vestre Engvej 61, 7100 Vejle, Denmark (55° 42′ 30″ N, 9° 32′ 0″ E) (Figure 5). The south extension of the Rosborg Gymnasium building is founded on 200 foundation pile heat exchangers. The thermo-active foundation has supplemented the heating and free cooling requirements of the building since 2011 (4,000 m² heated area). More information about the performance of the installation can be found in Alberdi-Pagola et al. (2016). The north extension of the gymnasium complex is currently under construction. To date, the foundation, that consists of 220 energy piles, has been constructed. The monitoring drilling was bored 30 meters away from the building towards the north.
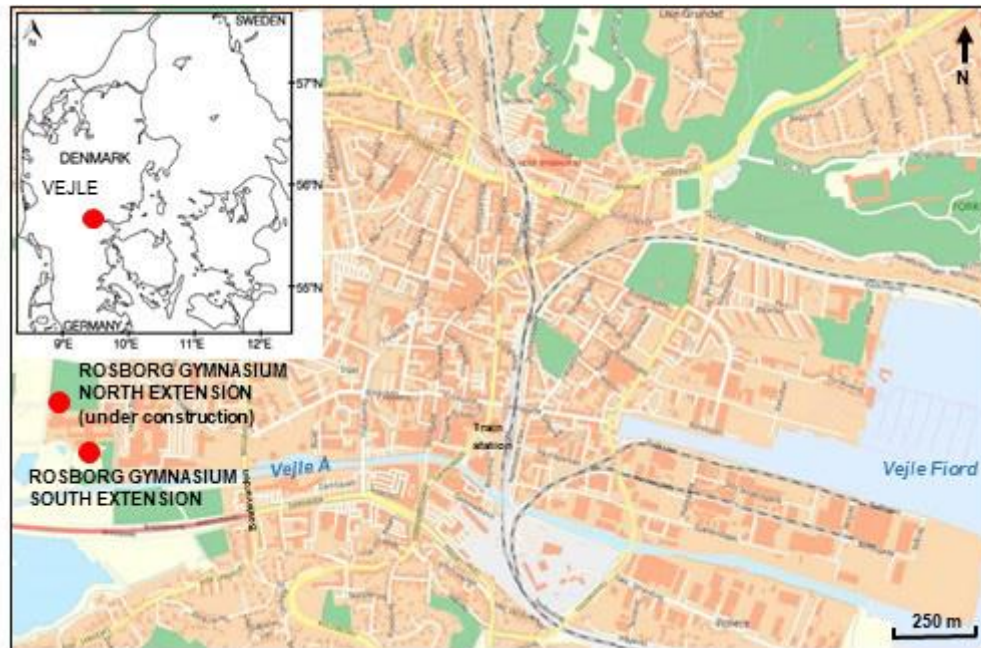
Figure 5: The Rosborg Gymnasium building at Vestre Engvej 61, 7100 Vejle, Denmark. The south and north extensions are founded on 200 and 220 energy piles, respectively.

3.2.1. Soil description

A stratigraphic column was developed (Figure 6). The piles are founded in glacial sand 5-6 m below terrain, which is overlain by postglacial, organic mud. The groundwater table is situated around 0.70 m below terrain (Dansk Geoteknik A/S, 1973, Franck Geoteknik A/S, 2013).
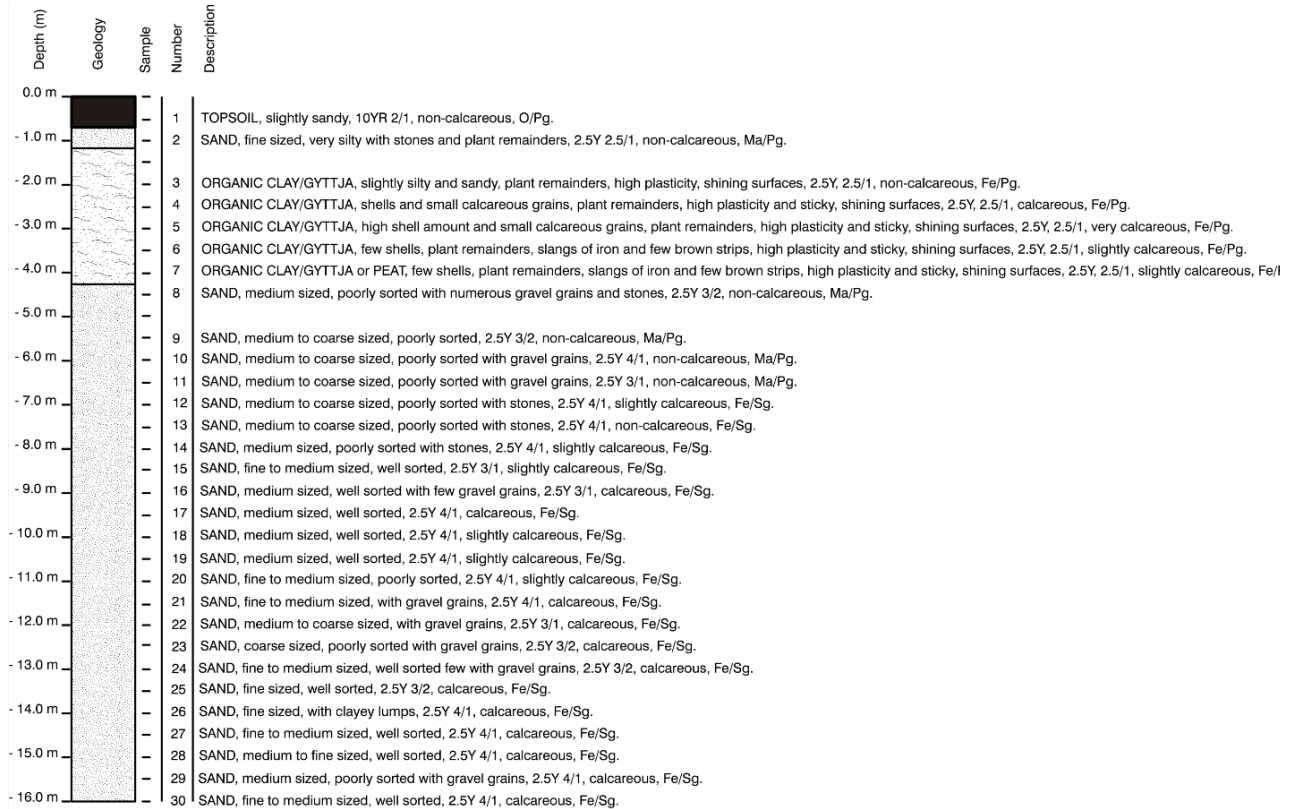
Figure 6: Soil description of the samples collected each 0.5 m in the drilling executed at Rosborg North.

3.2.2. Measurements

The samples were kept as intact as possible in sealed plastic bags and they were measured within the next 24 - 48 hours. Despite samples 1 to 7, which are cohesive, the rest (sand) needed to be reconstituted (repacked and compacted) to a realistic density to perform single sided measurements (see Appendix A).

Figure 7 illustrates the depth dependence of the bulk density ρ [g/cm^3], water content [%], thermal conductivity λ_s [W/m/K] and volumetric heat capacity ρc_p [MJ/m^3/K] of the samples. The weighted average estimates over the length of the drilling give an effective thermal conductivity λ_s of 2.14 ± 0.11 W/m/K and an effective volumetric heat capacity ρc_p of 2.47 ± 0.29 MJ/m^3/K. The organic matter content in the peat sample (samples 7 in Figure 6) is 33%, twice the one measured in the organic clay samples (11-15%).
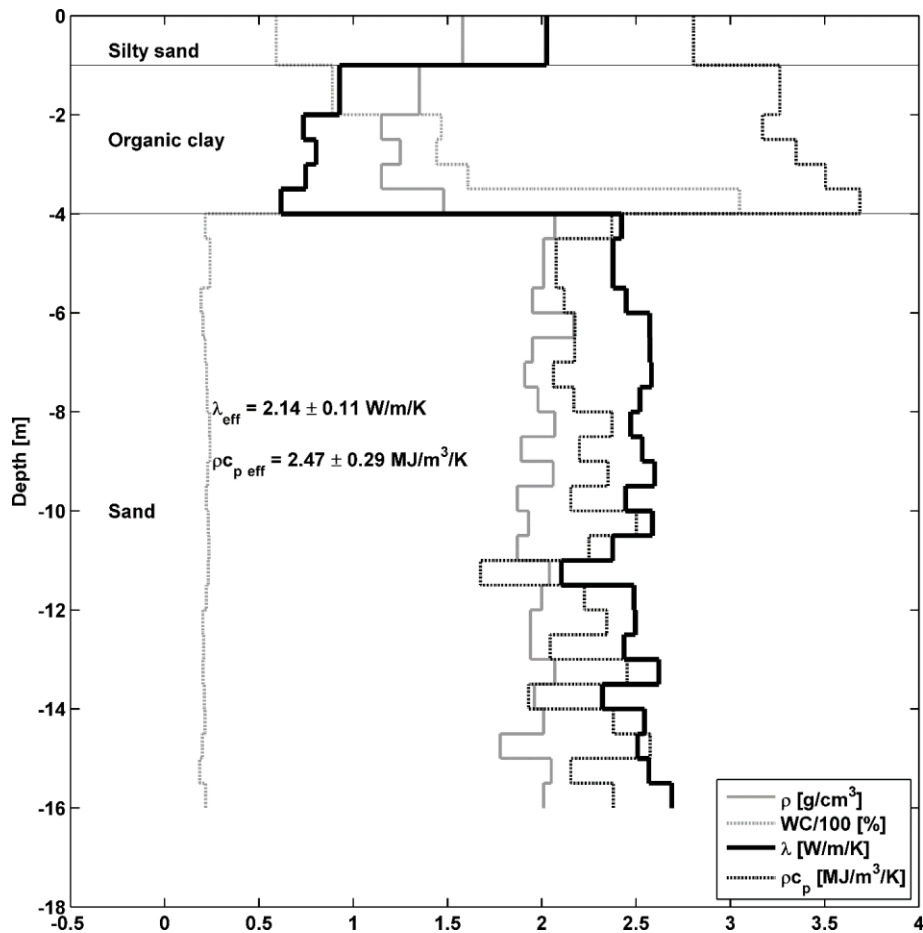
Figure 7: Stratigraphic profile at Rosborg Norht test site. Bulk density ρ, water content, thermal conductivity λ_s and volumetric heat capacity ρc_p measured in the laboratory using the Hot Disk apparatus are also provided. $\rho c_{p\ eff}$ and $\lambda_{s\ eff}$ are weighted average estimates over the length of the drilling.

4. Thermal properties of concrete

This section aims to measure the thermal properties of the standard concrete (S3 receipt) produced at Centrum Pæle A/S. This receipt is used in the production of precast pile heat exchangers. First, the experimental characterisation of the concrete is provided. Then, the goodness of fit of thermal conductivity and heat capacity prediction models is assessed, by comparing their estimations to the measurements.

4.1. Experimental characterisation

First, the mix constituents and the test specimens are described, after, the laboratory work is summarised and the measurements shown. Later, selected prediction models are applied and to finish, both approaches are compared. The thermal expansion is not measured in this study.

4.1.1. Mix constituents and test specimens

The studied mix is the one used in the production of precast pile heat exchangers (S3 receipt). Details of mix components, laboratory conditions for casting and compressive strength results are given in Table 1. A mineralogical analysis of the aggregates has been carried out (see Appendix B). Quartz is the main component (62%) for the pit sand, while crystalline rocks lead the gravel aggregates (61%). For the determination of the thermal properties, four sliced 100 x 200 mm cylinders were used: samples S1 and S2 belong to the same batch produced the 08/04/2016 while samples S3 and S4 belong to the batch produced the 19/01/2017. Every slide had a 65 mm thickness, approximately.

Table 1: Mix components and physical properties for the S3 receipt. Average values for the two batches. The dosage is kept confidential.

Components S3 receipt	
Cement (CEM I 52,5, Dyckerhoff Dreifach N)	-
Fly ash (Type B5)	-
Water	-
Air-entraining admixture (MicroAir)	-
Plasticizer (Glenium ACE 403)	-
Pit sand 0 - 2mm	-
Crushed stone 4 - 8 mm	-
Pea gravel 8 - 16 mm	-
Physical properties S3 receipt	
Water/cement ratio	0.40
Air content in fresh concrete [%]	3.25
Density [kg/m^3]	2370.00
Compressive strength at 28 days [Mpa]	66.2

4.1.2. Measurements

For each specimen the following properties were measured in the laboratory: bulk dry density ρ_d [kg/m^3], bulk saturated density ρ_s [kg/m^3], bulk natural density ρ_n [kg/m^3], water content or humidity [% of weight], porosity, absorption, thermal conductivity λ_c [W/m/K] and volumetric heat capacity ρc_{pc} [MJ/m^3/K].

The four specimens (S3 receipt) have been measured in oven dry, saturated and normally dry (ambient air) conditions. This way, the potential lower and upper limits and intermediate conditions for the thermal properties are covered. More information about these processes is provided in Appendix A. Table 2 provides the average porosity and absorption of the concrete specimens.

Table 2: Measured porosity and absorption of the concrete specimens.

Sample ID	Volume of permeable voids [%]	Absorption [%]
S1	9.4	4.1
S2	9.3	4.0
S3	8.5	3.6
S4	7.4	3.2
Average	8.6	3.7

Repeated measurements have been taken with the Hot Disk apparatus for each sample at a room temperature between 19 to 23°C for the three water content conditions (dry, saturated and normally dry), summarised in Table 3. More information about the measurements and the test are provided in Appendixes A and B.

Table 3: Summary of samples and measurements for each condition.

Sample ID	Condition	Number of measurements
S1	Oven dry	5
S1	Normally dry	15
S1	Saturated	10
S2	Oven dry	5
S2	Normally dry	15
S2	Saturated	10
S3	Oven dry	5
S3	Normally dry	5
S3	Saturated	10
S4	Oven dry	5
S4	Normally dry	5
S4	Saturated	10

The measured thermal properties of the four specimens are plotted in Figure 8. Each marker contains the average of five repeated measurements and the error bars comprise the 95% confidence interval, which account for systematic and random errors. The average values of the measurements in dry, normally dry and saturated conditions of the four specimens are summarised in Table 4 and illustrated in Figure 9. The measured values are in accordance with the values reported in Neville (1995).

Average values for 4 specimens:
Volume of permeable voids = 8.6 ± 0.8%; Absorption = 3.7 ± 0.3% (ASTM C642-13)
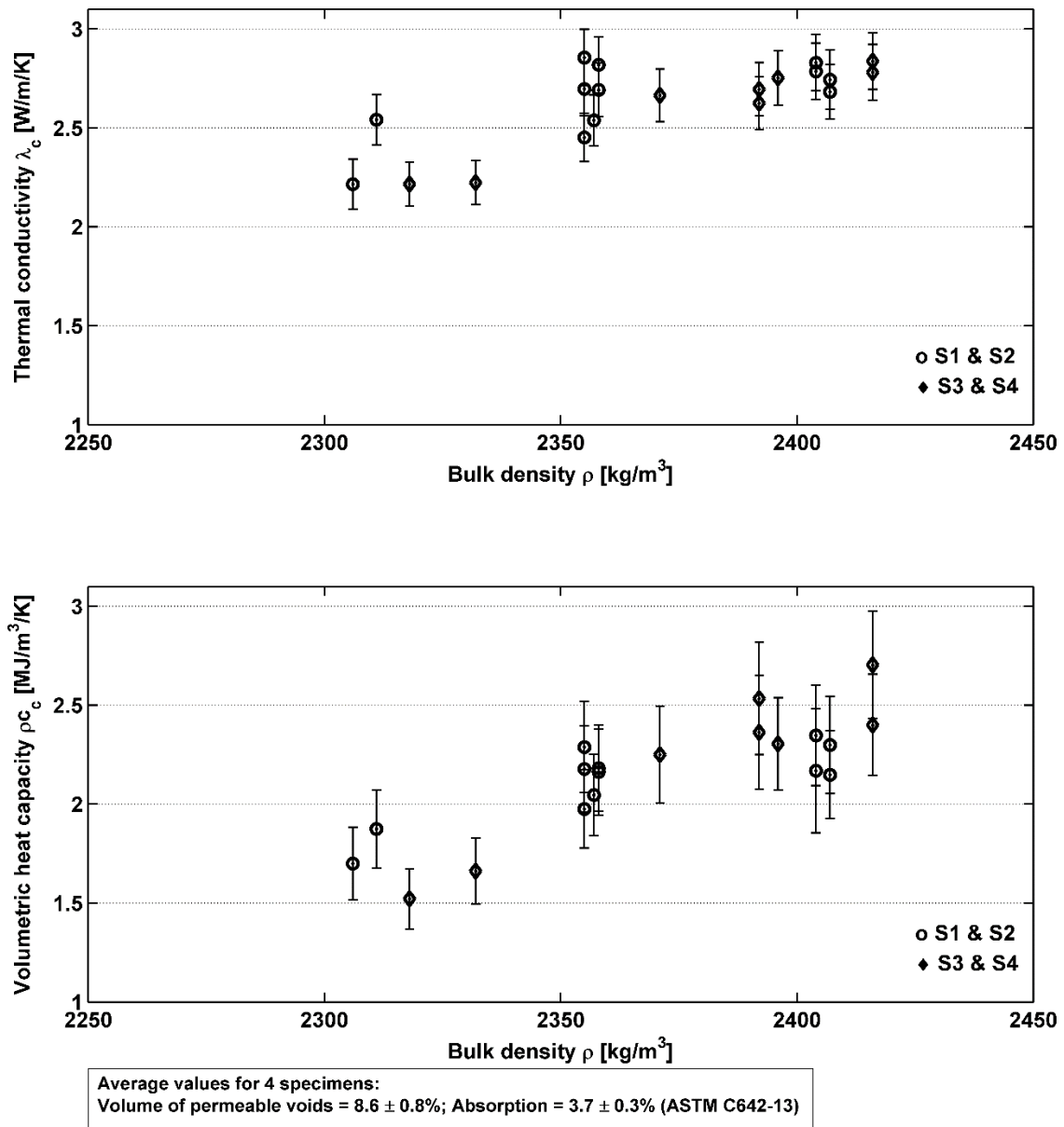
Figure 8: Measured thermal properties of S3 receipt concrete with the transient plane source method. The error bars indicate the 95% confidence level.

Due to a change in humidity of 3.7% (saturated conditions), the thermal conductivity of the dry concrete decreases up to 16% while the volumetric heat capacity decreases 28%. It is a considerable change, considering the low modification in humidity.

Table 4: Summary of mean values of the thermal property property measurements and their uncertainties.

Sample condition	Density ρ [kg/m^3]	Thermal conductivity λ_c [W/m/K]	Volumetric heat capacity ρc_{pc} [MJ/m^3/K]
Oven dry	2318 ± 8	2.30 ± 0.28	1.69 ± 0.29
Normally dry	2370 ± 16	2.69 ± 0.18	2.17 ± 0.24
Saturated	2405 ± 9	2.75 ± 0.15	2.37 ± 0.28

18
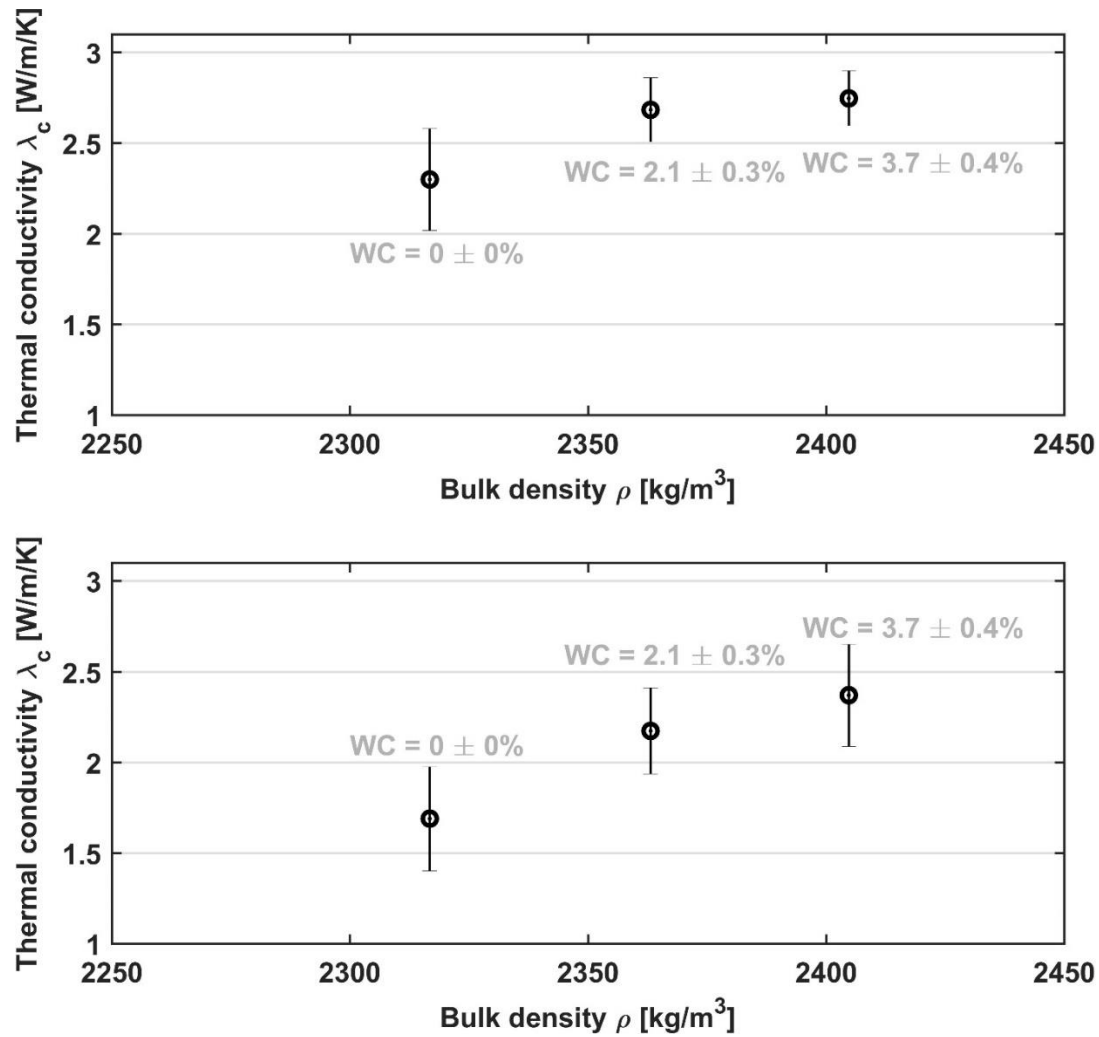
Figure 9: Average of measured thermal properties of S3 receipt concrete with the transient plane source method. The error bars indicate the 95% confidence level. Average values for 4 specimens, according to ASTM C642-13: volume of permeable voids: 8.6 ± 0.8%; absorption = 3.7 ± 0.3%.

Pomianowski M. (personal communication, January 2017) suggests that the drying process of the concrete could take months and, therefore, the results reported in this study might not have been measured in completely dry conditions.

4.2. Application of prediction models of thermal properties

Campbell-Thorne's model (Equation 3) and the Hashin-Strikman's model (Equation 4) have been selected, as they have been considered more suitable since the pore nature (connections and shapes) is unknown in the studied concrete. For the volumetric heat capacity, the model of mixing theory is applied.

The use of prediction models requires to know the materials compounding the concrete. A mineralogical analysis of the aggregates has been done (Appendix C) and the main components have been identified for each aggregate. The continuous phase is defined as the cement paste and fly ash while the particle phase involved all the aggregates (the air content was neglected). The thermal properties considered for each of the components are given in Table 5. These values are chosen from the literature (Appendix B).

Table 5: Thermal properties of the concrete components assumed for the prediction models.

Components	Density ρ [kg/m^3]	Mass fraction	Volume fraction	Thermal conductivity λ [W/m/K]		Volumetric heat capacity ρc_p [MJ/m^3/K]	
				Saturated state	Dry state	Saturated state	Dry state
Pit sand, 0/2 mm, main comp. quartz (62 %)	2640	0.27	0.25	6.00	5.00	2.10	2.00
Crushed stone, 4/8mm, main comp. crystalline (61 %)	2660	0.05	0.04	4.60	3.00	2.20	2.00
Pea gravel, 8/16mm, main comp. crystalline (61 %)	2650	0.45	0.40	4.60	3.00	2.20	2.00
Cement	3100	0.15	0.11	1.20	1.20	2.65	2.65
Fly ash (Bentz et al., 2011 & Kim et al., 2003)	2380	0.03	0.03	0.89	0.89	1.71	1.71
Water	1000	0.06	0.14	0.58	0.58	4.19	2.20
Air-entraining admixture (MicroAir)	-	-	-	-	-	-	-
Plasticizer (Glenium ACE 403)	-	-	-	-	-	-	-
Air (3%)	-	-	-	-	-	-	-

4.3. Discussion

As shown in Figure 10, the prediction models overestimate the measurements for dry conditions while they target very close the thermal properties in saturated conditions, as concluded by Khan (2002). Porous media approaches are recommended to get more information about the pore nature. The measured values are in accordance with the values reported in Neville (1995). However, the measurements seem very sensitive to the humidity content of the samples.
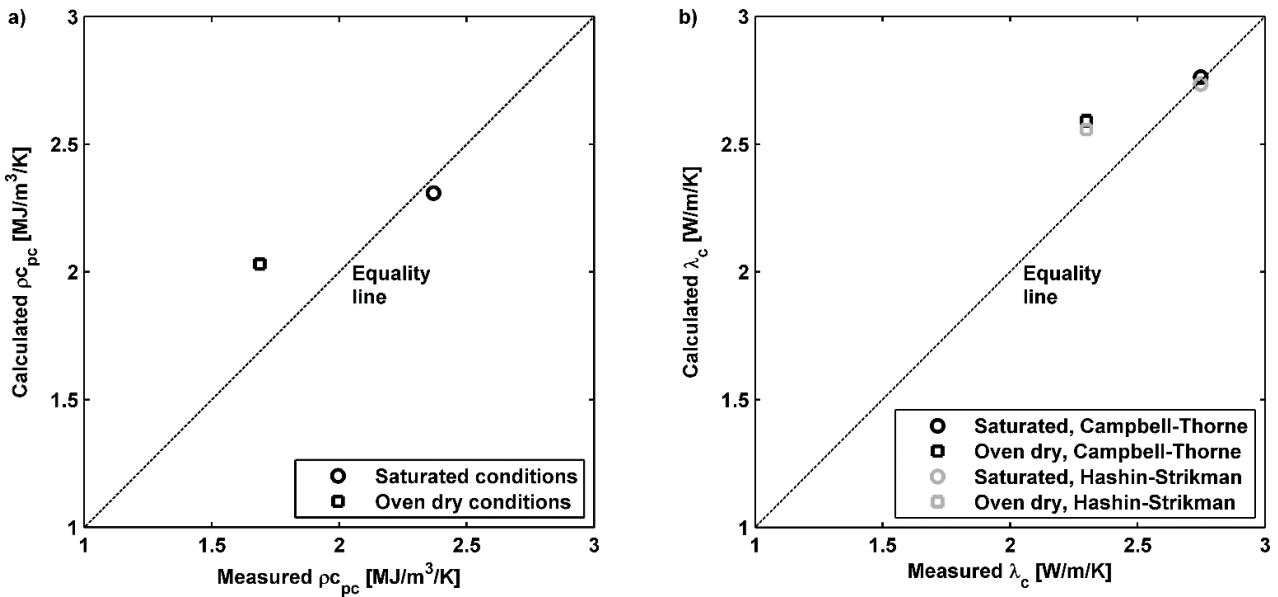
Figure 10: Predicted thermal properties of concrete against experimentally obtained values a) volumetric heat capacity ρc_p and b) thermal conductivity λ.

5. Conclusion

Pile heat exchangers, also known as energy piles, are thermally active building foundation elements with embedded geothermal pipes fixed to the steel reinforcement in which a circulating fluid exchanges heat with the pile and the surrounding soil. As such, the foundation of the building both serves as a structural component and a heating/cooling supply element. The precast piles act as heat exchangers and, therefore, the thermal properties of the concrete and the surrounding soil highly influence the heat transfer phenomena within the pile-soil system.

This document measures the thermal properties of the soil from two locations and the standard concrete (S3 receipt) produced at Centrum Pæle A/S by means of the Hot Disk apparatus (transient plane source method), following Dansk Standard (2015).

The measurements of the soil specimens are in agreement with the ranges proposed in VDI (2010) and Abu-Hamdeh (2003). And the measurements for the concrete specimens are in accordance with the values reported in Neville (1995). However, the measurements seem very sensitive to the humidity content of the samples. A further comparison with prediction models of thermal properties has been done for the concrete samples. These models closely reproduce the thermal properties in saturated conditions but they differ in dry conditions, due to the complexity of considering the nature of pores.

Future research on the thermal properties of concrete should focus on: i) performing more measurements at different water contents and with different mixes to establish empirical rules to compute the thermal properties in terms of the bulk density. ii) Further study the nature of the pores of the concrete and analyse the validity of more complex prediction models, such as the ones recommended in Khan (2002). Regarding soil thermal properties, due to the fact that non-cohesive soils are harder to measure, unified measurement protocols should be developed, putting together the experience from several laboratories, so that the measured values are comparable.

6. Acknowledgements

7. References

ABU-HAMDEH, N. H., 2003. Thermal Properties of Soils as affected by Density and Water Content. Biosystems Engineering, 86, 97-102.

ALBERDI-PAGOLA, M., JENSEN, R. L. & POULSEN, S. E., 2016. A performance case study of energy pile foundation at Rosborg Gymnasium (Denmark). 12th REHVA World Congress Clima2016, 22-25 May 2016 Aalborg, Denmark. Department of Civil Engineering, Aalborg University, p. 10.

ALBERDI-PAGOLA, M., POULSEN, S. E., JENSEN, R. L. & MADSEN, S., 2017. Thermal response testing of precast pile heat exchangers: fieldwork report. In: AALBORG UNIVERSITY, D. O. C. E. (ed.). Aalborg, Denmark: Aalborg University.

ASTM STANDARDS, 1998. ASTM D2974:1998: Standard Test Methods for Moisture, Ash, and Organic Matter of Peat and Other Organic Soils. 1916 Race St., Philadelphia, PA 19103.

ASTM STANDARDS, 2013. C642-13. Standard Test Method for Density, Absorption, and Voids in Hardened Concrete.

BENTZ, D., PELTZ, M., DURAN-HERRERA, A., VALDEZ, P. & JUAREZ, C., 2011. Thermal properties of high-volume fly ash mortars and concretes. Journal of Building Physics, 34, 263-275.

CHAN, J., 2014. Thermal properties of concrete with different Swedish aggregate materials. Rapport TVBM (5000-serie).

DANSK GEOTEKNIK A/S, 1973. Geoteknisk rapport. Grundundersøgelser for Amtsgymnasium i Vejle, Vestre Engvej, Vejle.

DANSK STANDARD, 2015. DS/EN ISO 22007-2 (2015): Plastics – Determination of the thermal conductivity and thermal diffusivity – Part 2: Transient plane heat source (hot disc) method.

DEMIRBOĞA, R., TÜRKMEN, İ. & KARAKOÇ, M. B., 2007. Thermo-mechanical properties of concrete containing high-volume mineral admixtures. Building and Environment, 42, 349-354.

DS/EN ISO/TS 17892-1: 2004 2004. Geotechnical investigation and testing - Laboratory testing of soil – Part 1: Determination of water content.

DS/EN ISO/TS 17892-2: 2004 2004. Geotechnical investigation and testing - Laboratory testing of soil – Part 2: Determination of density of fine-grained soil.

FRANCK GEOTEKNIK A/S, 2013. Geoteknisk rapport, parameterundersøgelse. Rosborg Gymnasium, Vestre Engvej 61, Vejle. Ny Nordfløj.

GARBOCZI, E. J. & BENTZ, D. P., 1992. Computer simulation of the diffusivity of cement-based materials. Journal of Materials Science, 27, 2083-2092.

HANSEN, K. K., 1986. Sorption isotherms: a catalogue. Technical University of Denmark Danmarks Tekniske Universitet, Department of Structural Engineering and MaterialsInstitut for Bærende Konstruktioner og Materialer.

HOT DISK AB, 2014. Hot Disk Thermal Constants Analyser TPS 1500 unit, Intruction Manual.

KHALIQ, W. & KODUR, V., 2011. Thermal and mechanical properties of fiber reinforced high performance self-consolidating concrete at elevated temperatures. Cement and Concrete Research, 41, 1112-1122.

KHAN, M., 2002. Factors affecting the thermal properties of concrete and applicability of its prediction models. Building and Environment, 37, 607-614.

KIM, K.-H., JEON, S.-E., KIM, J.-K. & YANG, S., 2003. An experimental study on thermal conductivity of concrete. Cement and Concrete Research, 33, 363-371.

LARSEN, G., 1995. A guide to engineering geological soil description, dgf-bulletin, 1, revision 1 (May 1995). Danish Geotechnical Society, Lyngby.

MARSHALL, A., 1972. The thermal properties of concrete. Building Science, 7, 167-174.

MEHTA, P. & MONTEIRO, P. J. M., 2006. Concrete: Microstructure, Properties, and Materials, McGraw-Hill Education.

NEVILLE, A. M., 1995. Properties of concrete.

POMIANOWSKI, M., HEISELBERG, P., JENSEN, R. L., CHENG, R. & ZHANG, Y., 2014. A new experimental method to determine specific heat capacity of inhomogeneous concrete material with incorporated microencapsulated-PCM. Cement and Concrete Research, 55, 22-34.

POMIANOWSKI, M.

TAVMAN, I. H., 1996. Effective thermal conductivity of granular porous materials. International Communications in Heat and Mass Transfer, 23, 169-176.

VDI, V. D. I., 2010. VDI 4640 Thermal Use of the Underground. Part 1: Fundamentals, approvals, environmental aspect. Berlin: VDI-Gessellschaft Energie und Umwelt (GEU).

WADSÖ L., 2012. Thermal properties of concrete with various aggregates. Cement and Concrete Research.

8. Appendices

A) Soils

This appendix provides pictures of the measurement process of soil thermal properties and information about the measurement parameters.

The cohesive samples were halved and in undisturbed conditions (Figures 11 and 12).
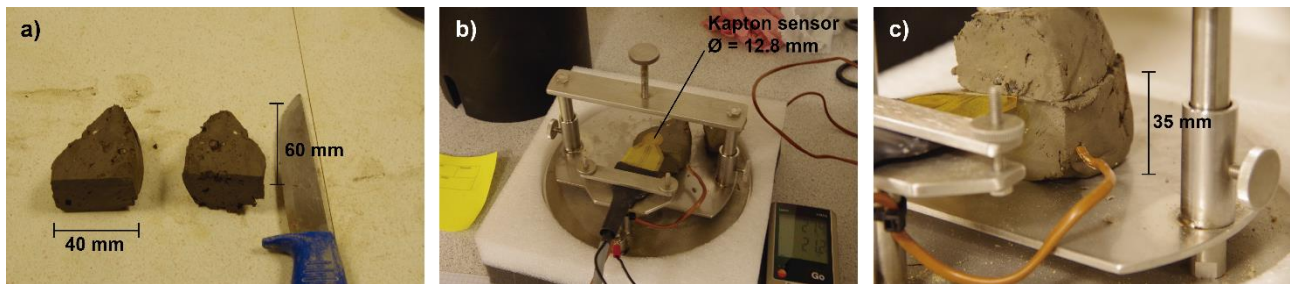
Figure 11: a) Halved moraine clay sample. b) Hot Disk kapton sensor ready to be placed between two specimens of soil. c) On-going Hot Disk testing, two-side measurement of a moraine clay sample (depth 8.5 m at Langmarskvej test site).
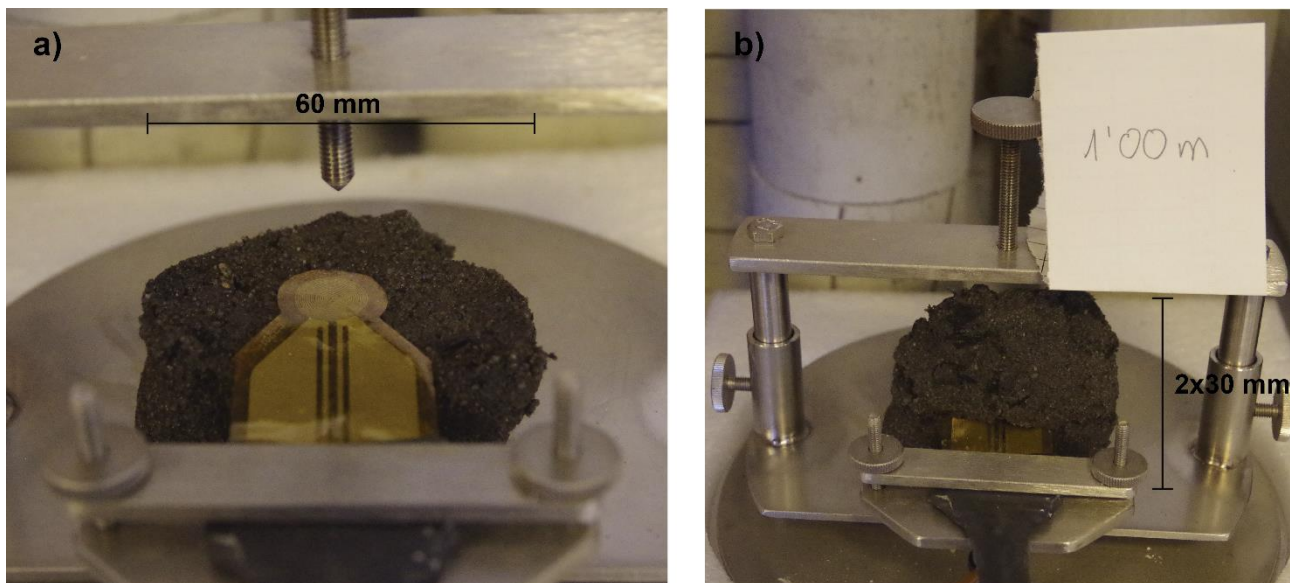
Figure 12: a) Hot Disk kapton sensor (15 mm in diameter) ready to be placed between two specimens of a silty sand sample. b) On-going Hot Disk testing, two-side measurement of the silty sand sample (depth 1.0 m at Rosborg North site).

Regarding non-cohesive samples, the sand was repacked into small containers to allow the single sided measurement procedure (Figure 13). The non-cohesive sample was taken off the sealed bag and placed into the containers layer by layer (1.5 cm approx.), compacting them with a hammer until the water (natural moist content) emerged to the surface.
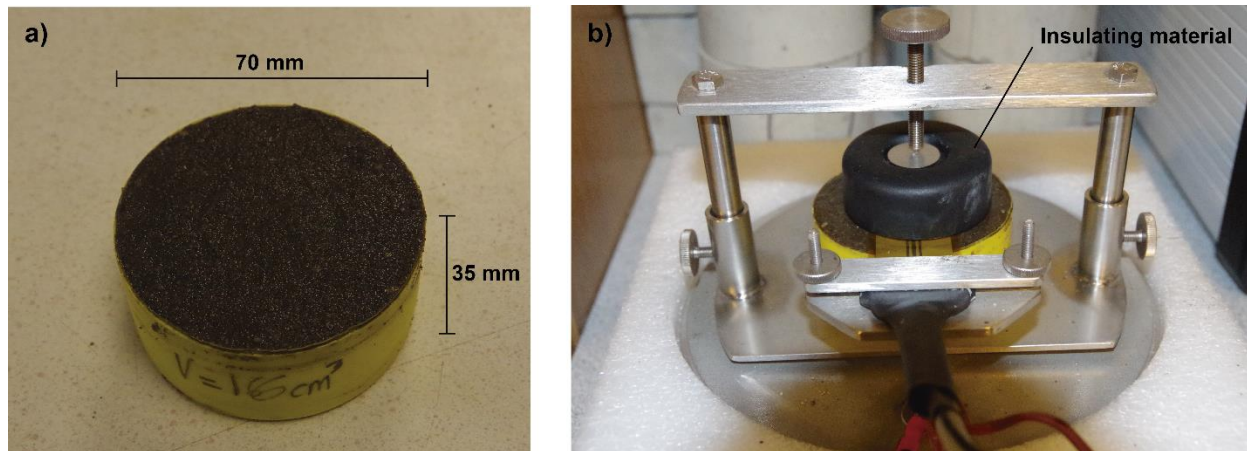
Figure 13: a) Sand sample in a container; b) On-going Hot Disk test, single-sided measurement of a sand sample (depth 4.5 m).

Table 6 shows the parameters and sensors used for the measurement of different type of soils.

Table 6: Summary of recommended experimental parameters for different soils based on measurements performed at the GeoLab at VIA University College, Horsens, DK, for the present study.

Type of sample	Sand	Plastic clay	Clay till	Silty sand	Organic clay
Thermal conductivity [W/m/K]	2.40	1.30	2.30	2.03	0.80
Thermal diffusivity [mm^2/s]	1.10	0.45	0.96	0.72	0.24
Temperature increase [K]	2.6	5.5	2.6	2.7	4.1
Sensor to use: Name/radius [mm]	8563 / 10	5501 / 6.5	5501 / 6.5	5501 / 6.5	5501 / 6.5
Specimen thickness [mm]	30	30	25	30	30
Specimen diameter [mm]	70	70	40	40	40
Measurement time [s]	80	80	40	40, 80	80
Heating Power [mW]	400, 800	250	400	250, 300	250

B) Concrete

This appendix provides pictures of the measurement process of concrete thermal properties and gives information about the measurement parameters, the drying and saturating processes and the mineralogical analysis.

Measurement process and parameters

The concrete samples were halved and measured as shown in Figure 14.
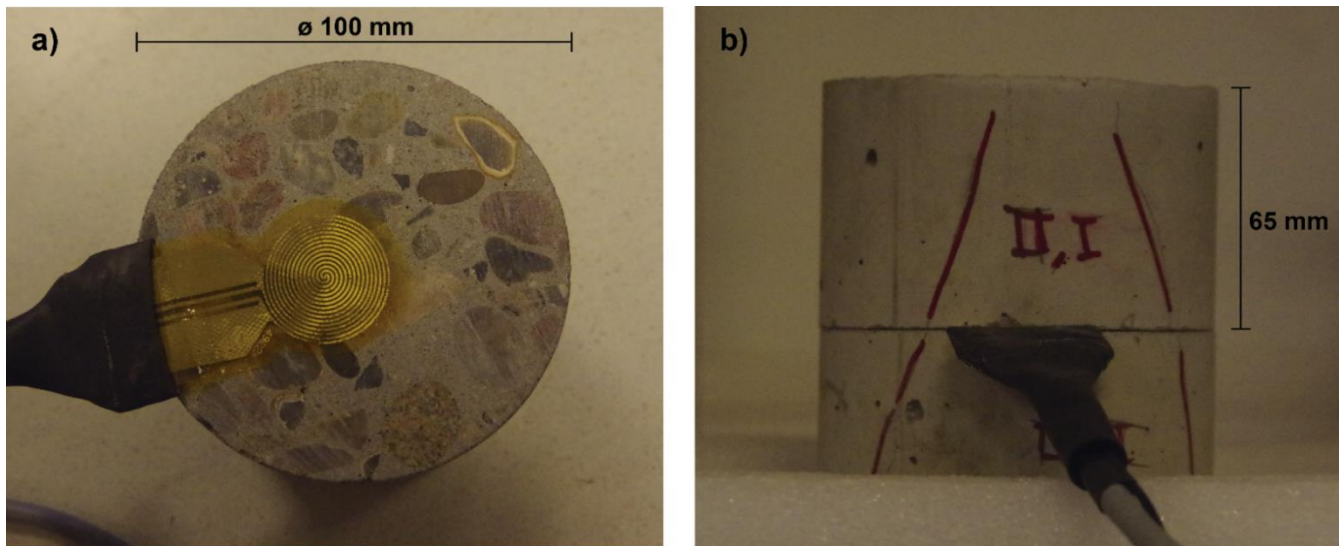
Figure 14: a) Hot Disk kapton sensor (15 mm in diameter) ready to be placed between two specimens of concrete. b) On-going Hot Disk testing, two-side measurement of a concrete sample.

Table 7 shows the parameters and sensors used for the measurement of concrete samples.

Table 7: Summary of recommended experimental parameters for concrete specimens based on measurements performed at the GeoLab at VIA University College, Horsens, DK, for the present study.

Type of sample	Concrete
Thermal conductivity [W/m/K]	2.11
Thermal diffusivity [mm²/s]	1.12
Temperature increase [K]	7.3
Sensor to use: Name/radius [mm]	4922/14.61
Specimen thickness [mm]	70
Specimen diameter [mm]	100
Measurement time [s]	80, 160
Heating Power [mW]	1000, 1200

Oven drying and saturating concrete specimens

First, the drying in the oven was performed. After 48 hours of drying, the lost in humidity was below 0.2% from day 2 to 3 (Figure 15).
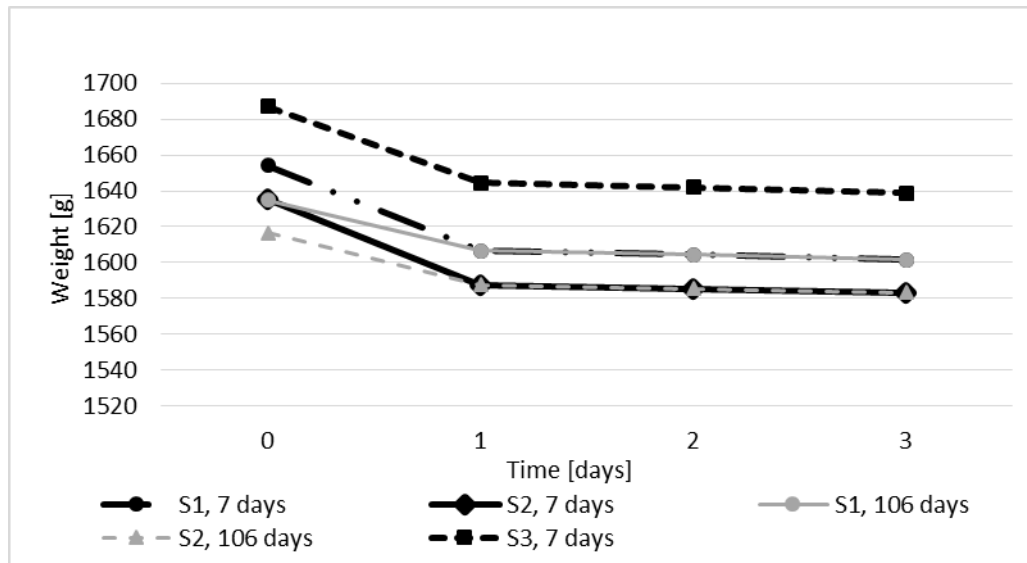
Figure 15: Weight evolution over oven-drying process for each specimen. Concrete drying at 105 °C.

Second, to measure the porosity and absorption of the concrete the following standard was followed ASTM C 642: 1975 (ASTM Standards, 2013). The specimens were vacuumed in a desiccator instead of boiled (Figure 16). Once saturated, the second round of measurements was made.

Figure 16: Desiccator.

Measuring relative humidity in GeoLab and determining water content of normally dried specimens

The specimens, after saturation, were kept in the GeoLab at VIA University College for some days in order to normally dry them. The relative humidity and the temperature has been monitored over 2 days (Figure 17). The average temperature is 21 °C while the relative humidity is 40.5 %. According to Hansen (1986) in pp- 41, a concrete with a water-cement ratio of 40 at 20 °C the hygroscopic content at a relative humidity of 40 % is around 1.2 weight %. In this study it has been measured as 2.1%.
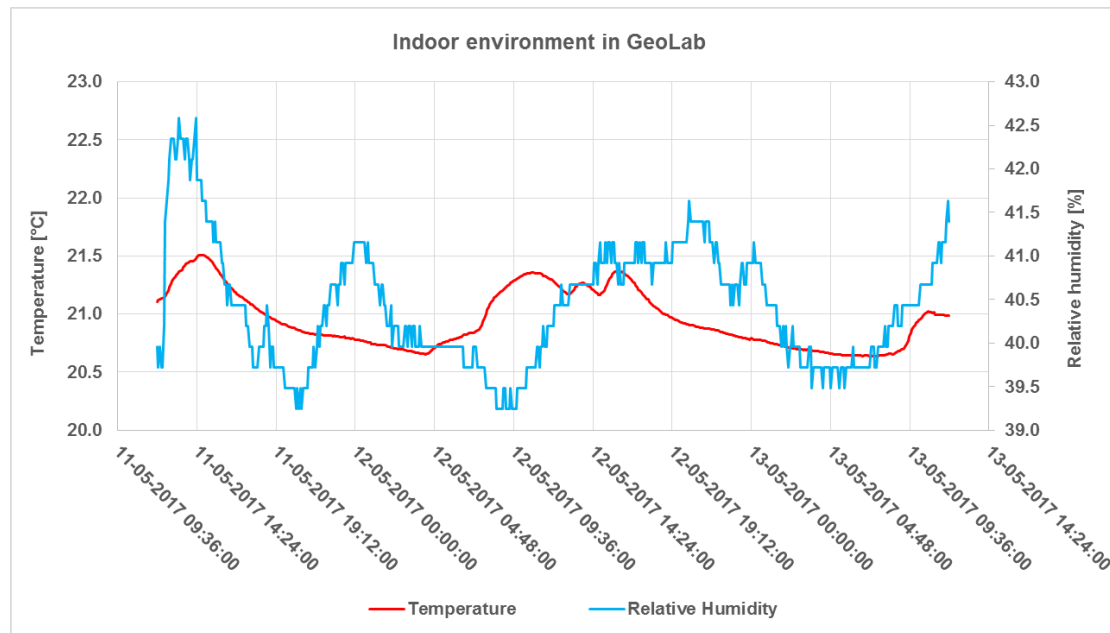
Figure 17: temperature and relative humidity measurements in the GeoLab at VIA University College in Horsens (DK).

Mineralogical analysis

The three types of aggregate have been analysed, prior cleaning and drying. For the Sand 0 – 2 mm, the fraction bigger than 1 mm has been analysed. Table 8 shows the composition of the sample. The main component in the pit sand is quartz.

Table 8: Mineralogical analysis of sand 0-2 mm.

Type	Number of grains	Composition [%]
Quartz	247	62
Crystalline	79	20
Flint	34	9
Sedimentary	14	4
Unstable	24	6
Total	398	100

For the Gravel 4 – 8 mm, Table 9 shows the composition of the sample. The main components in the crushed stone are crystalline rocks, such as granite.

Table 9: Mineralogical analysis of sand 4-8 mm.

Type	Number of grains	Composition [%]
Quartz	2	2
Crystalline	60	61
Flint	26	26
Sedimentary	11	11
Unstable	0	0
Total	99	100

For the gravel 8-16 mm the same mineralogy as for gravel 4-8 mm has been assumed.

Thermal property values from literature

The reference values for the thermal properties have been obtained from VDI (2010) and they are summarised in Table 10. These values are used for the prediction models.

Table 10: Thermal property values considered for prediction models.

Type of rock	Thermal conductivity [W/m/K]	Volumetric heat capacity [MJ/m^3/K]	Density [kg/m^3]	Reference
Quartzite	5.0 - 6.0	2.1	2500 - 2700	
Crystalline	1.9 - 4.6	1.8 - 2.6	2500 - 2700	VDI 4640
Flint	4.5 - 5.0	2.2	2500 - 2700	(2010)
Sedimentary	2.1 - 4.1	2.1 - 3.0	2200 - 2700	
Unstable rock	-	-	-	-

Appendix V. Multiple pile g-functions (Technical report III)

Alberdi-Pagola, M., Jensen, L.J., Madsen, S. And Poulsen, S.E., 2018. "Method to obtain g-functions for multiple precast quadratic pile heat exchangers". Aalborg: Department of Civil Engineering, Aalborg University. DCE Technical Reports; nr. 243, pp. 34. Available online:

http://vbn.aau.dk/files/274763046/Method_to_obtain_g_functions_for_multiple_precast_quadratic_pile_heat_exchangers.pdf

Aalborg Universitet

Method to obtain g-functions for multiple precast quadratic pile heat exchangers

Pagola, Maria Alberdi; Jensen, Rasmus Lund; Madsen, Søren; Poulsen, Søren Erbs

[Link to publication from Aalborg University](#)

DEPARTMENT OF CIVIL ENGINEERING
AALBORG UNIVERSITY

Method to obtain g-functions for multiple precast quadratic pile heat exchangers

Maria Alberdi-Pagola
Rasmus Lund Jensen
Søren Madsen
Søren Erbs Poulsen (VIA University College, Horsens)

Aalborg University
Department of Civil Engineering
Group Name

DCE Technical Report No. 243

Method to obtain g-functions for multiple precast quadratic pile heat exchangers

by

Maria Alberdi-Pagola
Rasmus Lund Jensen
Søren Madsen
Søren Erbs Poulsen (VIA University College, Horsens)

May 2018

Scientific Publications at the Department of Civil Engineering

Technical Reports are published for timely dissemination of research results and scientific work carried out at the Department of Civil Engineering (DCE) at Aalborg University. This medium allows publication of more detailed explanations and results than typically allowed in scientific journals.

Technical Memoranda are produced to enable the preliminary dissemination of scientific work by the personnel of the DCE where such release is deemed to be appropriate. Documents of this kind may be incomplete or temporary versions of papers—or part of continuing work. This should be kept in mind when references are given to publications of this kind.

Contract Reports are produced to report scientific work carried out under contract. Publications of this kind contain confidential matter and are reserved for the sponsors and the DCE. Therefore, Contract Reports are generally not available for public circulation.

Lecture Notes contain material produced by the lecturers at the DCE for educational purposes. This may be scientific notes, lecture books, example problems or manuals for laboratory work, or computer programs developed at the DCE.

Theses are monograms or collections of papers published to report the scientific work carried out at the DCE to obtain a degree as either PhD or Doctor of Technology. The thesis is publicly available after the defence of the degree.

Latest News is published to enable rapid communication of information about scientific work carried out at the DCE. This includes the status of research projects, developments in the laboratories, information about collaborative work and recent research results.

Recent publications in the DCE Technical Report Series

The present report complements a series of technical reports:

Alberdi-Pagola, M., Poulsen, S. E., Jensen, R. L., & Madsen, S. (2017). Thermal response testing of precast pile heat exchangers: Fieldwork report. Aalborg: Aalborg University. Department of Civil Engineering. DCE Technical Reports, No. 234.

Alberdi-Pagola, M., Jensen, R. L., Madsen, S., & Poulsen, S. E. (2017). Measurement of thermal properties of soil and concrete samples. Aalborg: Aalborg University. Department of Civil Engineering. DCE Technical Reports, No. 235.

Contents

Introduction

The average fluid temperature circulating through the ground loop is one of the main parameters required when choosing the most adequate heat pump for a ground source heat pump installation. Besides, the analysis of the fluid temperature over time will show the sustainability of the energy supply over the lifetime of the installation. The average fluid temperature is subjected to the type of ground heat exchangers and the thermal interactions between them, which also depend on the soil thermal properties. For the case of precast piles, the thermal interactions become significant as they are usually placed within short distances (0.5 to 4 metres). Fast models that can account for these interactions are required to enable feasibility studies and support the design phase. Besides, since pile heat exchangers have a main structural role, it is also relevant to develop models that can determine the temperature changes that the foundation might be subjected to, to assess thermo-mechanical implications.

3D finite element model (FEM) computation of the thermal behaviour of multiple pile heat exchanger foundations is not cost effective nor for feasibility studies, nor for most design applications. Therefore, this report describes a method to obtain simpler semi-empirical models based on 3D FEM simulations, called multiple pile g-functions.

The precast quadratic cross section pile heat exchangers analysed in this report have single-U and W-shape pipe heat exchangers and their aspect ratios (AR = Length/Diameter) are limited to 15, 30, 45 and 53. They are further described in [1] and [2]. The proposed g-functions account for the transient heat storage within the pile and are applicable over a range of timescales up to 20 years. This report builds on the methodology described in [3,4] and uses a similar notation. Different g-functions are used to describe the temperature responses of the ground surrounding the pile (ground G-functions G_g) and of the pile itself (concrete G-functions G_c).

The report first defines the g-functions, and then it explores each element required for the calculation of the average fluid temperature. After, some examples are studied, and an error analysis derived from using simplifications in the model is performed before the model is applied to analyse field thermal response test (TRT) data.

G-functions: definitions

The average fluid temperature T_f [°C] circulating through the ground-loop is one of the main parameters required to choose the most adequate heat pump for a ground source heat pump installation. The average fluid temperature T_f can be defined as:

$$T_f = T_0 + \frac{q}{2\pi\lambda_s}G_g + qR_cG_c + qR_{pipe} \tag{1}$$

Where T_0 [°C] is the undisturbed soil temperature, q [W/m] is the heat transfer rate per metre length of pile heat exchanger, λ_s [W/m/K] is the thermal conductivity of the soil, G_g is the g-function describing the ground temperature response, R_c [K·m/W] is the steady state concrete thermal resistance, G_c is the concrete g-function describing the transient concrete response and R_{pipe} [K·m/W] is the thermal resistance of the pipes. In the following, each term of Equation 1 will be analysed.

G-functions are dimensionless response factors that describe the change in temperature in the ground around a heat exchanger with time as a result of an applied thermal load q [5]. Usually, both temperature change and time are normalised. In this study, the normalised temperature changes Φ and time Fo are defined as:

$$\Phi = \frac{2\pi\lambda_s\Delta T}{q} \tag{2}$$

$$Fo = \frac{\alpha_s t}{r_b^2} \tag{3}$$

where ΔT [K] is the temperature change between the undisturbed soil temperature T_0 [°C] and the average pile wall temperature T_b [°C], α_s [m²/s] is the thermal diffusivity, i.e., the ratio between the thermal conductivity λ_s [W/m/K] and the volumetric heat capacity of the soil ρc_{ps} [J/m³/K], t [s] is the time and r_b [m] is the pile equivalent radius. The pile radius is the radius that provides an equivalent circumference to the square perimeter.

G-functions are used to calculate the pile wall temperature. For a single pile, the pile wall temperature depends on time and its aspect ratio ($L/2r_b$), and it can be determined as:

$$T_b = T_0 + \frac{q}{4\pi\lambda_s} \cdot G(Fo, \frac{L}{2r_b}) \tag{4}$$

G-functions can be obtained by analytical, numerical and empirical methods. The pile g-functions presented in this study are semi-empirical models based on 3D FEM of a single pile heat exchanger,

where temporal and spatial superposition techniques ease the consideration of the thermal influence between piles.

Single pile G-function G_g

The methods to obtain single pile g-functions are given before the simulation results are analysed.

Methods

The ground temperature response functions G_g, or single pile G-functions, are based on 3D numerical analyses and are valid for time ranges $0.1 < Fo < 10000$. These functions describe the time dependent pile wall temperature evolution under a constant thermal load. As this temperature response will be affected by the surface boundary, i.e., it will be affected by the length of the pile heat exchanger, different pile aspect ratios AR have been considered. Based on the most common produced precast piles, aspect ratios of 15, 30, 45 and 53 and single-U and W-shape pipe arrangements have been considered. The numerical models were constructed using the software COMSOL Multiphysics [6] and they comprise a full representation of the pile, the built-in pipes and the surrounding soil (Figure 1).

The model contains the ground surrounding the pile up to a radial distance of 25 m and beneath the base of the pile to 25 m. The soil and concrete properties used in the model are given in Table 1. The properties are assumed constant with temperature changes due to the relatively small temperature changes related to energy geostructure applications. The radial outer, top and base boundaries are kept at a constant temperature of 10 °C. The initial temperature is set to 10 °C everywhere in the model and groundwater flow was neglected.

Model tests were made to ensure that the modelled temperatures are independent to the chosen temporal and spatial discretisation. The mesh is refined in the immediate vicinity of the pile, it expands towards the model outer boundary and it comprises tetrahedral, prismatic, triangular, quadrilateral, linear and vertex elements. The models have been verified in [1].

To guarantee the maintenance of a specific heat injection rate [W/m], an inlet temperature history was dynamically generated during the simulation by coupling the inlet to the outlet temperature of the previous time step. The water flow is ensured turbulent. 20-year simulations are performed. The temperature response at the pipe boundary, at the edge of the pile and the soil are recorded by the model.

Table 1: Properties of the materials used in the models.

Parameters [units]	Values
Volumetric heat capacity concrete ρc_{pc} [MJ/m³/K]	2.00
Thermal conductivity concrete λ_c [W/m/K]	2.00
Volumetric heat capacity soil ρc_{ps} [MJ/m³/K]	2.00
Thermal conductivity soil λ_s [W/m/K]	1.00, 2.00, 4.00
Thermal conductivity pipe λ_{pipe} [W/m/K]	0.42
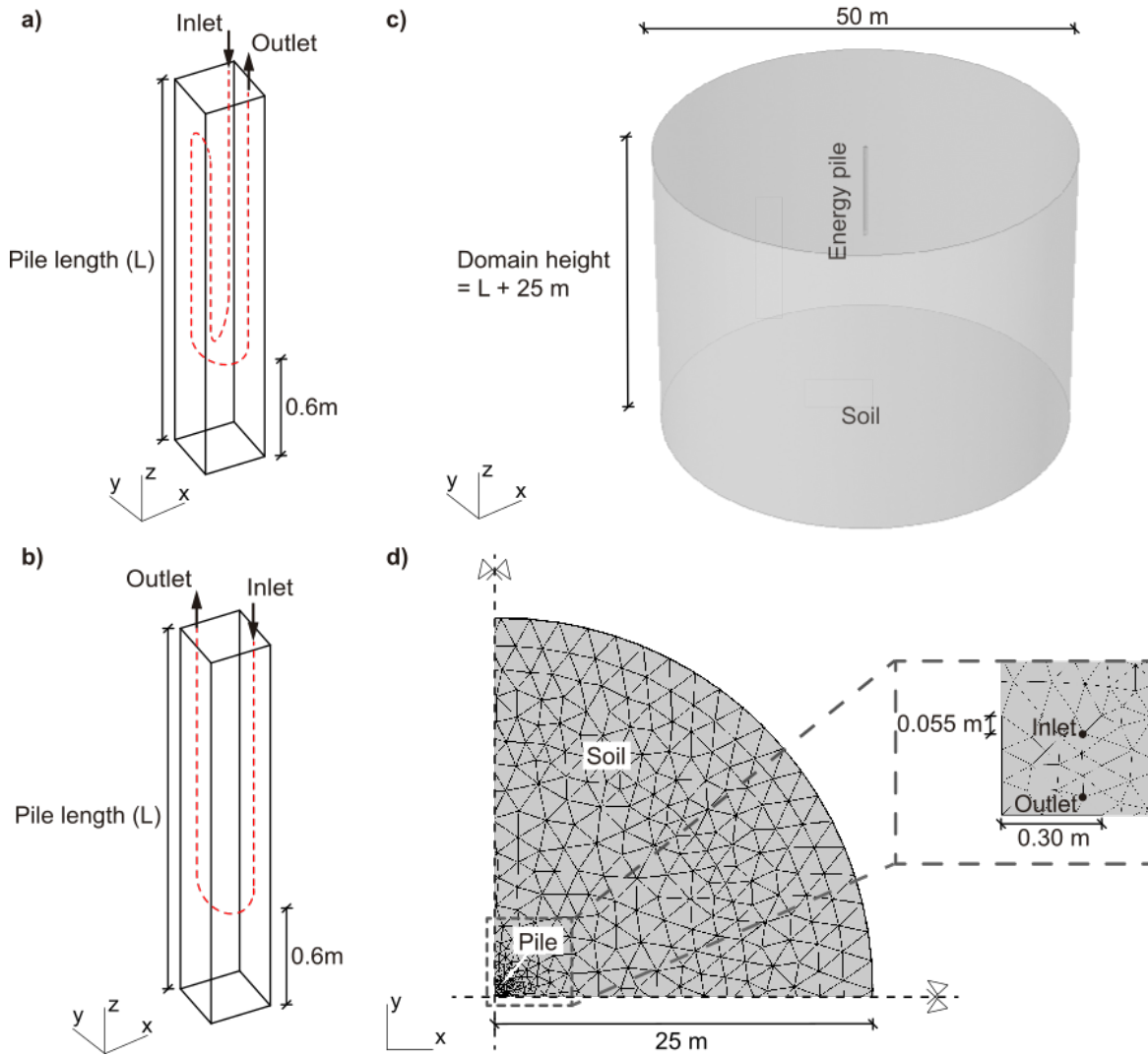
Figure 1: Description of the 3D finite element model: a) schematic of the W-shape pile heat exchanger; b) schematic of the single-U pile heat exchanger; c) simulated domains; d) top view of a quarter domain.

To sum up, the following assumptions have been considered for the derivation of the model:

- The ground is regarded as homogeneous medium and its thermo-physical properties do not change with temperature.
- The medium has a uniform initial temperature.

- The heating rate per unit length is constant from the starting instant.

- A constant ground surface temperature has been imposed.

- No heat convection due to groundwater flow has been considered.

- The steel reinforcement is not modelled since it has not a significant effect on the overall thermal performance of the pile [7].

Simulation results

A common way to show the temperature response factors in literature, is by computing the dimensionless temperature Φ over time Fo as a result of a constant thermal load, i.e., resembling a long thermal response test. Based on simulated average temperatures around the pile perimeter, a summary of the model ground temperature responses G_g are presented in Figure 2. A range of curves is possible depending on the aspect ratio AR, the size of the pile and the relative properties of the pile concrete and the surrounding ground. Figure 2 depicts the cases where the thermal conductivities of soil λ_s and concrete λ_c are the same.

For easier implementation of the temperature response functions G_g curve fitting has been carried out for the G-functions presented in Figure 2, in a similar way to the process followed by [3,8]. The results are contained in Appendix A.

The impact of the concrete thermal conductivity λ_c will be taken into account by consideration of the relative conductivities of the ground and the concrete (λ_c/λ_s) in the temperature response of the pile concrete itself, which is discussed in the next section.
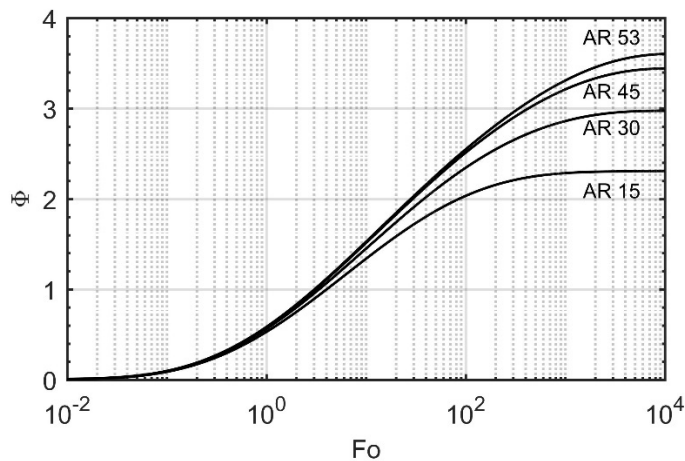
Figure 2: Pile G-functions for precast pile heat exchangers with different aspect ratios (AR) 15, 30, 45 and 53.

Concrete G-functions *G_c*

First, the method to obtain the transient concrete G-function G_c is described and simulation results are analysed afterwards.

Methods

The concrete G-function, as defined by [3,9], describes the transient thermal resistance of the pile heat exchangers. It depends on the shape of the pile cross section, the position of the pipes and the thermal conductivity of the concrete λ_c. That is, it defines the thermal resistance of the concrete part. To incorporate the transient response of the pile concrete into the overall temperature response function (Equation 1), the proportion of the steady state thermal resistance that has been achieved at a given value of time Fo has been calculated using the temperature field output from the 3D FEM. Ref. [1] demonstrated that 96% of the steady state in the concrete is reached by 100 hours (Fo ≈ 10). The thermal resistance of the concrete part of the pile is calculated over time as:

$$R_c = \frac{T_p - T_b}{q} \tag{5}$$

where T_p [°C] is the average temperature on the outer wall of the pipe.

Simulation results

The steady state resistance is the asymptotic value of Equation 5 calculated at large values of time, when Fo approaches 1000 [3]. It can be calculated numerically, as it was done in [1], for different pipe arrangements and a range of concrete thermal conductivities λ_c. As presented in [1], the aspect ratio of the pile does not considerably affect the concrete thermal resistance R_c. Figure 3a shows the most conservative cases. The range of laboratory measurements of the thermal conductivity of the concrete λ_c, reported in [1,10], have been added. This limits the concrete thermal resistances to a narrower range.

The proportion of the steady state value of the concrete thermal resistance R_c is shown in Figure 3b for single-U and W-shape piles. The case for $\lambda_c/\lambda_s = 1$ is shown. Curves for different λ_c/λ_s ratios (0.5 and 2) are given in the corresponding Appendix C.

To allow the calculation of the steady state R_c values and to ease the implementation of the response curves as concrete G-functions, curve fit data are presented in Appendix B and Appendix C, respectively.

a)

b)
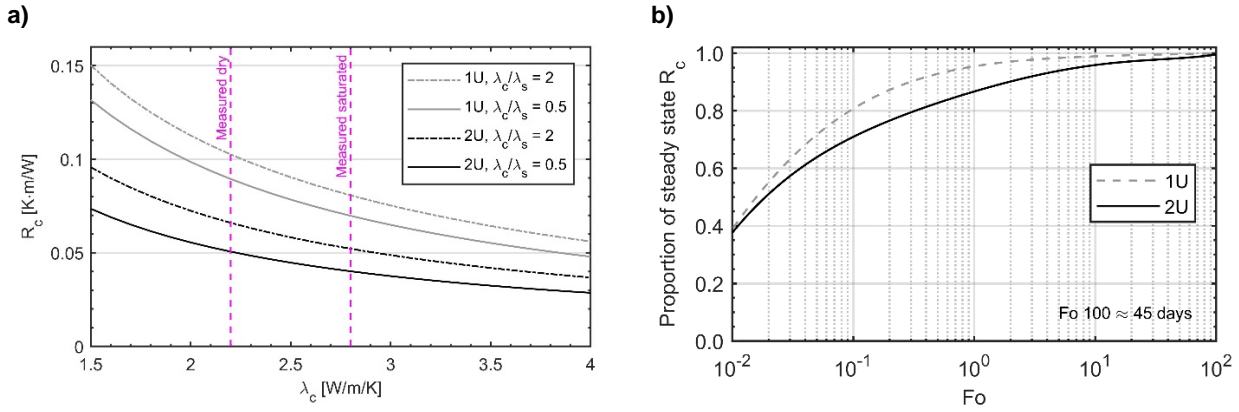
Figure 3: a) Upper and lower bounds for the steady state concrete thermal resistance R_c for square precast pile heat exchangers for 30x30 cm^2 with single-U (1U) and W-shape (2U) pipes obtained from 3D FEM modelling for a range of concrete thermal conductivities, after [1]. b) Proportion of steady state R_c for time for single-U (1U) and W-shape (2U) piles.

Pipe thermal resistance R_{pipe}

The method to obtain the pipe thermal resistance is shortly described before an analysis of the results is given.

Methods

The heat exchanger pipes pose an obstacle for the heat to be dissipated from the circulating fluid towards the pile and the soil and vice versa. Thus, a pipe thermal resistance needs to be considered. The heat transfer process within the pipes will reach steady state rapidly and, hence, the pipe thermal resistance is considered constant. The pipe thermal resistance R_{pipe} [K·m/W] is defined in Equation 6 as the sum of the pipe convective (first term on right hand side) and conductive (second term on right hand side) resistances:

$$R_{pipe} = \frac{1}{2n\pi r_i h_i} + \frac{\ln(r_o/r_i)}{2n\pi \lambda_{pipe}} \tag{6}$$

where n is the number of pipes in the pile heat exchanger cross section, r_i [m] is the inner radius of the pipe, r_o [m] is the outer radius of the pipe, h_i [W/m^2/K] is the heat transfer coefficient and λ_{pipe} [W/m/K] is the thermal conductivity of the pipe material. h_i can be calculated using the Gnielinski correlation as described in [11,12].

Results

The pipe thermal resistances for different pipe configurations (single-U and W-shape) and different pipe diameters Ø are shown in Figure 4 for a range of Reynolds numbers. The Reynolds number is

a dimensionless quantity that establishes whether a circulating fluid flows at laminar, transient or turbulent regime [11,12]. The pipe thermal resistance significantly decreases in the change from laminar to turbulent flow. However, it does not meaningfully improve once turbulence is reached.
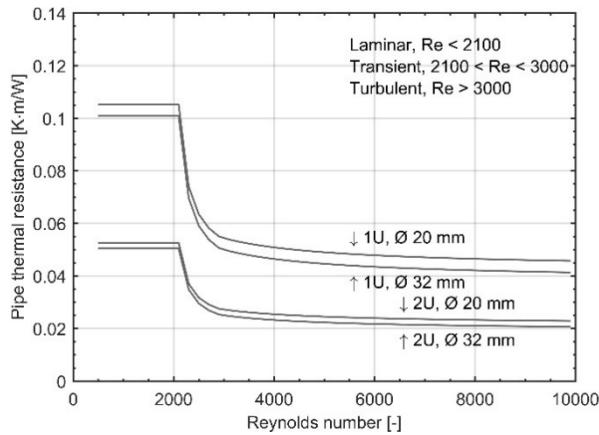
Figure 4: Pipe thermal resistance VS Reynolds number for different pipe arrangements and pipe diameters Ø.

Multiple pile g-functions

First, the methods to obtain multiple pile g-functions are described and simulation results are analysed afterwards.

Methods

The multiple pile heat exchanger g-functions are based on the temperature fields extracted from the 3D FEM described in the section "Single pile G-functions G_g" and in Figure 1. The simulations are used to obtain, in addition to the pile wall temperature, soil temperatures at required radial distances, r = S [m], that would resemble pile spacing.

The multiple pile g-functions provide the change in the average pile wall temperature over time of all the piles comprising the foundation. I.e., the g-function gives the pile wall temperature for a specific foundation configuration due to a constant heat input rate [13]:

$$T_b = T_0 - \frac{q}{4\pi\lambda_s} \cdot g(Fo, \frac{L}{2r_b}, \frac{S}{2r_b}) \tag{7}$$

where T_b [°C] is the pile wall temperature common to all piles, T_0 [°C] is the undisturbed ground temperature, q [W/m] is the average heat extraction rate per pile length, λ_s [W/m/K] is the ground thermal conductivity, g is the multiple pile g-function. For the case of pile heat exchanger foundations or groups, the multiple g-functions depend on three non-dimensional parameters: the dimensionless time, the AR ($L/2r_b$), being L [m] the active length of the pile heat exchanger and the foundation aspect ratio $S/2r_b$, being S the centre to centre pile spacing, as defined in [4].

For various piles, the g-function can be calculated by applying temporal and spatial superposition of the single pile G-function and radial temperatures. This principle relies on the heat conduction equation and boundary conditions on being linear [13].

In the spatial superposition the temperature distributions around every ground heat exchanger are added in order to calculate the overall temperature variation at the pile walls [14]:

$$\Delta T_b(t) = \frac{1}{n_p} \sum_{i=1}^{n_p} \sum_{j=1}^{n_p} \Delta \overline{T}(d_{ij}, t) \tag{8}$$

$$d_{ij} = \begin{cases} r_b, & i = j \\ \sqrt{(x_i - x_j)^2 + (y_i - y_j)^2}, & i \neq j \end{cases} \tag{9}$$

where ΔT_b [K] is the average temperature variation at the pile heat exchanger wall, (x_i, y_i) [m] are the coordinates of the ith pile heat exchanger, n_p is the number of pile heat exchangers in the foundation and d_{ij} [m] is the pile distance.

Time variations can be applied by deconvolution of the time varying heat transfer rate [13]. The temperature at discrete time step in the pile heat exchanger foundation is computed as:

$$\Delta T_n = \sum_{i=1}^{i=n} \frac{q_i}{2\pi\lambda_s} \left(G(Fo_n - Fo_{(i-1)}) - G(Fo_n - Fo_i) \right) \tag{10}$$

In an energy foundation, the pile heat exchangers can be connected in series and/or in parallel. This study analyses pile heat exchangers connected in parallel. This has an impact on the temperatures that develop around each individual heat exchanger. It is assumed that the heat extraction rates are uniform and equal for all the energy piles. As a result of this boundary condition, identified as boundary condition BC I in [15], the average temperatures along the length of all the piles are unequal. Hence, the average of the mean pile wall temperatures is used in the evaluation of the g-function.

Simulation results

Radial soil temperatures

Based on simulated average soil temperatures at increasing radial distances S from the pile centre, a summary of the dimensionless ground temperature responses Φ plotted against normalised time Fo are presented in Figure 5. The uppermost curve corresponds to the earlier described single pile G-function (Figure 2) as it represents the pile wall temperature. The rest of the curves correspond to

increasing normalised radial distances, from top to bottom, i.e., the bigger the distance, the smaller the thermal influence.
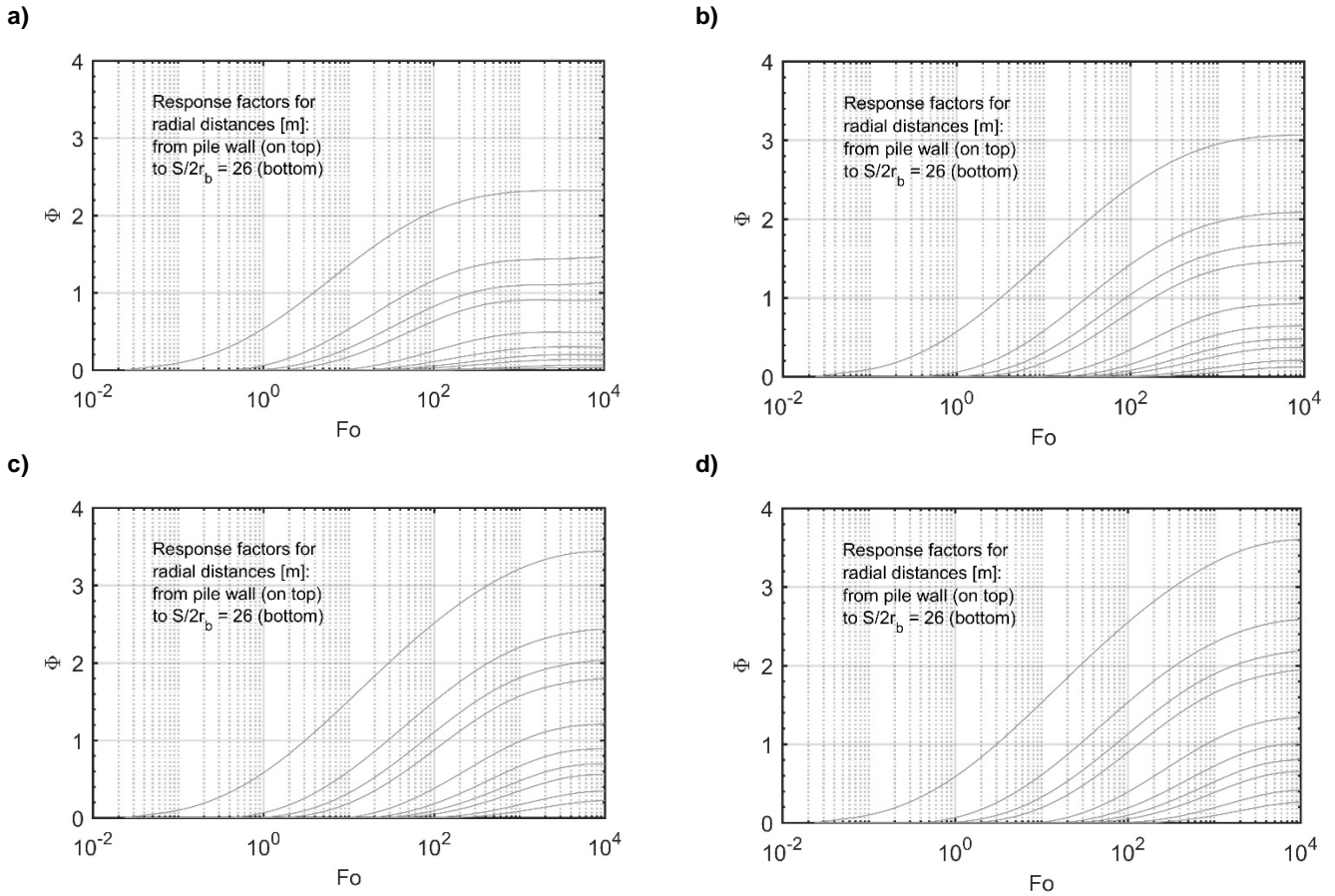
Figure 5: Dimensionless temperature responses for soil temperature changes at normalised distances $S/2r_b = T_b$, 1.3, 2, 2.6, 5.2, 7.9, 10.5, 13.1, 19.6, 26: a) aspect ratio 15; b) aspect ratio 30; c) aspect ratio 45; d) aspect ratio 53.

To ease the implementation, empirical equations for the curves have been calculated. The curve fitting parameters are provided in the corresponding Appendix D. For values of AR and distances that are not considered in the tables of coefficients, a linear interpolation needs to be applied to obtain the g-functions. Linear interpolations are considered sufficient precise and quick [8]. This issue is further described in the following section "Error analysis".

The curves provided in Figure 5 can be superimposed in time and space to account for multiple piles. A thorough analysis of two interacting piles is used to analyse the main implications on the response factors [4]. Figure 6 reproduces the influence of the aspect ratio for several pile spacings: i) the closer the piles, the greater the temperature changes at steady state; ii) the higher the aspect ratio, the greater the degree of interaction between piles. Piles with higher aspect ratios have a higher overall temperature change and they influence a further distance in the ground due to the later influence of the surface boundary, in contrast to the piles with lower aspect ratios. Therefore, low aspect ratio piles might be more efficient.

a)

b)

c)

d)
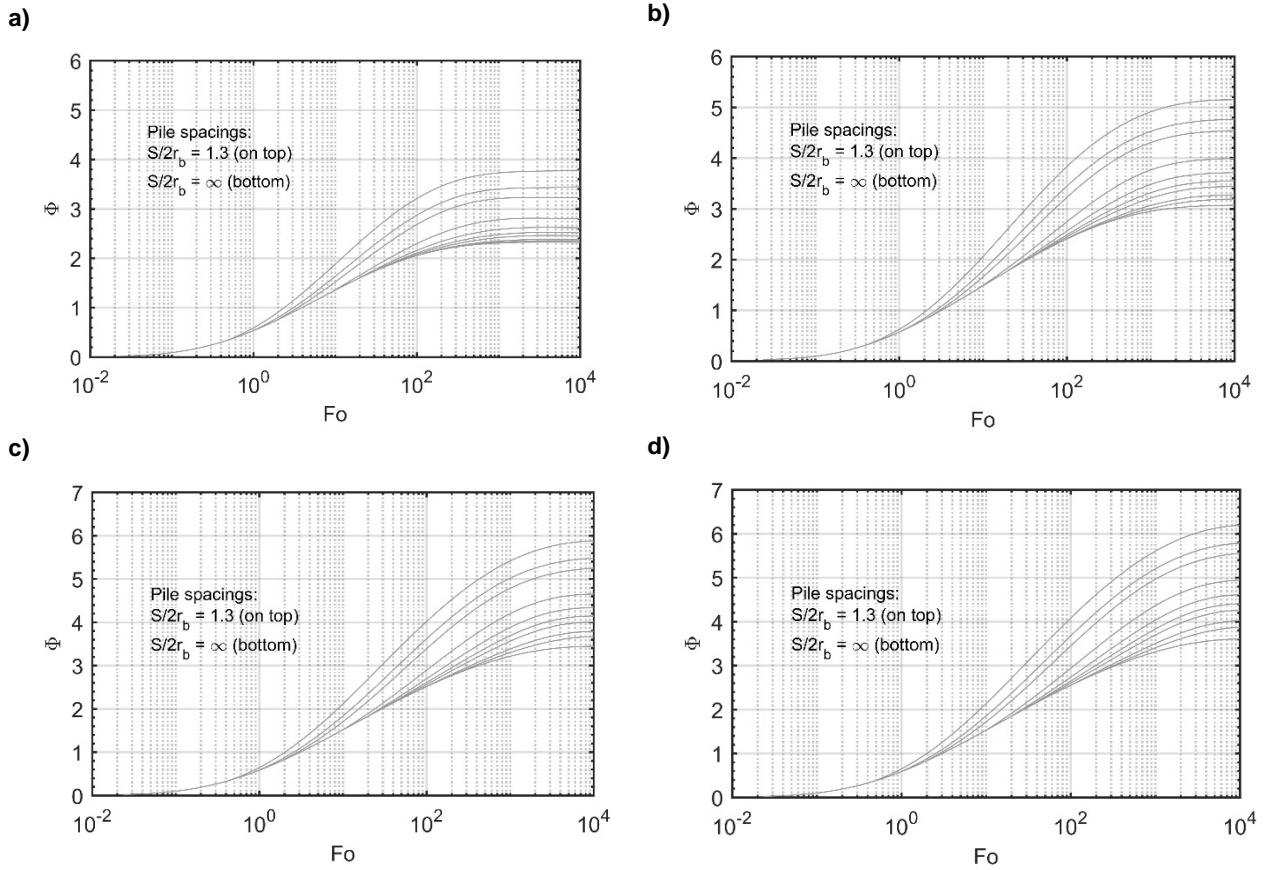
Figure 6: Response factors for two interacting piles at pile spacings S/2r$_b$ = 1.3, 2, 2.6, 5.2, 7.9, 10.5, 13.1, 19.6, 26.2, ∞ (= single pile); a) aspect ratio 15; b) aspect ratio 30; c) aspect ratio 45 and d) aspect ratio 53.

Figure 7 plots the percentage increase of the dimensionless temperature Φ with normalised distance S/2r$_b$ for normalised times Fo equal to 0.1, 1, 10, 100, 1000 and 10000. The interactions are mild at small values of time regardless of the pile spacing and pile geometry. However, as time increases, larger aspect ratio piles interact more and for longer.
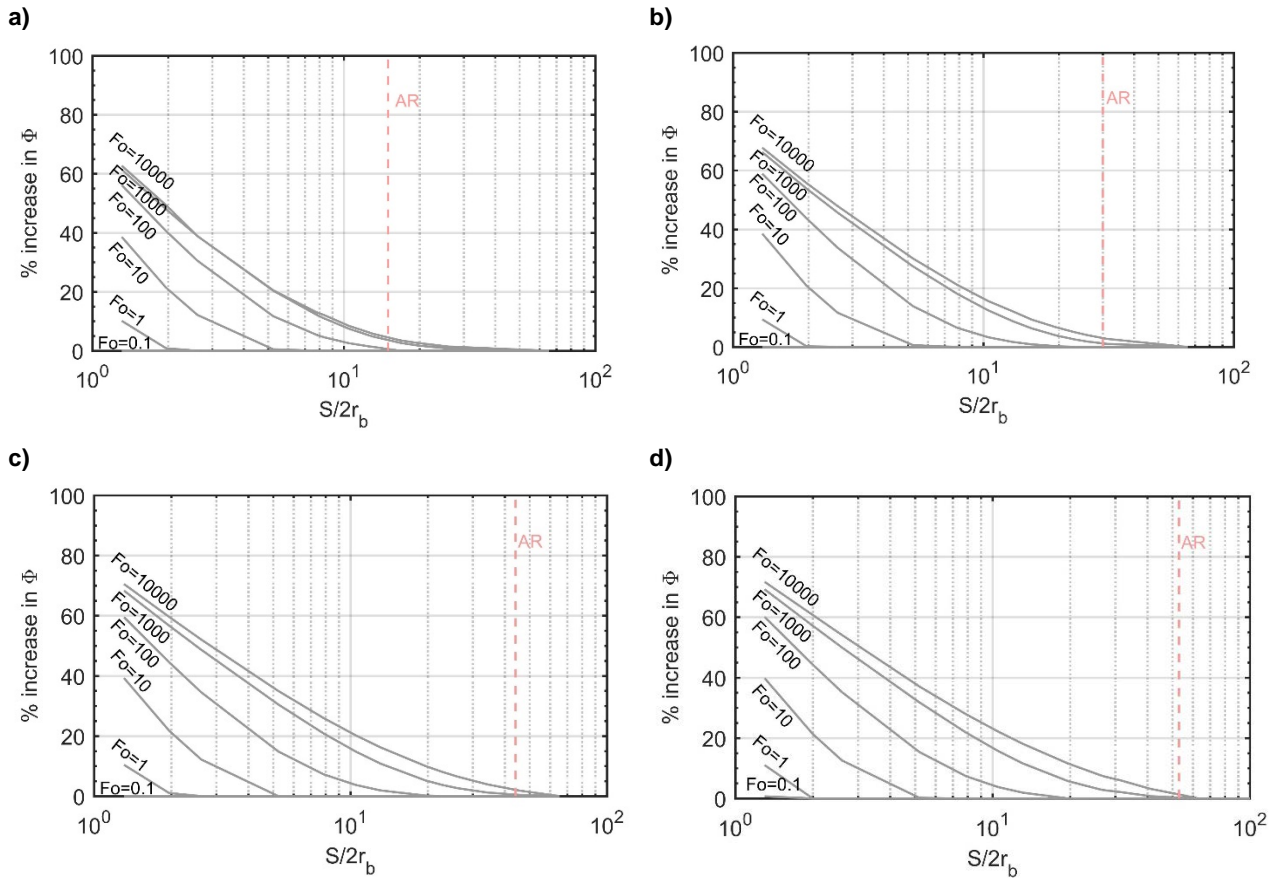
Figure 7: Percentage increase in dimensionless temperature for different normalized pile spacings; a) aspect ratio 15; b) aspect ratio 30; c) aspect ratio 45; d) aspect ratio 53.

It is assumed that there is no interference between borehole heat exchangers if the borehole spacing is bigger than its length and interactions are small for spacings half the length [5]. Loveridge and Powrie [4] defined that for pile heat exchangers, that criterion is equivalent to $S/2r_b > AR$. For a pile heat exchanger foundation, where the pile positions and spacings are governed by structural and geotechnical requirements of the building, interaction will happen since the minimum pile spacing will be lower than 5 m, for the case of precast pile heat exchangers.

Representative foundation patterns

Specific regular patterns (listed in Table 2) for pile aspect ratio 45 have been selected to investigate multiple pile g-functions with different pile spacings.

Table 2: Selected pile heat exchanger field configurations.

Pile arrangement	Pile spacing S [m]
1x2	1, 3, 5
1x3	1, 3, 5
2x3	1, 3, 5
2x4	1, 3, 5
3x3	1, 3, 5
4x4	1, 3, 5

Figure 8 shows g-functions in the form of non-dimensional curves Φ and the significant impact that multiple pile heat exchangers can have when interacting is illustrated for aspect ratio 45. For a single pile, i.e., when the pile spacing approaches infinity, the long term steady state normalized temperature response is approximately 3.4. For two piles at 1 m, the response increases to 5, for three piles and sixteen piles at the same spacing is 6.5 and 21.5, respectively. These increases will result in a corresponding decrease in the energy that can be exchanged per linear metre of the pile, as demonstrated in [4].
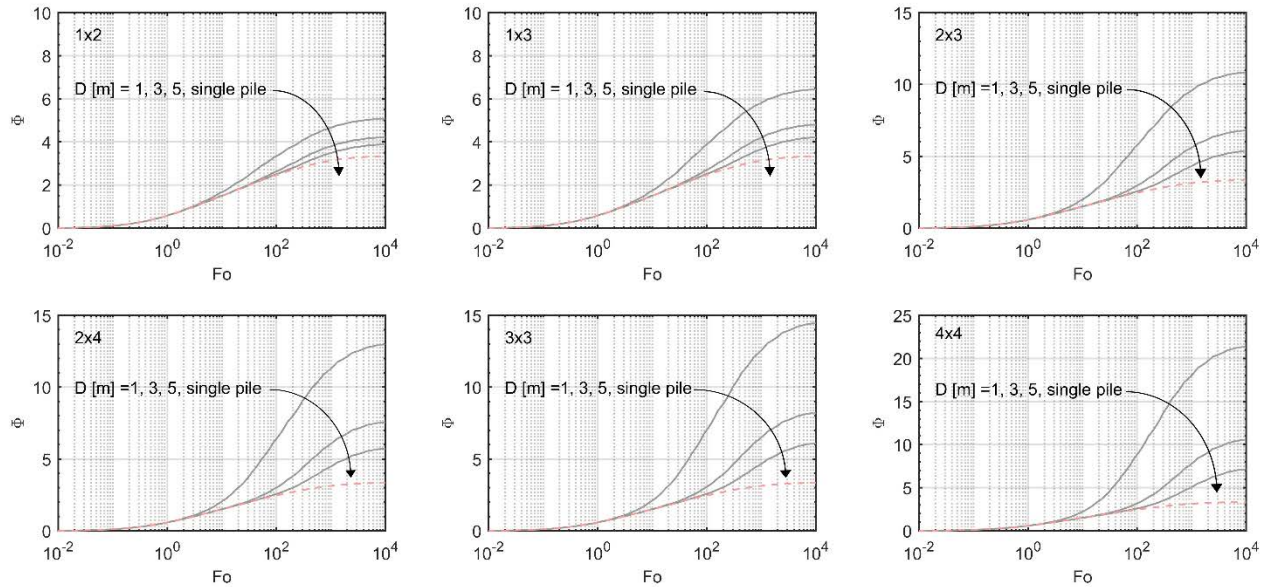
Figure 8: Multiple pile g-functions for different pile arrangements for aspect ratio AR 45 pile heat exchangers. The red dashed line represents the single pile g-function, i.e., an infinite pile spacing.

Table 3 summarises the increase in dimensionless temperature Φ for spacings of 1, 3 and 5 m and Table 4 provides the energy output percentage for different pile arrangements compared to a single pile. It is highlighted that at steady state with six piles in a 2x3 grid, each pile is only delivering 31% of the energy of an individual isolated pile.

For the case of precast piles, it is common to drive them in clusters, sometimes placed at distances below 1 m. In the case that all piles are equipped as pile heat exchangers, this would lead to an increase of the interactions, what is detrimental for the installation. It may be more cost-effective to equip only some of these piles with heat transfer pipes.

Table 3: Steady state increase in Φ for different pile arrangements compared to a single pile (AR = 45).

Pattern Spacing	Single pile	1x2	1x3	2x3	2x4	3x3	4x4
1 m	-	52	93	225	290	334	542
3 m	-	26	44	104	127	147	217
5 m	-	17	26	61	72	83	114

Table 4: Energy output [%] for different pile arrangements compared to a single pile (AR = 45).

Pattern / Spacing	Single pile	1x2	1x3	2x3	2x4	3x3	4x4
1 m	-	66	52	31	26	23	16
3 m	-	79	69	49	44	41	32
5 m	-	86	79	62	58	55	47

Limitations of the model

There are several error sources when developing the semi-empirical multiple pile g-functions and that will affect its accuracy. There are errors derived from: i) fitting polynomials to the raw 3D FEM data; ii) interpolating between distances where data is not given; iii) simplifying the pile to a point without considering its volume.

The errors derived from the polynomial simplification are minimal, as it can be checked in the goodness of fit available in the appendix tables. I.e., the errors derived from the data fit for the selected distances extracted from the single pile with soil 3D FEM model are low.

The main errors are expected to come from the spatial interpolation, for pile spacings where raw data are not available. Tables 5 and 6 show the errors derived from using interpolation and the sensitivity of the error to the type of interpolation (linear or cubic). Here, the last time step of the multiple pile g-function is compared for the 4x4 pattern with 1 and 3 m pile spacings.

Table 5: g-function value for the 4x4 pattern with 1 m pile spacing.

Type of interpolation	Interpolated g-function	No-interpolated g-function	Error [%]
Linear	22.3	21.7	2.6
Cubic	22.1		1.8
Error [%]	0.9	-	

Table 6: g-function value for the 4x4 pattern with 3 m pile spacing.

Type of interpolation	Interpolated g-function	No-interpolated g-function	Error [%]
Linear	11.0	10.7	2.5
Cubic	10.9		1.7
Error [%]	0.9	-	

The errors assigned to the spatial interpolation are small for the purpose of this study, around 2.5%. Hence, linear interpolation is assumed acceptable, yet cubic interpolation is advised. However, it needs to be considered that these errors will accumulate as the amount of piles increases. The inaccuracies derived from these errors will be analysed in a journal paper, where the discrepancies between the temperatures computed with the proposed g-functions and full 3D finite element models of multiple piles will be discussed.

Besides, the model has the following limits:

- It does not account for the case of groundwater flow.
- It is applicable when soil stratification does not affect thermal properties significantly.
- It does not account for heat gains/losses from surface, such as heat gains from the building or solar gains.

Interpretation of TRT data

Once all the terms are analysed, the average fluid temperature in the ground-loop is calculated following Equation 1. To explore the applicability of these semi-empirical models, interpretation of precast pile heat exchanger TRT data has been performed.

Methods

The analysed precast pile heat exchanger TRT data are available in [16]. The inverse modelling approach is the same as described in [1]: the parameter estimation is performed with PEST [17] and the model is based on Equation 1, from where the inverse modelling yields estimates of the thermal conductivity of the soil λ_s [W/m/K] and the steady state concrete thermal resistance R_c [Km/W].

Results

Five TRTs have been analysed: LM1 corresponds to a single-U pile heat exchanger while the other four have a W-shape pipe arrangement. The results are compared to the 3D FEM calibration estimates reported in Table 5 in [1]. Figure 9 shows the parameter estimates normalised by the 3D FEM results.
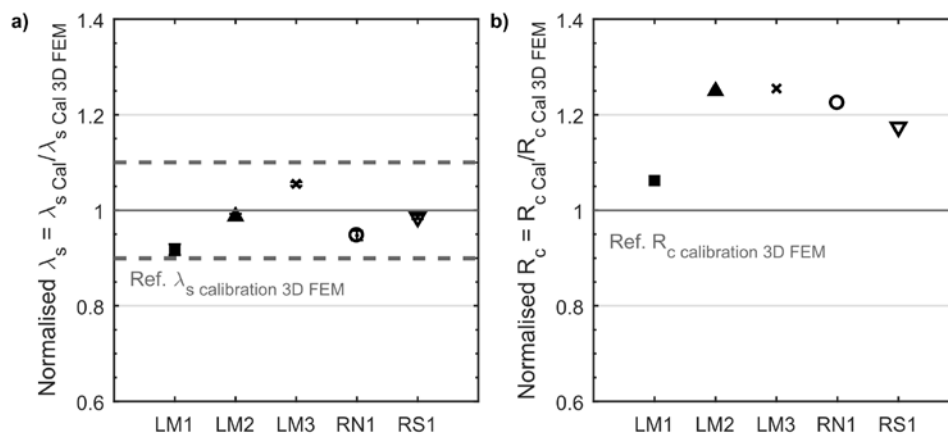
Figure 9: Parameter estimates from calibration of the semi-empirical models normalised by the 3D EFM based estimates. a) Thermal conductivity of soil λ_s; the uncertainty bounds correspond to the largest uncertainty obtained in the calibration of the 3D FEM models (test RN1); b) Concrete thermal resistance; uncertainties are not shown as they are insignificant (order of 10^{-2} Km/W). LM1: single-U. LM2, LM3, RN1 and RS1: W-shape.

The semi-empirical models provide a reliable estimation of the thermal conductivity of the soil λ_s. However, they tend to overestimate the concrete thermal resistance R_c by 20% and 6% for the W-shape and single-U piles, respectively. The proposed models show acceptable results and can be used for TRT interpretation.

Conclusions

This report presented in detail the methodology to obtain multiple precast pile heat exchanger g-functions, its different parameters, errors and applications. It has been demonstrated that this energy pile heat flux model is able to yield acceptable estimates of thermal conductivity of the soil λ_s [W/m/K] and pile concrete thermal resistance R_c [Km/W], when is used to interpret thermal response test data. The proposed method allows a fast assessment of the ground-loop fluid temperatures.

The polynomial expressions presented in this report will be compared to multiple pile 3D finite element models in a journal paper, where their suitability will be assessed, and the nature of the discrepancies will be discussed.

References

[1] M. Alberdi -Pagola, S.E. Poulsen, F. Loveridge, S. Madsen, R.L. Jensen, Comparing heat flow models for interpretation of precast quadratic pile heat exchanger thermal response tests, Energy. 145 (2018) 721–733. doi:10.1016/j.energy.2017.12.104.

[2] M. Alberdi -Pagola, S.E. Poulsen, R.L. Jensen, S. Madsen, Thermal response testing of precast pile heat exchangers: fieldwork report, Aalborg University, Aalborg, Denmark, 2017. http://vbn.aau.dk/files/266379225/Thermal_response_testing_of_precast_pile_heat_exchangers_fieldwork_report.pdf.

[3] F. Loveridge, W. Powrie, Temperature response functions (G-functions) for single pile heat exchangers, Energy. 57 (2013) 554–564. doi:http://dx.doi.org/10.1016/j.energy.2013.04.060.

[4] F. Loveridge, W. Powrie, G-Functions for multiple interacting pile heat exchangers, Energy. 64 (2014) 747–757. doi:http://dx.doi.org/10.1016/j.energy.2013.11.014.

[5] P. Eskilson, Thermal Analysis of Heat Extraction, University of Lund, Sweden, 1987.

[6] COMSOL Multiphysics, Introduction to COMSOL Multiphysics version 5.3, Burlington, 2017.

[7] S.L.A.M. Abdelaziz, Deep energy foundations: geotechnical challenges and design considerations, Virginia Polytechnic Institute and State University, Blacksburg, Virginia, 2013.

[8] E. Zanchini, S. Lazzari, Temperature distribution in a field of long Borehole Heat Exchangers (BHEs) subjected to a monthly averaged heat flux, Energy. 59 (2013) 570–580. doi:https://doi.org/10.1016/j.energy.2013.06.040.

[9] F. Loveridge, W. Powrie, 2D thermal resistance of pile heat exchangers, Geothermics. 50 (2014) 122–135. doi:http://dx.doi.org/10.1016/j.geothermics.2013.09.015.

[10] M. Alberdi-Pagola, R.L. Jensen, S. Madsen, S.E. Poulsen, Measurement of thermal properties of soil and concrete samples, Aalborg University, Aalborg, Denmark, 2017. http://vbn.aau.dk/files/266378485/Measurement_of_thermal_properties_of_soil_and_concrete_samples.pdf.

[11] R. Al-Khoury, Computational modeling of shallow geothermal systems, CRC Press, 2011.

[12] H.-J.G. Diersch, FEFLOW Finite Element Modeling of Flow, Mass and Heat Transport in Porous and Fractured Media, Springer Science & Business Media, 2014. doi:10.1007/978-3-642-38739-5.

[13] J.D. Spitler, M. Bernier, 2 - Vertical borehole ground heat exchanger design methods A2 - Rees, Simon J, in: Adv. Ground-Source Heat Pump Syst., Woodhead Publishing, 2016: pp.

29–61. doi:http://dx.doi.org/10.1016/B978-0-08-100311-4.00002-9.

[14]   M. Cimmino, M. Bernier, F. Adams, A contribution towards the determination of g-functions using the finite line source, Appl. Therm. Eng. 51 (2013) 401–412. doi:http://dx.doi.org/10.1016/j.applthermaleng.2012.07.044.

[15]   M. Cimmino, M. Bernier, A semi-analytical method to generate g-functions for geothermal bore fields, Int. J. Heat Mass Transf. 70 (2014) 641–650. doi:10.1016/j.ijheatmasstransfer.2013.11.037.

[16]   M. Alberdi-Pagola, Thermal response test data of five quadratic cross section precast pile heat exchangers, Data Br. 18 (2018) 13–15. doi:10.1016/j.dib.2018.02.080.

[17]   J. Doherty, PEST Model-Independent Parameter Estimation. User Manual, 5th Editio, 2010. file:///C:/Users/maap/Downloads/pestman.pdf.

Appendix

A) Curve fit results for ground temperature response functions: pile G-functions G_g

The ground temperature response G-functions for each AR are valid for $0.1 < Fo < 10000$. G_g can be described as:

$$G_g = a \cdot \ln(Fo)^9 + b \cdot \ln(Fo)^8 + c \cdot \ln(Fo)^7 + d \cdot \ln(Fo)^6 + e \cdot \ln(Fo)^5$$
$$+ f \cdot \ln(Fo)^4 + g \cdot \ln(Fo)^3 + h \cdot \ln(Fo)^2 + i \cdot \ln(Fo) + j \tag{11}$$

The curve fitting parameters are defined in Table 5. For $Fo < 0.1$, G_g should be set to zero.

Table 7: Curve fitting parameters for ground response factors G_g.

	AR = 15	AR = 30	AR = 45	AR = 53
a	4.04E-09	-6.133E-09	4.199E-09	4.938E-09
b	-6.28E-08	1.568E-07	-3.525E-08	-4.061E-08
c	-7.71E-07	-1.134E-06	-8.541E-07	-9.857E-07
d	1.31E-05	-2.850E-06	8.311E-06	8.874E-06
e	6.89E-05	1.151E-04	6.477E-05	7.218E-05
f	-1.06E-03	-7.257E-04	-8.423E-04	-8.504E-04
g	-4.70E-03	-4.868E-03	-3.519E-03	-3.562E-03
h	4.04E-02	4.514E-02	4.648E-02	4.713E-02
i	2.97E-01	3.243E-01	3.245E-01	3.272E-01
j	5.34E-01	5.689E-01	5.817E-01	5.854E-01
RMSE*	6.35E-06	1.138E-05	1.658E-05	1.665E-05
R^{2}**	9.999E-01	9.999E-01	9.999E-01	9.998E-01

*RMSE: Root Mean Squared Error
**R^2: Coefficient of Determination

B) *Steady state concrete thermal resistance values R_c*

The upper and lower bounds for the concrete thermal resistance R_c for square precast pile heat exchangers with single-U- and W-shape pipes for a range of thermal conductivities of concrete ($1 < \lambda_c < 4$) take the form:

$$R_c = a \cdot \lambda_c^5 + b \cdot \lambda_c^4 + c \cdot \lambda_c^3 + d \cdot \lambda_c^2 + e \cdot \lambda_c + f \tag{12}$$

The curve fitting parameters are defined in Table 6. Perform linear interpolation for non-computed values.

Table 8: Curve fitting parameters for upper and lower bounds for the concrete thermal resistance R_c.

λ_c/λ_s	Single-U shape		W-shape	
	2	**0.5**	**2**	**0.5**
a	-0.00255	-0.00151	-0.00105	-0.00096
b	0.03765	0.02234	0.01557	0.01422
c	-0.22166	-0.13312	-0.09284	-0.08438
d	0.66019	0.40771	0.28459	0.25660
e	-1.03559	-0.67667	-0.47303	-0.42066
f	0.79525	0.57674	0.40727	0.35237

C) Curve fit results for transient pile temperature response functions: concrete G-functions G_c

The transient concrete thermal resistance differs depending on the relation between the soil and the concrete, as shown in Figure 9.
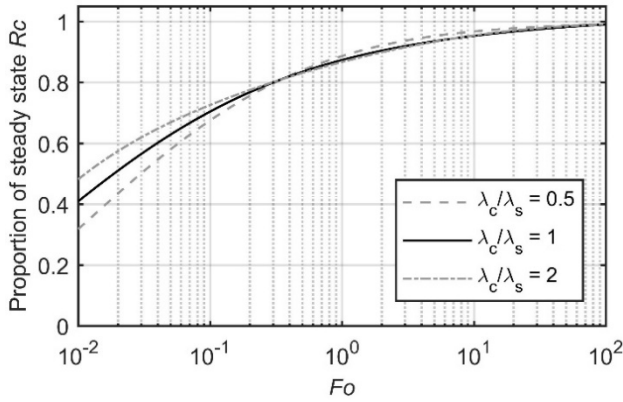
Figure 10: Proportion of steady state R_c for time of the W-shape pile heat exchanger and for different λ_c/λ_s ratios.

The concrete temperature response G-function G_c are valid for $0.01 < Fo < 100$ and it takes the form:

$$G_c = a \cdot \ln(Fo)^6 + b \cdot \ln(Fo)^5 + c \cdot \ln(Fo)^4 + d \cdot \ln(Fo)^3 + e \cdot \ln(Fo)^2 + f \cdot \ln(Fo) + g \qquad (13)$$

The curve fitting parameters are defined in Table 7. For $Fo > 100$ G_c should be set to 1 and for $Fo < 0.01$ G_c should be set to zero.

Table 9: Curve fitting parameters for concrete G-functions G_c.

	1U	2U		
λ_c/λ_s	1	0.5	1	2
a	1.7874E-06	7.4143E-07	3.2209E-06	-6.8329E-07
b	-9.9483E-06	-1.6587E-05	3.5142E-05	1.2454E-05
c	-1.5283E-04	6.6686E-05	-2.3294E-04	-4.7563E-05
d	1.9418E-03	1.0464E-03	-1.0900E-04	3.1674E-05
e	-9.8678E-03	-1.2676E-02	-5.0508E-03	-4.8439E-03
f	2.9573E-02	5.8398E-02	5.3798E-02	4.9111E-02
g	9.5364E-01	8.8640E-01	8.6614E-01	8.6694E-01
RMSE*	0.00032	0.0039	0.0025	0.00003
R^{2}**	0.99998	0.9991	0.9997	0.99992

*RMSE: Root Mean Squared Error
**R^2: Coefficient of Determination

D) Curve fit results for ground temperature response functions for distances

The ground temperature response G-functions for each distance are valid for min(Fo) < Fo < 10000. G_g can be described as:

$$G_g = a \cdot \ln(Fo)^9 + b \cdot \ln(Fo)^8 + c \cdot \ln(Fo)^7 + d \cdot \ln(Fo)^6 + e \cdot \ln(Fo)^5 + f \cdot \ln(Fo)^4 + g \cdot \ln(Fo)^3 + h \cdot \ln(Fo)^2 + i \cdot \ln(Fo) + j \qquad (14)$$

The curve fitting parameters are defined in Table 8, 9, 10 and 11 for aspect ratios 15, 30, 45 and 50, respectively. For Fo < min(Fo), G_g should be set to zero.

Table 10: Spatial G-functions for AR 15.

S/2r	∞	1.3	2.0	2.6	5.2	7.8	8.4	10.5	12.6	13.1	16.7	19.6	26.2
Distance from pile edge [m]	0.00	0.50	0.75	1.00	2.00	3.00	3.20	4.00	4.80	5.00	6.40	7.50	10.00
a	4.04E-09	2.79E-09	-4.83E-09	-9.30E-09	-1.01E-08	-5.40E-09	-4.59E-09	-2.09E-09	-5.66E-10	-3.03E-10	6.97E-10	8.89E-10	7.16E-10
b	-6.28E-08	-1.22E-07	-4.22E-08	2.21E-08	9.75E-08	7.23E-08	6.56E-08	4.13E-08	2.35E-08	2.01E-08	4.40E-09	-1.10E-09	-4.25E-09
c	-7.71E-07	2.85E-07	1.57E-06	2.15E-06	1.74E-06	8.07E-07	6.65E-07	2.45E-07	9.48E-09	-2.91E-08	-1.63E-07	-1.77E-07	-1.27E-07
d	1.31E-05	2.11E-05	8.02E-06	-2.16E-06	-1.42E-05	-1.08E-05	-9.84E-06	-6.35E-06	-3.76E-06	-3.26E-06	-9.14E-07	-6.25E-08	4.92E-07
e	6.89E-05	-7.33E-05	-0.00015	-0.00018	-0.00012	-4.87E-05	-3.93E-05	-1.27E-05	1.34E-06	3.55E-06	1.07E-05	1.11E-05	7.63E-06
f	-1.06E-03	-1.39E-03	-6.71E-04	-1.26E-04	5.76E-04	4.77E-04	4.40E-04	2.98E-04	1.88E-04	1.66E-04	6.10E-05	2.03E-05	-1.12E-05
g	-4.70E-03	2.50E-03	5.06E-03	5.75E-03	3.77E-03	1.73E-03	1.45E-03	6.54E-04	2.17E-04	1.45E-04	-1.22E-04	-1.74E-04	-1.43E-04
h	4.04E-02	4.55E-02	3.02E-02	1.83E-02	-7.87E-04	-3.30E-03	-3.26E-03	-2.61E-03	-1.81E-03	-1.63E-03	-7.04E-04	-3.00E-04	5.20E-05
i	2.97E-01	1.03E-01	3.91E-02	8.33E-03	-1.61E-02	-1.03E-02	-9.01E-03	-4.83E-03	-2.19E-03	-1.72E-03	1.75E-04	6.69E-04	7.13E-04
j	5.34E-01	5.41E-02	0.004521	-0.0081	-0.00508	2.62E-04	7.53E-04	1.65E-03	1.66E-03	1.61E-03	1.06E-03	6.76E-04	1.78E-04
RMSE*	6.35E-06	1.60E-05	2.80E-05	2.33E-05	7.23E-06	6.09E-06	5.45E-06	3.95E-06	2.23E-06	1.95E-06	7.39E-07	3.30E-07	4.60E-08
R²**	1.00E+00	9.99E-01	9.98E-01	9.99E-01	9.99E-01	9.45E-01	9.28E-01	9.81E-01	9.92E-01	9.66E-01	1.00E+00	9.87E-01	9.93E-01
min Fo [-]	0.01	0.46	0.95	2.10	9.00	20.00	20.00	33.50	41.00	58.00	100.00	115.00	175.00
min time [h]	0.10	4.66	9.63	21.28	91.20	202.67	202.67	339.48	415.48	587.75	1013.36	1165.37	1773.38
max Phi	2.33	1.44	1.13	0.92	0.49	0.30	0.28	0.20	0.15	0.14	0.09	0.06	0.03
max Fo	10000	10000	10000	10000	10000	10000	10000	10000	10000	10000	10000	10000	10000

*RMSE: Root Mean Squared Error

**R²: Coefficient of Determination

Table 11: Spatial G-functions for AR 30.

S/2r	∞	1.3	2.0	2.6	5.2	7.8	10.5	13.1	15.6	19.6	23.4	26.2	31.2
Distance from pile edge [m]	0.00	0.50	0.75	1.00	2.00	3.00	4.00	5.00	5.95	7.50	8.93	10.00	11.90
a	-6.133E-09	1.592E-08	1.462E-08	3.032E-09	-3.090E-08	-2.950E-08	-1.835E-08	-8.193E-09	-1.423E-09	4.478E-09	6.338E-09	6.524E-09	5.694E-09
b	1.568E-07	-3.884E-07	-4.648E-07	-2.610E-07	5.431E-07	6.249E-07	4.464E-07	2.521E-07	1.103E-07	-2.753E-08	-8.293E-08	-9.809E-08	-9.627E-08
c	-1.134E-06	1.065E-06	3.224E-06	3.712E-06	1.042E-06	-8.417E-07	-1.408E-06	-1.386E-06	-1.177E-06	-7.791E-07	-4.822E-07	-3.166E-07	-1.265E-07
d	-2.850E-06	3.737E-05	3.045E-05	8.788E-06	-4.946E-05	-4.916E-05	-3.272E-05	-1.717E-05	-6.483E-06	3.368E-06	7.014E-06	7.845E-06	7.355E-06
e	1.151E-04	-1.932E-04	-3.436E-04	-3.290E-04	6.678E-06	1.488E-04	1.576E-04	1.253E-04	8.948E-05	4.287E-05	1.593E-05	3.510E-06	-7.582E-06
f	-7.257E-04	-1.620E-03	-8.398E-04	1.088E-05	1.501E-03	1.312E-03	8.230E-04	4.161E-04	1.529E-04	-7.755E-05	-1.577E-04	-1.739E-04	-1.598E-04
g	-4.868E-03	6.314E-03	1.010E-02	9.692E-03	1.601E-03	-2.005E-03	-2.544E-03	-2.093E-03	-1.493E-03	-6.775E-04	-2.039E-04	1.077E-05	1.941E-04
h	4.514E-02	5.190E-02	3.323E-02	1.794E-02	-6.802E-03	-8.278E-03	-5.495E-03	-2.838E-03	-1.079E-03	4.586E-04	9.856E-04	1.090E-03	9.959E-04
i	3.243E-01	9.452E-02	2.136E-02	-5.962E-03	-5.438E-03	6.321E-03	8.970E-03	7.734E-03	5.664E-03	2.646E-03	8.179E-04	-2.910E-05	-7.663E-04
j	5.689E-01	5.337E-02	1.583E-03	-8.649E-03	2.333E-03	7.817E-03	6.984E-03	4.715E-03	2.745E-03	5.910E-04	-4.216E-04	-7.884E-04	-9.730E-04
RMSE*	1.138E-05	9.286E-06	8.246E-06	8.402E-06	6.814E-06	5.272E-06	5.359E-06	5.164E-06	4.005E-06	1.858E-06	7.265E-07	3.368E-07	1.107E-07
R²**	1.000E+00	9.997E-01	9.997E-01	9.999E-01	9.992E-01	9.999E-01	1.000E+00	1.000E+00	9.998E-01	1.000E+00	9.999E-01	1.000E+00	9.998E-01
min Fo [-]	0.01	0.43	0.95	2.10	8.00	20.00	26.00	33.50	41.00	58.00	100.00	115.00	175.00
min time [h]	0.10	4.36	9.63	21.28	81.07	202.67	263.47	339.48	415.48	587.75	1013.36	1165.37	1773.38
max Phi	3.07	2.07	1.71	1.46	0.92	0.65	0.48	0.37	0.29	0.21	0.15	0.12	0.09
max Fo	10000	10000	10000	10000	10000	10000	10000	10000	10000	10000	10000	10000	10000

*RMSE: Root Mean Squared Error
**R²: Coefficient of Determination

Alberdi-Pagola et. al (2018)
DCE Technical Report No. 243
Method to obtain g-functions for multiple precast quadratic pile heat exchangers

Table 12: Spatial G-functions for AR 45.

$S/2r_b$	∞	1.3	2.0	2.6	5.2	7.9	10.5	13.1	19.6	22.8	26.2	34.2	45.6
Distance from pile edge [m]	0.00	0.50	0.75	1.00	2.00	3.00	4.00	5.00	7.50	8.70	10.00	13.05	17.40
a	4.199E-09	2.392E-09	-5.884E-09	-1.052E-08	-9.248E-09	-1.870E-09	3.169E-09	5.693E-09	6.248E-09	5.406E-09	4.353E-09	2.246E-09	6.536E-10
b	-3.525E-08	-9.048E-08	-3.823E-10	7.076E-08	1.389E-07	8.660E-08	3.149E-08	-5.976E-09	-4.042E-08	-4.138E-08	-3.801E-08	-2.521E-08	-1.085E-08
c	-8.541E-07	3.281E-07	1.694E-06	2.267E-06	1.404E-06	1.246E-08	-8.020E-07	-1.156E-06	-1.115E-06	-9.385E-07	-7.394E-07	-3.666E-07	-1.007E-07
d	8.311E-06	1.546E-05	6.875E-07	-1.062E-05	-2.182E-05	-1.446E-05	-6.407E-06	-7.995E-07	4.745E-06	5.122E-06	4.852E-06	3.348E-06	1.493E-06
e	6.477E-05	-8.856E-05	-1.714E-04	-1.926E-04	-9.560E-05	2.152E-06	5.308E-05	7.320E-05	6.764E-05	5.643E-05	4.419E-05	2.190E-05	6.226E-06
f	-8.423E-04	-1.116E-03	-2.979E-04	3.158E-04	1.021E-03	7.615E-04	4.225E-04	1.714E-04	-1.086E-04	-1.435E-04	-1.492E-04	-1.130E-04	-5.328E-05
g	-3.519E-03	4.209E-03	6.877E-03	7.437E-03	4.321E-03	1.341E-03	-2.729E-04	-1.015E-03	-1.256E-03	-1.092E-03	-8.816E-04	-4.597E-04	-1.418E-04
h	4.648E-02	4.981E-02	3.187E-02	1.806E-02	-4.088E-03	-6.134E-03	-4.251E-03	-2.209E-03	5.635E-04	1.016E-03	1.179E-03	9.919E-04	4.997E-04
i	3.245E-01	1.100E-01	3.877E-02	4.341E-03	-2.050E-02	-1.030E-02	-1.528E-03	3.378E-03	6.238E-03	5.696E-03	4.760E-03	2.627E-03	8.745E-04
j	5.817E-01	6.060E-02	5.990E-03	-7.559E-03	-2.580E-03	3.802E-03	4.919E-03	4.112E-03	1.336E-03	4.792E-04	-1.042E-04	-5.966E-04	-4.694E-04
RMSE*	1.658E-05	1.609E-05	2.035E-05	1.374E-05	1.418E-05	1.943E-05	1.491E-05	9.313E-06	2.111E-06	1.382E-06	1.152E-06	8.269E-07	3.081E-07
R²**	9.999E-01	1.000E+00	1.000E+00	1.000E+00	1.000E+00	9.998E-01	1.000E+00	9.997E-01	9.971E-01	9.894E-01	9.925E-01	9.962E-01	9.972E-01
min Fo [-]	0.01	0.43	0.85	1.7	10	20	25	32	78	115	155	240	350
min time [h]	0.10	4.36	8.61	17.23	101.34	202.67	253.34	324.28	790.42	1165.37	1570.71	2432.07	3546.76
max Phi	3.45	2.43	2.05	1.79	1.21	0.90	0.70	0.56	0.35	0.28	0.22	0.14	0.06
max Fo	10000	10000	10000	10000	10000	10000	10000	10000	10000	10000	10000	10000	10000

*RMSE: Root Mean Squared Error
**R²: Coefficient of Determination

32

Table 13: Spatial G-functions for AR 53.

| B/2r | ∞ | 1.31 | 1.96 | 2.62 | 5.24 | 7.85 | 10.47 | 13.09 | 19.63 | 26.96 | 26.18 | 40.45 | 53.93 |
Distance from pile edge [m]	0.00	0.50	0.75	1.00	2.00	3.00	4.00	5.00	7.50	10.30	10.00	15.45	20.60
a	4.938E-09	3.084E-09	-5.240E-09	-9.889E-09	-8.448E-09	-8.617E-10	4.286E-09	6.818E-09	7.137E-09	4.909E-09	4.632E-09	1.265E-09	1.785E-10
b	-4.061E-08	-9.555E-08	-4.755E-09	6.688E-08	1.343E-07	7.969E-08	2.257E-08	-1.607E-08	-5.046E-08	-4.597E-08	-4.457E-08	-1.958E-08	-5.788E-09
c	-9.857E-07	2.068E-07	1.579E-06	2.151E-06	1.250E-06	-1.756E-07	-1.004E-06	-1.354E-06	-1.264E-06	-8.295E-07	-7.793E-07	-1.984E-07	-2.413E-08
d	8.874E-06	1.597E-05	1.083E-06	-1.030E-05	-2.142E-05	-1.371E-05	-5.342E-06	4.615E-07	6.067E-06	5.932E-06	5.778E-06	2.681E-06	8.227E-07
e	7.218E-05	-8.203E-05	-1.651E-04	-1.860E-04	-8.600E-05	1.404E-05	6.576E-05	8.556E-05	7.692E-05	4.987E-05	4.683E-05	1.227E-05	1.784E-06
f	-8.504E-04	-1.121E-03	-2.961E-04	3.226E-04	1.027E-03	7.525E-04	3.989E-04	1.374E-04	-1.508E-04	-1.859E-04	-1.834E-04	-9.448E-05	-3.024E-05
g	-3.562E-03	4.206E-03	6.882E-03	7.431E-03	4.215E-03	1.155E-03	-4.981E-04	-1.249E-03	-1.447E-03	-1.006E-03	-9.500E-04	-2.750E-04	-4.904E-05
h	4.713E-02	5.039E-02	3.226E-02	1.831E-02	-4.099E-03	-6.096E-03	-4.100E-03	-1.959E-03	9.196E-04	1.508E-03	1.508E-03	8.739E-04	2.945E-04
i	3.272E-01	1.113E-01	3.954E-02	4.817E-03	-2.004E-02	-9.465E-03	-4.331E-04	4.580E-03	7.300E-03	5.489E-03	5.220E-03	1.667E-03	3.426E-04
j	5.854E-01	6.101E-02	5.999E-03	-7.650E-03	-2.495E-03	3.967E-03	5.036E-03	4.137E-03	1.166E-03	-3.514E-04	-4.481E-04	-7.647E-04	-3.388E-04
RMSE*	1.665E-05	1.766E-05	2.274E-05	1.554E-05	1.423E-05	1.877E-05	1.419E-05	8.605E-06	2.254E-06	1.740E-06	1.831E-06	8.595E-07	1.460E-07
R²**	9.998E-01	1.000E+00	1.000E+00	1.000E+00	1.000E+00	9.998E-01	9.999E-01	9.989E-01	9.973E-01	9.943E-01	9.964E-01	9.969E-01	9.954E-01
min Fo [-]	0.02	0.50	1.00	2.00	10.00	20.00	30.00	40.00	115.00	180.00	220.00	350.00	400.00
min time [h]	0.20	5.07	10.13	20.26	101.32	202.64	303.96	405.28	1165.19	1823.78	2229.07	3546.24	4052.85
max Phi	3.61	2.58	2.20	1.94	1.34	1.02	0.81	0.66	0.42	0.28	0.27	0.12	0.04
max Fo	10000	10000	10000	10000	10000	10000	10000	10000	10000	10000	10000	10000	10000

*RMSE: Root Mean Squared Error
**R²: Coefficient of Determination

Appendix VI. Literature review on thermo-mechanical aspects (Technical report IV)

Alberdi-Pagola, M., Madsen, S., Jensen, L.J. & Poulsen, S.E., 2018. "Thermo-mechanical aspects of pile heat exchangers: background and literature review". Aalborg: Department of Civil Engineering, Aalborg University. DCE Technical Reports, nr. 250, pp. 37. Available online:

http://vbn.aau.dk/files/281634409/Thermo_mechanical_aspects_of_pile_heat_exchangers_background_and_literature_review.pdf

AALBORG UNIVERSITY

DENMARK

Thermo-mechanical aspects of pile heat exchangers

Pagola, Maria Alberdi; Madsen, Søren; Jensen, Rasmus Lund; Poulsen, Søren Erbs

Link to publication from Aalborg University

Thermo-mechanical aspects of pile heat exchangers: background and literature review

Maria Alberdi-Pagola
Søren Madsen (COWI)
Rasmus Lund Jensen
Søren Erbs Poulsen (VIA University College, Horsens)

Aalborg University
Department of Civil Engineering
Group Name

DCE Technical Report No. 250

Thermo-mechanical aspects of pile heat exchangers: background and literature review

by

Maria Alberdi-Pagola
Søren Madsen (COWI)
Rasmus Lund Jensen
Søren Erbs Poulsen (VIA University College, Horsens)

June 2018

Scientific Publications at the Department of Civil Engineering

Technical Reports are published for timely dissemination of research results and scientific work carried out at the Department of Civil Engineering (DCE) at Aalborg University. This medium allows publication of more detailed explanations and results than typically allowed in scientific journals.

Technical Memoranda are produced to enable the preliminary dissemination of scientific work by the personnel of the DCE where such release is deemed to be appropriate. Documents of this kind may be incomplete or temporary versions of papers—or part of continuing work. This should be kept in mind when references are given to publications of this kind.

Contract Reports are produced to report scientific work carried out under contract. Publications of this kind contain confidential matter and are reserved for the sponsors and the DCE. Therefore, Contract Reports are generally not available for public circulation.

Lecture Notes contain material produced by the lecturers at the DCE for educational purposes. This may be scientific notes, lecture books, example problems or manuals for laboratory work, or computer programs developed at the DCE.

Theses are monograms or collections of papers published to report the scientific work carried out at the DCE to obtain a degree as either PhD or Doctor of Technology. The thesis is publicly available after the defence of the degree.

Latest News is published to enable rapid communication of information about scientific work carried out at the DCE. This includes the status of research projects, developments in the laboratories, information about collaborative work and recent research results.

Recent publications in the DCE Technical Report Series

This report complements a series of technical reports:

Alberdi-Pagola, M., Poulsen, S. E., Jensen, R. L., & Madsen, S. (2017). Thermal response testing of precast pile heat exchangers: Fieldwork report. Aalborg: Aalborg University. Department of Civil Engineering. DCE Technical Reports, No. 234.

Alberdi-Pagola, M., Jensen, R. L., Madsen, S., & Poulsen, S. E. (2017). Measurement of thermal properties of soil and concrete samples. Aalborg: Aalborg University. Department of Civil Engineering. DCE Technical Reports, No. 235.

Alberdi-Pagola, M., Jensen, L.J., Madsen, S. & Poulsen, S.E., 2018. Method to obtain g-functions for multiple precast quadratic pile heat exchangers. Aalborg: Department of Civil Engineering, Aalborg University. DCE Technical Reports, No. 243.

Abstract

Pile heat exchangers are thermo-active ground structures with built in geothermal heat exchanger pipes. As such, the foundation of the building both serves as a structural component and a heating/cooling supply element. The existing geotechnical and structural design standards do not consider the nature of the thermo-active foundations, what hampers their implementation. Several studies tackle different aspects of the thermo-mechanical behaviour of pile heat exchangers by experimental and numerical approaches. This document aims to compile the main literature in the field. We depart from understanding how an energy pile behaves under mechanical and thermal loads and then, we look into the different aspects affecting the phenomena. It is concluded that, even though the thermal loads resulted from the geothermal use applied to the energy piles are not likely to lead to geotechnical or structural failure, they need to be considered in the analysis and design of such structures. More data under operational conditions will ease the development of regulations and unified guidelines.

Abstract

Scope

First, the main principles of ground source heat pump (GSHP) systems are presented in order to establish a framework. Then, the main challenges associated to the mechanical aspects of pile heat exchangers are treated. This document does not look into the thermal aspects of energy piles, treated in other documents linked to this series of technical reports.

Foundation piles as ground heat exchangers

Ground source heat pump (GSHP) systems produce renewable thermal energy that offer high levels of efficiency for space heating and cooling [1,2]. Ground heat exchangers are critical components in any GSHP system. Horizontal heat exchangers, vertical borehole heat exchangers and energy piles comprise the main different types of closed loop ground heat exchangers (Figure 1). Energy piles are concrete piles with built in geothermal pipes, i.e., they are thermo-active ground structures that utilize reinforced concrete foundation piles as vertical closed-loop heat exchangers [3]. They vary in length from 7 to 50 m with a cross section of 0.3 to 1.5 m and can be either cast in place or precast driven.
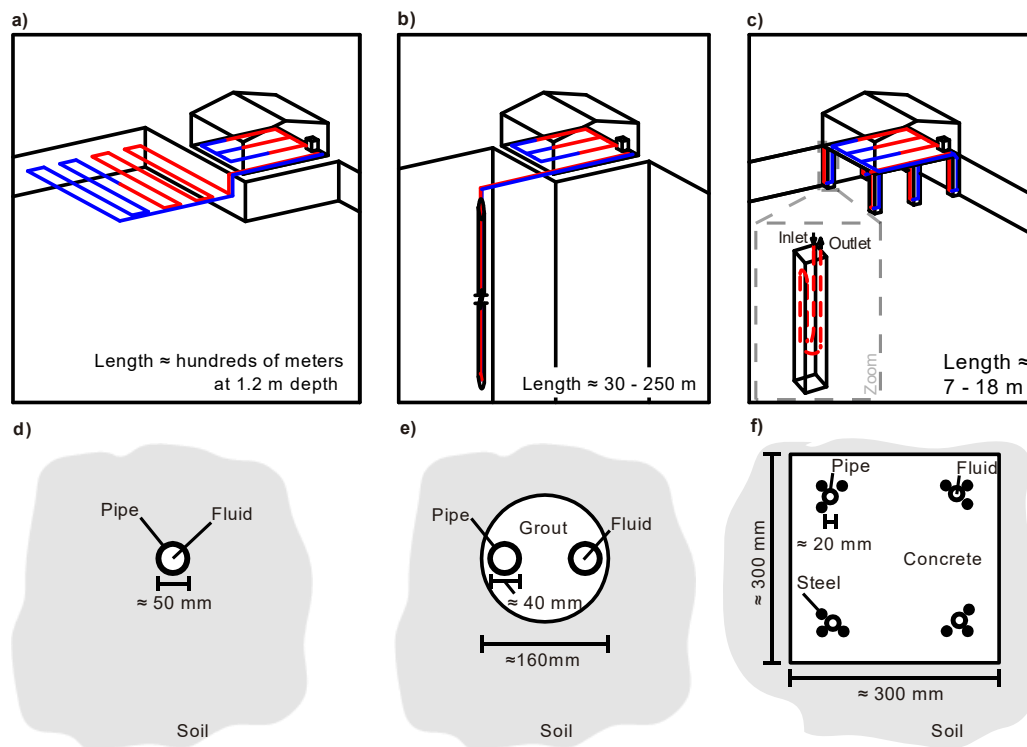
Figure 1: Description of main closed loop GSHP systems: a) horizontal heat exchangers; b) vertical borehole heat exchangers; c) pile heat exchangers. d), e) and f) illustrate the cross sections for horizontal, borehole and pile heat exchangers, respectively. Reproduced after [4]**.**

The foundation of the building both serves as a structural and a heating and/or cooling component. Therefore, different aspects need to be considered (Figure 2). Thermal aspects affect the mechanical behaviour of soils and piles, whereas the influence of the mechanical loads on the temperature field is usually insignificant. Thermal loads may induce changes in pore pressure and in groundwater flow regime and fluids can transport heat through the pores of the soil. Finally, effective stresses are affected by variations of pore pressure [5]. The analysis of pile heat exchangers is mainly governed by thermo-mechanical influences, hence, the focus of this report.
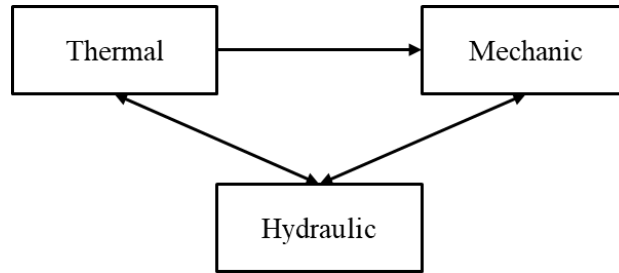
Figure 2: Relevant couplings in shallow geothermal energy systems, after [5]**.**

Load transfer mechanisms of pile heat exchangers

Pile heat exchangers are structural elements subject to time varying thermal loads, additional to those due to static axial loading, and as such, an assessment of the structural implications needs to be carried out in any project. Pile design approaches in Europe are based on the determination of the ultimate and serviceability limit states, ULS and SLS respectively, according to the Eurocode 7 (DS/EN 1997-1/AC, 2010 [6]). Yet regulations do not consider the geothermal use in the foundation design process with regards to structural and geotechnical requirements.

Energy piles will be subject to a net change of the temperature relative to the initial condition over time, which causes thermal stresses and head displacements. Under thermo-elastic conditions, if the pile is a free body, i.e. it has no restraints, it will expand while heating and contract during cooling to yield a thermal free strain $\varepsilon_{T\text{-Free}}$:

$$\varepsilon_{T-Free} = \alpha \cdot \Delta T \tag{1}$$

where α [1/K] is the coefficient of thermal expansion of the reinforced concrete and ΔT [K] is the net change in temperature of the pile. This strain will provoke a change in the pile geometry and this way no axial load will be mobilised:

$$\Delta L = L_0 \cdot \varepsilon_{T-Free} \tag{2}$$

Where ΔL [m] is the change in length caused by the temperature change and L_0 [m] is the initial length of the body. If the pile is perfectly restrained, it will keep its length, but thermally induced stresses will be created $\Delta\sigma_T$ [N/m^2]:

$$\Delta\sigma_T = \alpha \cdot \Delta T \cdot E \tag{3}$$

where E [MPa] is the Young's modulus of the pile material.

In reality, a pile will not expand or contract freely as it will be confined by the structure on top and the surrounding soil, at different levels of restrain (Figure 3). As a result, the measured strain changes due to temperature changes $\varepsilon_{T\text{-Obs}}$ will be less than the free axial thermal strain $\varepsilon_{T\text{-Free}}$ [7]:
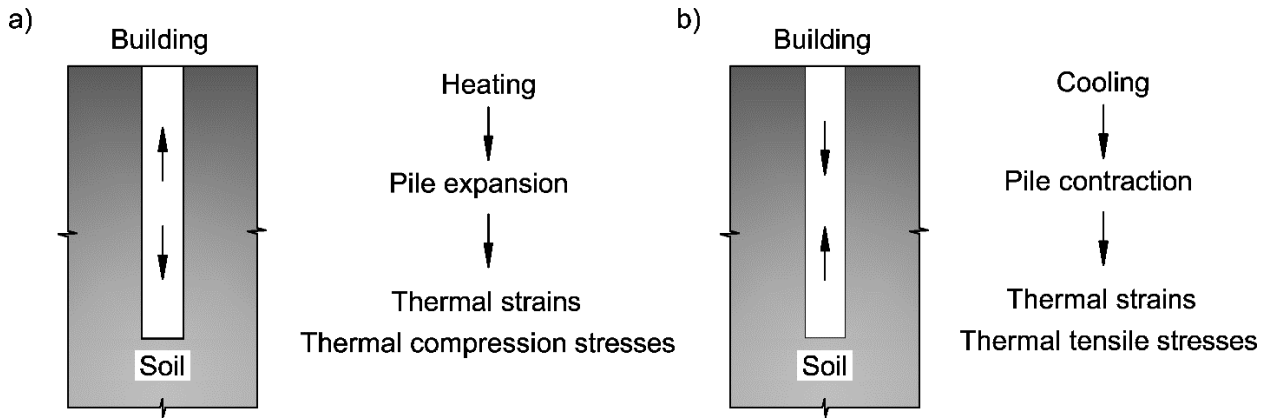
Figure 3: Response mechanism of a pile heat exchanger to thermal loading; a) for heating and b) for cooling. Reproduced after [8].

$$\varepsilon_{T-Free} \geq \varepsilon_{T-Obs} \tag{4}$$

From here, the restrained axial strain $\varepsilon_{T\text{-Rstr}}$ can be estimated as:

$$\varepsilon_{T-Rstr} = \varepsilon_{T-Free} - \varepsilon_{T-Obs} \tag{5}$$

The restrained strain provokes a thermal stress in the pile and the thermally induced axial load P_T [N] for a given strain increment is calculated as:

$$P_T = -E \cdot A \cdot \varepsilon_{T-Rstr} = -E \cdot A \cdot (\alpha \cdot \Delta T - \varepsilon_{T-Obs}) \tag{6}$$

where A [m^2] is the cross-sectional area of the body. When a mechanically loaded pile is heated or cooled, the total mobilised strain ε_{Total} is the sum of the mechanically imposed strain ε_M and thermal strains $\varepsilon_{T\text{-Obs}}$:

$$\varepsilon_{Total} = \varepsilon_M + \varepsilon_{T-Obs} \tag{7}$$

The mechanical strain is directly developed by a mechanical load P_M applied in the pile head:

$$P_M = -E \cdot A \cdot \varepsilon_M \tag{8}$$

Consequently, the total load P_{Total} is the sum of the mechanical load P_M and the thermal load P_T:

$$P_{Total} = P_M + P_T \tag{9}$$

Pile foundations are used when settlements of buildings need to be limited, to increase bearing capacities or to reach a deeper soil layer which is more resistant. Therefore, the geotechnical bearing capacity of the pile and the prediction of its displacements need to be considered when designing a pile [9].

Under structural (mechanical) load only (Figure 4a), the maximum axial stress is found at the pile head, reducing with depth as load is transferred into the ground by the shaft friction (or side shear resistance) mobilised at the soil-pile interface. I.e., the surrounding soil confines the movement of the pile and mobilises the reaction forces along the pile shaft and the pile toe. The axial stress will decrease to zero if the shaft resistance is enough to support the building load; otherwise, the remaining load is transferred at the pile toe and supported by the underlying material, known as end-bearing resistance [10–12].

The maximum load that an axially loaded pile can support Q_{LIM} is defined as a sum of the tip (toe or base) and friction (side shear or shaft) resistances:

$$Q_{LIM} = Q_S + Q_P - W_P \tag{10}$$

Where Q_S is the share of the pile bearing capacity provided by the friction between the pile and the soil and Q_P is the share of the pile bearing capacity delivered by the soil below the pile tip and W_P is its own weight. The tip resistance Q_P depends on the resistance of the soil below the pile toe (undrained shear strength and vertical stress) whereas the shaft resistance Q_S depends on the friction angle at the interface and the stress state of the pile-soil interface. The total load applied to the pile P_{Total} should be less than the design limit, considering a safety factor [6].

Depending on the way the load is transferred to the soil, we may find three different types of piles: i) end-bearing piles where the main resistive mechanism is the pile tip resistance; ii) floating piles (a.k.a. friction piles or surface bearing piles) where the shaft friction provides the main resistance capacity; iii) semi-floating piles which involve an intermediate configuration between the previous two.

The pile-soil interaction under working mechanical and thermal loads provokes complex systems which depend on: ground conditions, different levels of pile confinement and magnitude of the thermal loads. Therefore, the behaviour of the piles is place dependent and it makes it hard to establish general rules. Fortunately, simple descriptive mechanistic frameworks have been established based on observed behaviours, which make it easier to understand the phenomena [13–15].

In the following the main load transfer mechanisms occurring due to combined mechanical and thermal solicitations are described. Simplified axial load and shaft resistance distribution diagrams are shown where the effect of standard mechanical load and combined thermo-mechanical loads are described. A soil with uniform strength, a linear elastic pile with constant cross-sectional area and a linear variation in strain and load along the pile's length are considered. When temperature changes are applied, the change is considered uniform over the pile length.

Figure 4 represents a floating pile heat exchanger. It is assumed that the mechanical load (Figure 4a) will be resisted by the shaft resistance, which is assumed uniform along the shaft for this simple model. When cooling occurs, the pile contracts and any restriction offered to the pile shaft will lead to tensile strains and stresses developing. Along the upper part of the shaft, shear stress on the pile-soil interface will be mobilised in the same direction as that mobilised by compression loading applied at the pile head. It will take the opposite direction in the lower part of the pile (Figure 4b). When heating (Figure 4d), the pile expands, and any restriction offered to the pile shaft will lead to compressive strains and/or loads developing. At the shaft resistance development, the opposite effect to a cooling load will occur. Shear on the pile-soil interface will have the same direction in the lower part of the pile and will oppose that induced by compressive pile loading in the upper. When cooling occurs in combination with compression loading (Figure 4c), axial loads become less compressive (potentially tensile stresses), while the mobilised shaft resistance reduces in the lower part of the pile and increases in the upper part. When a heating cycle is applied to a pile under compressive mechanical load (Figure 4e), the axial load will become more compressive and while the mobilised shaft resistance reduces in the upper part of the pile, it increases in the lower part.

a)

In pile shaft: ε, P
On interface: qₛ

ε = axial strain in pile
P = axial load in pile (P = εAE)
qₛ = pile-soil interface shear stress
A = pile cross-sectional area
E = pile elastic modulus

b)

In pile shaft: ε, P
On interface: qₛ

Stronger cooling

c)

In pile shaft: ε, P
On interface: qₛ

Stronger cooling

d)

In pile shaft: ε, P
On interface: qₛ

Stronger heating

e)

In pile shaft: ε, P
On interface: qₛ

Stronger heating

Figure 4: Response mechanism for pile undergoing thermo-mechanical loading: heating and cooling with no end restraint: a) load only; b) cooling only; c) combined load and cooling; d) heating only; e) combined load and heating. After [13]. The figure is not to scale neither to relative scale.

Figure 5 represents the effects of end-restraints, provided by the building and a stiff bearing layer around the tip. During heating, the restricted pile expansion strains will generate additional compressive stresses. Therefore, the resultant load profile will change depending on the relative stiffness of the end-restrains (Figure 5a). And because of the restrained axial deformation, the mobilised shaft resistance will be less than for the case of the pile without end-restraint. Pile cooling will result in opposite responses (Figure 5b) [16].
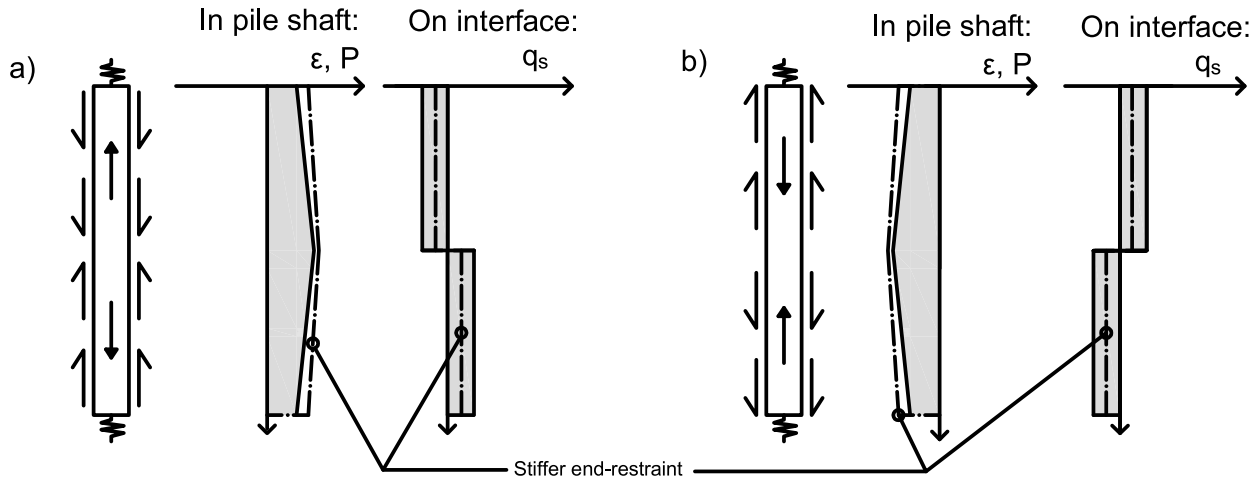
Figure 5: Effect of end-restraint on the thermal response: a) pile heated; b) pile cooled. After [16]**. The figure is not to scale neither to relative scale.**

A pile heat exchanger will expand or contract at different levels of restraint [7]. The level of restraint n is defined as the ratio between the observed and the free axial strains [15] and it is minimal in the null-point, which represents the plane where zero thermally induced displacement occurs in the pile [17]:

$$n = \frac{\varepsilon_{T-Obs}}{\varepsilon_{T-Free}} \tag{11}$$

The section of the pile above the null point experiences upward displacements when heated and downward displacements during cooling, whereas the pile section below the null point experiences downward displacements during heating and upward movements when cooled down. As it has been shown in Figures 4 and 5, as a result of the temperature change, the mobilised end-bearing and shaft resistances of energy piles will vary and will be redistributed according to the position of the null point [18].

Influence of temperature on soil behaviour

In the previous section, it has been described how the load transfer from the pile to the soil is expected to rearrange due to temperature variations of the pile. In the following, it is analysed whether the temperature variations resulted from the geothermal use affect the stress state at the pile-soil interface and the shear strength of the soil. I.e., a review of the influences of temperature on the soil resistance parameters is provided.

The temperature range imposed by the geothermal exploitation of the foundations are relatively modest, falling between 2 °C to 30 °C [15], and the nature of the ground thermal loads depend on the needs of the building [19]. The upper temperature limit might be more restrictive due to environmental regulations. E.g. in Denmark, the injection temperature can be limited to 25 °C [20]. Ref. [21] shows operational temperatures in cooling mode of a 1.2 m diameter energy pile, with centrally placed pipes: the temperature of the fluid in the geothermal pipes shows quick variation in response to the building thermal needs while the temperature changes near the edge of the pile are smoother. The changes in pile temperature in the centre vary from 12.5 °C (end of winter) to 27 °C (end of summer), while the corresponding temperatures near the edge vary from 14 °C to 19 °C. Therefore, any temperature change in the ground will show rather small amplitude and seasonal period. The temperature disturbance and its magnitude in the pile-soil system will also depend on the thermal properties of the concrete and the surrounding soil. Hence, an assessment of the induced temperature changes with respect to the initial undisturbed temperature needs to be carried out in order to estimate the induced thermal stresses and strains.

Soil behaviour

The temperature dependency of the geotechnical properties of the soil has mainly been treated by the nuclear waste disposal research, where much greater temperature variations are expected [21]. The principal thermo-hydro-mechanical processes that affect the mechanical behaviour of soils are the thermal hardening, the thermally induced water flow, the excess pore pressure development and the volume changes due to thermal consolidation, possibly the most critical factor [21,22].

When a thermal load is transmitted from the pile to the soil, the soil reacts by changing its volume (expansion or contraction of the porewater and soil structure) and by modifying the strength of contact between soil particles [23,24]. Coarse-grained soils do not seem to be affected by temperature variations due to their drained behaviour [25]. On the other hand, fine-grained soils show a densification and a reduction in the undrained shear strength with increasing temperature due to an increase in the pore water pressure that cannot be dissipated. This results in a reduction in effective stresses (short-term). Ref. [26] reported that an excess pore water pressure of 0.7% of the effective stress is generated by 1 °C increase in soil temperatures. In the long term (drained

conditions), the behaviour differs for over- and normally-consolidated clays since the void ratio might increase for the first while it may decrease for the latter (Figure 6a) [7]. Normally consolidated clays show an irreversible volume change while highly over-consolidated clays show reversible behaviour, as shown in Figure 6b. The thermally induced volumetric strains expected for energy pile applications fall in the lower part of the curves in Figure 6, where the thermally induced volumetric strains are very low. To the knowledge of the authors, the range from 0 to 10 °C has not been measured.

a)
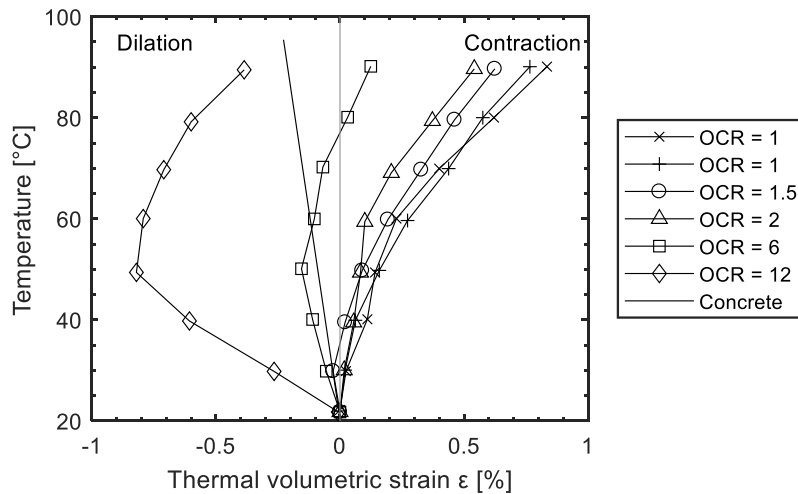
b)
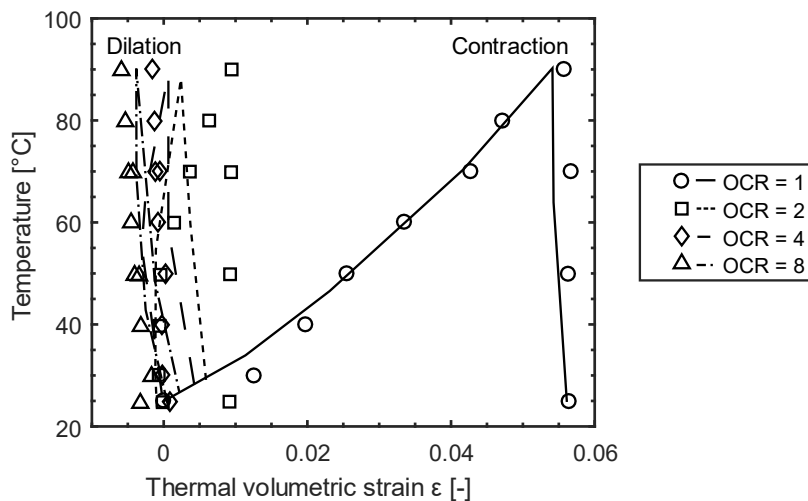
Figure 6: a) Thermal volumetric strain of Kaolin clay during drained heating from 22 to 90 °C; initial consolidation pressure 600 kPa, after [27] **and** [28]**. b) Numerical simulations of a heating-cooling cycle at different degrees of consolidation under oedometric conditions (vertical preconsolidation pressure= 200 kPa). Points: experimental results; lines: numerical simulations, after** [29]**. OCR stays for Over-Consolidation Ratio, defined as the ratio of the vertical effective preconsolidation stress to the current effective stress.**

According to [21], soft normally consolidated clays require main attention because large plastic volume changes may occur upon heating. However, after hardening, further cycles of temperature

change within the same temperature range will show an elastic behaviour. Hence, temperature changes can affect the stress state at the pile-soil interface and the shear strength of the soil that affects the tip resistance of the pile [22].

The stress and strain relations occurring in soils due to temperature changes is described by constitutive models. Ref. [30] proposed a thermo-plastic model based on the modified cam-clay and Prager's thermo-plasticity theory. Ref. [29,31] developed a thermo-elastoplastic model, which considers the possible plastic behaviour under non-isothermal conditions. This type of models define yield surfaces that depend on temperature and outside their limits, the soil behaves thermoplastically. Further discussions and literature reviews are available in [5,32].

Soil-pile interface behaviour

Recent studies on the impact of thermal loading at the pile-soil interface indicate that the pile bearing capacity is not reduced to a critical level in terms of structural integrity [7,9,33,34]. Mechanical cyclic load studies of the pile-soil interface at +1.1 °C to -16 °C are reported by [35–37] but studies of the long-term behaviour of energy piles under cyclic thermal loads for the operational range have not been reported. Ref. [9,34] have analysed monotonic temperature variations in the range from 6 °C to 50 °C - 60 °C and have concluded that higher temperatures increase the strength of the clay-concrete contact. This is explained by the thermal consolidation of the clay that results in an increase of the contact surface, even though the interface friction angle is reduced. Ref. [38] analysed the interface between concrete and a low plasticity clay and observed no impact of temperature on the interface shear strength as observed in Figure 7. The sand-concrete interface is hardly affected by the monotonic temperature changes [9].
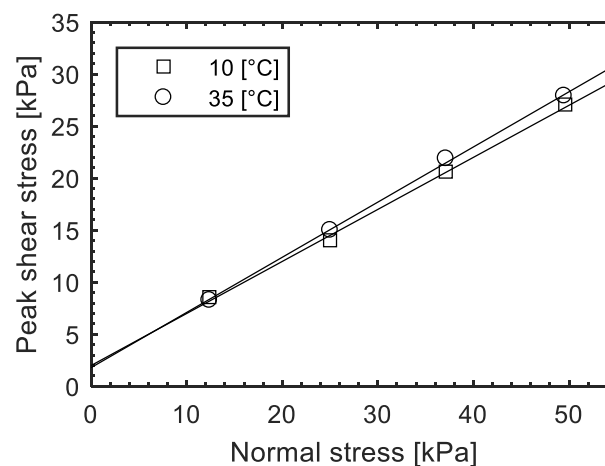
Figure 7: Clay/concrete interface behaviour assessed using thermal borehole shear device. Impact of temperature on failure envelope, after [38]**.**

In order to characterize the degradation of the pile-soil interface under thermal cyclic loads, constitutive laws, such as the Modjoin law [39] and numerical models [40,41], can be applied to reproduce the cyclic behaviour of energy piles.

Observed behaviour of energy piles

The main research programs covering the thermo-mechanical behaviour of the energy pile-soil systems encompass full-scale, lab-scale and numerical studies which are shortly described in the following and in appended tables. A comprehensive review on published studies is available in [26].

Full-scale setups

Two main full scale studies of energy piles have leaded the investigation in the field: the Lambeth College setup in London [13,42], which behaves as a floating pile, and the EPFL setup in Lausanne [33,43,44], which shows a semi-floating behaviour. Both studies conclude: i) short-term plastic response of soils has not been observed due to the geothermal use since effective stresses typically are within yield surfaces, i.e., within the thermo-elastic domain; ii) the additional stresses produced in the energy pile due to thermal loads depend on the level of restraint of the pile, i.e., they depend on the allowance of the pile to move (expand or contract).

Full scale demonstrations of precast energy piles have also been reported in [45]. The 17.4 m long pile, with a 35-cm side size and centrally placed pipes, is subjected to 14 cycles of heat injection at 80 W/m during 14 hours per day, resembling cooling operation mode. The results show that the increase of the axial load in the pile (compared to the existing mechanical) is in the order of 12% and that the maximum increase of temperature in the pile during the test does not reach 5 °C at any depth. The maximum displacement observed during heating is 0.4 mm after 6 cycles and the elastic recovery is 0.2 mm. An accumulated permanent upward displacement of 0.2 mm is measured. The recovery to initial conditions is not shown.

A similar behaviour has been reported in [46], where the thermal strains and stresses for intermittent tests (20 days long at different operation modes resembling building heating, i.e., pile cooling) were cyclic and returned to initial values, i.e., the pile experiences thermo-elastic behaviour for daily thermal cycles. The maximum thermal strain measured 0.09 mm downwards and the thermally induced average stress are around 900 kPa for 8 hours working cycles. The absolute decrease of temperature in the pile at the end of the test is 9 °C and 10 °C, for 8 hours and 16 hours operation cycles, respectively. It was concluded that intermittent operation (resembling operational conditions) is advantageous in terms of generating lower pile thermal loading for long term operations and regarding a more efficient heat transfer capacity than a continuous operation.

As a rule of thumb, it could be said that 1 °C of increased temperature results in an increase of the pile axial stress of approximately 100 - 200 kPa and a change in mobilised shaft friction at the soil-pile interface of - 2.1 to + 2.5 kPa, corresponding to the upper- and the lower-half of the pile [13,14,43].

Group effects

Current research focuses on the analysis of energy pile group effects [44,47–50]. Combined experimental and numerical studies of energy piles operating in groups [51] suggest that the assessment of thermally induced vertical strains needs to be assessed by considering group effects. This happens because, as the number of operating energy piles increases, higher thermally induced vertical strains arise. Conversely, as the number of operating energy piles increases, lower thermally induced vertical stresses arise. Hence, analyses of single energy piles are valid and conservative for the assessment of additional stresses. In addition, the same authors suggest in [48] that the serviceability mechanical performance of energy pile groups (i.e., deformation related) depends on the relative thermally induced deformation of the soil to that of the energy piles, i.e., the ratio between the linear thermal expansion coefficient of the soil and the pile. Meaning that in the long term, if the thermal expansion coefficient of the soil exceeds the pile's, the deformation of energy pile groups is governed by the thermally induced deformation of the soil surrounding the piles.

Numerical studies

Numerical tools are used to analyse not just experimental conditions but also potential scenarios, supporting the understanding of the physics behind the problem and assisting the development of behavioural rules. Several numerical studies explore the thermo-mechanical phenomena of energy piles by different methods. Regarding load transfer mechanisms, [43,52–54] encompass good examples of finite element models validated with experimental data. The load transfer method [15,55], modified to account for thermal loads has been used by [15,18,40,56,57]. This method allows reliable analysis of mechanical and monotonic thermal changes in a practical way. Computational tools such as ThermoPile [58] and Oasys Pile [59] have been develop based on this approach. Ref. [26,40,60] have adapted the load transfer model to account for cyclic thermal loads.

Operational demonstration

Ref. [61] analyses two energy piles that have been coupled to a conventional GSHP system. Measurements under operational conditions over a period of 658 days show fluid temperatures ranging from 7 to 35 °C. It concludes that the values of thermal axial displacement and the thermo-mechanical axial stresses are within reasonable limits and are not expected to cause any structural damage to the building. However, it is highlighted that in complex soil layers, the pile soil systems might not behave in a thermo-elastic manner in the long term. This is also in accordance with

numerical studies [54] that highlight that it is critical to maintain stable temperature of the ground over seasons for long-term sustainability of heat exchange operations to avoid potential plastic effects on the soil around the piles. Ref. [3] states that appropriate operating conditions of energy pile installations, where the temperatures range from 5 to 20 °C, hardly affect the shaft resistance of the pile. More operational data will aid the understanding of the performance of energy foundations in terms of structural integrity.

Recent developments on the design of energy pile foundations

Regulations do not consider the geothermal use in the foundation design process with regards to geotechnical and structural requirements. To ensure that the geotechnical performance of the pile is not negatively affected, conservative safety procedures are applied, which potentially reduce their cost-effectiveness. The fluid temperature in the ground loop is not allowed to go below 0 - 2 °C, to avoid freezing of the pile interface, and there is a tendency to place more energy piles than required [7,33,62–65].

The analysed research concludes that the thermal loads and displacements resulted from the geothermal use of the energy piles are not likely to lead to geotechnical or structural failure. However, energy piles are structural elements and they need to be treated as such. Therefore, the energy pile design needs to integrate geotechnical, structural and heat transfer considerations [66].

Ref. [57] launched the development of a design method that could be incorporated within the Eurocode agenda, based on the load transfer method. The pile (15 m long and 0.6 m square section) head-building structural interaction was modelled by means of a spring restraint with different stiffness. For a typical application of +10 K temperature change from initial undisturbed soil temperature and a 200 MN/m pile head stiffness, the thermally induced compression axial load is 175 kN and the pile heave, 0.5 mm. See Figure 8 for more stiffness. A discussion about this can be followed in [67,68].

To build a design framework, it needs to be decided how the thermal loads derived from the geothermal use are considered in the load combination processes and whether their consideration is relevant just for SLS or it also needs to be addressed in ULS.

Ref. [18] demonstrated that under monotonic thermal loading the null point (previously described) will always move towards the pile end in order to maintain the equilibrium, even if the ultimate bearing force (friction and base) is mobilised, as it happened at the Lambeth College pile [13]. Regarding serviceability, it was demonstrated that over-sizing energy piles, by projecting a longer length, can have a negative impact. This happens because the null point will prevent excessive settlement/heave since at least, this point remains stable under temperature variations. If a pile is over dimensioned

structurally, the head heave or settlement will increase with temperature because there is a considerable amount of bearing force that the pile could still mobilise after mechanical loading. This has been observed in the Lambeth College test pile [18]. Therefore, enlengthening for geothermal reasons could go against safety.
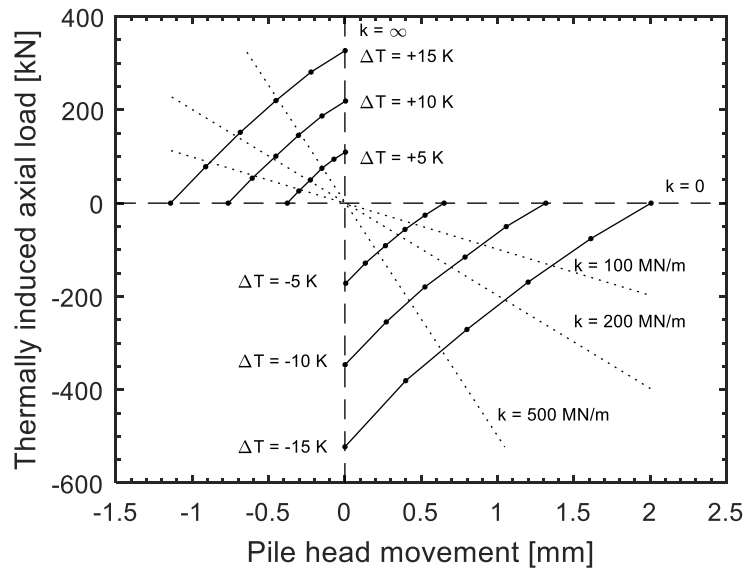
Figure 8: Interaction diagram relating change in thermally induced pile axial load and pile head movement as function of applied temperature change and pile head stiffness, after [57]**.**

Based on these findings, the EPFL research team has continued developing a method to consider the thermal loads within the Eurocode framework. The latest work is still under review [69], but personal communication with the authors and the recent attendance to a course in EPFL [70], provided the following main outcomes:

The thermal loads are deformation related problems. Hence, for geotechnical design, the thermal loads are more relevant in SLS than in ULS. This happens because the presence of the null point will always ensure equilibrium with regards to a collapse mechanism. Hence, it should suffice with checking that the thermally induced pile head heave or settlement resulted from thermal expansion or contraction, respectively, remain within acceptable limits for the structure. For this verifications, numerical tools such as the load transfer method [15,26,40,60,71], can be used. Stresses caused by thermal loads may be generated in the reinforced concrete section. Hence, sufficient compressive and tensile strengths need to be ensured to verify structural ULS [26]. Extensive reviews about this topic are available in [10,67,68].

Conclusions

The literature review shows a vast amount of information and studies regarding thermo-mechanical aspects of pile heat exchangers. However, more data of the thermo-mechanical behaviour under operational conditions is required to ease the development of regulations and unified guidelines and to boost the implementation of this technology.

The analysed research concludes that the thermal loads and displacements resulted from the geothermal use of the energy piles are not likely to lead to geotechnical or structural failure. However, energy piles are structural elements and they need to be treated as such. Therefore, the energy pile design needs to incorporate geotechnical, structural and heat transfer considerations.

The induced thermal stresses and strains depend on the temperature change caused by the ground thermal load, which results from the building heating and/or cooling needs. The temperature disturbance and its magnitude in the pile-soil system will also depend on the thermal properties of the concrete and the surrounding soil. Hence, a prior assessment of the induced temperature changes with respect to the initial undisturbed temperature needs to be carried out in order to estimate the induced thermal stresses and strains. The ULS and SLS verifications for geotechnical design can be addressed by numerical tools such as the load transfer method.

Acknowledgements

References

[1] S.J. Rees, 1 - An introduction to ground-source heat pump technology, in: Adv. Ground-Source Heat Pump Syst., Woodhead Publishing, 2016: pp. 1–25. doi:http://dx.doi.org/10.1016/B978-0-08-100311-4.00001-7.

[2] J.W. Lund, T.L. Boyd, Direct utilization of geothermal energy 2015 worldwide review, Geothermics. 60 (2016) 66–93.

[3] H. Brandl, Energy foundations and other thermo-active ground structures, Geotechnique. 56 (2006) 81–122. http://www.scopus.com/inward/record.url?eid=2-s2.0-33644596527&partnerID=40&md5=778cc8fddf57ca9555395cb6465c77e8.

[4] M. Alberdi -Pagola, S.E. Poulsen, F. Loveridge, S. Madsen, R.L. Jensen, Comparing heat flow models for interpretation of precast quadratic pile heat exchanger thermal response tests, Energy. 145 (2018) 721–733. doi:10.1016/j.energy.2017.12.104.

[5] A. Vieira, M. Alberdi-Pagola, P. Christodoulides, S. Javed, F. Loveridge, F. Nguyen, F. Cecinato, J. Maranha, G. Florides, I. Prodan, G. Van Lysebetten, E. Ramalho, D. Salciarini, A. Georgiev, S. Rosin-Paumier, R. Popov, S. Lenart, S.E. Poulsen, G. Radioti, Characterisation of Ground Thermal and Thermo-Mechanical Behaviour for Shallow Geothermal Energy Applications, Energies . 10 (2017). doi:10.3390/en10122044.

[6] DS/EN 1997-1/AC, Eurocode 7: Geotechnical design - Part 1: General rules, (2010).

[7] GSHP Association, Thermal Pile: Design, Installation & Materials Standards., (2012). http://www.gshp.org.uk/pdf/GSHPA_Thermal_Pile_Standard.pdf.

[8] M. Alberdi-Pagola, S. Madsen, R.L. Jensen, S.E. Poulsen, Numerical investigation on the thermo-mechanical behavior of a quadratic cross section pile heat exchanger, in: Proc. IGSHPA Tech. Conf. Expo, Denver, USA, March 14-16, 2017. doi:http://dx.doi.org/10.22488/okstate.17.000520.

[9] A. Di Donna, L. Laloui, Thermo-mechanical aspects of energy piles, École polytechnique fédérale de Lausanne EPFL, 2014. doi:doi:10.5075/epfl-thesis-6145.

[10] C.G. Olgun, J.S. McCartney, Outcomes from international workshop on thermoactive geotechnical systems for near-surface geothermal energy: from research to practice, DFI Journal-The J. Deep Found. Inst. 8 (2014) 59–73. doi:https://doi.org/10.1179/1937525514Y.0000000005.

[11] K.D. Murphy, J.S. McCartney, K.S. Henry, Evaluation of thermo-mechanical and thermal behavior of full-scale energy foundations, Acta Geotech. (2014) 1–17.

[12] M.E. Suryatriyastuti, S. Burlon, H. Mroueh, On the understanding of cyclic interaction mechanisms in an energy pile group, Int. J. Numer. Anal. Methods Geomech. 40 (2016) 3–24.

[13] P.J. Bourne-Webb, B. Amatya, K. Soga, T. Amis, C. Davidson, P. Payne, Energy pile test at lambeth college, London: Geotechnical and thermodynamic aspects of pile response to heat cycles, Geotechnique. 59 (2009) 237–248. http://www.scopus.com/inward/record.url?eid=2-s2.0-58049214205&partnerID=40&md5=8847275985af4148a4ad28dad671efb6.

[14] B.L. Amatya, K. Soga, P.J. Bourne-Webb, T. Amis, L. Laloui, Thermo-mechanical behaviour of energy piles, Geotechnique. 62 (2012) 503–519. http://www.scopus.com/inward/record.url?eid=2-s2.0-84871024108&partnerID=40&md5=fda0d47a907be64a2115ed30ee55c501.

[15] C. Knellwolf, H. Peron, L. Laloui, Geotechnical analysis of heat exchanger piles, J. Geotech. Geoenvironmental Eng. 137 (2011) 890–902.

[16]   P.J. Bourne-Webb, B. Amatya, K. Soga, A framework for understanding energy pile behaviour, Proc. Inst. Civ. Eng. Geotech. Eng. 166 (2013) 170–177. http://www.scopus.com/inward/record.url?eid=2-s2.0-84885000834&partnerID=40&md5=a1ff5f429f63d45acedf0447c7856dac.

[17]   L. Laloui, M. Moreni, L. Vulliet, Comportement d'un pieu bi-fonction, fondation et échangeur de chaleur, Can. Geotech. J. 40 (2003) 388–402. doi:10.1139/t02-117.

[18]   T. Mimouni, L. Laloui, Towards a secure basis for the design of geothermal piles, Acta Geotech. 9 (2014) 355–366.

[19]   A. Di Donna, L. Laloui, Soil Response under Thermomechanical Conditions Imposed by Energy Geostructures, in: Energy Geostructures, John Wiley & Sons, Inc., 2013: pp. 3–21. doi:10.1002/9781118761809.ch1.

[20]   S. Haehnlein, P. Bayer, P. Blum, International legal status of the use of shallow geothermal energy, Renew. Sustain. Energy Rev. 14 (2010) 2611–2625. doi:10.1016/j.rser.2010.07.069.

[21]   F. Loveridge, J. Low, W. Powrie, Site investigation for energy geostructures, Q. J. Eng. Geol. Hydrogeol. 50 (2017) 158–168. doi:10.1144/qjegh2016-027.

[22]   C.G. Olgun, T.Y. Ozudogru, C.F. Arson, Thermo-mechanical radial expansion of heat exchanger piles and possible effects on contact pressures at pile–soil interface, Géotechnique Lett. 4 (2014) 170–178. doi:10.1680/geolett.14.00018.

[23]   R.G. Campanella, J.K. Mitchell, Influence of temperature variations on soil behavior, J. Soil Mech. Found. Div. (1968).

[24]   M. Boudali, S. Leroueil, B.R. Srinivasa Murthy, Viscous behaviour of natural clays., in: 13th Int. Conf. Soil Mech. Found. Eng. ICSMFE, New Delhi, India, 1994.

[25]   T. Hueckel, B. François, L. Laloui, Explaining thermal failure in saturated clays, Geotechnique. 59 (2009) 197–212.

[26]   M. Sutman, Thermo-Mechanical Behavior of Energy Piles: Full-Scale Field Testing and Numerical Modeling, (2016).

[27]   C. Cekerevac, L. Laloui, Experimental study of thermal effects on the mechanical behaviour of a clay, Int. J. Numer. Anal. Methods Geomech. 28 (2004) 209–228. doi:10.1002/nag.332.

[28]   T.M. Bodas Freitas, F. Cruz Silva, P.J. Bourne-Webb, The response of energy foundations under thermo-mechanical loading, in: Proc. 18th Int. Conf. Soil Mech. Geotech. Eng., 2013: pp. 1–4.

[29]   L. Laloui, B. François, ACMEG-T: soil thermoplasticity model, Artic. J. Eng. Mech. (2009).

doi:10.1061/ASCÊEM.1943-7889.0000011.

[30]   T. Hueckel, R. Pellegrini, Thermoplastic modeling of undrained failure of saturated clay due to heating, Soils Found. 31 (1991) 1–16.

[31]   L. Laloui, C. Cekerevac, Non-isothermal plasticity model for cyclic behaviour of soils, Int. J. Numer. Anal. Methods Geomech. 32 (2008) 437–460.

[32]   L. Laloui, C.G. Olgun, M. Sutman, J.S. McCartney, C.J. Coccia, H.M. Abuel-Naga, G.A. Bowers, Issues involved with thermoactive geotechnical systems: characterization of thermomechanical soil behavior and soil-structure interface behavior, DFI J. - J. Deep Found. Inst. 8 (2014) 108–120. doi:10.1179/1937525514Y.0000000010.

[33]   T. Mimouni, Lyesse Laloui, Thermomechanical Characterization of Energy Geostructures with Emphasis on Energy Piles, École polytechnique fédérale de Lausanne EPFL, 2014. doi:doi:10.5075/epfl-thesis-6452.

[34]   X. Suguang, M.T. Suleiman, J.S. McCartney, S. Xiao, M.T. Suleiman, J.S. McCartney, Shear behavior of silty soil and soil-structure interface under temperature effects, in: Geo-Congress 2014 Tech. Pap. Geo-Characterization Model. Sustain., ASCE, Atlanta, Georgia, USA, 2014: pp. 4105–4114. doi:doi:10.1061/9780784413272.399.

[35]   L. Zhao, P. Yang, J.G. Wang, L.C. Zhang, Cyclic direct shear behaviors of frozen soil–structure interface under constant normal stiffness condition, Cold Reg. Sci. Technol. 102 (2014) 52–62. doi:http://dx.doi.org/10.1016/j.coldregions.2014.03.001.

[36]   J. Liu, Y. Cui, P. Wang, P. Lv, Design and validation of a new dynamic direct shear apparatus for frozen soil, Cold Reg. Sci. Technol. 106–107 (2014) 207–215. doi:http://dx.doi.org/10.1016/j.coldregions.2014.07.010.

[37]   J. Liu, P. Lv, Y. Cui, J. Liu, Experimental study on direct shear behavior of frozen soil–concrete interface, Cold Reg. Sci. Technol. 104–105 (2014) 1–6. doi:http://dx.doi.org/10.1016/j.coldregions.2014.04.007.

[38]   K.D. Murphy, J.S. McCartney, Thermal Borehole Shear Device, Geotech. Test. J. 37 (2014) 20140009. doi:10.1520/GTJ20140009.

[39]   I. Shahrour, F. Rezaie, An elastoplastic constitutive relation for the soil-structure interface under cyclic loading, Comput. Geotech. 21 (1997) 21–39. doi:http://dx.doi.org/10.1016/S0266-352X(97)00001-3.

[40]   M.E. Suryatriyastuti, H. Mroueh, S. Burlon, A load transfer approach for studying the cyclic behavior of thermo-active piles, Comput. Geotech. 55 (2014) 378–391.

doi:10.1016/J.COMPGEO.2013.09.021.

[41]   Suryatriyastuti M. E., Mroueh H., Burlon S., Habert J, Numerical analysis of the bearing capacity in thermo-active piles under cyclic axial loading, in: Energy Geostructures Innov. Undergr. Eng., Hoboken, ISTE Ltd. and John Wiley and Sons, 2013: pp. 139–154.

[42]   T. Amis, P.J. Bourne-Webb, The effects of heating and cooling energy piles under working load at Lambeth College, UK, 2009. http://www.slideshare.net/Tonyamis/the-effects-of-heating-and-cooling-energy-piles-under-working-load-at-lambeth-college-uk.

[43]   L. Laloui, M. Nuth, L. Vulliet, Experimental and numerical investigations of the behaviour of a heat exchanger pile, Int. J. Numer. Anal. Methods Geomech. 30 (2006) 763–781. doi:10.1002/nag.499.

[44]   A. Di Donna, A.F. Rotta Loria, L. Laloui, Numerical study of the response of a group of energy piles under different combinations of thermo-mechanical loads, Comput. Geotech. 72 (2016) 126–142. doi:http://dx.doi.org/10.1016/j.compgeo.2015.11.010.

[45]   F.P. de Santayana, C. de Santiago, M. de Groot, J. Uchueguía, J.L. Arcos, B. Badenes, Effect of Thermal Loads on Precast Concrete Thermopile, Environ. Geotech. 0 (n.d.) 1–54. doi:10.1680/jenge.17.00103.

[46]   M. Faizal, A. Bouazza, R.M. Singh, An experimental investigation of the influence of intermittent and continuous operating modes on the thermal behaviour of a full scale geothermal energy pile, Geomech. Energy Environ. 8 (2016) 8–29. doi:10.1016/j.gete.2016.08.001.

[47]   A.F. Rotta Loria, L. Laloui, The interaction factor method for energy pile groups, Comput. Geotech. 80 (2016) 121–137. doi:http://dx.doi.org/10.1016/j.compgeo.2016.07.002.

[48]   A.F. Rotta Loria, L. Laloui, Impact of Thermally Induced Soil Deformation on the Serviceability of Energy Pile Groups, in: Springer, Cham, 2017: pp. 421–428. doi:10.1007/978-3-319-52773-4_50.

[49]   A.F. Rotta Loria, Thermo-mechanical performance of energy pile groups, (2018). doi:10.5075/EPFL-THESIS-8138.

[50]   A.F.R. Loria, L. Laloui, The equivalent pier method for energy pile groups Thermo-mechanical performance of energy pile groups View project Reduction of fuel consumption by farming, a new practice-oriented Tool View project, (2017). doi:10.1680/jgeot.16.P.139.

[51]   A.F. Rotta Loria, L. Laloui, Group action effects caused by various operating energy piles, Géotechnique. (2017) 1–8. doi:10.1680/jgeot.17.P.213.

[52] M.E. Suryatriyastuti, H. Mroueh, S. Burlon, Understanding the temperature-induced mechanical behaviour of energy pile foundations, Renew. Sustain. Energy Rev. 16 (2012) 3344–3354. doi:http://dx.doi.org/10.1016/j.rser.2012.02.062.

[53] E. Hassani Nezhad Gashti, M. Malaska, K. Kujala, Evaluation of thermo-mechanical behaviour of composite energy piles during heating/cooling operations, Eng. Struct. 75 (2014) 363–373. doi:http://dx.doi.org/10.1016/j.engstruct.2014.06.018.

[54] C.G. Olgun, T.Y. Ozudogru, S.L. Abdelaziz, A. Senol, Long-term performance of heat exchanger piles, Acta Geotech. 10 (2015) 553–569. doi:10.1007/s11440-014-0334-z.

[55] H.M. Coyle, L.C. Reese, Load transfer for axially loaded piles in clay, J. Soil Mech. Found. Div. 92 (1966).

[56] H. Péron, C. Knellwolf, L. Laloui, A method for the geotechnical design of heat exchanger piles, in: Proc. Geo-Frontiers 2011 Conf., 2011: pp. 470–479.

[57] S. Burlon, J. Habert, F. Szymkievicz, M. Suryatriyastuti, H. Mroueh, Towards a design approach of bearing capacity of thermo-active piles, in: Eur. Geotherm. Congr., 2013: pp. 1–6.

[58] T. Mimouni, L. Laloui, Thermo-Pile: A Numerical Tool for the Design of Energy Piles, in: Energy Geostructures, John Wiley & Sons, Inc., 2013: pp. 265–279. doi:10.1002/9781118761809.ch13.

[59] Oasys, Pile Version 19.5. Pile Oasys Geo Suite for Windows. User manual., London, UK, 2014.

[60] M. Suryatriyastuti, Numerical study of the thermoactive piles behavior in cohesionless soils, (2013). https://www.researchgate.net/publication/259829225 (accessed June 22, 2018).

[61] K.D. Murphy, J.S. McCartney, Seasonal response of energy foundations during building operation, Geotech. Geol. Eng. 33 (2015) 343–356.

[62] VDI, VDI 4640 Thermal use of the underground. Part 2: Ground source heat pump systems, The Association of German Engineers (VDI), 2001.

[63] SIA, Utilisation de la chaleur du sol par des ouvrages de fondation et de soutènement en béton: guide pour la coneption, la réalisation et la maintenance, SIA, Société suisse des ingénieurs et des architectes, 2005. http://books.google.dk/books?id=Ki.

[64] A. Phillips, B.R. Establishment, B.R.E. Staff, N. Foundation, N.F. Staff, NHBC Foundation, Efficient Design of Piled Foundations for Low-Rise Housing: Design Guide, Building Research Establishment, 2010. http://www.nhbcfoundation.org/Portals/0/NF_Pubs1/NF21 Efficient

design of piled foundations for low-rise housing.pdf.

[65]   F. Loveridge, T. Amis, W. Powrie, Energy pile performance and preventing ground freezing, 2012 Int. Conf. Geomech. Eng. 1 (2012). http://eprints.soton.ac.uk/342799/.

[66]   S.L.A.M. Abdelaziz, Deep energy foundations: geotechnical challenges and design considerations, Virginia Polytechnic Institute and State University, Blacksburg, Virginia, 2013.

[67]   P. Bourne-Webb, J.-M. Pereira, G.A. Bowers, T. Mimouni, F.A. Loveridge, S. Burlon, C.G. Olgun, J.S. McCartney, M. Sutman, Design tools for thermoactive geotechnical systems, DFI Journal-The J. Deep Found. Inst. 8 (2014) 121–129.

[68]   P. Bourne-Webb, S. Burlon, S. Javed, S. Kürten, F. Loveridge, Analysis and design methods for energy geostructures, Renew. Sustain. Energy Rev. 65 (2016) 402–419. doi:10.1016/J.RSER.2016.06.046.

[69]   A.F. Rotta Loria, M. Bocco, C. Garbellini, A. Muttoni, L. Laloui, The role of thermal loads in the performance-based design of energy piles, Géotechnique. (2018).

[70]   L. Laloui, A.F. Rotta Loria, Energy geostructures analysis and design, (n.d.).

[71]   L. Laloui, Thermo-Pile. A software for the geotechnical design of energy piles. Theoretical aspects. , 2016.

[72]   P. Bourne-Webb, J.-B. Bernard, W. Friedemann, N. von der hude, N. Pralle, V.M. Uotinen, B. Widerin, Delivery of Energy Geostructures, in: Energy Geostructures, John Wiley & Sons, Inc., 2013: pp. 229–263. doi:10.1002/9781118761809.ch12.

[73]   M. Alberdi-Pagola, R.L. Jensen, S.E. Poulsen, A performance case study of energy pile foundation at Rosborg Gymnasium (Denmark), in: 12th REHVA World Congr. Clima2016, Department of Civil Engineering, Aalborg University, Aalborg, Denmark, 2016: p. 10. http://vbn.aau.dk/files/233716932/paper_472.pdf.

[74]   D. Pahud, M. Hubbuch, Measured thermal performances of the energy pile system of the Dock Midfield at Zürich Airport, in: Proc. Eur. Geotherm. Congr., 2007.

[75]   F. Bockelmann, H. Kipry, S. Plesser, M.N. Fisch, Evaluation and optimization of underground thermal energy storage systems of Energy Efficient Buildings (WKSP) - A project within the new German R&D-framework EnBop, in: Proc. Eighth Int. Conf. Enhanc. Build. Oper., Berlin, Germany, 2008.

[76]   Y. Hamada, H. Saitoh, M. Nakamura, H. Kubota, K. Ochifuji, Field performance of an energy pile system for space heating, Energy Build. 39 (2007) 517–524.

[77]   H.I. Henderson, S.W. Carlson, A.C. Walburger, North American monitoring of a hotel with

room size GSHPS, 1999.

[78] C.J. Wood, H. Liu, S.B. Riffat, Comparison of a modelled and field tested piled ground heat exchanger system for a residential building and the simulated effect of assisted ground heat recharge, Int. J. Low-Carbon Technol. 5 (2010) 137–143. http://www.scopus.com/inward/record.url?eid=2-s2.0-79551701460&partnerID=40&md5=ecc189d295c6f554d6f5bea55918f34c.

[79] K. Sekine, R. Ooka, S. Hwang, Y. Nam, Y. Shiba, M. Eng, Development of a ground-source heat pump system with ground heat exchanger utilizing the cast-in-place concrete pile foundations of buildings, 2007.

[80] M.N. Fisch, R. Himmler, International Solar Centre, Berlin-A Comprehensive Energy Design, (2005).

[81] C.J. Wood, H. Liu, S.B. Riffat, An investigation of the heat pump performance and ground temperature of a piled foundation heat exchanger system for a residential building, Energy. 35 (2010) 4932–4940. doi:http://dx.doi.org/10.1016/j.energy.2010.08.032.

[82] Małgorzata JASTRZĘBSKA, B. WAWRZYŃCZYK, The analysis of the direct foundation with energy foundations on the basis of the office building "A4 Business Park" in Katowice at Francuska street, ACEE Silesian Univ. Technol. 2 (2016).

[83] Y. Ouyang, K. Soga, Y.F. Leung, Numerical back-analysis of energy pile test at Lambeth College, London, in: 211 GSP, 2011: pp. 440–449. http://www.scopus.com/inward/record.url?eid=2-s2.0-79956367294&partnerID=40&md5=07b724c34a506741bb2aca22dc4a3940.

[84] L. Laloui, M. Moreni, A. Fromentin, D. Pahud, L. Vuillet, In-situ thermo-mechanical load test on a heat exchanger pile, (1999).

[85] L. Laloui, M. Nuth, Numerical modelling of the behaviour of a heat exchanger pile, Rev. Eur. Génie Civ. 9 (2005) 827–839.

[86] T. Mimouni, L. Laloui, Behaviour of a group of energy piles, Can. Geotech. J. 52 (2015) 1913–1929. doi:10.1139/cgj-2014-0403.

[87] A. Di Donna, A.F. Rotta Loria, L. Laloui, Numerical study of the response of a group of energy piles under different combinations of thermo-mechanical loads, Comput. Geotech. 72 (2016) 126–142. doi:10.1016/J.COMPGEO.2015.11.010.

[88] J.S. McCartney, K.D. Murphy, Strain Distributions in Full-Scale Energy Foundations (DFI Young Professor Paper Competition 2012), DFI J. - J. Deep Found. Inst. 6 (2012) 26–38.

doi:10.1179/dfi.2012.008.

[89]   K.D. Murphy, J.S. McCartney, K.S. Henry, Evaluation of thermo-mechanical and thermal behavior of full-scale energy foundations, Acta Geotech. 10 (2015) 179–195. doi:10.1007/s11440-013-0298-4.

[90]   M. De Groot, C. De Santiago, F. Pardo de Santayana, Heating and cooling an energy pile under working load in Valencia, 23rd Eur. Young Geotech. Eng. Conf. (2014).

[91]   M. Sutman, T. Brettmann, C.G. Olgun, Thermo-mechanical behavior of energy piles: full-scale field test verification, in: DFI 39th Annu. Conf. Deep Found. Atlanta, GA, 2014: pp. 1–11.

[92]   S. Baycan, C. Haberfield, G. Chapman, B. Wang, A. Bouazza, R.M. Singh, D. Barry-Macaulay, Field investigation of a geothermal energy pile: Initial observations, in: 18th Int. Conf. Soil Mech. Geotech. Eng., Paris (France), 2013.

[93]   A. Bouazza, R.M. Singh, B. Wang, D. Barry-Macaulay, C. Haberfield, G. Chapman, S. Baycan, Y. Carden, Harnessing on site renewable energy through pile foundations, (n.d.).

[94]   R. Poudyal, Thermal-mechanical Behavior of a Multiple-loop Geothermal Heat Exchanger Pile, (2014). https://shareok.org/handle/11244/25704 (accessed June 26, 2018).

[95]   J.S. McCartney, J.E. Rosenberg, Impact of heat exchange on side shear in thermo-active foundations, in: Geo-Frontiers 2011 Adv. Geotech. Eng., ASCE, 2011: pp. 488–498.

[96]   C.A. Kramer, An Experimental Investigation on Performance of a Model Geothermal Pile in Sand, The Pennsylvania State University, 2013.

[97]   C.A. Kramer, P. Basu, Performance of a model geothermal pile in sand, in: Proc. 8th Int. Conf. Phys. Model. Geotech. Perth (Gaudin, C. White, D. (Eds)). Leiden CRC Press. Pp. 771–777., 2014.

[98]   A. Kalantidou, A.M. Tang, J.-M. Pereira, G. Hassen, Preliminary study on the mechanical behaviour of heat exchanger pile in physical model, Geotechnique. 62 (2012) 1047.

[99]   N. Yavari, A.M. Tang, J.-M. Pereira, G. Hassen, Experimental study on the mechanical behaviour of a heat exchanger pile using physical modelling, Acta Geotech. 9 (2014) 385–398.

[100] A.-M. Tang, A. Kalantidou, J.-M. Pereira, G. Hassen, N. Yavari, Mechanical Behaviour of Energy Piles in Dry Sand, 2014.

[101] A. Marto, A. Amaludin, M.H. Bin Satar, Experiments on Shallow Geothermal Energy Model Piles Embedded in Soft Soil, EJGE. 20 (2015).

[102] A.F.R. Loria, A. Gunawan, C. Shi, L. Laloui, C.W.W. Ng, Numerical modelling of energy piles in saturated sand subjected to thermo-mechanical loads, Geomech. Energy Environ. 1 (2015) 1–15.

[103] A.F. Rotta Loria, A. Di Donna, L. Laloui, Numerical study on the suitability of centrifuge testing for capturing the thermal-induced mechanical behavior of energy piles, J. Geotech. Geoenvironmental Eng. 141 (2015) 4015042.

[104] W. Wang, R.A. Regueiro, M. Stewart, J.S. McCartney, Coupled thermo-poro-mechanical finite element analysis of an energy foundation centrifuge experiment in saturated silt, in: GeoCongress 2012 State Art Pract. Geotech. Eng., ASCE, 2012: pp. 4406–4415.

Appendix

Table A: Main case studies reported in literature.

More case studies are available in [72].

Pile type, length [m] / diameter [m]	Pipe configuration	Number of energy piles	Seasonal performance factor [SPF]	Heat transfer rate [W/m]	Reference
Precast driven, 15 / 0.3m x 0.3m	W-shape	220	Heating: 3	Max. 43; average 12.	[73], updated
Precast driven, 12	-	52	Heating: 4.3	-	[72]
Cast in place, 26.8 / 0.9 to 1.5	5U	306	Heating: 3.9	Max. 72; average 45.	[74]
Cast in place, 8.5	1U	196	Cooling: 6.5	Average heating 50; average cooling 5-35.	[75]
Precast driven, 9 / 0.30	1U	26	Heating: 3.2		[76]
Cast in place, 26	-	198	Heating: 4.0; cooling: 4.4	Max. heating 18.5; average heating 1; max. Cooling 23.3; average cooling 11.6.	[77]
Cast in place, 10/0.3	1U	21	Heating: 3.2	Average heating 26.	[78]
Cast in place, 14.8/0.91	3U	1		Average heating 91.	[61]
Cast in place, 13.4/0.91	4U	1		Average heating 95.	
Cast in place, 20/1.5	8U	2	Heating: 3.2; cooling: 3.7	Average heating 44-52; average cooling 100-120.	[79]
Cast in place (-)	-	196	Heating 5.4; free-cooling: 24.5	Max. heating: 12 heating; Max. cooling: 17.	[80]
Cast in place, 10 / 0.3	1U	16	Heating: 3.62	Average heating 26 W/m.	[81]
Cast in place, 15 / 0.5	1U	54	-	Max. 300.	[82]

Table B: Main full-scale studies reported in literature.

Pile type, length [m]/ diameter [m]	Ground conditions	Restrain condition	Induced temperature changes	Mechanical load	Main conclusions	Source
2 cast in place piles, 23-26/0.6	5 m river deposits over London clay	Floating pile	Fluid temperature imposed in test pile: - 6 to 40 °C; test pile ΔT = - 20 °C; sink pile: ΔT = + 30 °C, 3-day tests.	1200 kN (failure 3600 kN)	Pile-soil system shows thermo-elastic behaviour. Sufficient margin between mobilised shaft.	[13,42,83] Lambeth College (UK)
Cast in place, 25.8/0.88	Alluvial deposits 12 m, glacial till to 25 m, driven to sandstone	End-bearing	TRT conditions: ΔT = + 21 and + 15 °C, 12 days heating and 16 days recovery.	Building load (1300 kN)	Pile strain shows thermo-elastic behaviour and depends on the surrounding soil.	[43,84] and numerical analysis [85]. EPFL (CH)
4 cast in place piles, 25.8/0.88	Alluvial deposits 12 m, glacial till to 25 m, driven to sandstone	End-bearing	Two test modes: i) 1 pile heated at a time; ii) 3 piles heated before last. TRT for 6 days and recovery, ΔT = + 10 °C.	Building load (800 - 2100 kN)	Group effect: differential displacements between test piles are reduced as more piles are heated.	[86,87] EPFL (CH)
Cast in place, 9/1.2	Silty sand/clayey silt over highly fissured weathered stiff clayey, sandy silt	Head restrained (raft) + floating	Operational conditions: 5 to 20 °C.	1100 kN	Appropriate operating of energy piles hardly affects the shaft resistance.	[3]
2 cast in place piles, 13.4 - 14.8/0.91	Embedded into 7.6 m of claystone (Denver Blue Shale)	End-bearing	Operational conditions: 7 to 35 °C.	Building load (3700 kN)	Thermal axial strains are within acceptable limits.	[61,88]
8 cast in place piles, 15.2/0.61	12 m of dense sand, silt and gravel on top of sandstone	End-bearing	TRT conditions: 10 - 50 °C, 120 - 500 hours.	Building load (833 kN)	Linear thermo-elastic behaviour observed. Pile head displacements should not cause significant angular distortions.	[89]
Precast driven, 17/0.35x0.35	Driven into gravel with coarse sand	End-bearing	TRT conditions: 23-29 °C, 120 hours; stages TRT 20 days and cyclic thermal loads for 15 days.	1000 kN	The increase of the axial load in the pile is around 12% of the mechanical load. The maximum increase of temperature in the pile does not reach 5 °C at any depth.	[45,90]
3 cast in place piles, 14/0.46	8.7 m of clay on top of dense sand	-	Different thermal patterns between 7 and 45 °C, 4 to 14 days.	2560 kN	The thermal loads need to be considered during the design of energy piles. The behaviour of energy piles depends on the level of restrictions of the pile.	[26,91] Virginia Tech (Richmond, Texas, USA)

Pile type, length [m] / diameter [m]	Ground conditions	Restrain condition	Induced temperature changes	Mechanical load	Main conclusions	Source
5 cast in place piles, 35/0.25	Silty sand layer (13-19 m) underlain by a shale layer	End-bearing	Different thermal patterns between 6 and 50 °C, 2 to 16 days.	1300 kN (ultimate load)	The thermal loads need to be considered during the design of energy piles.	[66] Virginia Tech (Virginia, USA)
Cast in place, 16.1/0.6	Unsaturated, very dense sand	-	TRT conditions: 15 - 50 °C; 3 to 52 days.	1850 kN	The pile shaft resistance gained strength during thermal heating loads.	[92,93] Monash University (AU)
Cast in place, 16.1/0.6	Unsaturated, very dense sand	-	Intermittent thermal loads for 20 days.	-	Thermal strains and stresses for intermittent tests were cyclic and returned to initial values. Intermittent operation is advantageous since generates lower pile thermal loading for long term operations.	[46] Monash University (AU)
Cast in place, 12.20/1.07	3 m soft clay topping shale	End-bearing	TRT conditions: 17 - 37 °C, 39 days.	-	The load transfer model reproduces the monotonic thermal load implications.	[94] Oklahoma State University (USA)

Table C: Main laboratory-scale studies reported in literature.

Laboratory studies, either physical or centrifuge models, allow to uncouple uncertainties as they are reproduced under controlled environments.

Pile type	Methodology	Soil	Heat source	Restraints	Main conclusions	Source
Concrete	Experimental data	Dry sand	PVC 1U tube	Free thermal expansion	Increase in bearing capacity after heating pile. Similar behaviour in [95].	[96,97]
Aluminium pipe pile	Experimental data	Dry sand	Aluminium 1U	End-bearing	During thermal cycles under constant axial head load, for a head load lower than 30 % of the pile resistance, thermo-elastic behaviour of the pile is observed. For higher head load, significant cumulative settlement can be observed.	[98–100]
Stainless steel	Experimental data	Soft Kaolin clay	Metallic 1U	-	The working load for shallow geothermal energy pile embedded in soft soil should be reduced adequately to prevent failure of the pile.	[101]
Steel pipe pile	Centrifuge experimental data + THM* FEM analysis	Saturated sand	Heating wire	-	The null point position depends on the magnitude of the thermal and mechanical loads.	[102]
Reinforced concrete	Centrifuge experimental data + TM FEM analysis	Dry Nevada sand	-	-	Negligible variation between the evolutions of the load settlement curves. This indicates a very limited impact of temperature on the bearing behaviour of the pile.	[103]
Concrete	Centrifuge data + axisymmetric TPM*2 FEM analysis	Partially saturated silt	PFA 3U tube	Semi-floating	Thermally-induced liquid water and water vapor flow inside the soil were found to have an impact on soil-structure interaction.	[104]
Reinforced concrete	Centrifuge experimental data + load transfer analysis	Bonny silt	Aluminium 1U	-	By heating the pile, its bearing capacity increased, because of an increase in drained shear distribution along the pile due to soil compression during the heating phase.	[95]

* THM: Thermo-hydro-mechanical; *2 TPM: Thermo-poro-mechanical

Appendix VII.   Complete list of references

The following reference list covers all the references used in this PhD thesis, including journal papers, conference papers and technical reports.

Abdelaziz, S. L. A. M. (2013). 'Deep energy foundations: geotechnical challenges and design considerations', PhD thesis, Virginia Polytechnic Institute and State University, Blacksburg, Virginia.

Abdelaziz, S. L., Olgun, C. G. and Martin Ii, J. R. (2015). 'Equivalent energy wave for long-term analysis of ground coupled heat exchangers', *Geothermics*, *53*, pp. 6*7-84*. https://doi.org/10.1016/j.geothermics.2014.04.006

Abu-Hamdeh, N. H. (2003). 'Thermal Properties of Soils as affected by Density and Water Content', *Biosystems Engineering*, *86*, pp. 97-102.

Acuña, J., Fossa, M., Monzó, P. and Palm, B. (2012). 'Numerically Generated g-functions for Ground Coupled Heat Pump Applications', In *Proceedings of the COMSOL Conference in Milan*.

Acuña, J., Mogensen, P. & Palm, B. (2009). 'Distributed thermal response test on a U-pipe borehole heat exchanger'. *Effstock 2009, 11th International Conference on Thermal Energy Storage*, Stockholm, June 14-17 2009. Academic Conferences Publishing.

Ahmad, M. (2017). *Operation and Control of Renewable Energy Systems*. John Wiley & Sons. ISBN:9781119281689

Alberdi-Pagola, M. and Poulsen, S. E. (2015). 'Thermal response testing and performance of quadratic cross section energy piles (Vejle, Denmark)', in *XVI European Conference for Soil Mechanics and Geotechnical Engineering 2015*.

Alberdi-Pagola, M. (2018). 'Thermal response test data of five quadratic cross section precast pile heat exchangers', *Data in Brief*, *18*, pp. 13–15, https://doi.org/10.1016/j.dib.2018.02.080

Alberdi-Pagola, M., Jensen, L.J., Madsen, S. And Poulsen, S.E. (2018). Method to obtain g-functions for multiple precast quadratic pile heat exchangers. Aalborg: Department of Civil Engineering, Aalborg University. DCE Technical Reports; nr. 243, pp. 34. Available online: http://vbn.aau.dk/files/274763046/Method_to_obtain_g_functions_for_multiple_precast_quadratic_pile_heat_exchangers.pdf

Alberdi-Pagola, M., Jensen, R. L. and Poulsen, S. E. (2016). 'A performance case study of energy pile foundation at Rosborg Gymnasium (Denmark)', in *12th REHVA World Congress Clima2016*. Aalborg, Denmark: Department of Civil Engineering, Aalborg University. Available at: http://vbn.aau.dk/files/233716932/paper_472.pdf.

Alberdi-Pagola, M., Jensen, R. L., Madsen, S. and Poulsen, S. E. (2017). 'Measurement of thermal properties of soil and concrete samples'. Aalborg: Department of Civil Engineering, Aalborg University. DCE Technical Reports, nr. 235, pp. 30. Available online: http://vbn.aau.dk/files/266378485/Measurement_of_thermal_properties_of_soil_and_concrete_samples.pdf

Alberdi-Pagola, M., Madsen, S., Jensen, R. L. and Poulsen, S. E. (2017). 'Numerical investigation on the thermo-mechanical behavior of a quadratic cross section pile heat exchanger', in *Proceedings of the IGSHPA Technical/Research Conference and Expo*; Denver, USA, March 14-16, 2017. http://dx.doi.org/10.22488/okstate.17.000520

Alberdi-Pagola, M., Madsen, S., Jensen, R. L. and Poulsen, S. E. (2018). 'Thermo-mechanical aspects of pile heat exchangers: background and literature review', Aalborg: Department of Civil Engineering, Aalborg University. DCE Technical Reports, nr. 250, pp. 37. Available online: http://vbn.aau.dk/files/281634409/Thermo_mechanical_aspects_of_pile_heat_exchangers_background_and_literature_review.pdf

Alberdi-Pagola, M., Poulsen, S. E., Jensen, L. J. and Madsen, S. (2018). 'A case study of the sizing and optimisation of an energy pile foundation (Rosborg, Denmark). *Renewable Energy (under-review)*.

Alberdi-Pagola, M., Poulsen, S. E., Jensen, R. L. and Madsen, S. (2017). 'Thermal response testing of precast pile heat

exchangers: fieldwork report' Aalborg: Department of Civil Engineering, Aalborg University. DCE Technical Reports, nr. 234, pp. 43. Available online: http://vbn.aau.dk/files/266379225/Thermal_response_testing_of_precast_pile_heat_exchangers_fieldwork_report.pdf

Alberdi-Pagola, M., Poulsen, S. E., Loveridge, F., Madsen, S. and Jensen, R. L. (2018). 'Comparing heat flow models for interpretation of precast quadratic pile heat exchanger thermal response tests', *Energy, 145*, pp. 721–733. https://doi.org/10.1016/j.energy.2017.12.104

Alberdi-Pagola, M., Poulsen, S.E., Jensen, R.L., and Madsen, S. (2018). 'Design methodology for precast quadratic pile heat exchanger-based shallow geothermal ground-loops: multiple pile g-functions' *Geothermics (under-review)*.

Al-Khoury, R. (2011). *Computational modeling of shallow geothermal systems*, CRC Press; ISBN 0415596270.

Amatya, B. L., Soga, K., Bourne-Webb, P. J., Amis, T. and Laloui, L. (2012). 'Thermo-mechanical behaviour of energy piles', *Geotechnique*, *62*, pp. 503–519. https://doi.org/10.1680/geot.10.P.116

Amis, T. and Bourne-Webb, P. J. 82008). 'The effects of heating and cooling energy piles under working load at Lambeth College'*, in 33rd Annual and 11th International DFI Conference UK*.

Ardehali, M. (2008). 'Energy performance monitoring and examination of electrical demand and consumption of a geothermal heat pump system', *Energy Engineering*, *105*(5), p. 44-54.

ASHRAE (2009). *ASHRAE Handbook. Fundamentals (2009).* 1791 Tullie Circle, N.E., Atlanta, GA 30329: American Society of Heating, Refrigerating and Air-Conditioning Engineers, Inc.

ASHRAE, (2011). *2011 ASHRAE Handbook - Heating, Ventilating, and Air-Conditioning Applications (SI Edition)*. American Society of Heating, Refrigerating and Air-Conditioning Engineers, Inc.

ASTM STANDARDS (1998). 'ASTM D2974:1998: Standard Test Methods for Moisture, Ash, and Organic Matter of Peat and Other Organic Soils'. 1916 Race St., Philadelphia, PA 19103.

ASTM STANDARDS (2013). 'C642-13. Standard Test Method for Density, Absorption, and Voids in Hardened Concrete'.

Austin, W. A. (2000). 'Development of an in-situ system and analysis procedure for measuring ground thermal properties', *ASHRAE Transactions. 106* (1), pp. 365–379.

Badenes, B., de Santiago, C., Nope, F., Magraner, T., Urchueguía, J., de Groot, M., Pardo de Santayana, F., Arcos, J. L. and Martín, F. (2016). 'Thermal characterization of a geothermal precast pile in Valencia (Spain)', in *European Geothermal Congress 2016*; Strasbourg, France, 19-24 Sept 2016.

Balfour Beatty Ground Engineering (2016). 'Geothermal driven piles'. Available online: http://www.balfourbeatty.com/media/29535/geothermal-driven-piles.pdf. [Accessed on March 2016].

Bandos, T. V, Campos-Celador, Á., López-González, L. M. and Sala-Lizarraga, J. M. (2014). 'Finite cylinder-source model for energy pile heat exchangers: Effects of thermal storage and vertical temperature variations', *Energy*, *78*, pp. 639–648. https://doi.org/10.1016/j.energy.2014.10.053.

Banks, D. *An Introduction to Thermogeololy. Ground Source Heating and Cooling*, Blackwell Publishing, Oxford, 2008. ISBN 9780470670347.

Baycan, S., Haberfield, C., Chapman, G., Wang, B., Bouazza, A., Singh, R. M. and Barry-Macaulay, D. (2013). 'Field investigation of a geothermal energy pile: Initial observations', in *18th International Conference on Soil Mechanics and Geotechnical Engineering*. Paris (France).

Beck, M., Bayer, P., de Paly, M., Hecht-Méndez, J. and Zell, A. (2013). 'Geometric arrangement and operation mode adjustment in low-enthalpy geothermal borehole fields for heating', *Energy*, *49*, pp. 434–443, https://doi.org/10.1016/j.energy.2012.10.060

Bentz, D., Peltz, M., Duran-Herrera, A., Valdez, P. & Juarez, C. (2011). 'Thermal properties of high-volume fly ash mortars and concretes', *Journal of Building Physics*, *34*, pp. 263-275.

Bernier, M. A., Chahla, A. and Pinel, P. (2008). 'Long-Term Ground-Temperature Changes in Geo-Exchange Systems', *ASHRAE Transactions*, *114*.

Bernier, M. A., Pinel, P., Labib, R. and Paillot, R. (2004). 'A Multiple Load Aggregation Algorithm for Annual Hourly Simulations of GCHP Systems', *HVAC&R Research, 10*, pp. 471–487. doi:10.1080/10789669.2004.10391115.

Bjorn, H. (2018). 'Shallow geothermal energy from a Danish standpoint', *Geothermal Energy,* press note.

Bockelmann, F., Kipry, H., Plesser, S. and Fisch, M.N. (2008). 'Evaluation and optimization of underground thermal energy storage systems of Energy Efficient Buildings (WKSP) - A project within the new German R&D-framework EnBop', in *Proceedings of the Eighth International Conference for Enhanced Building Operations*. Berlin, Germany.

Bodas Freitas, T. M., Cruz Silva, F. and Bourne-Webb, P. J. (2013). 'The response of energy foundations under thermo-mechanical loading', in *Proceedings of the 18th International Conference on Soil Mechanics and Geotechnical Engineering*.

Bouazza, A., Singh, R. M., Wang, B., Barry-Macaulay, D., Haberfield, C., Chapman, G., Baycan, S. and Carden, Y. (2011). 'Harnessing on site renewable energy through pile foundations', *Australian Geomechanics*, *46*.

Boudali, M., Leroueil, S. and Srinivasa Murthy, B. R. (1994). 'Viscous behaviour of natural clays', in *13th International Conference Soil Mechanics and Foundation Engineering ICSMFE,* New Delhi, India.

Bourne-Webb, P. *et al.* (2013). 'Delivery of Energy Geostructures', in *Energy Geostructures*. John Wiley & Sons, Inc., pp. 229–263. doi: 10.1002/9781118761809.ch12.

Bourne-Webb, P. J., Amatya, B. and Soga, K. (2013). 'A framework for understanding energy pile behaviour', in *Proceedings of the Institution of Civil Engineers: Geotechnical Engineering*, 166(2), pp. 170–177.

Bourne-Webb, P. J., Amatya, B., Soga, K., Amis, T., Davidson, C. and Payne, P. (2009). 'Energy pile test at Lambeth College, London: Geotechnical and thermodynamic aspects of pile response to heat cycles', *Geotechnique*, *59*, pp. 237–248. https://doi.org/10.1680/geot.2009.59.3.237

Bourne-Webb, P., Burlon, S., Javed, S., Kürten, S. and Loveridge, F. (2016). 'Analysis and design methods for energy geostructures', *Renewable Sustainable Energy Reviews, 65*, pp. 402–419, https://doi.org/10.1016/j.rser.2016.06.046.

Bourne-Webb, P., Pereira, J.-M., Bowers, G. A., Mimouni, T., Loveridge, F. A., Burlon, S., Olgun, C. G., McCartney, J. S. and Sutman, M. (2014). 'Design tools for thermoactive geotechnical systems'. *DFI Journal - The Journal of Deep Foundation Institute*, *8*, pp. 121–129. https://doi.org/10.1179/1937525514Y.0000000013

Brandl, H. (2006). 'Energy foundations and other thermo-active ground structures', *Geotechnique*, 56, pp. 81–122. https://doi.org/10.1680/geot.2006.56.2.81

Brettman, T. P. E., Amis, T. and Kapps, M. (2010). 'Thermal conductivity analysis of geothermal energy piles', in *Proceedings of the Geotechnical Challenges in Urban Regeneration Conference,* pp. 26–28.

British Standard (2007). 'BS EN 15450:2007. Heating systems in buildings - Design of heat pump heating systems'.

Building Physics (2017) 'Earth Energy Designer EED 4'. Available at: https://www.buildingphysics.com/manuals/EED4.pdf.

Buildingphysics (2008). 'Earth Energy Designer EED 3'.

Burlon, S., Habert, J., Szymkievicz, F., Suryatriyastuti, M. and Mroueh, H. (2013). 'Towards a design approach of bearing capacity of thermo-active piles', in *European Geothermal Congress*.

Campanella, R. G. and Mitchell, J. K. (1968). 'Influence of temperature variations on soil behavior', *Journal of the Soil Mechanics and Foundations Division*, *94*, Issue 3, pp. 609-734.

Capozza, A., De Carli, M. and Zarrella, A. (2012). 'Design of borehole heat exchangers for ground-source heat pumps: A literature review, methodology comparison and analysis on the penalty temperature', *Energy and Buildings*, *55*, pp. 369–379. https://doi.org/10.1016/j.enbuild.2012.08.041

Carslaw, H. S. and Jaeger, J. C. (1959). *Conduction of Heat in Solids*. Clarendon Press.

Cecinato, F. and Loveridge, F. A. (2015). 'Influences on the thermal efficiency of energy piles'. *Energy*, *82*, pp. 1021–1033. https://doi.org/10.1016/j.energy.2015.02.001

Cekerevac, C. and Laloui, L. (2004). 'Experimental study of thermal effects on the mechanical behaviour of a clay', *International Journal for Numerical Analysis Methods in Geomechanics*, *28*, pp. 209–228, https://doi.org/10.1002/nag.332

Centrum Paele A/S (2014). *Statiske Beregninger, Centrum Pæle System. Udgave Marts 2014.* Available at: http://www.centrumpaele.dk/files/manager/statiske-beregninger/statiske beregninger udgave 2014_rev.marts2016.pdf.

Centrum Paele A/S (2016). 'Energipæle'. Available online: http://www.centrumpaele.dk/paele/energipaele.html. [Accessed 14-February 2016].

Chan, J. (2014). 'Thermal properties of concrete with different Swedish aggregate materials'. Rapport TVBM (5000-serie).

Churchill, S. W. (1977). 'Friction factor equations spans all fluid-flow regimes', *Chemical Engineering, 84*.

Cimmino, M. and Bernier, M. (2014). 'A semi-analytical method to generate g-functions for geothermal bore fields'. *International Journal of Heat Mass Transfer*, *70*, pp. 641–650. https://doi.org/10.1016/j.ijheatmasstransfer.2013.11.037

Cimmino, M., Bernier, M. and Adams, F. (2013). 'A contribution towards the determination of g-functions using the finite line source', *Applied Thermal Engineering*, *51*, pp. 401–412. https://doi.org/10.1016/j.applthermaleng.2012.07.044

Claesson, J. and Hellström, G. (2000). 'Analytical Studies of the Influence of Regional Groundwater Flow by on the Performance of Borehole Heat Exchangers', in *Proceedings TERRASTOCK 2000, 8th International Conference on Thermal Energy Storage*. University of Stuttgart, Germany.

COMSOL Multiphysics (2012). *Pipe Flow Module - User's guide*.

COMSOL Multiphysics (2017). *Introduction to COMSOL Multiphysics version 5.3*. Edited by COMSOL. Burlington.

Costa, N. R., Lourenço, J. and Pereira, Z. L. (2011). 'Desirability function approach: A review and performance evaluation in adverse conditions', *Chemometrics and Intelligent Laboratory Systems, 107*, pp. 234–244, https://doi.org/10.1016/j.chemolab.2011.04.004

Coyle, H. M. and Reese, L. C. (1966). 'Load transfer for axially loaded piles in clay', *Journal of Soil Mechanics & Foundations Division.*

Danish Energy Agency (2012). *Energy Policy in Denmark*. Solid Media Solutions ed. Amaliegade 44, 1256 Copenhagen K, Denmark: Danish Energy Agency.

Danish Energy Agency (2017). *Denmark's Energy and Climate Outlook*, ISBN 978-87-93180-28-4.

Danish Energy Agency (2017). *Regulation and planning of district heating in Denmark*. URL: https://ens.dk/sites/ens.dk/files/Globalcooperation/regulation_and_planning_of_district_heating_in_denmark.pdf

Danish Energy Agency (2018). *Basisfremskrivning 2018*, ISBN 978-87-93180-33-8.

Danish Standard (2004). 'DS/EN ISO/TS 17892-1: 2004 2004. Geotechnical investigation and testing - Laboratory testing of soil – Part 1: Determination of water content'.

Danish Standard (2004). 'DS/EN ISO/TS 17892-2: 2004 2004. Geotechnical investigation and testing - Laboratory testing of soil – Part 2: Determination of density of fine-grained soil'.

Danish Standard (2010). 'DS/EN 1997-1/AC: 2010: Eurocode 7: Geotechnical design - Part 1: General rules'. Dansk Standard.

Danish Standard (2010). 'DS/EN 1997-1/AC:2010 Eurocode 7: Geotechnical design - Part 1: General rules'.

Danmarks Meteorologiske Institut (2018). 'Vejrarkiv'. Available online: http://www.dmi.dk/vejr/. [Accessed on Jun 1, 2018].

Dansk Geoteknik A/S (1973). *Geoteknisk rapport. Grundundersøgelser for Amtsgymnasium i Vejle, Vestre Engvej, Vejle.*

Dansk Standard (2015). 'DS/EN ISO 22007-2 (2015): Plastics – Determination of the thermal conductivity and thermal diffusivity – Part 2: Transient plane heat source (hot disc) method'.

De Groot, M., De Santiago, C., and Pardo de Santayana, F. (2014). 'Heating and cooling an energy pile under working load in Valencia', in *23rd European Young Geotechncal Engineers Conference.*

de Paly, M., Hecht-Méndez, J., Beck, M., Blum, P., Zell, A. and Bayer, P. (2012). 'Optimization of energy extraction for closed shallow geothermal systems using linear programming', *Geothermics*, *43*, pp. 57–65, https://doi.org/10.1016/j.geothermics.2012.03.001

de Santayana, F. P., de Santiago, C., de Groot, M., Uchueguía, J., Arcos, J. L. and Badenes, B. (2018). 'Effect of Thermal Loads on Precast Concrete Thermopile', *Environmental Geotechnics.* https://doi.org/10.1680/jenge.17.00103

Demirboğa, R., Türkmen, İ. & Karakoç, M. B. (2007). Thermo-mechanical properties of concrete containing high-volume mineral admixtures', *Building and Environment*, *42*, pp. 349-354.

Derringer, G. and Suich, R. (1980). 'Simultaneous Optimization of Several Response Variables', *Journal of Quality Technology*, *12*, pp. 214–219, doi:10.1080/00224065.1980.11980968.

Di Donna, A. and Laloui, L. (2013). 'Soil Response under Thermomechanical Conditions Imposed by Energy Geostructures', in *Energy Geostructures*. John Wiley & Sons, Inc., pp. 3–21. doi: 10.1002/9781118761809.ch1.

Di Donna, A. (2014). 'Thermo-mechanical aspects of energy piles'. PhD Thesis, École polytechnique fédérale de Lausanne EPFL.

Di Donna, A., Marco, B. and Tony, A. (2017). 'Energy Geostructures: Analysis from research and systems installed around the World'. In *DFI 2017: 42nd Annual Conference on Deep Foundations*, USA.

Di Donna, A., Rotta Loria, A. F. and Laloui, L. (2016). 'Numerical study of the response of a group of energy piles under different combinations of thermo-mechanical loads', *Computers and Geotechnics, 72*, pp. 126–142. https://doi.org/10.1016/j.compgeo.2015.11.010

Diersch, H.-J. G. (2014). 'FEFLOW Finite Element Modeling of Flow, Mass and Heat Transport in Porous and Fractured Media', Springer Science & Business Media; ISBN 364238739X.

Doherty, J. (2010). 'PEST Model-Independent Parameter Estimation. User Manual'; Computing, W. N., Ed.; 5th Edition.

Dupray, F., Laloui, L. and Kazangba, A. (2014). 'Numerical analysis of seasonal heat storage in an energy pile foundation', *Computers and Geotechnics*, *55*(0), pp. 67–77. https://doi.org/10.1016/j.compgeo.2013.08.004

Engineering Toolbox (2003). 'Ethylene Glycol Heat-Transfer Fluid'. Available at: https://www.engineeringtoolbox.com/ethylene-glycol-d_146.html [Accessed 30-March 2018].

EPA (1993). *Space conditioning: the next frontier. The potential of advanced residential space conditioning technologies for reducing pollution and saving money.* Environmental protection agency.

Eskilson, P. (1987). 'Thermal Analysis of Heat Extraction', PhD thesis, University of Lund, Sweden.

Fadejev, J., Simson, R., Kurnitski, J. and Haghighat, F. (2017). 'A review on energy piles design, sizing and modelling', *Energy*, *122*, pp. 390–407. https://doi.org/10.1016/j.energy.2017.01.097

Faizal, M., Bouazza, A. and Singh, R. M. (2016). 'An experimental investigation of the influence of intermittent and continuous operating modes on the thermal behaviour of a full scale geothermal energy pile', *Geomechanics for Energy and the Environment*, *8*, pp. 8–29. https://doi.org/10.1016/j.gete.2016.08.001

Faizal, M., Bouazza, A. and Singh, R. M. (2016). 'Heat transfer enhancement of geothermal energy piles', *Renewable and Sustainable Energy Reviews*, *57*, pp. 16–33. https://doi.org/10.1016/j.rser.2015.12.065

Farouki, O. T. (1981). 'Thermal properties of soils', *Cold Regions Research and Engineering Laboratory,* Hanover*,* The Netherlands.

Fisch, M. N. and Himmler, R. (2005). 'International Solar Centre, Berlin-A Comprehensive Energy Design'. Energy Systems Laboratory.

Fødevareministeriet (2017). 'M. BEK nr 240 af 27/02/2017 Bekendtgørelse om jordvarmeanlæg'.

Fossa, M. and Rolando, D. (2014). 'Fully analytical finite line source solution for fast calculation of temperature response factors in geothermal heat pump borefield design', In *Proceedings, IEA Heat Pump Conference, 12-16 May, Montreal (Québec), Canada.*

Fossa, M. and Rolando, D. (2015). 'Improving the Ashrae method for vertical geothermal borefield design', *Energy and Buildings*, *93*, pp. 315–323. https://doi.org/10.1016/j.enbuild.2015.02.008

Fossa, M. (2011). 'A fast method for evaluating the performance of complex arrangements of borehole heat exchangers'. *HVAC&R Research*, *17*, pp. 948–958. doi:10.1080/10789669.2011.599764.

Fossa, M., Cauret, O. and Bernier, M. (2009). 'Comparing the thermal performance of ground heat exchangers of various lengths', in *Proceedings from the 11th International Conference on Energy Storage, EFFSTOCK*.

Franck Geoteknik A/S (2013). *Geoteknisk rapport, parameterundersøgelse. Rosborg Gymnasium, Vestre Engvej 61,*

Vejle. Ny Nordfløj.

Fritsch, F. N. and Carlson, R. E. (1980). 'Monotone Piecewise Cubic Interpolation', *SIAM Journal on Numerical Analysis*, *17*, pp. 238–246, https://doi.org/10.1137/0717021

Gaia Geothermal. 'GLD Overview'. Available online: http://www.gaiageo.com/products.html. [Accessed May 2018].

Gao, J., Zhang, X., Liu, J., Li, Kui S. and Yang, J. (2008). 'Thermal performance and ground temperature of vertical pile-foundation heat exchangers: A case study', *Applied Thermal Engineering, 28*(17–18), pp. 2295-2304. https://doi.org/10.1016/j.applthermaleng.2008.01.013

Garboczi, E. J. & Bentz, D. P. (1992). 'Computer simulation of the diffusivity of cement-based materials', *Journal of Materials Science*, *27*, pp. 2083-2092.

Geelen, C., Krosse, L., Sterrenburg, P., Bakker, E.-J. and Sijpheer, N. (2003). 'Handboek Energiepalen', TNO Milieu, Energie en Procesinnovatie: Laan van Westenenk 501, Postbus 342, 7300 AH Apeldoorn, The Netherlands.

Gehlin, S. (2002). 'Thermal Response Test. Method Development and Evaluation', PhD thesis, Luleå University of Technology, Sweden.

Geo Connections Loop. 'Link PRO'. Available online: https://looplinkpro.com/features/ [Accessed March 2016].

Geotechdata.Info. (2013). Soil elastic Young's modulus. Available online: http://www.geotechdata.info/parameter/soil-young's-modulus.html. [Accessed 16-September 2016]

Geotrainet (2011). 'Geotrainet Training Manual for Design of Shallow Geothermal Systems', Geotrainet: Geo-Education for sustainable geothermal heating and cooling market.

Global, M. (2008). *Ethylene Glycol Product Guide*. Available online: http://www.meglobal.biz/media/product_guides/MEGlobal_MEG.pdf.

Ground Energy Support LLC (2013). Ground Source Heat Pumps System Performance: Monitoring, Measuring, and Metering.

GSHP Association (2012). 'Thermal Pile: Design, Installation & Materials Standards'. http://www.gshp.org.uk/pdf/GSHPA_Thermal_Pile_Standard.pdf

Haehnlein, S., Bayer, P. and Blum, P. (2010). 'International legal status of the use of shallow geothermal energy', *Renewable Sustainable Energy Reviews, 14*, pp. 2611–2625. https://doi.org/10.1016/j.rser.2010.07.069.

Hamada, Y., Saitoh, H., Nakamura, M., Kubota, H. and Ochifuji, K. (2007). 'Field performance of an energy pile system for space heating', *Energy and Buildings*, *39*(5), pp. 517–524. https://doi.org/10.1016/j.enbuild.2006.09.006

Hansen, K. K. (1986). *Sorption isotherms: a catalogue*. Technical University of Denmark Danmarks Tekniske Universitet, Department of Structural Engineering and Materials Institut for Bærende Konstruktioner og Materialer.

Harris, M. (2011). 'Thermal energy storage in Sweden and Denmark. Potentials for technology transfer', Master thesis, Lund University, Lund, Sweden.

Hassani Nezhad Gashti, E., Malaska, M. and Kujala, K. (2014). 'Evaluation of thermo-mechanical behaviour of composite energy piles during heating/cooling operations'. *Engineering Structures, 75*, pp. 363–373. https://doi.org/10.1016/j.engstruct.2014.06.018

Hellström, G. (1991). 'Ground Heat Storage: Thermal Analyses of Duct Storage Systems I. Theory', Lund University,

Department of Mathematical Physics, Sweden.

Hellström, G. (1998). 'Thermal Performance of Borehole Heat Exchangers'. Swedish Council for Building Research (BFR).

Henderson, H. I., Carlson, S. W. and Walburger, A. C. (1999). 'North American monitoring of a hotel with room size GSHPS'. Available online: http://cloud.cdhenergy.com/presentations/IEA%20Room%20HP%20June%201998%20-%20GeoExchange%20Hotel.pdf

Hot Disk AB (2014). 'Hot Disk Thermal Constants Analyser TPS 1500 unit, Instruction Manual'.

Hu, P., Zha, J., Lei, F., Zhu, N. and Wu, T. (2014). 'A composite cylindrical model and its application in analysis of thermal response and performance for energy pile', *Energy and Buildings*, *84*, pp. 324–332, https://doi.org/10.1016/j.enbuild.2014.07.046.

Hueckel, T. and Pellegrini, R. (1991). 'Thermoplastic modeling of undrained failure of saturated clay due to heating', *Soils and Foundations*, *31*(3).

Hueckel, T., François, B. and Laloui, L. (2009). 'Explaining thermal failure in saturated clays', *Geotechnique*, *59*, pp. 197–212. https://doi.org/10.1680/geot.2009.59.3.197

Ingersoll, L. R. (1954). 'Heat Conduction - With Engineering and Geological Application', The Univer.; Read Books, 1954; ISBN 9781443730747.

Jalaluddin, A. M., Tsubaki, K., Inoue, S. and Yoshida, K. (2011). 'Experimental study of several types of ground heat exchanger using a steel pile foundation'. *Renewewable Energy, 36*, pp. 764–771, https://doi.org/10.1016/j.renene.2010.08.011

Jastrzębska, M. And Wawrzyńczyk, B. (2016). 'The analysis of the direct foundation with energy foundations on the basis of the office building 'A4 Business Park' in Katowice at Francuska street', ACEE The Silesian University of Technology. Available online: http://www.acee-journal.pl/cmd.php?cmd=download&id=dbitem:article:id=398&field=fullpdf

Javed, S., Fahlén, P. and Claesson, J. (2009). 'Vertical ground heat exchangers: A review of heat flow models'. In *Effstock 2009-Stockholm*.

Javed, S., Spitler, J. D. and Fahlén, P. (2011). 'An experimental investigation of the accuracy of thermal response tests used to measure ground thermal properties', *ASHRAE Transactions*, 117(1), pp. 13–21.

Kalantidou, A., Tang, A.M., Pereira, J.-M. and Hassen, G. (2012). 'Preliminary study on the mechanical behaviour of heat exchanger pile in physical mode', *Geotechnique*, *62*(11). https://doi.org/10.1680/geot.11.T.013

Katsura, T., Nagano, K. and Takeda, S. (2008). 'Method of calculation of the ground temperature for multiple ground heat exchangers'. *Applied Thermal Engineering*, *28*, pp. 1995–2004. https://doi.org/10.1016/j.applthermaleng.2007.12.013

Kelvin, T. W. (1982). 'Mathematical and physical papers'. *Cambridge University Press. London.*

Khaliq, W. & Kodur, V. (2011). 'Thermal and mechanical properties of fiber reinforced high performance self-consolidating concrete at elevated temperatures', *Cement and Concrete Research*, *41*, pp. 1112-1122. https://doi.org/10.1016/j.cemconres.2011.06.012

Khan, M. (2002). 'Factors affecting the thermal properties of concrete and applicability of its prediction models', *Building and Environment*, *37*, pp. 607-614. https://doi.org/10.1016/S0360-1323(01)00061-0

Kim, K.-H., Jeon, S.-E., Kim, J.-K. and Yang, S. (2003). 'An experimental study on thermal conductivity of concrete', *Cement and Concrete Research*, 33, pp. 363-371. https://doi.org/10.1016/S0008-8846(02)00965-1

Knellwolf, C., Peron, H and; Laloui, L. (2011). 'Geotechnical analysis of heat exchanger piles', *Journal of Geotechnical and Geoenvironmental Engineering*, *137*, *pp. 890–902*. https://doi.org/10.1061/(ASCE)GT.1943-5606.0000513.

Kramer, C. A. and Basu, P. (2014). 'Performance of a model geothermal pile in sand', *in Proc. 8th Int. Conf. on Physical Modelling in Geotechnics*, Perth (Gaudin, C. & White, D. (eds)). Leiden: CRC Press/Balkema, pp. 771–777.

Kramer, C. A. (2013). 'An Experimental Investigation on Performance of a Model Geothermal Pile in Sand'. MSc thesis, The Pennsylvania State University, USA.

Laloui, L. and Cekerevac, C. (2008). 'Non-isothermal plasticity model for cyclic behaviour of soils', *International Journal for Numerical and Analytical Methods in Geomechanics*, 32(5), pp. 437–460. https://doi.org/10.1002/nag.629

Laloui, L. and Di Donna, A. (2011). 'Understanding the behaviour of energy geo-structures', in *Proceedings of the Institution of Civil Engineers-Civil Engineering*. Thomas Telford Ltd, 184-191.

Laloui, L. and Di Donna, A. (2013). *Energy Geostructures: Innovation in Underground Engineering*, John Wiley & Sons, Inc.

Laloui, L. and Di Donna, A. (2013). *Energy Geostructures: Innovation in Underground Engineering*, John Wiley & Sons, Inc., 2013; ISBN 978-1-84821-572-6.

Laloui, L. and François, B. (2009). 'ACMEG-T: soil thermoplasticity model', *Journal of Engineering Mechanics*, *135*. https://doi.org/10.1061/(ASCE)EM.1943-7889.0000011

Laloui, L. and Nuth, M. (2005). 'Numerical modelling of the behaviour of a heat exchanger pile', *Revue européenne de génie civil*, 9(5–6), pp. 827–839.

Laloui, L. and Nuth, M. (2009). 'Investigations on the mechanical behaviour of a Heat Exchanger Pile', *In Deep Foundations on Bored and Auger Piles*, VanImpe, W. F., VanImpe, P. O., Eds.; Crc Press-Taylor & Francis Group: Boca Raton; ISBN 978-0-415-47556-3.

Laloui, L. and Rotta Loria, A. F. (2018). 'Energy geostructures analysis and design. Intensive course in EPFL, Lausanne, Switzerland.

Laloui, L. et al. (1999). 'In-situ thermo-mechanical load test on a heat exchanger pile'. Available online: http://repository.supsi.ch/3617/1/50-Pahud-1999-Singapore.pdf

Laloui, L. et al. (2014). 'Issues involved with thermoactive geotechnical systems: characterization of thermomechanical soil behavior and soil-structure interface behavior', *DFI Journal - The Journal of the Deep Foundations Institute,* 8(2), pp. 108–120. doi: 10.1179/1937525514Y.0000000010. https://doi.org/10.1179/1937525514Y.0000000010

Laloui, L. (2016). 'Thermo-Pile. A software for the geotechnical design of energy piles. Theoretical aspects', Edited by L. of soil mechanics. S. F. I. of T. Lausanne.

Laloui, L., Moreni, M. and Vulliet, L. (2003). 'Comportement d'un pieu bi-fonction, fondation et échangeur de chaleur', *Canadian Geotechnical Journal,* 40(2), pp. 388–402. doi: 10.1139/t02-117.

Laloui, L., Moreni, M. and Vulliet, L. (2003). 'Comportement d'un pieu bi-fonction, fondation et échangeur de chaleur', *Canadian Geotechnical Journal*, *40*, pp. 388–402. doi:10.1139/t02-117.

Laloui, L., Nuth, M. and Vulliet, L. (2006). 'Experimental and numerical investigations of the behaviour of a heat exchanger pile', *International Journal of Numerical Analysis Methods for Geomechanics*, *30*, pp. 763–781.

https://doi.org/10.1016/S1571-9960(05)80040-0

Laloui, L., Olgun, C. G., Sutman, M., McCartney, J. S., Coccia, C. J., Abuel-Naga, H. M. and Bowers, G. A. (2014). 'Issues involved with thermoactive geotechnical systems: characterization of thermomechanical soil behavior and soil-structure interface behavior'. *DFI Journal – Journal of Deep Foundation Institute*, *8*, pp.108–120. https://doi.org/10.1179/1937525514Y.0000000010

Lamarche, L. and Beauchamp, B. (2007). 'A new contribution to the finite line-source model for geothermal boreholes', *Energy and Buildings*, 39(2), pp. 188–198. https://doi.org/10.1016/j.enbuild.2006.06.003

Larsen, G. (1995). *A guide to engineering geological soil description*. DGF-bulletin, 1, revision 1 (May 1995). Danish Geotechnical Society, Lyngby.

Lennon, D. J., Watt, E. and Suckling, T. P. (2009). 'Energy piles in Scotland', in *Proceedings of the Fifth International Conference on Deep Foundations on Bored and Auger Piles*; (Eds), V. I. & V. I., Ed.; Taylor & Francis Group, London: Frankfurt.

Li, M. and Lai, A. C. K. (2012). 'New temperature response functions (G functions) for pile and borehole ground heat exchangers based on composite-medium line-source theory', *Energy*, 38(1), pp. 255–263. https://doi.org/10.1016/j.energy.2011.12.004

Li, M. and Lai, A. C. K. (2015). 'Review of analytical models for heat transfer by vertical ground heat exchangers (GHEs): a perspective of time and space scales', *Applied Energy*, 151, pp. 178–191. https://doi.org/10.1016/j.apenergy.2015.04.070

Liu, J., Cui, Y., et al. (2014). 'Design and validation of a new dynamic direct shear apparatus for frozen soil', *Cold Regions Science and Technology*, 106–107(0), pp. 207–215. doi: http://dx.doi.org/10.1016/j.coldregions.2014.07.010. https://doi.org/10.1016/j.coldregions.2014.07.010

Liu, J., Lv, P., et al. (2014). 'Experimental study on direct shear behavior of frozen soil–concrete interface', *Cold Regions Science and Technology*, 104–105(0), pp. 1–6. doi: http://dx.doi.org/10.1016/j.coldregions.2014.04.007. https://doi.org/10.1016/j.coldregions.2014.04.007

Loveridge, F. and Cecinato, F. (2016). 'Thermal performance of thermoactive continuous flight auger piles', *Environmental Geotechnics*, 3(4), pp. 265–279. doi: 10.1680/jenge.15.00023.

Loveridge, F. and Powrie, W. (2014). 'G-Functions for multiple interacting pile heat exchangers', *Energy*, *64*, pp. 747–757, https://doi.org/10.1016/j.energy.2013.11.014.

Loveridge, F. and Powrie, W. (2013). 'Temperature response functions (G-functions) for single pile heat exchangers'. *Energy*, *57*, pp. 554–564, https://doi.org/10.1016/j.energy.2013.04.060

Loveridge, F. and Powrie, W. (2014). '2D thermal resistance of pile heat exchangers', *Geothermics*, *50*, pp. 122–135, https://doi.org/10.1016/j.geothermics.2013.09.015

Loveridge, F. (2012). 'The thermal performance of foundation piles used as heat exchangers in ground energy systems', PhD thesis, University of Southampton, UK.

Loveridge, F., Amis, T. and Powrie, W. (2012). 'Energy pile performance and preventing ground freezing', in I*nternational Conference on Geotechnical Engineering and Geomechanics.*

Loveridge, F., Brettmann, T., Olgun, C. G. and Powrie, W. (2014). 'Assessing the applicability of thermal response testing to energy piles', in *At global perspectives on the sustainable execution of foundation works, Sweden, May 2014.*

Loveridge, F., Low, J. and Powrie, W. (2017). 'Site investigation for energy geostructures', *Quarterly Journal of*

Engineering Geology and Hydrogeology, *50*, pp. 158–168. doi.org/10.1144/qjegh2016-027

Loveridge, F., Olgun, C. G., Brettmann, T. and Powrie, W. (2014). 'The Thermal Behaviour of Three Different Auger Pressure Grouted Piles Used as Heat Exchangers', *Geotechnical and Geoogical. Engineering*, pp. 273-289. https://doi.org/10.1007/s10706-014-9757-4

Loveridge, F., Powrie, W. and Nicholson, D. (2014). 'Comparison of two different models for pile thermal response test interpretation', *Acta Geotechnica*, *9*, pp. 367–384. https://doi.org/10.1007/s11440-014-0306-3

Low, J. E. *et al.* (2014). 'A comparison of laboratory and in situ methods to determine soil thermal conductivity for energy foundations and other ground heat exchanger applications', *Acta Geotechnica*, 10(2), pp. 209–218. doi: 10.1007/s11440-014-0333-0. https://doi.org/10.1007/s11440-014-0333-0

Lund, H., Werner, S., Wiltshire, R., Svendsen, S., Thorsen, J. E., Hvelplund, F. and Mathiesen, B. V. (2014). '4th Generation District Heating (4GDH): Integrating smart thermal grids into future sustainable energy systems', *Energy*, *68*, https://doi.org/10.1016/j.energy.2014.02.089

Lund, J. W. and Boyd, T. L. (2016). 'Direct utilization of geothermal energy 2015 worldwide review', *Geothermics, 60*, pp. 66–93. https://doi.org/10.1016/j.geothermics.2015.11.004.

Magraner, T., Montero, Á., Quilis, S. and Urchueguía, J. F. (2010). 'Comparison between design and actual energy performance of a HVAC-ground coupled heat pump system in cooling and heating operation', *Energy and Buildings*, *42*, pp. 1394-1401. https://doi.org/10.1016/j.enbuild.2010.03.008.

Makasis, N., Narsilio, G. A. and Bidarmaghz, A. (2018). 'A machine learning approach to energy pile design', *Computers and Geotechnics*. Elsevier, 97, pp. 189–203. https://doi.org/10.1016/j.compgeo.2018.01.011

Maragna, C. and Rachez, X. (2015). 'Innovative Methodology to Compute the Temperature Evolution of Pile Heat Exchangers', in *World Geothermal Congress 2015*.

Maragna, C. (2016). 'Development of a numerical Platform for the Optimization of Borehole Heat Exchanger Fields', in *European Geothermal Congress 2016*, pp. 19–24.

Marshall, A. (1972). 'The thermal properties of concrete'. *Building Science*, 7, pp. 167-174.

Marto, A., Amaludin, A. and Satar, M. H. (2015). 'Experiments on Shallow Geothermal Energy Model Piles Embedded in Soft Soil', *EJGE*, 20.

McCartney, J. S. and Murphy, K. D. (2012). 'Strain Distributions in Full-Scale Energy Foundations (DFI Young Professor Paper Competition 2012)', *DFI Journal - The Journal of the Deep Foundations Institute*, 6(2), pp. 26–38. doi: 10.1179/dfi.2012.008.

McCartney, J. S. and Rosenberg, J. E. (2011). 'Impact of heat exchange on side shear in thermo-active foundations', in *Geo-Frontiers 2011: Advances in Geotechnical Engineering*. ASCE, pp. 488–498.

Mehta, P. & Monteiro, P. J. M. (2006). *Concrete: Microstructure, Properties, and Materials*, McGraw-Hill Education.

Midttømme, K., Banks, D., Ramstad, R. K., Sæther, O. M. and Skarphagen, H. (2008). 'Ground-Source Heat Pumps and Underground Thermal Energy Storage - Energy for the future', *NGU Special Publication*, *11*, pp. 93-98.

Mimouni, T. and Laloui, L. (2013). 'Thermo-Pile: A Numerical Tool for the Design of Energy Piles', in *Energy Geostructures*; John Wiley & Sons, Inc., 2013; pp. 265–279. ISBN 9781118761809.

Mimouni, T. and Laloui, L. (2014). 'Towards a secure basis for the design of geothermal piles', *Acta Geotechnica, 9*, pp. 355–366. https://doi.org/10.1007/s11440-013-0245-4

Mimouni, T. and Laloui, L. (2015). 'Behaviour of a group of energy piles', *Canadian Geotechnical Journal*. NRC Research Press, 52(12), pp. 1913–1929. doi: 10.1139/cgj-2014-0403.

Mimouni, T. (2014). 'Thermomechanical Characterization of Energy Geostructures with Emphasis on Energy Piles', PhD thesis, École Polytechnique Fédérale de Lausanne EPFL, Lausanne, Switzerland.

Mogensen P. (1983). 'Fluid to Duct Wall Heat Transfer in Duct System Heat Storage', In *Proceedings of the International Conference On Subsurface Heat Storage in Theory and Practice*; Swedish Council for Building Research: Stockholm. Sweden, June 6–8, 1983; pp. 652-657.

Møller, O., Frederiksen, J.K., Augustesen, A.H., Okkels, N. and Sorensen, K.G. (2016). 'Design of piles – Danish practice'*, in Proceedings of ISSMGE - ETC 3 International Symposium on Design of Piles in Europe.*

Montagud, C., Corberán, J. M., Montero, Á. and Urchueguía, J. F. (2011). 'Analysis of the energy performance of a ground source heat pump system after five years of operation', *Energy and Buildings*, *43*, pp. 3618–3626, https://doi.org/10.1016/j.enbuild.2011.09.036

Monzó, P. (2018). 'Modelling and monitoring thermal response of the ground in borehole fields', PhD thesis, KTH Stockholm, Sweden.

Murphy, K. D. and McCartney, J. S. (2014). 'Thermal Borehole Shear Device', *Geotechnical Testing Journal. ASTM International*, 37(6), p. 20140009. doi: 10.1520/GTJ20140009.

Murphy, K. D. and McCartney, J. S. (2015). 'Seasonal response of energy foundations during building operation', *Geotechnical and Geological Engineering, 33*, pp. 343–356. https://doi.org/10.1007/s10706-014-9802-3

Murphy, K. D., McCartney, J. S. and Henry, K. S. (2015). 'Evaluation of thermo-mechanical and thermal behavior of full-scale energy foundations', *Acta Geotechnica*, 10(2), pp. 179–195. doi: 10.1007/s11440-013-0298-4. https://doi.org/10.1007/s11440-013-0298-4

Neville, A. M. (1995). *Properties of concrete*, Wiley.

NHBC Foundation (2010). 'Efficient Design of Piled Foundations for Low-Rise Housing: Design Guide', Building Research Establishment. ISBN 9781848061064.

Nicholson, D., Smith, P., Bowers, G. A., Cuceoglu, F., Olgun, C. G., McCartney, J. S., Henry, K., Meyer, L. L. and Loveridge, F. A. (2014). 'Environmental impact calculations, life cycle cost analysis', *DFI Journal – The Journal of the Deep Foundations Institute, 8*, pp. 130–146, https://doi.org/10.1179/1937525514Y.0000000009

Nist Sematech (2018). 'Engineering statistics handbook. Multiple responses: The desirability approach'. Available online: https://www.itl.nist.gov/div898/handbook/pri/section5/pri5322.htm [Accessed on 11-May 2018].

Oasys (2014). 'Pile Version 19.5. Pile Oasys Geo Suite for Windows. User manual'; Ltd., O., Ed.; London, UK.

Oklahoma State University (1988). *Closed-loop/ground source heat pump systems. Installation guide.* Edited by O. S. University. International Ground Source Heat Pump Association.

Olgun, C. G. and McCartney, J. S. (2014). 'Outcomes from international workshop on thermoactive geotechnical systems for near-surface geothermal energy: from research to practice', DFI Journal - The Journal of Deep Foundation Institute, 8, pp. 59–73, https://doi.org/10.1179/1937525514Y.0000000005.

Olgun, C. G., Ozudogru, T. Y. and Arson, C. F. (2014). 'Thermo-mechanical radial expansion of heat exchanger piles and possible effects on contact pressures at pile–soil interface', *Géotechnique Letters*, *4*, pp. 170–178. https://doi.org/10.1680/geolett.14.00018

Olgun, C. G., Ozudogru, T. Y., Abdelaziz, S. L. and Senol, A. (2015). 'Long-term performance of heat exchanger piles', *Acta Geotechnica*, *10*, pp. 553–569. https://doi.org/10.1007/s11440-014-0334-z

Ouyang, Y., Soga, K. and Leung, Y. F. (2011). 'Numerical back-analysis of energy pile test at Lambeth College, London', in *Geo-Frontiers Congress 2011*, pp. 440–449.

Pahud, D. and Fromentin (1991). 'PILESIM - LASEN. Simulation Tool for Heating/Cooling Systems with Heat Exchanger Piles or Borehole Heat Exchangers. User Manual.', Available in: http://repository.supsi.ch/3047/

Pahud, D. and Fromentin, A. (1999). *PILESIM - LASEN. Simulation Tool for Heating/Cooling Systems with Heat Exchanger Piles or Borehole Heat Exchangers. User Manual.* Available at: http://repository.supsi.ch/id/eprint/3047.

Pahud, D. and Hubbuch, M. (2007). 'Measured thermal performances of the energy pile system of the Dock Midfield at Zürich Airport', in *Proceedings European geothermal congress 2007*.

Pahud, D. (2002). 'Geothermal energy and heat storage', SUPSI – DCT – LEEE. Scuola Universitaria Professionale della Svizzera Italiana, Cannobio.

Pardo, N., Montero, Á., Sala, A., Martos, J. and Urchueguía, J. F. (2011). 'Efficiency improvement of a ground coupled heat pump system from energy management', *Applied Thermal Engineering*, *31*, pp. 391–398, https://doi.org/10.1016/j.applthermaleng.2010.09.016

Park, H., Lee, S.R., Yoon, S. and Choi, J.C. (2013). 'Evaluation of thermal response and performance of PHC energy pile: Field experiments and numerical simulation', *Applied Energy*, *103*, pp. 12–24. https://doi.org/10.1016/j.apenergy.2012.10.012

Park, S., Lee, D., Choi, H. J., Jung, K. and Choi, H. (2015). 'Relative constructability and thermal performance of cast-in-place concrete energy pile: Coil-type GHEX (ground heat exchanger)', *Energy*, *81*, pp. 56–66. https://doi.org/10.1016/j.energy.2014.08.012.

Pavlov, G. K. and Olesen, B. W. (2011). 'Seasonal Ground Solar Thermal Energy Storage – Review of Systems and Applications', in *Proceedings ISES Sol. World Congress*, pp. 515–525. doi:10.18086/swc.2011.29.24.

Péron, H., Knellwolf, C. and Laloui (2011). L. 'A method for the geotechnical design of heat exchanger piles'. In *Proceedings of the geo-frontiers 2011 conference*, *211*, pp. 470–479.

Philippe, M., Bernier, M. and Marchio, D (2010). 'Sizing calculation spreadsheet: Vertical geothermal borefields'. *Ashrae Journal,52*, 20.

Philippe, M., Bernier, M. and Marchio, D. (2009). 'Validity ranges of three analytical solutions to heat transfer in the vicinity of single boreholes', *Geothermics*, *38*, pp. 407–413, https://doi.org/10.1016/j.geothermics.2009.07.002

Phillips, A. et al. (2010). *Efficient Design of Piled Foundations for Low-Rise Housing: Design Guide*. Building Research Establishment. Available online: https://www.nhbcfoundation.org/publication/efficient-design-of-piled-foundations-for-low-rise-housing/

Pomianowski, M., Heiselberg, P., Jensen, R. L., Cheng, R. and Zhang, Y. (2014). 'A new experimental method to determine specific heat capacity of inhomogeneous concrete material with incorporated microencapsulated-PCM', *Cement and Concrete Research*, 55, pp. 22-34. https://doi.org/10.1016/j.cemconres.2013.09.012

Poudyal, R. (2014). 'Thermal-mechanical Behavior of a Multiple-loop Geothermal Heat Exchanger Pile', MSc thesis, Oklahoma State University, USA.

Poulsen, S. E. and Alberdi-Pagola, M. (2015). 'Interpretation of ongoing thermal response tests of vertical (BHE) borehole heat exchangers with predictive uncertainty based stopping criterion', *Energy*, 88, pp. 157–167.

https://doi.org/10.1016/j.energy.2015.03.133

Rees, S. J. 'An introduction to ground-source heat pump technology', in *Advances in Ground-Source Heat Pump Systems*; Woodhead Publishing, 2016. ISBN 978-0-08-100311-4.

Rees, S. W., Adjali, M. H., Zhou, Z., Davies, M. and Thomas, H. R. (2000). 'Ground heat transfer effects on the thermal performance of earth-contact structures', *Renewable Sustainable Energy Reviews, 4*, pp. 213–265. https://doi.org/10.1016/S1364-0321(99)00018-0.

Rogelj, J., Den Elzen, M., Höhne, N., Fransen, T., Fekete, H., Winkler, H., Schaeffer, R., Sha, F.; Riahi, K. and Meinshausen, M. (2016). 'Paris Agreement climate proposals need a boost to keep warming well below 2 C', *Nature, 534*, pp. 631–639.

Røgen, B., Ditlefsen, C. and Vangkilde-Pedersen, T. (2015). 'Geothermal energy use, 2015 country update for Denmark', in *Proceedings World Geothermal Congress 2015.*

Rotta Loria A. F. and Laloui, L. (2017). 'Impact of Thermally Induced Soil Deformation on the Serviceability of Energy Pile Groups'. In: Ferrari A., Laloui L. (eds) *Advances in Laboratory Testing and Modelling of Soils and Shales (ATMSS).* ATMSS 2017. Springer Series in Geomechanics and Geoengineering. Springer, Cham.

Rotta Loria, A. F. and Laloui, L. (2016). 'The equivalent pier method for energy pile groups', *Geotechnique*, *67*, pp. 691-702. http://dx.doi.org/10.1680/jgeot.16.P.139

Rotta Loria, A. F. and Laloui, L. (2016). 'The interaction factor method for energy pile groups'. *Computers and Geotechnics, 80*, pp. 121–137. https://doi.org/10.1016/j.compgeo.2016.07.002

Rotta Loria, A. F. and Laloui, L. (2017). 'Group action effects caused by various operating energy piles', *Géotechnique.* https://doi.org/10.1680/jgeot.17.P.213.

Rotta Loria, A. F. et al. (2015). 'Numerical modelling of energy piles in saturated sand subjected to thermo-mechanical loads', *Geomechanics for Energy and the Environment*, 1, pp. 1–15. https://doi.org/10.1016/j.gete.2015.03.002

Rotta Loria, A. F. (2018). 'Thermo-mechanical performance of energy pile groups', PhD thesis, École Polytechnique Fédérale de Lausanne EPFL, Lausanne, Switzerland. doi:10.5075/EPFL-THESIS-8138.

Rotta Loria, A. F., Bocco, M., Garbellini, C., Muttoni, A. and Laloui, L. (2018). 'The role of thermal loads in the performance-based design of energy piles', *Géotechnique (under-review).*

Rotta Loria, A. F., Donna, A. Di and Laloui, L. (2015). 'Numerical study on the suitability of centrifuge testing for capturing the thermal-induced mechanical behavior of energy piles', *Journal of Geotechnical and Geoenvironmental Engineering*, 141(10), p. 4015042. https://doi.org/10.1061/(ASCE)GT.1943-5606.0001318

Schnürer, H., Sasse, C. and Fisch, M. N. (2005). 'Thermal Energy Storage in Office Buildings Foundations'. Available online: https://businessdocbox.com/Green_Solutions/70941158-Thermal-energy-storage-in-office-buildings-foundations.html [Accessed on 15-June 2016]

Schröder, B., Hanschke, T. (2003). 'Energiepfhähle - umweltfreundliches Heizen und Kühlen mit geothermisch aktivierten Stahlbetonfertigpfählen', *Bautechnik*, *80*, pp. 925–927. https://doi.org/10.1002/bate.200306210

Sekine, K. et al. (2007). 'Development of a ground-source heat pump system with ground heat exchanger utilizing the cast-in-place concrete pile foundations of buildings', *ASHRAE Transactions.*

Shahrour, I. and Rezaie, F. (1997). 'An elastoplastic constitutive relation for the soil-structure interface under cyclic loading', *Computers and Geotechnics, 21*(1), pp. 21–39. https://doi.org/10.1016/S0266-352X(97)00001-3

Shonder, J. A. and Beck, J. V. (2000). 'Field test of a new method for determining soil formation thermal conductivity and borehole resistance', *ASHRAE Transactions*, *106*, pp. 843–850.

SIA (2005). 'Utilisation de la chaleur du sol par des ouvrages de fondation et de soutènement en béton: guide pour la coneption, la réalisation et la maintenance'; SIA, Société suisse des ingénieurs et des architectes. ISBN 9783908483595.

Signorelli, S. et al. (2007). 'Numerical evaluation of thermal response tests', *Geothermics*, 36(2), pp. 141–166. https://doi.org/10.1016/j.geothermics.2006.10.006

Spitler, J. D. and Bernier, M. (2016). 'Vertical borehole ground heat exchanger design methods', Rees, S. J., in *Advances in Ground-Source Heat Pump Systems*; Woodhead Publishing, pp. 29–61 ISBN 978-0-08-100311-4.

Spitler, J. D. and Gehlin, S. E. A. (2015). 'Thermal response testing for ground source heat pump systems—An historical review', *Renewable and Sustainable Energy Reviews*, 50, pp. 1125–1137. https://doi.org/10.1016/j.rser.2015.05.061

Spitler, J. D. (2000). 'GLHEPRO-A design tool for commercial building ground loop heat exchangers', in *Proceedings of the fourth international heat pumps in cold climates conference*, Citeseer.

Suguang, X., Suleiman, M. T. & McCartney, J. S. (2014). 'Shear Behavior of Silty Soil and Soil-Structure Interface under Temperature Effects', in *Geo-Congress 2014*. Atlanta, Georgia, USA: American Society of Civil Engineers.

Suryatriyastuti, M. E., Burlon, S. and Mroueh, H. (2016). 'On the understanding of cyclic interaction mechanisms in an energy pile group', *International Journal for Numerical and Analytical Methods in Geomechanics*, 40(1), pp. 3–24. https://doi.org/10.1002/nag.2382

Suryatriyastuti, M. E., Mroueh, H. and Burlon, S. (2012). 'Understanding the temperature-induced mechanical behaviour of energy pile foundations', *Renewable and Sustainable Energy Reviews, 16*, pp. 3344–3354. https://doi.org/10.1016/j.rser.2012.02.062

Suryatriyastuti, M. E., Mroueh, H. and Burlon, S. (2014). 'A load transfer approach for studying the cyclic behavior of thermo-active piles'. *Computers and Geotechnics, 55*, pp. 378–391. https://doi.org/10.1016/j.compgeo.2013.09.021

Suryatriyastuti, M. E., Mroueh, H., Burlon, S. and Habert, J. (2013). 'Numerical analysis of the bearing capacity in thermo-active piles under cyclic axial loading'. In *Energy geostructures: Innovation in Underground Engineering*, Hoboken, ISTE Ltd. and John Wiley and Sons, 2013.

Suryatriyastuti, M. (2013). 'Numerical study of the thermoactive piles behavior in cohesionless soils', PhD thesis, Université Lille, France.

Sutman, M. (2016). 'Thermo-Mechanical Behavior of Energy Piles: Full Scale Field Testing and Numerical Modeling', PhD thesis, Virginia Polytechnic Institute and State University, USA.

Sutman, M., Brettmann, T. and Olgun, C. G. (2014). 'Thermo-mechanical behavior of energy piles: full-scale field test verification', in *DFI 39th Annual Conference on Deep Foundations*, Atlanta, GA, pp. 1–11.

Tang, A.-M. et al. (2014). 'Mechanical Behaviour of Energy Piles in Dry Sand', *Geotechnical Engineering Journal of the SEAGS & AGSSEA,* 45 (3). ISSN 0046-5828

Tavman, I. H. (1996). 'Effective thermal conductivity of granular porous materials', *International Communications in Heat and Mass Transfer*, 23, pp. 169-176.

Teza, G., Galgaro, A. and De Carli, M. (2012). 'Long-term performance of an irregular shaped borehole heat exchanger

system: Analysis of real pattern and regular grid approximation', *Geothermics*, *43*, pp. 45–56, https://doi.org/10.1016/j.geothermics.2012.02.004.

The MathWorks Inc. (2017). 'MATLAB R2017a and Global Optimization Toolbox'.

The MathWorks Inc. (2017). 'MATLAB R2017a'.

UBEG Umwelt Baugrund Geothermie Geotechnik (2013). Thermal Response Test Equipment Data. Germany.

Urchueguía, J.F., et al. (2008). 'Comparison between the energy performance of a ground coupled water to water heat pump system and an air to water heat pump system for heating and cooling in typical conditions of the European Mediterranean coast', *Energy Conversion and Management*, 49(10): p. 2917-2923. https://doi.org/10.1016/j.enconman.2008.03.001

VDI (2001). 'VDI 4640 Thermal use of the underground. Part 2: Ground source heat pump systems', The Association of German Engineers (VDI), Germany.

VDI (2001). 'VDI 4640 Thermal Use of the Underground. Part 3: Utilization of the Subsurface for Thermal Purposes'. Underground Thermal Energy Storage. German Engineers (VDI), Germany.

VDI (2010). 'VDI 4640 Thermal Use of the Underground. Part 1: Fundamentals, approvals, environmental aspect'. German Engineers (VDI), Germany.

Vieira, A., Alberdi-Pagola, M., Christodoulides, P., Javed, S.; Loveridge, F., Nguyen, F., Cecinato, F., Maranha, J., Florides, G., Prodan, I., Lysebetten, G. Van, Ramalho, E., Salciarini, D., Georgiev, A., Rosin-Paumier, S., Popov, R., Lenart, S., Poulsen, S. E. and Radioti, G. (2017). 'Characterisation of Ground Thermal and Thermo-Mechanical Behaviour for Shallow Geothermal Energy Applications', *Energies*, *10*(12), 2044. https://doi.org/10.3390/en10122044

Wang, W. et al. (2012). 'Coupled thermo-poro-mechanical finite element analysis of an energy foundation centrifuge experiment in saturated silt', in *GeoCongress 2012: State of the Art and Practice in Geotechnical Engineering. ASCE*, pp. 4406–4415.

Wheeler, A. J. & Ganji, A. R. (2004). *Introduction To Engineering Experimentation*, Upper Saddle River, New Jersey 07458, Usa, Pearson Education, Inc.

Witte, H. J. L. (2013). 'Error analysis of thermal response tests', *Applied Energy*, 109, pp. 302-311. https://doi.org/10.1016/j.apenergy.2012.11.060

Witte, H. J. L., Van Gelder, G. J. and Spitler, J. D. (2002). 'In Situ Measurement of Ground Thermal Conductivity: A Dutch Perspective', *ASHRAE Transactions 2002*, 108(Part 1), pp. 263–272.

Wood, C. J., Liu, H. and Riffat, S. B. (2010). 'An investigation of the heat pump performance and ground temperature of a piled foundation heat exchanger system for a residential building', *Energy*, 35(12), pp. 4932–4940. https://doi.org/10.1016/j.energy.2010.08.032

Wood, C. J., Liu, H. and Riffat, S. B. (2010). 'Comparison of a modelled and field tested piled ground heat exchanger system for a residential building and the simulated effect of assisted ground heat recharge', *International Journal of Low-Carbon Technologies*, 5(3), pp. 137–143. https://doi.org/10.1093/ijlct/ctq015

Xiao, J., Luo, Z., Martin Ii, J. R., Gong, W. & Wang, L. (2016). 'Probabilistic geotechnical analysis of energy piles in granular soils*, Engineering Geology*, 209, 119-127. https://doi.org/10.1016/j.enggeo.2016.05.006

Xiaolong, M. and Jürgen, G. (2010). 'Efficiency Increase of Soil Heat Exchangers due to Groundwater Flow and Air Injection', in *Proceedings World Geothermal Congress 2010*; Bali, Indonesia, 25-29 April 2010.

Yavari, N. et al. (2014). 'Experimental study on the mechanical behaviour of a heat exchanger pile using physical modelling', *Acta Geotechnica*, 9(3), pp. 385–398. https://doi.org/10.1007/s11440-014-0310-7

Yu, K. L., Singh, R. M., Bouazza, A. and Bui, H. (2015). 'Determining soil thermal conductivity through numerical simulation of a heating test on a heat exchanger pile'. *Geotechnical and Geological Engineering*, *33*, pp. 239–252. https://doi.org/10.1007/s10706-015-9870-z

Zanchini, E. and Lazzari, S. (2013). 'Temperature distribution in a field of long Borehole Heat Exchangers (BHEs) subjected to a monthly averaged heat flux', *Energy*, *59*, pp. 570–580, https://doi.org/10.1016/j.energy.2013.06.040

Zanchini, E. and Lazzari, S. (2014). 'New g-functions for the hourly simulation of double U-tube borehole heat exchanger fields', *Energy*, *70*, pp. 444–455. https://doi.org/10.1016/j.energy.2014.04.022

Zanchini, E., Lazzari, S. and Priarone, A. (2012). 'Long-term performance of large borehole heat exchanger fields with unbalanced seasonal loads and groundwater flow', *Energy*, *38*, pp. 66–77, https://doi.org/10.1016/j.energy.2011.12.038

Zarrella, A., Emmi, G., Zecchin, R. and De Carli, M. (2017). 'An appropriate use of the thermal response test for the design of energy foundation piles with U-tube circuits', *Energy and Buildings*, *134*, pp. 259–270, https://doi.org/10.1016/j.enbuild.2016.10.053

Zeng, H. Y., Diao, N. R. and Fang, Z. H. (2002). 'A finite line-source model for boreholes in geothermal heat exchangers', *Heat Transfer—Asian Research*, 31(7), pp. 558–567. https://doi.org/10.1002/htj.10057

Zhao, L. et al. (2014). 'Cyclic direct shear behaviors of frozen soil–structure interface under constant normal stiffness condition', *Cold Regions Science and Technology*, 102(0), pp. 52–62. doi: https://doi.org/10.1016/j.coldregions.2014.03.001

SUMMARY

Ground source heat pump systems (GSHP) are sustainable and cost-effective space conditioning systems based on shallow geothermal energy. A novel way to harvest the energy stored in the ground, is to use foundation piles as ground heat exchangers. Energy piles are standard concrete piles with built in geothermal pipes. Thus, the foundation of a building performs as a structural and a heating/cooling supply element.

This Industrial PhD project investigates the thermal behaviour of energy piles, in terms of pile testing and system sizing, and treats the main thermo-mechanical effects resulted from seasonally heating and cooling the piles. A tool has been developed to assess the thermal dimensioning of energy pile foundations, at a minimal computational cost, which will assist in building more cost-effective installations.

In combination with other renewable energies, shallow geothermal systems based on energy piles have great potential for realising the transition from fossil fuels to renewable energy resources.